# DRVNA INDUSTRIJA

SCIENTIFIC JOURNAL
OF WOOD TECHNOLOGY

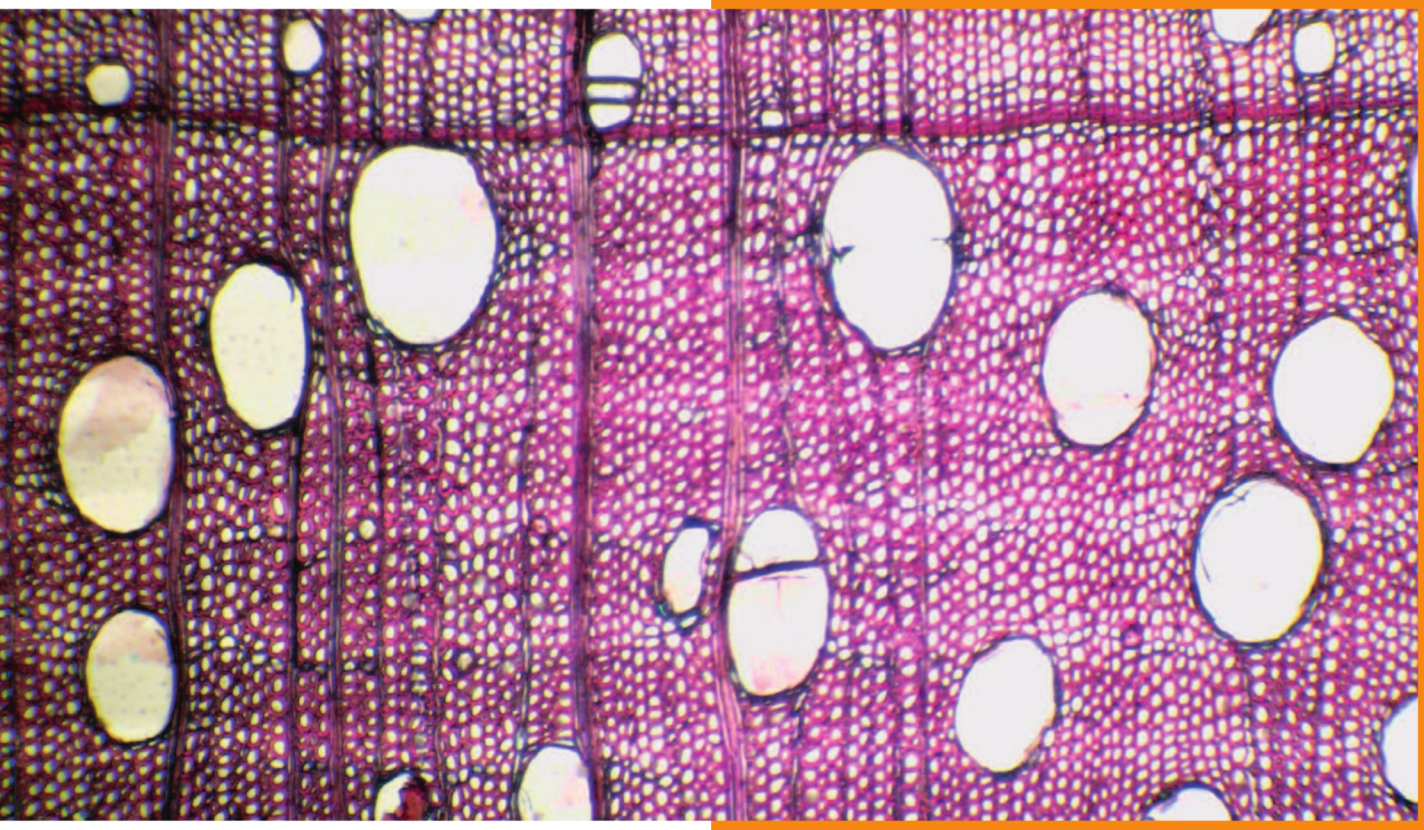

ZNANSTVENI ČASOPIS
IZ PODRUČJA DRVNE TEHNOLOGIJE

*Juglans nigra* L.

UDK 674.031.677.7
ISO: Drv. Ind.
CODEN: DRINAT
JCR: DRVNA IND
ISSN 0012-6772

4/24
VOLUME **75**

since 1913

UDK 630*8+674 Coden: Drinat ISSN 0012-6772

# DRVNA INDUSTRIJA

## SCIENTIFIC JOURNAL OF WOOD TECHNOLOGY

Znanstveni časopis iz područja drvne tehnologije

**PUBLISHER AND EDITORIAL OFFICE**
Izdavač i uredništvo
***University of Zagreb***
***Faculty of Forestry and Wood Technology***
*Sveučilište u Zagrebu*
*Fakultet šumarstva i drvne tehnologije*
*www.sumfak.unizg.hr*

**CO-PUBLISHER** / Suizdavač
*Hrvatska komora inženjera šumarstva i drvne tehnologije*

**FOUNDER** / Osnivač
*Institut za drvnoindustrijska istraživanja, Zagreb*



***The journal Drvna industrija is a public scientific journal for publishing research results on structure, properties and protection of wood and wood materials, application of wood and wood materials, mechanical woodworking, hydrothermal treatment and chemical processing of wood, all aspects of wood materials and wood products production and trade in wood and wood products.***
***The journal is published quarterly and financially supported by the Ministry of Science and Education of the Republic of Croatia***

*Časopis Drvna industrija javno je znanstveno glasilo za objavu rezultata istraživanja građe, svojstava i zaštite drva i drvnih materijala, primjene drva i drvnih materijala, mehaničke i hidrotermičke obrade te kemijske prerade drva, svih aspekata proizvodnje drvnih materijala i proizvoda te trgovine drvom i drvnim proizvodima.*
*Časopis izlazi četiri puta u godini uz financijsku potporu Ministarstva znanosti i obrazovanja Republike Hrvatske.*

# Contents
# Sadržaj

**CIRCULATION:** *400 pieces*

**INDEXED IN:** *Science Citation Index Expanded, Scopus, CAB Abstracts, Compendex, Environment Index, Veterinary Science Database, Geobase, DOAJ, Hrčak, Sherpa Romeo*

**MANUSCRIPTS ARE TO BE SUBMITTED** *by the link http://journal.sdewes.org/drvind*

**CONTACT WITH THE EDITORIAL** *e-mail: editordi@sumfak.hr*

**SUBSCRIPTION:** *Annual subscription is 55 EUR. For pupils, students and retired persons the subscription is 15 EUR. Subscription shall be paid to the IBAN HR0923600001101340148 with the indication "Drvna industrija".*

**PRINTED BY:** *DENONA d.o.o., Getaldićeva 1, Zagreb, www.denona.hr*

**DESIGN:** *Bernardić Studio*

**THE JOURNAL IS AVAILABLE ONLINE:** *https://drvnaindustrija.com*

**COVER:** *Cross-sectional microscopic view of Juglans nigra L., xylotheca of Institute for Wood Science, University of Zagreb Faculty of Forestry and Wood Technology*

**DRVNA INDUSTRIJA · VOL. 75, 4 · P. 383-490 · WINTER 2024. · ZAGREB EDITORIAL COMPLETED 15. 12. 2024.**

**NAKLADA:** *400 komada*

**ČASOPIS JE REFERIRAN U**: *Science Citation Index Expanded, Scopus, CAB Abstracts, Compendex, Environment Index, Veterinary Science Database, Geobase, DOAJ, Hrčak, Sherpa Romeo*

**ČLANKE TREBA SLATI** *putem poveznice http://journal.sdewes.org/drvind*

**KONTAKT S UREDNIŠTVOM:** *e-mail: editordi@sumfak.hr*

**PRETPLATA:** *Godišnja pretplata za pretplatnike u Hrvatskoj i inozemstvu iznosi 55 EUR. Za đake, studente i umirovljenike 15 EUR. Pretplata se plaća na IBAN HR0923600001101340148 s naznakom "Drvna industrija".*

**TISAK**: *DENONA d.o.o., Getaldićeva 1, Zagreb, www.denona.hr*

**DESIGN**: *Bernardić Studio*

**ČASOPIS JE DOSTUPAN NA INTERNETU:** *https://drvnaindustrija.com*

**NASLOVNICA**: *Mikroskopska slika poprečnog presjeka drva Juglans nigra L., ksiloteka Zavoda za znanost o drvu, Sveučilište u Zagrebu Fakultet šumarstva i drvne tehnologije*

**DRVNA INDUSTRIJA · VOL. 75, 4 · STR. 383-490 · ZIMA 2024. · ZAGREB REDAKCIJA DOVRŠENA 15. 12. 2024.**

## ORIGINAL SCIENTIFIC PAPERS
## Izvorni znanstveni radovi ..... 385-487

İsmail Özlüsoylu[1], Abdullah İstek[1], Mehmet Emin Ergün*[2], Deniz Aydemir[1]

# The Effect of Foamed Urea-Formaldehyde Adhesive on Physical and Mechanical Properties of Medium Density Fiberboards (MDF)

# Utjecaj upjenjenog urea-formaldehidnog ljepila na fizička i mehanička svojstva srednje guste ploče vlaknatice (MDF)

**ORIGINAL SCIENTIFIC PAPER**
**Izvorni znanstveni rad**
Received – prispjelo: 30. 11. 2023.
Accepted – prihvaćeno: 9. 4. 2024.
UDK: 630*83; 674.817-415
https://doi.org/10.5552/drvind.2024.0170



**ABSTRACT** • *In this study, the effect of using foamed urea-formaldehyde (UF) adhesive in the production of medium-density fiberboard (MDF) on the properties of the board was investigated. A commercial foaming agent was used to increase the volume of UF adhesive by approximately 2.5 times. MDFs were produced using 6, 9 and 12 % adhesive and 1 % ammonium chloride hardener relative to the dry weight of the adhesive. The thermal degradation behavior of the foamed and control adhesives was determined by thermal analysis i.e., thermogravimetric (TGA) and derivative thermogravimetric (DTG) analyses. It was found that the foaming agent did not affect the thermal degradation of the adhesive. Scanning electron microscope images showed that the volume of foamed adhesive and blending efficiency increased. It was determined that MDFs produced with foamed adhesive had better water absorption and thickness swelling properties than control boards. However, the internal bond strength (IB) and modulus of elasticity (MOE) were found to be 8-14 % and 3-16 % higher, respectively, compared to the control samples. As a result, it can be concluded that the foaming process had a positive effect on the board properties and had the potential to reduce the amount of adhesive used.*

**KEYWORDS:** *medium-density fiberboard; foamed urea-formaldehyde adhesive; physical and mechanical properties; foaming agent*

**SAŽETAK** • *U radu je istraživan utjecaj upotrebe upjenjenog urea-formaldehidnog (UF) ljepila u proizvodnji srednje gustih ploča vlaknatica (MDF) na njihova svojstva. Za povećanje volumena UF ljepila za otprilike 2,5 puta iskorišten je komercijalni dodatak za pjenjenje. MDF ploče proizvedene su uporabom 6, 9 i 12 %-tnog ljepila te 1 %-tnog otvrđivača amonijeva klorida u odnosu prema težini suhih vlakana. Toplinska degradacija upjenjenoga i kontrolnog ljepila utvrđena je termogravimetrijskom (TGA) i diferencijalnom toplinskom (DTG) analizom. Ustanovljeno je da dodatak za pjenjenje nije utjecao na toplinsku degradaciju ljepila. Pretražnim elektronskim mikroskopom uočeno je da se povećao volumen i mješivost upjenjenog ljepila. Rezultati su pokazali da je MDF*

* Corresponding author
[1] Authors are researchers at Bartin University, Faculty of Forestry, Department of Forest Industrial Engineering, Bartin, Turkiye.
[2] Author is researcher at Alanya Alaaddin Keykubat University, Forest and Forest Product Program, Department of Forestry, Antalya, Turkiye. https://orcid.org/0000-0002-9938-7561

*proizveden s upjenjenim ljepilom imao bolja svojstva upijanja vode i debljinskog bubrenja od kontrolnih ploča. Međutim, čvrstoća raslojavanja (IB) i modul elastičnosti (MOE) bili su 8 – 14 % odnosno 3 – 16 % veći od istih pokazatelja kontrolne ploče. Slijedom toga, može se zaključiti da pjenjenje ljepila pozitivno utječe na svojstva ploče i može pridonijeti smanjenju količine potrebnog ljepila.*

**KLJUČNE RIJEČI:** *srednje gusta ploča vlaknatica; upjenjeno urea-formaldehidno ljepilo; fizička i mehanička svojstva; dodatak za pjenjenje*

## 1 INTRODUCTION
## 1. UVOD

Fiberboards have a wide range of applications, including furniture, cladding, doors, flooring, and wall and ceiling coverings (Istek *et al.,* 2012). Urea-formaldehyde (UF) resin is commonly used in the production of fiberboards due to its economic viability, high reactivity, and good adhesive properties (Moslemi *et al.*, 2020). It is emphasized that 1 million tons of UF adhesive are used in wood-based panel production worldwide (Gadhave *et al*., 2017). However, in terms of the current emphasis on human and environmental health, as well as economic considerations, efforts have been directed towards reducing adhesive consumption and promoting its healthy use. For instance, considering a medium-sized factory producing 1000 $m^3$ per day, it is noted that the daily consumption of solid UF is around 45-50 thousand kg, and a monthly saving of 150 tons of solid UF could be achieved with a 10 % reduction (Kelleci *et al*., 2022). While achieving homogeneous adhesive distribution in practice is challenging, it is observed that the sprayed adhesive surface area is dependent on particle area measurements. Despite the fiber surface area being approximately 260 $cm^2$ for 1 g weight, the average droplet diameter of adhesive with 7 % solids is 40 µm, covering a total area of 82 $cm^2$ (Watters, 1974). Istek *et al*. (2019) indicated that an increase in adhesive surface area leads to enhanced internal bond (IB) strength in the board. Achieving the optimum bonding surface area also relies on the significant importance of the sprayed adhesive diameter (Zhan *et al*., 2021).

Among the disadvantages of UF resin are high formaldehyde emissions, low water resistance, and sensitivity to temperature changes (Bekhta *et al*., 2022). Formaldehyde emission is responsible for adverse effects on human health such as cancer, leukemia, genotoxicity, skin, and respiratory tract irritation, nausea, nasopharyngeal and skin sensitization (Chrobak *et al*., 2022; Istek *et al*., 2018; Kristak *et al.,* 2023). Intensive research has been conducted to reduce formaldehyde emissions and improve the mechanical properties in the production of fiber and particleboards. Some of these studies include encapsulated urea (Liu *et al*., 2021), zeolite (Camlibel, 2020), activated carbon (Zamani *et al*., 2022; Ergün *et al*., 2023), and adhesive foaming. The foaming process enhances adhesive homogeneity by reducing resin viscosity. Additionally, it allows for the use of less adhesive by increasing its volume, thereby reducing both cost and formaldehyde emission (Hu *et al*., 2021). Recently, bio-based foaming agents have emerged as a promising alternative to enhance the performance of UF adhesives. These agents are bio-based surfactants that can improve the foam stability and bubble size distribution of UF adhesives, enabling better penetration and distribution in wood structures (Bacigalupe *et al*., 2020). Bio-based foaming agents are considered environmentally and human-health-friendly compared to synthetic agents containing harmful chemicals (Benavides, 2022).

Studies have investigated the properties of low-density particleboards produced with UF adhesive prepared using chemical foaming agents, indicating that results obtained with the use of 2 % less adhesive were similar to control group boards (Boruszewski *et al*., 2022). Jiang *et al*. (2016) reported that particleboards produced with foamed adhesive generally meet international standards in terms of mechanical properties, providing a significant advantage of obtaining a product similar to the control with a lower solid content. Heri Iswanto *et al*. (2018), Nadhari *et al*. (2019), Widyorini *et al*. (2017), and Zhai *et al*. (2021) have conducted studies on the use of foam agents in adhesive foaming. Chemical foaming agents such as azodicarbonamide, sodium dodecyl sulfate, sodium laureth sulfate, commonly used in foam agents, have environmental and human health impacts. In the present world, moving away from products with such effects will likely restrict the use of chemical foaming agents in the near future.

In this study, a commercial foaming agent was used in the production of UF adhesive foamed fiberboard, aiming to produce boards with standard properties while consuming less adhesive. The physical and mechanical properties of the produced boards were examined, along with the thermal and morphological properties of foamed and unfoamed adhesives.

## 2 MATERIALS AND METHODS
## 2. MATERIJALI I METODE

### 2.1 Materials
### 2.1. Materijali

In this study, fibers obtained from oriental beech (*Fagus orientalis*) and pine (*Pinus brutia*) wood fibers were used as raw materials. The wood fibers were

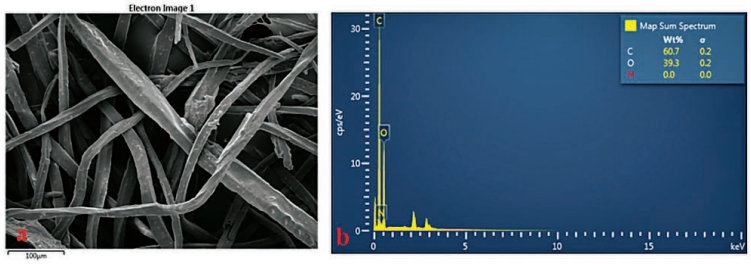


**Figure 1** SEM (a) and EDS (b) analyses of neat fiber
**Slika 1.** SEM (a) i EDS (b) analize čistih vlakana

sourced from the Kastamonu Integrated MDF Plant (Kastamonu, Turkey) and consist of a blend of 55 % beech and 45 % pine wood. SEM and EDS analyses of fiber are given in Figure 1.

The fibers determined the chemical composition, and they contained 60.7 % of carbon (C), 39.3 % of oxygen (O) and 0 % of nitrogen (N). The fibers used in the production were dried up to 2 % moisture content to be prepared for manufacturing. UF adhesive with a density of 1.28 g/cm$^3$ and a solids content of 65 %, supplied by a commercial wood-based board factory (Kastamonu, Turkey), was employed as the adhesive. The commercial foam agent used has a density of 1.05 and a pH value of 5.5. This foam agent is herbal resin-based and was supplied by ARTRA Construction Landscape Plastic Ltd. (İstanbul, Turkey).

## 2.2 Production of MDF
## 2.2. Proizvodnja MDF ploča

In this study, UF adhesive at usage ratio, 6, 9 and 12 % based on the dry fiber weight, along with a commercial foam agent at a 1.5 % concentration based on adhesive solids, was mixed for 5 minutes at 3000 rpm to foam the adhesive. The viscosity and pH of the foamed adhesive were found to be 41.15 CP and 7.20, respectively, at 22 °C, while the viscosity and pH of the unfoamed adhesive were determined to be 17.67 CP and 8.25 at the same temperature. MDF experimental boards were produced using the obtained foamed adhesive solution. Three groups of boards were manufactured, resulting in a total of 18 experimental boards, including control samples for each group. The experimental boards were produced with dimensions of 250 mm × 250 mm, a thickness of 12 mm, and a target density of 0.8 g/cm$^3$. The foamed adhesive solution prepared with fibers at 2 % moisture content was sprayed onto the fibers using a rotating drum, internal spray, and single injector system at 5.5 bars of compressed air pressure. The spraying process was completed by mixing the adhesive and fibers for approximately 3 minutes. The adhesive-coated fibers were manually formed in a mat with dimensions of 250×250×300 to form the board layout. Experimental boards were then produced using a hot press (SSP180 Cemil Usta, Turkey) under the conditions of 4.0 N/mm$^2$ of specific pressure, 175 °C temperature, and a 5-minute duration. Following the hot press, the boards were allowed to cool, and test samples were prepared. The MDFs were conditioned for one week under ambient conditions before preparing the test samples according to the EN 326-1 (1999) standard. Following one week at (20±2) °C and (65±5) % relative humidity, the samples were maintained in a controlled environment chamber.

## 2.3 Characterization of adhesive and MDF
## 2.3. Karakterizacija ljepila i MDF ploča

Thermogravimetric (TG) and derivative thermogravimetric (DTG) tests were conducted on the foamed and unfoamed adhesive samples using Hitachi-STA 7300 equipment (Hitachi, Ltd., Tokyo, Japan). The samples were heated at a rate of 10 °C per minute from room temperature to 600 °C while being subjected to a nitrogen environment with a gas flow rate of 50 mL/min. The foamed and unfoamed adhesive morphologies were studied using a scanning electron microscope (SEM) (MAIA3 XMU model, TESCAN, Brno, Czech Republic). To increase the conductivity of the adhesive, a 5 nm thick layer of gold was applied to the samples. The SEM microscope was operated at 20.0 kV voltages during the microstructure image analysis.

The EN 322 (1999) standard was used to measure moisture content (*MC*), while EN 323 (1999) was used to calculate densities. The EN 317 (1999) standard was used to evaluate thickness swelling (*TS*), and ASTM D1037-12 (2020) was followed for water absorption (*WA*). According to EN 319 (1999) and EN 310 (1999), respectively, the internal bond strength (*IB*), modulus of elasticity (*MOE*), and modulus of rupture (*MOR*) were assessed. All tests, except for the SEM and TGA analyses, were conducted on six samples for each group. The effect of foamed and unfoamed adhesives on the mechanical and physical properties of the MDF was statistically analyzed using one-way analysis of variance (ANOVA) within the SPSS 16 software.

## 3 RESULTS AND DISCUSSION
## 3. REZULTATI I RASPRAVA

### 3.1 Characterization of adhesive and MDF
### 3.1. Karakterizacija ljepila i MDF ploča

TG and DTG graphs of foamed UF adhesive (UF-F) and unfoamed UF adhesive are given in Figure 2.

The thermal decomposition behavior of UF and UF-F samples was determined through TGA measurements. Figure 1 shows the weight loss (%) ratios as a function of temperature. The weight loss (%) by weight of the resins was computed. At temperatures below 200 °C, surface evaporation and the gradual release of natural moisture and formaldehyde from UF are the main causes of the weight loss during the first stage (Jiang *et al*., 2010; Roumeli *et al*., 2012). The condensation reaction of unreacted amino and hydroxymethyl groups can cause water to evaporate. According to Zorba *et al*. (2008) and Zhao *et al*. (2013), the breakdown of methylene and methylene ether bonds takes place in the second stage, which is between 175 and 350 °C. The final stage involves additional carbonization, performed over a wide temperature range from 350 °C to 800 °C. Lower rates of O, N, and H element elimination are the cause of this stage (Chen *et al*., 2021). Similar studies have also found that TGA analyses of UF adhesives yield similar results (Singha and Thakur, 2009; Chen *et al*., 2017).

The TG and DTG results of UF-F, foamed by adding a commercial foam agent at a 1.5 % ratio based on the dry weight of UF, were found to be quite similar to UF. The amount of foam agent used was observed not to significantly impact the thermal properties of the adhesive either positively or negatively. Figure 3 displays SEM images of foamed and unfoamed (pure) UF adhesives.

The images reveal that, because of UF foaming, pores with different diameters are formed (Figure 3a), while unfoamed UF exhibits morphology similar to a flat film (Figure 3b). These pores increased the UF volume. The volumes of both foamed and unfoamed adhesive, which had the same amount, were determined through 5 repetitions each. The volume of the unfoamed and foamed adhesive was found to be (1238±25) $cm^3$ and (3056±99) $cm^3$, respectively. Chemical composition of neat UF adhesive, determined with EDS analyses, was 48 % C, 30.6 % O and 21.5 % N. Gul and Alrobei (2021) found via EDS analyses that neat UF adhesive had 27 % N content.

The increased volume enhances blending efficiency by allowing UF to come into contact with more fiber surfaces. As will be discussed in the mechanical experiments, foaming the adhesive enables achieving the same mechanical properties with less adhesive. Similar SEM images were obtained by foaming UF adhesive in the

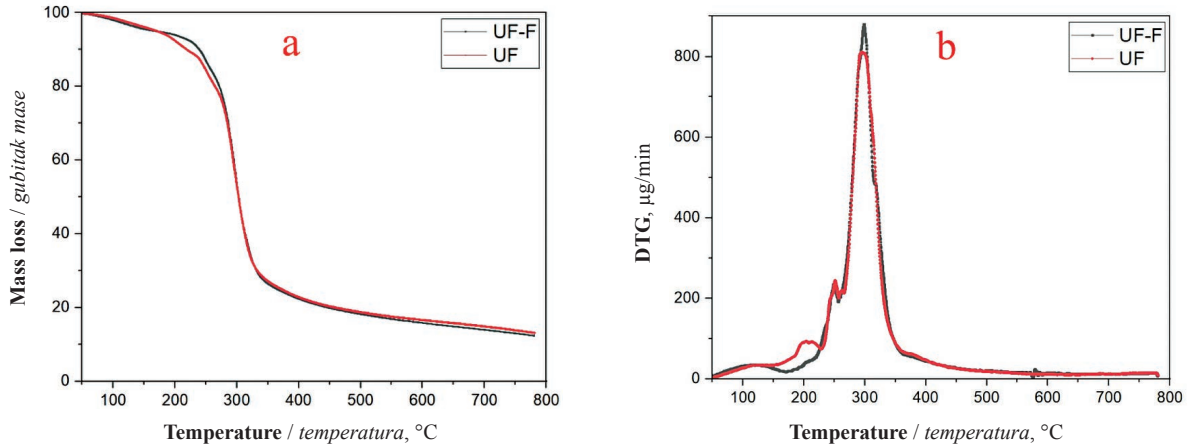


**Figure 2** TG (a) and DTG (b) results of foamed (UF-F) and unfoamed (UF) adhesive
**Slika 2.** TG (a) i DTG (b) rezultati za upjenjeno (UF-F) i neupjenjeno (UF) ljepilo

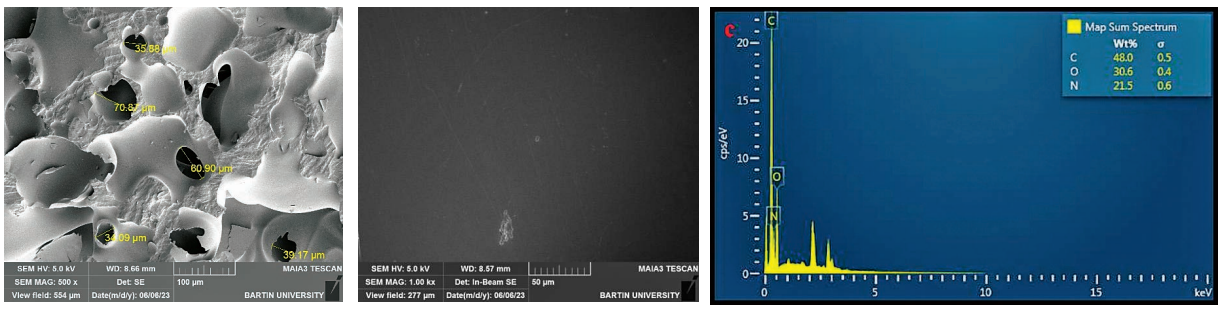


a) b) c)

**Figure 3** SEM images of foamed UF (a) and unfoamed UF (b); EDS analyses of UF (c)
**Slika 3.** SEM fotografije upjenjenoga (a) i neupjenjenog (b) UF ljepila; EDS analiza UF ljepila (c)

production of particleboards, and it was reported that the same or better mechanical properties could be achieved with less adhesive (Kelleci *et al*., 2022).

### 3.2 Chemical and morphological properties of MDF
### 3.2. Kemijska i morfološka svojstva MDF ploča

The SEM, mapping, and EDS analyses of MDFs produced with adhesives containing 12 % foam and adhesive without foam are given in Figure 4, aiming to identify the distribution of adhesive within the manufactured MDF.

The SEM image of MDF produced with 12 % foamed adhesive (Figure 4a) shows that the adhesive uniform distribution results in enhanced fiber binding (a tighter structure). In Figure 4d, MDFs manufactured with unfoamed adhesive exhibit distinct fibers with less interconnection (a looser structure). Additionally, the nitrogen distribution within the adhesive used in the manufactured MDFs was scrutinized using mapping images. The mapping image of MDF produced with foamed adhesive (Figure 4b) reveals a more homogeneous distribution, whereas MDFs produced with unfoamed adhesive show a more clustered nitrogen distribution with areas devoid of nitrogen (Figure 4e). Conducting EDS analyses on the SEM-imaged areas of the produced MDFs yielded disparate results despite the equal adhesive quantities used in MDF production. In Figure 4c, MDF manufactured with foamed adhesive contains 11.4 % nitrogen, while in MDF produced with unfoamed adhesive (Figure 4f), the nitrogen content attributed to the adhesive is 7.6 %. Although both samples used 12 % adhesive, a 3.8 % difference is observed in the analyzed part. The more heterogeneous distribution of adhesive in MDFs produced with unfoamed adhesive is also shown in the SEM images. These findings from SEM, mapping, and EDS analyses suggest that foamed adhesive ensures a more homogeneous distribution within the produced MDF. The concentration of total nitrogen in the wood is under 0.5 % by dry weight (Cowling and Merrill, 1966; Khanina *et al.*, 2023). So, this amount of N is negligible. In the study conducted by Fletes and Rodrigue (2021), the nitrogen content was neglected in the analysis of wood fiber using EDS, similar to our study (Figure 1b), due to its significantly low concentration. On the other hand, the ultimate analysis, which provides more precise information about the chemical composition of wood, has indicated that the nitrogen (N) content in various wood species ranges from 0.1 % to 0.5 % (Telmo *et al.,* 2010). On the other hand, the low signals observed are considered normal and expected. This situation is related to the addition of adhesive in proportions of 6, 9 and 12 % by weight of the fiber content. The detection of 7.6 % and 11.4 % nitrogen (N) attributed to UF adhesive is in line with the expected results, considering that neat UF contains 21.5 % N as determined by EDS analysis. Similar studies have also reported low signal intensities for nitrogen (N) (Hashim *et al.,* 2005). Additionally, Gul *et al.* (2019) found that the UF adhesive filled the gaps between the fibers in the manufactured MDF, and the presence of nitrogen (N) was confirmed through EDS analysis. In another study, the distribution and chemical composition of the adhesive in wood-based panels were examined, and it

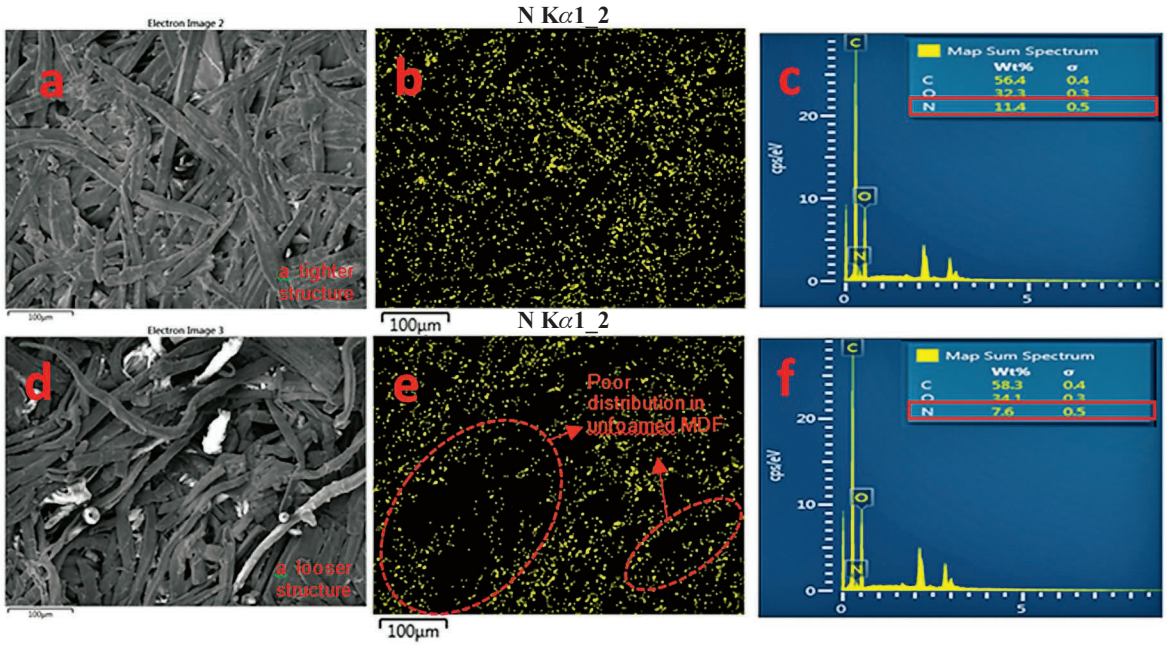


**Figure 4** SEM, mapping, and EDS analyses of 12 % foamed MDF (a, b, c) and unfoamed MDF (d, e, f)
**Slika 4.** SEM, mapiranje i EDS analiza 12 %-tnog upjenjenog MDF-a (a, b, c) i neupjenjenog MDF-a (d, e, f)

was emphasized that the nitrogen (N) element originated from the adhesive. The distribution of the adhesive and the nitrogen (N) element were visualized using SEM-mapping (Lin *et al.,* 2023).

### 3.3 Physical properties of MDF
### 3.3. Fizička svojstva MDF ploča

In this study, MDF was produced by adding a commercial foam agent to urea-formaldehyde adhesive at concentrations of 6, 9 and 12 %, and by using adhesive with added foam. The water absorption (*WA*), thickness swelling (*TS*), moisture content (*MC*), and density values of the produced MDFs are provided in Table 1.

The highest density among the produced MDFs is observed in the 12 % unfoamed MDF. On the other hand, the *MC* values of the produced MDFs varied between 4.13 % and 4.58 %. Both the increased adhesive content and foaming of the adhesive resulted in a decrease in *MC* values. However, statistically, no significant differences were observed in density and *MC* values. Due to the manual production of MDFs, some density fluctuations are inevitable. As shown in Table 1, the foaming process reduced the *WA* and *TS* values of the MDFs. For instance, the 24-hour *WA* value for 6 % unfoamed MDF was 43.61 %, whereas the 24-hour *WA* value for 6 % foamed MDF was 42.76 %. Similarly, the 24-hour *TS* value for 6 % unfoamed MDF was 23.35 %, while the 24-hour *TS* value for 6 % foamed MDF was 22.71 %. This result indicates that the foaming process fills the voids between the fibers with adhesive, thereby enhancing the resistance of MDFs to water, influenced by the foam agent used. Additionally, *WA* and *TS* values decreased as the adhesive addition ratio increased. For example, the 24-hour *WA* value for 6 % unfoamed MDF was 43.61 %, whereas the 24-hour *WA* value for 12 % unfoamed MDF was 30.75 %. Similarly, the 24-hour *TS* value for 6 % unfoamed MDF was 23.35 %, while the 24-hour *TS* value for 12 % unfoamed MDF was 18.47 %. This result indicates that the commercial foam agent used strengthens the bonding between the fibers, allowing the foaming process to penetrate the fibers more effectively and prevent moisture absorption. Statistically significant differences were found in the *TS* and *WA* values of the produced MDFs. In previous studies, MDFs produced using urea-formaldehyde adhesive at concentrations of 10-13 % had 24-hour *TS* and *WA* values ranging from 12-23 % and 42-92 %, respectively (Ashori *et al*., 2009; Selakjani *et al*., 2021). On the other hand, in a study conducted by Kelleci *et al*. (2022), different ratios of UF adhesives were foamed and used in the production of particleboards. An increase in adhesive content and foaming resulted in a reduction in the 24-hour TS and WA values of the particleboards, creating a trend similar to that of the current study.

### 3.4 Mechanical properties of MDF
### 3.4. Mehanička svojstva MDF ploča

The *IB* results of MDFs containing foamed and unfoamed UF adhesive at 6, 9 12 % ratios are presented in Figure 5.

When evaluating the *IB* values, it was observed that foamed MDF samples generally had higher *IB* values compared to unfoamed samples. This observation was particularly pronounced in the foamed samples at 9 % and 12 % concentrations. The *IB* values of MDF ranged from 0.11 N/mm² to 0.16 N/mm². Although there was an increase in *IB* values due to the foaming process allowing better penetration of the adhesive into the fibers, statistically, there was no significant difference in *IB* values among the groups. MDFs produced using UF adhesive at concentrations of 10-13 % had *IB* values ranging from 0.10 to 0.32 N/mm² (Mohebby *et al*., 2008; Ashori *et al*., 2009).

The *MOR* and *MOE* results of MDFs containing foamed and unfoamed UF adhesive at 6, 9 and 12 % ratios are given in Figure 6.

As seen in Figure 6, the *MOR* value of 6 % unfoamed MDF was 15.62 N/mm², while the *MOR* value of 6 % foamed MDF was 18.08 N/mm². On the other hand, an increase in adhesive content also resulted in an increase in *MOR* values (23.33 N/mm² for 12 % Foamed MDF). When examining *MOR* values, it was generally observed that foamed MDF samples had

**Table 1** Physical test results of produced MDFs
**Tablica 1.** Rezultati mjerenja fizičkih svojstava proizvedenih MDF ploča

| **Codes** *Oznaka* | **Density, g/cm³** *Gustoća,* g/cm³ | ***MC*, %** | ***TS*, % (2 h)** | ***TS*, % (24 h)** | ***WA*, % (2 h)** | ***WA*, % (24 h)** |
|---|---|---|---|---|---|---|
| % 6 Unfoamed | 0.78±0,07a | 4.58±0.01a | 11.53±1.91b | 23.35±1.79c | 21.17±5.06bc | 43.61±9.20c |
| % 6 Foamed | 0.79±0.03a | 4.45±0.01a | 11.08±1.99b | 22.71±0.91c | 22.10±7.63c | 42.76±9.12c |
| % 9 Unfoamed | 0.79±0.05a | 4.54±0.06a | 9.94±2.20ab | 18.79±2.39b | 20.96±5.21bc | 40.35±5.31bc |
| % 9 Foamed | 0.80±0.04a | 4.37±0.1a | 9.83±0.74ab | 18.84±1.16b | 17.40±2.74abc | 32.19±4.17ab |
| % 12 Unfoamed | 0.82±0.05a | 4.29±0.7a | 9.71±2.41ab | 18.47±3.50b | 14.86±2.94ab | 30.75±5.31a |
| % 12 Foamed | 0.80±0.05a | 4.13±0.02a | 8.23±0.97a | 15.28±1.99a | 11.39±3.26a | 27.20±6.91a |

Means followed by the same letters (*a*, *b*, *c*) in the same column are not significantly ($p$ <0.05) different; ± Standard deviation.
*Srednje vrijednosti iza kojih su ista slova (a, b, c) u istom stupcu nisu značajno različite ($p$ < 0,05); ± označuje standardnu devijaciju.*

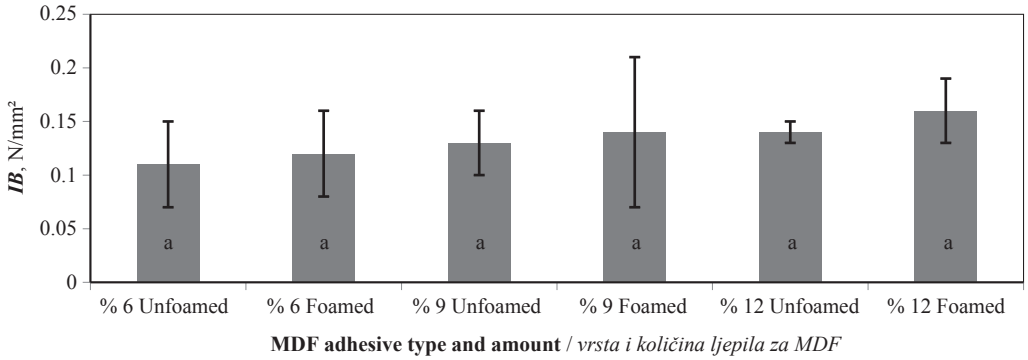


**Figure 5** *IB* values of MDFs containing varying amounts of foamed and unfoamed adhesives (means with the same letters (a) in columns are not significantly ($p < 0.05$) different; standard deviation is given with error bars)
**Slika 5.** *IB* vrijednosti MDF ploča koje sadržavaju različite količine upjenjenoga i neupjenjenog ljepila; srednje vrijednosti s istim slovom (a) u stupcima nisu značajno različite ($p < 0,05$); trake pogrešaka predočuju standardnu devijaciju

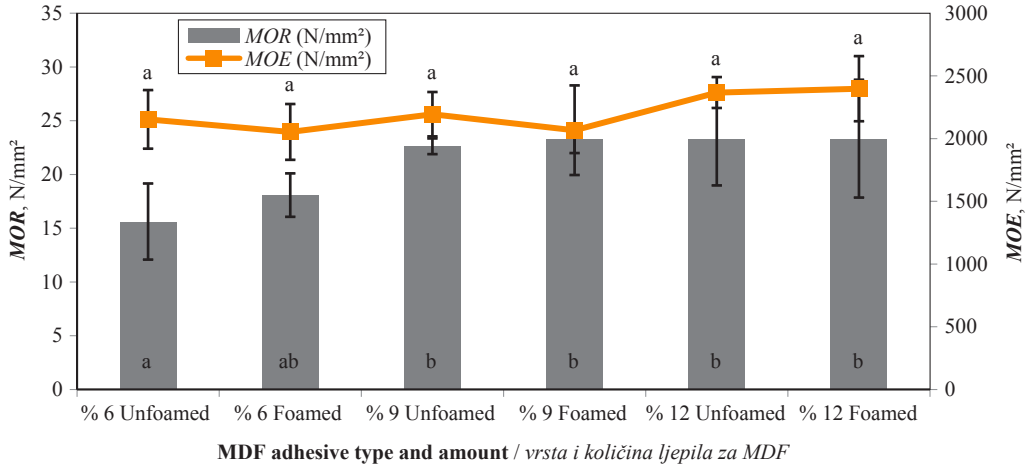


**Figure 6** *MOR* and *MOE* values of MDFs containing varying amounts of foamed and unfoamed adhesives (means with the same letters (a, b) in columns are not significantly ($p < 0.05$) different; standard deviation is given with error bars)
**Slika 6.** *MOR* i *MOE* vrijednosti MDF ploča koje sadržavaju različite količine upjenjenoga i neupjenjenog ljepila; srednje vrijednosti s istim slovima (a, b) u stupcima nisu značajno različite ($p < 0,05$); trake pogrešaka označuju standardnu devijaciju

higher bending strength than unfoamed samples. There was a statistically significant difference among the groups, with the group produced with 6 % unfoamed adhesive showing the lowest result. Especially, it was observed that bending strength of foamed samples was increased at concentrations of 6, 9 and 12 %.

When evaluating *MOE* values, it was observed that foamed MDF samples generally had lower *MOE* values compared to unfoamed samples. This suggests that foamed MDF samples have slightly lower flexibility than unfoamed samples. However, statistically, there was no significant difference between them. This result indicates that the adhesive foamed with a commercial foam agent, by increasing its volume, strengthens the bonding between the fibers, thereby improving the mechanical properties of MDFs. In previous studies, MDFs produced using urea-formaldehyde adhesive at concentrations of 10-13 % had *MOR* and *MOE* values ranging from 12-21 N/mm² and 1400-2650 N/mm², respectively (Mohebby *et al*., 2008; Gul and Alrobei, 2021; Zamani *et al*., 2022). Foaming UF adhesives at different ratios in particleboard production led to an increase in *MOR* and *MOE* values, similar to the findings in the present study (Kelleci *et al*., 2022).

## 4 CONCLUSIONS
## 4. ZAKLJUČAK

This study investigated the effects of foamed and unfoamed versions of urea-formaldehyde (UF) adhesive at different ratios on Medium Density Fiberboard (MDF) production. Foamed and unfoamed MDF samples were produced by adding a commercial foam agent to UF adhesive at various ratios. The physical and mechanical properties of the produced MDF samples were examined. In terms of physical properties, unfoamed MDF samples exhibited higher density; however, the addition of the commercial foam agent and the foaming process reduced water absorption and thickness swelling. Foamed MDF samples showed increased resistance to water and exhibited less swelling thickness. Additionally, the addition of the commercial

foam agent contributed to enhanced water resistance in the produced MDFs. Regarding mechanical properties, foamed MDF samples generally demonstrated higher internal bond strength and bending strength compared to unfoamed samples. This suggests that the foamed adhesive strengthened the bonding between fibers, improving the mechanical durability of the MDF. However, the modulus of elasticity (*MOE*) of foamed MDF samples was generally lower than that of unfoamed samples, indicating a higher flexibility of the foamed samples.

In conclusion, the addition of a commercial foam agent and the use of foamed adhesive contributed to improvements in various physical and mechanical properties in MDF production. These results could facilitate the development of more efficient and environmentally friendly products in the MDF manufacturing industry. However, further studies and optimization efforts may help better understand the commercial applicability of this method.

## 5 REFERENCES
## 5. LITERATURA


1. Ashori, A.; Nourbakhsh, A.; Karegarfard, A., 2009: Properties of medium density fiberboard based on bagasse fibers. Journal of Composite Materials, 43 (18): 1927-1934. https://doi.org/10.1177/0021998309341099
2. Bacigalupe, A.; Molinari, F.; Eisenberg, P.; Escobar, M. M., 2020: Adhesive properties of urea-formaldehyde resins blended with soy protein concentrate. Advanced Composites and Hybrid Materials, 3 (2): 213-221. https://doi.org/10.1007/s42114-020-00151-7
3. Bekhta, P.; Kozak, R.; Gryc, V.; Sebera, V.; Tippner, J., 2022: Effects of wood particles from deadwood on the properties and formaldehyde emission of particleboards. Polymers, 14 (17): 3535. https://doi.org/10.3390/polym14173535
4. Benavides, L., 2023: Using bio-based surfactants as frothers in froth flotation to improve renewable carbon index. In: Proceedings of the 61st Conference of Metallurgists, COM 2022. Springer International Publishing, Cham: 907-909. https://doi.org/10.1007/978-3-031-17425-4_101
5. Boruszewski, P.; Borysiuk, P.; Jankowska, A.; Pazik J., 2022: Low-density particleboards modified with blowing agents – characteristic and properties. Materials, 15 (13): 4528. https://doi.org/10.3390/ma15134528
6. Camlibel, O., 2020: Mechanical and formaldehyde-related properties of medium density fiberboard with zeolite additive. BioResources, 15 (4): 7918-7932. https://doi.org/10.15376/biores.15.4.7918-7932
7. Chen, K.; Cheng, X.; Chen, Y.; Qi, J.; Xie, J.; Huang, X.; Jiang, Y.; Xiao, H., 2021: Thermal degradation kinetics of urea-formaldehyde resins modified by almond shells. ACS Omega, 6 (39): 25702-25709. https://doi.org/10.1021/acsomega.1c03896
8. Chen, S.; Lu, X.; Pan, F.; Wang, T.; Zhang, Z., 2017: Preparation and characterization of urea-formaldehyde resin/reactive montmorillonite composites. Journal of Wuhan University of Technology – Materials Science Edition, 32 (4): 783-790. https://doi.org/10.1007/s11595-017-1668-9
9. Chrobak, J.; Iłowska, J.; Chrobok, A., 2022: Formaldehyde-free resins for the wood-based panel industry: alternatives to formaldehyde and novel hardeners. Molecules, 27 (15): 4862. https://doi.org/10.3390/molecules27154862
10. Cowling, E. B.; Merrill, W., 1966: Nitrogen in wood and its role in wood deterioration. Canadian Journal of Botany, 44 (11): 1539-1554.
11. Ergun, M. E.; Özlüsoylu, İ.; İstek, A.; Can, A., 2023: Analysis and impact of activated carbon incorporation into urea-formaldehyde adhesive on the properties of particleboard. Coatings, 13 (9): 1476. https://doi.org/10.3390/coatings13091476
12. Fletes, R. C. V.; Rodrigue, D., 2021: Effect of wood fiber surface treatment on the properties of recycled hdpe/maple fiber composites. Journal of Composites Science, 5 (7): 177. https://doi.org/10.3390/jcs5070177
13. Gadhave, R. V.; Mahanwar, P. A.; Gadekar, P. T., 2017: Factor affecting gel time/process-ability of urea formaldehyde resin based wood adhesives. Open Journal of Polymer Chemistry, 7 (2): 33-42. https://doi.org/10.4236/ojpchem.2017.72003
14. Gul, W.; Alrobei, H., 2021: Effect of graphene oxide nanoparticles on the physical and mechanical properties of medium density fiberboard. Polymers, 13 (11): 1818. https://doi.org/10.3390/polym13111818
15. Gul, W.; Akbar, S. R.; Khan, A.; Ahmed, S., 2019: Investigation of the surface morphology and structural characterization of MDF & HDF. In: Proceedings of the 5th International Conference on Advances in Mechanical Engineering. Istanbul, Turkey.
16. Hashim, R.; How, L. S.; Kumar, R. N.; Sulaiman, O., 2005: Some of the properties of flame retardant medium density fiberboard made from rubberwood and recycled containers containing aluminum trihydroxide. Bioresource Technology, 96 (16): 1826-1831. https://doi.org/10.1016/j.biortech.2005.01.023
17. Hu, L.; Wang, J.; Qin, L.; Xu, H.; Yang, Z., 2021: Foaming performance and bonding strength of a novel urea-formaldehyde foaming resin facilely prepared with thermo-expandable microspheres. International Journal of Adhesion and Adhesives, 105: 102783. https://doi.org/10.1016/j.ijadhadh.2020.102783
18. Istek, A.; Aydin, U.; Ozlusoylu, I., 2019: The effect of mat layers moisture content on some properties of particleboard. Drvna industrija, 70 (3): 221-228. https://doi.org/10.5552/drvind.2019.1821
19. Istek, A.; Özlüsoylu, I.; Onat, S. M.; Özlüsoylu, Ş., 2018: Formaldehyde emission problems and solution recommendations on wood-based boards. Bartın Orman Fakültesi Dergisi, 20(2): 382-387.
20. Istek, A.; Aydemir, D.; Eroglu, H., 2012: Surface properties of MDF coated with calcite/clay and effects of fire retardants on these properties. Maderas. Ciencia y Tecnología, 14 (2): 135-144. https://doi.org/ 10.4067/S0718-221X2012000200001
21. Jiang, X.; Li, C.; Chi, Y.; Yan, J., 2010: TG-FTIR study on urea-formaldehyde resin residue during pyrolysis and combustion. Journal of Hazardous Materials, 173 (1): 205-210. https://doi.org/10.1016/j.jhazmat.2009.08.070
22. Kelleci, O.; Koksal, S. E.; Aydemir, D.; Sancar, S., 2022: Eco-friendly particleboards with low formaldehyde emission and enhanced mechanical properties produced with foamed urea-formaldehyde resins. Journal of Cleaner Production, 379: 134785. https://doi.org/10.1016/j.jclepro.2022.134785
23. Khanina, L.; Bobrovsky, M.; Smirnov, V.; Romanov, M., 2023: Wood decomposition, carbon, nitrogen and pH values in logs of 8 tree species 14 and 15 years after a cata-

strophic windthrow in a mesic broad-leaved forest in the East European plain. Forest Ecology and Management, 545: 121275. https://doi.org/10.1016/j.foreco.2023.121275
24. Kristak, L.; Antov, P.; Bekhta, P.; Lubis, M. A. R.; Iswanto, A. H.; Reh, R.; Hejna, A., 2023: Recent progress in ultra-low formaldehyde emitting adhesive systems and formaldehyde scavengers in wood-based panels: A review. Wood Material Science & Engineering, 18 (2): 763-782. https://doi.org/10.1080/17480272.2022.2056080
25. Lin, C. F.; Zhang, C.; Karlsson, O.; Martinka, J.; Mantanis, G. I.; Rantuch, P.; Jones, D.; Sandberg, D., 2023: Phytic acid-silica system for imparting fire retardancy in wood composites. Forests, 14 (5): 1021. https://doi.org/10.3390/f14051021
26. Liu, Y.; Qin, X.; Zhu, X.; Wu, L.; Xu, Y.; Huang, K.; Huang, J.; Chen, Y., 2021: Microencapsulation of formaldehyde scavenger agent and its application to veneered panels. European Journal of Wood and Wood Products, 79 (3): 579-588. https://doi.org/10.1007/s00107-021-01656-8
27. Mohebby, B.; Ilbeighi, F.; Kazemi-Najafi, S.; 2008: Influence of hydrothermal modification of fibers on some physical and mechanical properties of medium density fiberboard (MDF). Holz als Roh- und Werkstoff, 66 (3): 213-218. https://doi.org/10.1007/s00107-008-0231-y
28. Moslemi, A.; Behzad, T.; Pizzi, A., 2020: Addition of cellulose nanofibers extracted from rice straw to urea formaldehyde resin; effect on the adhesive characteristics and medium density fiberboard properties. International Journal of Adhesion and Adhesives, 99: 102582. https://doi.org/10.1016/j.ijadhadh.2020.102582
29. Roumeli, E.; Papadopoulou, E.; Pavlidou, E.; Vourlias, G.; Bikiaris, D.; Paraskevopoulos, K. M.; Chrissafis, K., 2012: Synthesis, characterization and thermal analysis of urea–formaldehyde/nano$SiO_2$ resins. Thermochimica Acta, 527: 33-39. https://doi.org/10.1016/j.tca.2011.10.007
30. Selakjani, P. P.; Dorieh, A., Pizzi, A.; Shahavi, M. H.; Hasankhah, A.; Shekarsaraee, S.; Ashouri, M.; Movahed, S. G.; Abatari, M. N., 2021: Reducing free formaldehyde emission, improvement of thickness swelling and increasing storage stability of novel medium density fiberboard by urea-formaldehyde adhesive modified by phenol derivatives. International Journal of Adhesion and Adhesives, 111: 102962. https://doi.org/10.1016/j.ijadhadh.2021.102962
31. Singha, A. S.; Thakur, V. K., 2009: Study of mechanical properties of urea-formaldehyde thermosets reinforced by pine needle powder. BioResources, 4 (1): 292-308. https://doi.org/10.15376/biores.4.1.292-308
32. Telmo, C.; Lousada, J.; Moreira, N., 2010: Proximate analysis, backwards stepwise regression between gross calorific value, ultimate and chemical analysis of wood. Bioresource Technology, 101 (11): 3808-3815. https://doi.org/10.1016/j.biortech.2010.01.021
33. Zamani, R.; Kazemi Najafi, S.; Younesi, H., 2022: Utilization of activated carbon as an additive for urea-formaldehyde resin in medium density fiberboard (MDF) manufacturing. Journal of Adhesion Science and Technology, 36 (21): 2285-2296. https://doi.org/10.1080/01694243.2021.2012029
34. Zhan, X.; Liu, Y.; Yi, P.; Feng, W.; Feng, Z.; Jin, Y., 2021: Effect of substrate surface texture shapes on the adhesion of plasma-sprayed Ni-based coatings. Journal of Thermal Spray Technology, 30 (1): 270-284. https://doi.org/10.1007/s11666-020-01126-2
35. Zhao, Y.; Yan, N.; Feng, M. W., 2013: Thermal degradation characteristics of phenol-formaldehyde resins derived from beetle infested pine barks. Thermochimica Acta, 555: 46-52. https://doi.org/10.1016/j.tca.2012.12.002
36. Zorba, T.; Papadopoulou, E.; Hatjiissaak, A.; Paraskevopoulos, K.; Chrissafis, K., 2008: Urea-formaldehyde resins characterized by thermal analysis and FTIR method. Journal of Thermal Analysis and Calorimetry, 92 (1): 29-33. https://doi.org/10.1007/s10973-007-8731-2
37. *** ASTM D1037-12, 2020: Standard test methods for evaluating properties of wood-base fiber and particle panel materials.
38. *** EN 326-1, 1999: Wood-based panels-sampling, cutting and inspection. Part 1: Sampling test pieces and expression of test results.
39. *** EN 322, 1999: Wood – Based panels – Determination of moisture content.
40. ***EN 317, 1999: Particleboards and fibreboards – Determination of swelling in thickness after immersion in water.
41. ***EN 319, 1999: Particleboards and fibreboards – Determination of tensile strength perpendicular to the plane of the board.
42. ***EN 323, 1999: Wood – Based panels – Determination of density.
43. *** EN 310, 1999: Wood – Based panels – Determination of modulus of elasticity in bending and of bending strength.

**Corresponding address:**

**MEHMET EMIN ERGÜN**
Alanya Alaaddin Keykubat University, Antalya, TURKEY, e-mail: mehmet.ergun@alanya.edu.tr

# LIn

Laboratorij za namještaj
Laboratory for Furniture

accredited testing laboratory for furniture according to HRN EN ISO/IEC 17025

**more than 40 methods in the scope of the testing of furniture**

outside the scope of accreditation:
coatings and parts for furniture
children's playgrounds and playground equipment
research of constructions and ergonomics of furniture
testing of finishing materials and proceses
testing of flammability and ecology of upholstered furniture
furniture expertise

***Laboratory*** **is a member of the Laboratoria Croatica CROLAB – an association whose goal is the development of Croatian laboratories as an infrastructure for the development of production and the economy within a demanding open market, using common potentials and synergy effects of the association, while the**

***Faculty of Forestry and Wood technology*** **is a full member of the INNOVAWOOD – association whose aim it to contribute to business successes in forestry, wood industry and furniture industry, stressing the increase of competitiveness of the European industry.**

**Research of beds and sleeping, research of children's beds, optimal design of tables, chairs and corpus furniture, healthy and comfort sitting at school, office and in home are some of numerous researches performed by the *Institute for furniture and wood in construction*, which enriched the treasury of knowledge on furniture quality.**

17025-HAA
1998
TEST

**Good cooperation with furniture manufacturers, importers and distributors makes us recognizable**

**Knowledge is our capital**

CROLAB

INNOVAWOOD

**University of Zagreb • Faculty of forestry and wood technology**
Testing laboratory for furniture and playground equipment
Institute for furniture and wood in construction
Svetošimunska cesta 23
HR-10000 Zagreb, Croatia

Miran Merhar*[1], Aldin Bjelić[2], Atif Hodžić[2]

# Modelling of Peripheral Wood Milling Power Using Design of Experiment Approach

# Modeliranje snage obodnoga glodanja drva primjenom pristupa dizajna eksperimenta

**ORIGINAL SCIENTIFIC PAPER**
**Izvorni znanstveni rad**
Received – prispjelo: 5. 12. 2023.
Accepted – prihvaćeno: 3. 5. 2024.
UDK: 630*82; 674,02
https://doi.org/10.5552/drvind.2024.0173



**ABSTRACT** • *For efficient production planning, it is necessary to know the power consumption of a particular woodworking operation in advance. In the past, many power measurement tests have been carried out based on a large number of different combinations of technological parameters. However, in this paper, the effects of technological parameters and wood properties on the power magnitude of peripheral milling are analysed using experimental design methods, where the effects of the different factors can be tested with a much smaller number of combinations. Therefore, a central composite experimental design was used to plan the experiments. Three different tree species with different densities were milled with three different numbers of cutting knives and three depths of cut at constant feeding speed and rotational velocity. For each milling combination, the power was measured continuously and then the average power was calculated. Based on the measurements, a suitable model was determined that allowed the magnitude of the cutting power to be determined for each combination of technological parameters and wood species tested. The model proved to be suitable, as the deviations between the measured and modelled power values are minimal.*

**KEYWORDS:** *wood cutting; milling; power consumption; response surface methodology; central composite design*

**SAŽETAK** • *Za učinkovito planiranje proizvodnje potrebno je unaprijed znati potrošnju energije za pojedine operacije u obradi drva. U prošlosti su mnoga istraživanja snage mehaničke obrade drva provedena na temelju velikog broja različitih kombinacija tehnoloških parametara. Međutim, u ovom se radu analiziraju utjecaji tehnoloških parametara i svojstava drva na vrijednosti snage obodnoga glodanja primjenom metoda dizajniranja eksperimenta kojima se utjecaji različitih parametara mogu ispitati s mnogo manjim brojem kombinacija tih parametara. Stoga je za planiranje eksperimenta primijenjen centralni kompozitni dizajn eksperimenta. Tri različite vrste drva različitih gustoća obrađivane su s tri različita broja oštrica i tri dubine glodanja pri konstantnoj posmičnoj brzini i frekvenciji vrtnje alata. Za svaku kombinaciju parametara glodanja kontinuirano je mjerena snaga, a zatim je izračunan prosjek te snage. Na temelju mjerenja izrađen je odgovarajući model koji omogućuje određivanje snage rezanja za svaku ispitivanu kombinaciju tehnoloških parametara i vrstu drva. Model se pokazao prikladnim jer su odstupanja između izmjerene i modelirane snage bila minimalna.*

**KLJUČNE RIJEČI:** *rezanje drva; glodanje; potrošnja energije; metoda odzivne površine; centralni kompozitni dizajn*

* Corresponding author
[1] Author is researcher at University of Ljubljana, Biotechnical Faculty, Department of Wood Science and Technology, Ljubljana, Slovenia. https://orcid.org/0000-0003-0420-787X
[2] Authors are researchers at Faculty of Technical Engineering, University of Bihać, Bihać, Bosnia and Herzegovina.

## 1 INTRODUCTION
## 1. UVOD

Nowadays, energy consumption is a very important factor in the production process, where it is desirable to minimise energy consumption as much as possible. Reducing energy consumption has an important impact on greenhouse gas emissions and the economic efficiency of the product. In addition to these factors, energy consumption also has an impact on the capacity of the production process. In woodworking, for example, where a specific machine with limited capacity is available, the maximum load on the machine can be calculated so as not to exceed the available capacity of the machine.

The average power required for milling or cutting wood is influenced by a number of factors, which can be divided into technological factors and factors related to material properties (Kollmann and Côte, 1975). Technological factors include the feeding speed, rotational velocity and diameter of the tool, number of cutting blades, rake angle of the blades, coefficient of friction between the blade and the chip, sharpness of the blade, depth of cut, cutting direction, *etc.* (Ettelt, 2004; Kivimaa, 1952). Among the properties of the working material, the mechanical properties, such as the strength of the material and fracture toughness have the greatest influence on the cutting performance and vary with the type of wood or wood density, direction of loading and moisture content of wood (Ettelt, 2004; Kivimaa, 1952).

Depending on the factors described, there are many ways to calculate the cutting force or power. The first is modelling based on the mechanical properties of wood, where both the stress-strain conditions must be considered and compared with the properties of wood, such as wood strength and fracture toughness. In the author's opinion, this method is not very suitable for an industrial user who wants to quickly calculate the cutting power and thus predict the energy consumption for a specific type of wood and specific cutting conditions as the user would need to know all the mechanical properties of the wood being cut. Imagine that a company must cut hundreds of cubic metres of wood, for which there is little information about mechanical properties of wood, and the company's technologist has only a limited amount of time to calculate the energy. This approach makes it impossible to acquire all information needed to calculate in a short time.

This method has been studied by many authors who have analysed more or less complex models taking into account different parameters (Aboussafy and Guilbault, 2021; Hlásková *et al.*, 2021; Kubík *et al.*, 2023; Liao and Axinte, 2016; Merhar and Bucar, 2012; Minagawa *et al.*, 2018; Orlowski *et al.*, 2022; Radmanovic *et al.*, 2018; Yang *et al.*, 2023), while others studied the influence of various woodworking tools on power consumption (Kopecký *et al.*, 2022; Svoreň *et al.*, 2022). However, since wood is an anisotropic material that can be described as orthotropic under certain conditions, the models must consider different mechanical properties for each tissue orientation. In addition, the tensile strength of wood is higher than the compressive strength, which must also be taken into account as both tensile and compressive failure of the fabric occurs when wood is cut. Thus, despite the many models for cutting wood that have already been developed and contain different variables, there is still no universal model that can calculate the cutting forces for different combinations of technological parameters and different tree species.

In the other way of calculating the cutting force, the mechanistic approach, the force is calculated using specific coefficients that are determined by the user for each operation (Axelsson *et al.*, 1993; Cristóvão *et al.*, 2012; Ettelt, 2004; Goli *et al.*, 2010; Kivimaa, 1952; Li *et al.*, 2022; Mandic *et al.*, 2015; Pałubicki, 2021; Porankiewicz *et al.*, 2007; Wang *et al.*, 2023). Thus, the specific coefficient should be determined as a function of wood density, cutting direction, angle between the tissue orientation and the blade velocity vector, coefficient for a given rake angle of the blade, moisture content of wood and sharpness of the blade. The value of these coefficients is also based on the mechanical properties of wood described above and can be determined based on these mechanical properties. The first way to calculate these coefficients can be by using the models described in the previous paragraph, which are complex and still unsatisfactory. The second way to determine these coefficients is through experiments in which the coefficients are calculated from measurements of the forces at different combinations of technological parameters and wood properties. Of course, these coefficients are only applicable within the range of values of the variables in which the experiment was carried out. For the above case, this method of calculating force or power offers the technologist in industry the possibility of calculating the cutting force or power required for a particular woodworking operation quickly and relatively accurately. From the technological side, the user only needs the technological parameters that must be known for the specific case and only the wood density in terms of wood properties.

To calculate the cutting power in the mechanistic model, the mean force for one chip $F_m$ is calculated first (Ettelt, 2004),

$$F_m = k_s \cdot b \cdot h_m \tag{1}$$

where $k_s$ is the specific cutting force in N/mm$^2$, $b$ is the cutting width in mm and $h_m$ is the mean thickness of the chip in mm (Figure 1), calculated as

$$h_m = f_z \cdot \sqrt{\frac{a}{d}} \tag{2}$$

where $a$ is the depth of cut in mm, $d$ is the diameter of the milling head in mm and $f_z$ is the feed per tooth in mm calculated as

$$f_z = \frac{v_f}{n \cdot z} \quad (3)$$

$v_f$ is the feeding speed in mm/min, $n$ is the tool rotational velocity in rpm in and $z$ is the number of cutting edges on the circumference of the blade. The above equations show that the average thickness of the chip is influenced by the feed per tooth $f_z$ , which in turn depends on the feeding speed $v_f$, rotational velocity $n$ and the number of cutting edges $z$ on the circumference of the cutting head. This means that the feed per tooth $f_z$ and therefore the average chip thickness $h_m$ can be the same for different workpiece feeding speeds and tool rotational velocities, provided that the relationship between the parameters in equation 3 is constant.

The specific cutting force $k_s$ in Eq. 1 is therefore influenced by various technological parameters and the properties of the material to be cut (Ettelt, 2004; Kivimaa, 1952). In addition to the strength properties of the material, which are related to the density of the material, the specific cutting force $k_s$ is also influenced by the cutting direction or the angle between the current cutting direction $v_c$ and the tissue orientation as shown in Figure 1. For example, the angle between the wood tissue and the cutting direction $v_c$ is 0 when the blade starts to cut (Figure 1). As the tool rotates, the angle j increases until the blade leaves the workpiece where the angle is $\varphi_{out}$. At this point, the specific cutting force is also the greatest, as for example in Figure 1, where the blade cuts almost perpendicular to the grain. The total force is therefore greatest at the angle $\varphi_{out}$, which is the consequence of the maximum specific cutting force $k_s$ and the maximum thickness of the chip $h_{max}$. An exact calculation of the cutting force would therefore require an integral that takes into account both the changing specific cutting force due to the increasing angle between the cutting vector and the orientation of the wood tissue and the increasing thickness of the chip. However, as this is impractical for industrial applications, the calculation can also be simplified by taking into account the mean thickness of the chip $h_m$ and the specific cutting force $k_s$ at the mean cutting angle $\varphi_m$ (Figure 1).

The magnitude of the specific cutting force $k_s$ is also influenced by the rake angle of the blade, where the specific cutting force increases with decreasing rake angle (Ettelt, 2004). Thus, for the calculation of the mean angle $\varphi_m$, the following equations can be used

$$\varphi_m = \frac{\varphi_{out}}{2} \quad (4)$$

$$\varphi_{out} = \arccos\left(\frac{r-a}{r}\right) \quad (5)$$

where $r$ is the radius of the milling head in *mm*. If the angular function (cos) is developed into a Taylor series, it can also be written

$$\varphi_{out} = 2 \cdot \sqrt{\frac{a}{d}} \quad (6)$$

where $d$ is the diameter of the milling head in mm. The latter equation shows that the exit angle $\varphi_{out}$ depends on both the depth of cut $a$ and the diameter of the blade $d$. Thus, for smaller blade diameters, the exit angle $\varphi_{out}$ is larger, and hence the mean angle $\varphi_m$ as well as specific cutting force $k_s$.

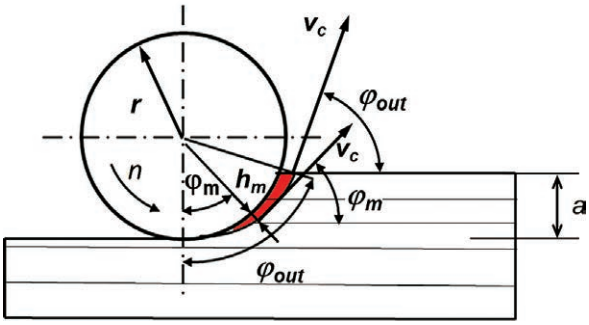


**Figure 1** Schematic of cutting principle; $v_c$ – cutting direction, $a$ – depth of cut, $r$ – cutting tool radius, $n$ – rotational velocity, $\varphi_{out}$ – tool exit angle, $\varphi_m$ – mean cutting angle, $h_m$ – mean chip thickness
**Slika 1.** Shema načela rezanja; $v_c$ – smjer rezanja, $a$ – dubina rezanja, $r$ – radijus alata, $n$ – frekvencija vrtnje alata, $\varphi_{out}$ – izlazni kut alata, $\varphi_m$ – srednji kut rezanja, $h_m$ – srednja debljina strugotine

Once the mean force per cut $F_m$ has been determined (Eq. 1), it is necessary to calculate the average or effective number of blades cutting in the process

$$z_{ef} = \frac{z \cdot \hat{\varphi}_{out}}{2\pi} \quad (7)$$

where $\hat{\varphi}_{out}$ out is the exit angle in radians. If equation 5 is also taken into account, it can be written as

$$z_{ef} = \frac{z \cdot \hat{\varphi}_{out}}{2\pi} = \frac{z \cdot 2 \cdot \sqrt{\frac{a}{d}}}{2\pi} = \frac{z}{\pi}\sqrt{\frac{a}{d}} \quad (8)$$

Thus, from the mean force for one chip $F_m$ and the effective number of teeth $z_{ef}$, the mean force of the operation is calculated

$$F_{op} = F_m \cdot z_{ef} \quad (9)$$

and further, the cutting moment and cutting power

$$M_c = F_{op} \cdot \frac{d}{2} \quad (10)$$

$$P_c = M_c \cdot \omega \quad (11)$$

where ω is angular velocity in rad/s. Putting all together the final theoretical equation for power calculation is

$$P_c = k_s \cdot b \cdot h_m \cdot z_{ef} \cdot \frac{d}{2} \cdot \omega \quad (12)$$

However, with the advent of computers and Design of Experiments (DOE) methods, it is possible to improve the power calculation using functions determined according to the DOE principle. This method has been used by a number of researchers to vary certain cutting parameters and measure cutting forces and cutting power (Mandic *et al.*, 2015; Porankiewicz *et al.*, 2021; Xu *et al.*, 2022; Zhu *et al.*, 2022).

The disadvantage of these studies is that the relationships obtained are only useful for a limited range of cutting conditions and cannot be used in other condi-

tions. Moreover, the models are usually obtained from linear cutting experiments (Axelsson *et al.*, 1993; Cristóvão *et al.*, 2012), so in the case of a circular cut, the mean thickness of the chip $h_m$ must be calculated, and the mean angle $\varphi_m$ between the tooth velocity vector and the direction of the wood tissue varies, which in turn requires additional calculations. In other cases, the authors have developed very complex models that include, in addition to linear relationships, power relationships and higher degree polynomials with dozens of coefficients, that, although they describe the measured forces very accurately, are too complicated and therefore impractical for the industrial end user (Mandic *et al.*, 2015; Porankiewicz *et al.*, 2007). Furthermore, the question arises whether such precise models are useful at all, especially when considering the general variability of the mechanical properties of wood and the resulting variability of cutting forces.

The aim of this research is therefore to develop a simple model that can be used to calculate the average cutting power required in peripheral milling of wood. The model will take into account the most important technological parameters in the case of peripheral milling, the input parameters being technological variables that are known to the operator. At the same time, the model will take into account the fact that some conditions change during circular cutting, such as the specific cutting force due to the increasing angle between the cutting direction vector and the wood tissue, as well as the increasing chip thickness.

## 2 MATERIALS AND METHODS
## 2. MATERIJALI I METODE

14 samples measuring 650 mm × 45 mm × 25 mm (Figure 2) were milled longitudinally on a table milling machine with a milling width of 45 mm. 4 samples of linden (*Tilia platyphyllos*) with the average density of 390 kg/m³ and standard deviation of 8.9 kg/m³, 4 samples of ash (*Fraxinus excelsior*) with the density of 640 kg/m³ and standard deviation of 10.5 kg/m³ and 6 samples of hornbeam (*Carpinus betulus*) with the average density of 790 kg/m³ and standard deviation of 11.1 kg/m³ were used, where all samples had a moisture content of (12±0.5) %. Samples of the same tree species were made from a single board. The feeding speed was 23 m/min, the diameter of the milling cutter 125 mm and the rotational velocity 5900 rpm. Three different cutters were used, each with 4, 6 and 8 cutting edges (Figure 2), consisting of new and sharp carbide inserts with a wedge angle of 60° and rake angle of 20°. The milling depths $a$ (Figure 1) were 2.5, 4.5 and 7 mm. The milling head had an inclination of the cutting edge of 15° where the cutting edge was segmented. The two facts have no influence on the cutting force and power, as shown in Appendix A and B.

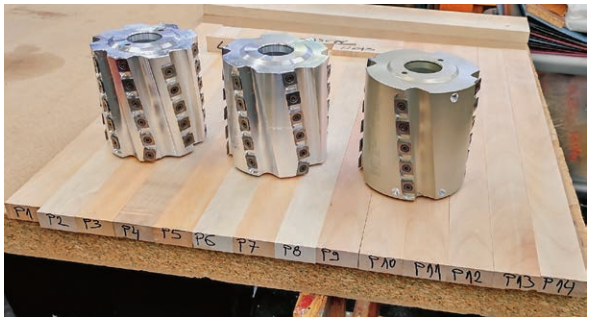

**Figure 2** Wood samples together with milling heads
**Slika 2.** Uzorci drva i alati za glodanje

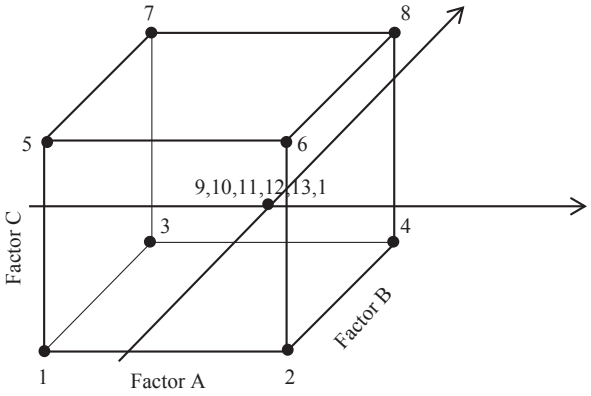


**Figure 3** Graphical representation of central composite design (CCD)
**Slika 3.** Grafički prikaz centralnoga kompozitnog dizajna (CCD)

To plan the experiment, an experimental design was developed using the Design-Expert software (V10, Stat-Ease, Inc., Minneapolis, USA). A conventional two-stage factorial experimental design with three unknowns and 6 central points was used, as shown in Figure 3.

As already mentioned, the density of the wood $\rho$, the number of knives $z$ and the depth of the cut $a$ varied in the experiment. From these variables, the feed per tooth $f_z$ can be calculated according to Eq. 3, which is different for each number of knives. However, the feed per tooth can also change with different feeding speeds $v_f$ or rotational speed $n$, but since they were constant in the experiment, the feed per tooth was included as an input parameter in the power equation. Similarly, the depth of cut $a$ influences the mean angle $\varphi_m$ (Eq. 4) between the vector of blade speed $v_c$ and tissue orientation (Figure 1), which influences the specific cutting force $k_s$. However, the mean angle $\varphi_m$ can also be changed if the cutting depth $a$ is constant but the tool diameter $d$ changes. Since different parameters can be influenced by different process factors, the material density ρ, the mean cutting angle $\varphi_m$ and the feed per tooth $f_z$ were selected as input parameters for the cutting power model. For all input parameters, the values have been converted to base units, i.e. density in kg/m³, $\varphi_m$ in radians and feed per tooth $f_z$ in metres, as shown in Table 2, using Eqs. 2-5, to

**Table 1** Real value parameters used in experiment
**Tablica 1.** Stvarne vrijednosti parametara obuhvaćenih eksperimentom

| | | | |
|---|---|---|---|
| Cutting depth – $a$<br>*Dubina rezanja – a,* mm | 2.5 | 4.5 | 7 |
| Corresponding medium cutting angle – $\varphi_m$, rad<br>*Odgovarajući srednji kut rezanja* – $\varphi_m$, rad | 0.141 | 0.190 | 0.237 |
| Number of cutting edges – $z$<br>*Broj oštrica – z* | 4 | 6 | 8 |
| Corresponding feed per tooth – $f_z$, m<br>*Odgovarajući posmak po zubu* – $f_z$, m | 0.000975 | 0.00065 | 0.000487 |

**Table 2** Parameters used in DOE cutting model
**Tablica 2.** Parametri korišteni u DOE modelu rezanja

| | **Encoded values**<br>*Kodirane vrijednosti* | | |
|---|---|---|---|
| | -1 | 0 | 1 |
| Factor A – $\rho$, kg/m$^3$ | 390 | 640 | 790 |
| Factor B – $\varphi_m$, rad | 0.141 | 0.190 | 0.237 |
| Factor C – $f_z$, m | 0.000487 | 0.00065 | 0.000975 |

avoid confusion when obtaining the power equation. At the end, the units of the basic variables are converted back to the commonly used units.

The cutting power was measured for different combinations of technological parameters and material properties. First, the idle power of the machine was measured and then the total power during milling under different conditions, from which the idle power was then subtracted. The power was calculated by measuring the voltage ($U$) and current ($I$) in all three phases of the electric motor that drives the table cutter. An electrical voltage transformer was used to convert the electrical voltage from the -400 to +400 V range to the -10 to +10 V range, and an electrical current transformer was used to generate a voltage proportional to the current, also in the -10 to +10 V range. All voltages were acquired using a National Instruments NI-USB 6351(Austin, Teksas, USA) acquisition board with a sampling frequency of 2500 Hz and then converted to the real value of the voltage and current. National Instruments LabVIEW (Austin, Teksas, USA) software was used for the acquisition and calculation. The power for each phase was calculated 10 times per second, where for each calculation 250 samples of $U$ and $I$ were used (2500/10) and the total power was the sum of the power of all three phases.

The cutting power was therefore determined as an average value over the entire length of the workpiece. The cutting power was used to calculate the cutting forces, which were further normalised ($F_{mb}$) to a cutting width of 1 m, dividing by the cutting width $b$ of 0.045 m. An ANOVA analysis was then carried out using the Design-Expert software and significant factors for the model were determined.

## 3 RESULTS AND DISCUSSION
## 3. REZULTATI I RASPRAVA

Figure 4 shows the measured power when milling with 4 cutting edges with a cutting depth of 2.5 mm, which corresponds to an average angle $\varphi_m$ of 0.19 rad and a feed per tooth $f_z$ of 0.974 mm. The increase in power from an initial value of 959 W to 1726 W is due to the transition from idling to cutting, where a slight fluctuation in power can be observed due to the variability of wood properties.

Table 3 shows the parameter combinations at which the measurements were carried out, together with the measured cutting powers $P_{c\text{-}eksp}$ and the normalised cutting forces per 1 m chip width ($F_{mb}$) calculated from the power. The values used in the DOE analysis are highlighted in grey. In addition to the input parameters for the analysis ($\rho$, $\varphi_m$, $f_z$, $F_{mb}$), the parameters $a$ and $z$, from which the values of the input parameters were obtained, are also given.

Table 4 shows the results of the ANOVA analysis. All main factors and their correlations are significant for the model ($p$ = 0.05), except for the combination AB, i.e. $\rho^*$ $\varphi_m$, while the combination AC has only a slightly increased $p$-value and was therefore also included in the model. The $R^2$ for the model is 0.9556, while the adjusted $R^2$ and the predicted $R^2$ are 0.9279 and 0.8067, respectively, and are therefore in reasonable agreement. The Adequate Precision, which measures the ratio of signal to noise as 20.8, is also well above the desirable value of 4.

The model in terms of coded and actual factors is shown in Table 5. The model in coded factors shows that all factors have approximately equal values and thus all have equal significant influence on the determination of the cutting force.

The distribution of the residuals is shown in Figure 5. The residuals are normally distributed, as there are no major deviations from the ideal distribution.

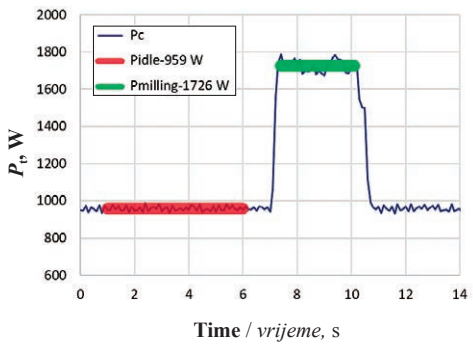


**Figure 4** Variation of power during specimen milling
**Slika 4.** Varijacije snage tijekom glodanja uzorka

**Table 3** Combinations of analysis parameters
**Tablica 3.** Kombinacije analiziranih parametara

| Run | $\rho$, kg/m$^3$ | $\varphi_m$, rad | $f_z$, m | $a$, mm | $z$ | $P_{c\text{-}eksp}$, kW | $F_m$, N | $F_{mb}$, N/m |
|---|---|---|---|---|---|---|---|---|
| 1 | 390 | 0.237 | 0.000975 | 7 | 4 | 2.79 | 239.8 | 5328.77 |
| 2 | 640 | 0.190 | 0.000650 | 4.5 | 6 | 1.81 | 129.3 | 2874.44 |
| 3 | 640 | 0.190 | 0.000650 | 4.5 | 6 | 2.02 | 144.4 | 3207.94 |
| 4 | 640 | 0.190 | 0.000650 | 4.5 | 6 | 2.01 | 143.6 | 3192.05 |
| 5 | 790 | 0.141 | 0.000975 | 2.5 | 4 | 1.15 | 165.4 | 3675.36 |
| 6 | 790 | 0.237 | 0.000975 | 7 | 4 | 3.44 | 295.7 | 6570.24 |
| 7 | 390 | 0.141 | 0.000975 | 2.5 | 4 | 0.76 | 109.3 | 2428.93 |
| 8 | 640 | 0.190 | 0.000650 | 4.5 | 6 | 1.9 | 135.8 | 3017.36 |
| 9 | 390 | 0.141 | 0.000487 | 2.5 | 8 | 1.5 | 107.9 | 2396.97 |
| 10 | 390 | 0.237 | 0.000487 | 7 | 8 | 3.15 | 135.4 | 3008.18 |
| 11 | 790 | 0.237 | 0.000487 | 7 | 8 | 3.58 | 153.8 | 3418.82 |
| 12 | 640 | 0.190 | 0.000650 | 4.5 | 6 | 1.86 | 132.9 | 2953.84 |
| 13 | 640 | 0.190 | 0.000650 | 4.5 | 6 | 1.97 | 140.8 | 3128.53 |
| 14 | 790 | 0.141 | 0.000487 | 2.5 | 8 | 1.71 | 123.0 | 2732.55 |

**Table 4** Result of ANOVA analysis
**Tablica 4.** Rezultati ANOVA analize

| **Source** *Izvor* | **Sum of squares** *Zbroj kvadrata* | **df** | **Mean square** *Srednji kvadrat* | ***F*-value** *F-vrijednost* | ***p*-value** *p-vrijednost* |
|---|---|---|---|---|---|
| Model | 16400000 | 6 | 2733000 | 25.130 | 0.000 |
| A – $\rho$ | 1056000 | 1 | 1056000 | 9.710 | 0.017 |
| B – $\varphi_m$ | 6250000 | 1 | 6250000 | 57.450 | 0.000 |
| C – $f_z$ | 6445000 | 1 | 6445000 | 59.250 | 0.000 |
| AB | 523.34 | 1 | 523.34 | 0.005 | 0.947 |
| AC | 434900 | 1 | 434900 | 4.000 | 0.086 |
| BC | 2536000 | 1 | 2536000 | 23.310 | 0.002 |

There are also no significant deviations between the calculated and measured values (Figure 5). The significance of the parameters can be clearly seen in Figure 6.

The resulting model with actual factors must then be multiplied by the cutting width $b$ to get the $F_m$,

$$Fm = \left(5105. - 8426276 f_z - 16866\varphi_m + 4.84\times10^7 f_z\varphi_m - \right.$$
$$\left. - 1.694\rho + 4771 f_z\rho\right)b \qquad (13)$$

In this model (Eq. 13), $f_z$ and $b$ are the feed per tooth and the cutting width still in metres, respectively, is the mean angle in radians, and ρ is the wood density in kg/m$^3$.

**Table 5** Model for calculating cutting forces in terms of coded and actual factors
**Tablica 5.** Model za proračun sila rezanja u smislu kodiranih i stvarnih čimbenika

| **Coded factors** *Kodirani čimbenici* | | **Actual factors** *Stvarni čimbenici* | |
|---|---|---|---|
| $F_{mb}$ | = | $F_{mb}$ | = |
| +3530.52 | | +5105.04 | |
| +358.66 | *A | -1.69 | * $\rho$ |
| +928.17 | *B | -16866 | *$\varphi_m$ |
| +877.85 | *C | -8.42E+06 | *$f_z$ |
| +232.85 | *AC | +4771.50 | * $\rho$ * $\varphi_m$ |
| +591.31 | *BC | +4.84E+07 | *$\varphi_m$ * $f_z$ |

However, since $f_z$ and $\varphi_m$ are not basic technological parameters but, as already mentioned, depend on the basic technological parameters, they must be replaced by equations 3 to 5. Multiplying the resulting equation by $z_{ef}$ (Eq. 7) gives the force of the operation $F_{op}$, which is further multiplied by the cutting radius to obtain the torque, and then by the angular velocity to obtain the final equation for the cutting power. Changing the units of the input parameters, $b$ and $a$ back to mm, the final model that takes into account the relevant technological parameters for the power calculation will be

$$Pc = b\left(a\left(0.807 v_f - 0.000281 nz\right) + \sqrt{\frac{a}{d}} d\left(\left(-0.14 + 0.0000795\rho\right)v_f \right.\right.$$
$$\left.\left. + n\left(0.0000850 - 2.82\times10^{-8}\rho\right)z\right)\right) \qquad (14)$$

Where $v_f$ is the feeding speed in m/min, $n$ is the rotational speed of the tool in rpm, $z$ is the number of cutting edges on the circumference of the tool, $a$ is the cutting depth in mm, $d$ is the diameter of the tool in mm and ρ is the density of the material in kg/m$^3$.

The measured and calculated cutting powers from Eq. 14 are shown in Table 6 together with their ratios. The latter show that the average deviation of the calculated values from the measured values is 6.6 %, which represents a good agreement between the measured and calculated values.

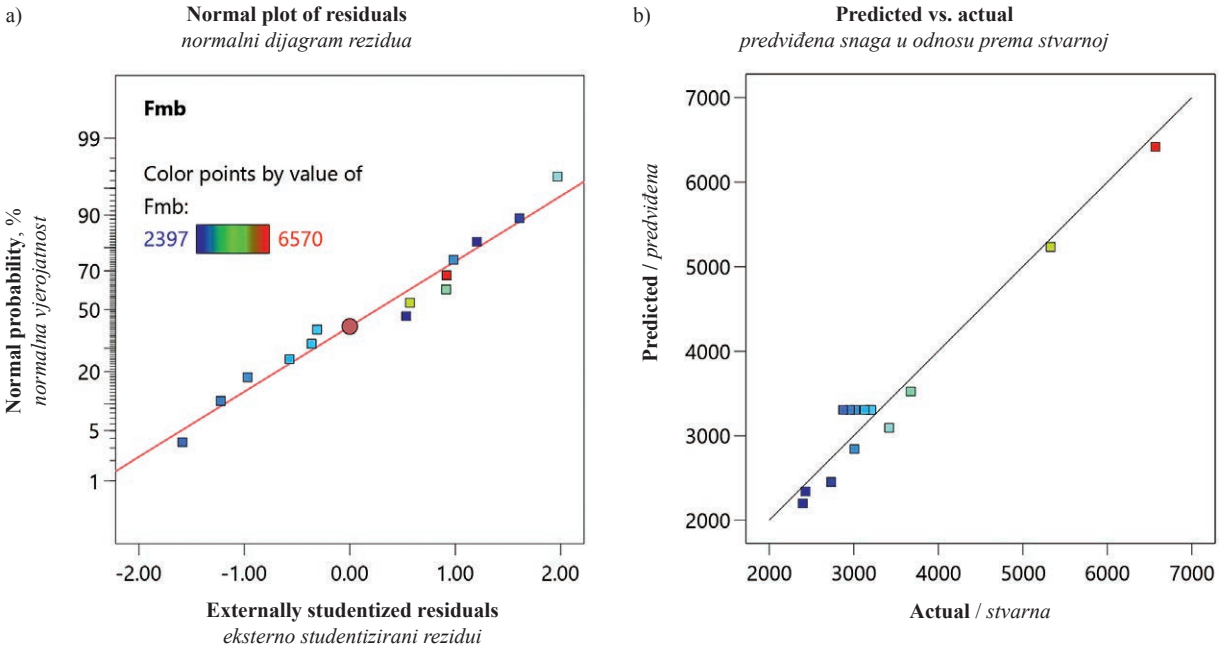


**Figure 5** Distribution of residuals (a) and predicted vs. actual cutting forces for DOE model (b)
**Slika 5.** Distribucija rezidua (a) i predviđene sile rezanja u odnosu prema stvarnima za DOE model (b)

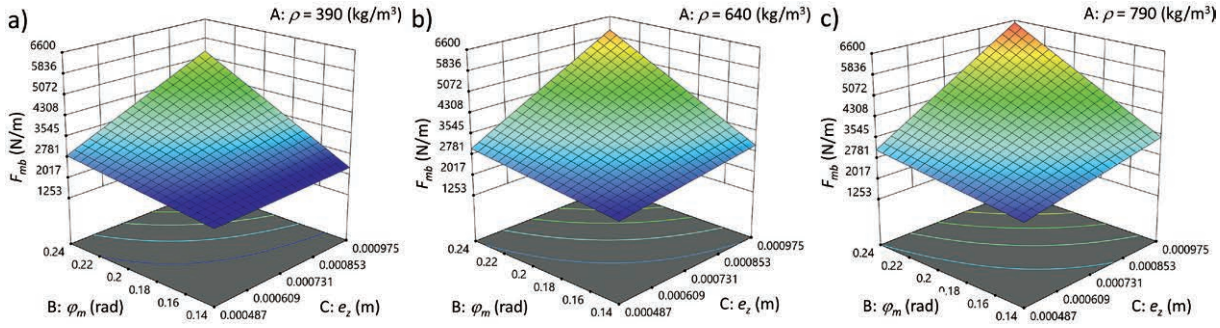


**Figure 6** 3D plot of cutting model with various factors
**Slika 6.** 3D dijagram modela rezanja pri različitim čimbenicima

**Table 6** Measured and calculated cutting power values (ρ – density, $a$ – depth of cut, $z$ – number of cutting knives, $P_{c\text{-}eksp}$ – measured cutting power, $P_{c\text{-}cal}$ – calculated cutting power)
**Tablica 6.** Izmjerene i izračunane vrijednosti snage rezanja (ρ – gustoća, $a$ – dubina rezanja, $z$ – broj oštrica, $P_{c\text{-}eksp}$ – izmjerena snaga rezanja, $P_{c\text{-}cal}$ – proračunana snaga rezanja)

| Run | $\rho$, kg/m$^3$ | $a$, mm | z | $P_{c\text{-}eksp}$, kW | $P_{c\text{-}cal}$, kW | $P_{c\text{-}eksp}/P_{c\text{-}cal}$ |
|---|---|---|---|---|---|---|
| 1 | 390 | 7 | 4 | 2.79 | 2.74 | 1.02 |
| 2 | 640 | 4.5 | 6 | 1.81 | 2.08 | 0.87 |
| 3 | 640 | 4.5 | 6 | 2.02 | 2.08 | 0.97 |
| 4 | 640 | 4.5 | 6 | 2.01 | 2.08 | 0.97 |
| 5 | 790 | 2.5 | 4 | 1.15 | 1.10 | 1.04 |
| 6 | 790 | 7 | 4 | 3.44 | 3.36 | 1.02 |
| 7 | 390 | 2.5 | 4 | 0.76 | 0.73 | 1.04 |
| 8 | 640 | 4.5 | 6 | 1.9 | 2.08 | 0.91 |
| 9 | 390 | 2.5 | 8 | 1.5 | 1.38 | 1.09 |
| 10 | 390 | 7 | 8 | 3.15 | 2.98 | 1.06 |
| 11 | 790 | 7 | 8 | 3.58 | 3.24 | 1.10 |
| 12 | 640 | 4.5 | 6 | 1.86 | 2.08 | 0.89 |
| 13 | 640 | 4.5 | 6 | 1.97 | 2.08 | 0.95 |
| 14 | 790 | 2.5 | 8 | 1.71 | 1.53 | 1.11 |

## 4 CONCLUSIONS
## 4. ZAKLJUČAK

From the results presented in this research, it can be concluded that:

The resulting model can be used to predict the average cutting power during peripheral milling of tested wood species in the machining conditions similar to the ones used in the experiment with an accuracy of 6.6 % as a function of tool diameter, tool rotational speed, number of cutting blades, feed rate, depth of cut and wood density.

With modern methods of experimental design, it is possible to obtain reliable and accurate models with a relatively small number of measurements.

The resulting model can also be used to calculate the cutting power for other tree species with densities in the range of 390 to 790 kg/m$^3$, as it is known that the mechanical properties and thus the cutting power vary with the density of the wood.

Using the same procedure, it is possible to develop a model for calculating the cutting power in other cutting directions.

**Acknowledgements** – Zahvala

The research was supported by the Programs P2-0182, co-financed by the Slovenian Research Agency.

## 5 REFERENCES
## 5. LITERATURA

1. Aboussafy, C.; Guilbault, R., 2021: Chip formation in machining of anisotropic plastic materials – —a finite element modeling strategy applied to wood. International Journal of Advanced Manufacturing Technology, 114 (5-6): 1471-1486. https://doi.org/10.1007/s00170-021-06950-6
2. Axelsson, B. O. M.; Lundberg, Å. S.; Grönlund, J. A., 1993: Studies of the main cutting force at and near a cutting edge. Holz als Roh- und Werkstoff, 51 (1): 43-48. https://doi.org/10.1007/BF02615376
3. Cristóvão, L.; Broman, O.; Grönlund, A.; Ekevad, M.; Sitoe, R., 2012: Main cutting force models for two species of tropical wood. Wood Material Science and Engineering, 7 (3): 143-149. https://doi.org/10.1080/17480272.2012.662996
4. Ettelt, B., 2004: Sägen, Fräsen, Hobeln, Bohren: die Spanung von Holz und ihre Werkzeuge (3rd ed.). Stuttgart, DRW-Verlag.
5. Goli, G.; Fioravanti, M.; Marchal, R.; Uzielli, L.; Busoni, S., 2010: Up-milling and down-milling wood with different grain orientations – the cutting forces behaviour. European Journal of Wood and Wood Products, 68 (4): 385-395. https://doi.org/10.1007/s00107-009-0374-5
6. Hlásková, L.; Procházka, J.; Novák, V.; Čermák, P.; Kopecký, Z., 2021: Interaction between thermal modification temperature of spruce wood and the cutting and fracture parameters. Materials, 14 (20): 6218. https://doi.org/10.3390/ma14206218
7. Kivimaa, E., 1952: Die Schnittkraft in der Holzbearbeitung. Holz als Roh- und Werkstoff, 10 (3): 94-108. https://doi.org/10.1007/BF02608840
8. Kollmann, F. F. P.; Côte, W. A., 1975: Principles of Wood Science and Technology. Solid Wood. Berlin, Germany, Springer-Verlag.
9. Kopecký, Z.; Novák, V.; Hlásková, L.; Rak, J., 2022: Impact of circular saw blade design on forces during cross-cutting of wood. Drvna industrija, 73 (4): 475-483. https://doi.org/10.5552/drvind.2022.2142
10. Kubík, P.; Šebek, F.; Krejčí, P.; Brabec, M.; Tippner, J.; Dvořáček, O.; Lechowicz, D.; Frybort, S., 2023: Linear woodcutting of European beech: experiments and computations. Wood Science and Technology, 57 (1): 51-74. https://doi.org/10.1007/s00226-022-01442-6
11. Li, R.; Yang, F.; Wang, X., 2022: Modeling and predicting the machined surface roughness and milling power in Scot's pine helical milling process. Machines, 10 (5), 331. https://doi.org/10.3390/machines10050331
12. Liao, Z.; Axinte, D. A., 2016: On chip formation mechanism in orthogonal cutting of bone. International Journal of Machine Tools and Manufacture, 102: 41-55. https://doi.org/10.1016/j.ijmachtools.2015.12.004
13. Mandic, M.; Porankiewicz, B.; Danon, G., 2015: An attempt at modelling of cutting forces in oak peripheral milling. BioResources, 10 (3): 5476-5488. https://doi.org/10.15376/biores.10.3.5476-5488
14. Merhar, M.; Bucar, B., 2012: Cutting force variability as a consequence of exchangeable cleavage fracture and compressive breakdown of wood tissue. Wood Science and Technology, 46 (5): 965-977. https://doi.org/10.1007/s00226-011-0457-4
15. Minagawa, M.; Matsuda, Y.; Fujiwara, Y.; Fujii, Y., 2018: Relationship between crack propagation and the stress intensity factor in cutting parallel to the grain of hinoki (Chamaecyparis obtusa). Journal of Wood Science, 64 (6): 758-766. https://doi.org/10.1007/s10086-018-1760-6
16. Orlowski, K. A.; Chuchala, D.; Sinn, G., 2022: Analyses of shear angle in orthogonal cutting of pine wood. Drvna industrija, 73 (3): 309-315. https://doi.org/10.5552/drvind.2022.0022
17. Pałubicki, B., 2021: Cutting forces in peripheral up-milling of particleboard. Materials, 14 (9): 2208. https://doi.org/10.3390/ma14092208
18. Porankiewicz, B.; Bermudez, E. J. C.; Tanaka, C., 2007: Cutting forces by peripheral cutting of low density wood species. BioResources, 2 (4): 671-681.
19. Porankiewicz, B.; Wieczorek, D.; Djurkovic, M.; Idzikowski, I.; Węgrzyn, Z., 2021: Modelling cutting forces using the moduli of elasticity in oak peripheral milling. BioResources, 16 (1): 1424-1437. https://doi.org/10.15376/biores.16.1.1424-1437
20. Radmanovic, K.; Dukic, I.; Merhar, M.; Safran, B.; Jug, M.; Lucic, R. B., 2018: Longitudinal and tangential coefficients of chip compression in orthogonal wood cutting. BioResources, 13 (4): 7998-8011. https://doi.org/10.15376/biores.13.4.7998-8011
21. Svoreň, J.; Naščák, L.; Barcík, Š.; Koleda, P.; Stehlík, Š., 2022: Influence of circular saw blade design on reducing energy consumption of a circular saw in the cutting process. Applied Sciences, 12 (3): 1276. https://doi.org/10.3390/app12031276
22. Wang, H.; Satake, U.; Enomoto, T., 2023: Serrated chip formation mechanism in orthogonal cutting of cortical bone at small depths of cut. Journal of Materials Processing Technology, 319. https://doi.org/10.1016/j.jmatprotec.2023.118097
23. Xu, W.; Wu, Z.; Lu, W.; Yu, Y.; Wang, J.; Zhu, Z.; Wang, X., 2022: Investigation on cutting power of wood-plastic

composite using response surface methodology. Forests, 13 (9): 1397. https://doi.org/10.3390/f13091397
24. Yang, C.; Liu, T.; Ma, Y.; Qu, W.; Ding, Y.; Zhang, T.; Song, W., 2023: Study of the movement of chips during pine wood milling. Forests, 14 (4): 849. https://doi.org/10.3390/f14040849
25. Zhu, Z.; Jin, D.; Wu, Z.; Xu, W.; Yu, Y.; Guo, X.; Wang, X., 2022: Assessment of surface roughness in milling of beech using a response surface methodology and an adaptive network-based fuzzy inference system. Machines, 10 (7): 567. https://doi.org/10.3390/machines10070567

# APPENDIX A
# DODATAK A

## Inclination of the cutting edge
## Nagib oštrice

The milling head had an inclination angle of 15°, which can have two effects. First, the inclination increases the effective rake angle and secondly, the time course of the forces is not the same as without inclination, as the cutting edge does not begin to cut all at once, but gradually.

The effect of the inclination on the effective rake angle is shown in Figure A1.

In the case of an inclination for an angle $\lambda$, for a blade with a nominal rake angle $\gamma_{eff}$, the following can be written

$$\tan\gamma_{eff} = \frac{AC}{AD} \tag{A1}$$

$$\tan\gamma_{nom} = \frac{AB}{AD} \rightarrow AD = \frac{AB}{\tan\gamma_{nom}} \tag{A2}$$

and also

$$\cos\lambda = \frac{AB}{AC} \rightarrow AC = \frac{AB}{\cos\lambda}. \tag{A3}$$

Combining AC and AD from Eqs. A2 and A3 and inserting into Eq. A1 gives the following expression for the effective rake angle

$$\tan\gamma_{eff} = \frac{\frac{AB}{\cos\lambda}}{\frac{AB}{\tan\gamma_{nom}}} = \frac{\tan\gamma_{nom}}{\cos\lambda} \tag{A4}$$

$$\gamma_{eff} = \operatorname{atan}\frac{\tan\gamma_{nom}}{\cos\lambda} \tag{A5}$$

If the nominal rake angle is 20° and the inclination angle is 15°, the effective rake angle is 20.6°, which practically corresponds to the nominal rake angle and, in our case, the influence of the inclination on the effective rake angle can be neglected.

Another factor that influences the inclination is the progression of the force over time, because the cutting edge does not start to cut all at once, but penetrates into the wood gradually. The effect of the inclination on the total cutting force can be analysed as follows.

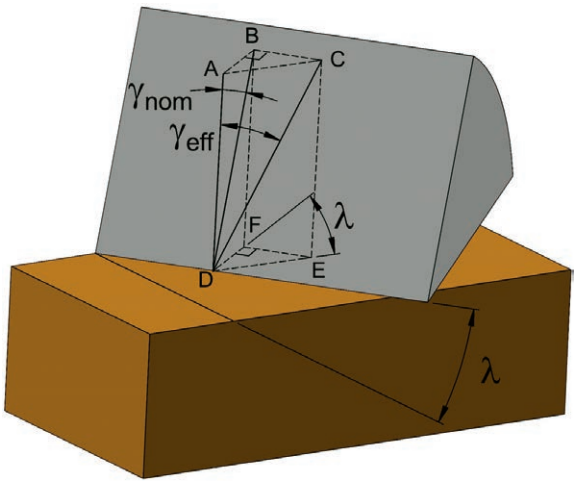


**Figure A1** Inclined cutting
**Slika A1.** Rezanje pod kutom

If the cutting edge is divided into infinitesimal lengths $\Delta b$, the average force for each $\Delta b$ to create a chip can be calculated as follows

$$\Delta F_m = k_s \cdot \Delta b \cdot h_m. \tag{A6}$$

For each $\Delta b$, the $\Delta F_{op}$ can then be calculated

$$\Delta F_{op} = \Delta F_m \cdot z_{ef} \tag{A7}$$

and further $\Delta M_c$ and $\Delta P_c$

$$\Delta M_c = \Delta F_{op} \cdot \frac{d}{2} \tag{A8}$$

$$\Delta P_c = \Delta M_c \cdot \omega \tag{A9}$$

Since $\Delta P_c$ for the individual $\Delta b$ can be added together, the total power is equal to

$$P_c = \sum\Delta P_c = \sum(\Delta M_c \cdot \omega) = \sum(\Delta F_{op} \cdot \frac{d}{2} \cdot \omega) = \sum(\Delta F_m \cdot z_{ef} \cdot \frac{d}{2} \cdot \omega)$$
$$= \sum\left(k_s \cdot \Delta b \cdot h_m \cdot z_{ef} \cdot \frac{d}{2} \cdot \omega\right) = k_s \cdot h_m \cdot z_{ef} \cdot \frac{d}{2} \cdot \omega \cdot \sum\Delta b \tag{A10}$$

Considering further

$$\sum\Delta b = b \tag{A11}$$

The final equation for calculating the cutting power of inclined cutting edge is

$$P_c = k_s \cdot h_m \cdot z_{ef} \cdot \frac{d}{2} \cdot \omega \cdot b \tag{A12}$$

which is the same as Eq. 12, meaning that the overall cutting force is unaffected by the inclination in terms of the temporal distribution of forces.

## APPENDIX B
## DODATAK B

### Segmented cutting edge
### Segmentirana oštrica

As the cutting edge is segmented, the resulting chip does not have a uniform cross-section across the entire width of the workpiece, as the wood between the two cutting edges remains in the running cut and is only removed by the next cutting edge. This means that the thickness of the chip varies across the width of the workpiece.

The milling head has a segmented cutting edge where the length of the insert is 15 mm and the distance between the inserts is 9 mm (Figure 2). If a crosscut is made through the workpiece at the point where the chip has an average thickness as shown in Figure B1, the cross-section can be seen in Figure B2.

The cross-section of a single cut is represented by the same colour and a number. If any position is taken and the next following cut is marked with the number 1, blue cross-section chips with the number 1 are made. Then comes the next cutting edge with the number 2, which produces red cross-section chips with the number 2. This is followed by 3, 4... As the cutting edge is segmented, the thickness of the chip varies. At the point where the cutting inserts overlap, each cutting edge cuts a chip with an average chip thickness of $h_{m1}$, and at the point where they do not overlap, every second cutting edge cuts a chip with an average thickness of $h_{m2}$. The force of a segmented cutting edge (Equation 1) can therefore be described as follows

$$F_m = k_s \cdot \frac{6}{24} b \cdot h_{m1} + k_s \cdot \frac{9}{24} b \cdot h_{m2} \qquad \text{(B1)}$$

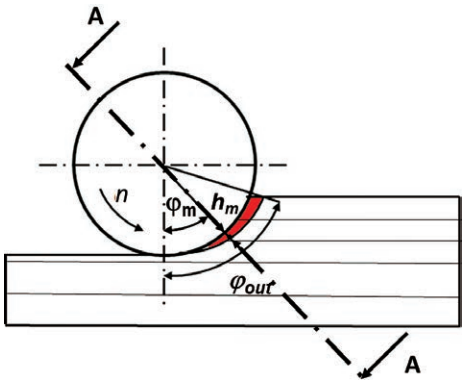


**Figure B1** Schematic of cutting principle
**Slika B1.** Shema načela rezanja

Considering Eqs. 2 and 3, the mean thickness of the chip $h_{m1}$ is

$$h_{m1} = \frac{v_f}{n \cdot z} \cdot \sqrt{\frac{a}{d}} \qquad \text{(B2)}$$

and $h_{m2}$

$$h_{m2} = \frac{v_f}{n \cdot \frac{z}{2}} \cdot \sqrt{\frac{a}{d}} = 2\frac{v_f}{n \cdot z} \cdot \sqrt{\frac{a}{d}} = 2 \cdot h_{m1} \qquad \text{(B3)}$$

Inserting Eq. B3 into B1, the following relationship can be written

$$F_m = k_s \cdot \frac{6}{24} b \cdot h_{m1} + k_s \cdot \frac{9}{24} b \cdot 2h_{m1}$$
$$= k_s \cdot \frac{6}{24} b \cdot h_{m1} + k_s \cdot \frac{18}{24} b \cdot h_{m1} = k_s \cdot b \cdot h_{m1} \qquad \text{(B4)}$$

Considering that $h_m = h_{m1}$, it follows that the mean force per cut with a segmented cutting edge is equal to the mean force per cut with a non-segmented cutting edge, which proves that a segmented cutting edge has no influence on the magnitude of the total cutting force.

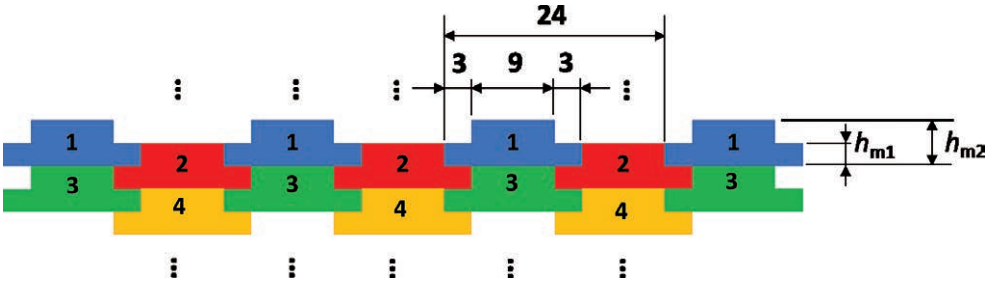


**Figure B2** Cross section A – A from Figure B1. The numbers show the order of cutting edges ($h_{m1}$ – mean thickness of the chip where the cutting inserts overlap, and each cutting edge cuts a chip; $h_{m2}$ – mean thickness of the chip where consecutive cutting edges do not overlap, and every second cutting edge cuts a chip)
**Slika B2.** Presjek A – A na slici B1. Brojevi pokazuju redoslijed reznih rubova ($h_{m1}$ – srednja debljina strugotine gdje se rezne pločice preklapaju i svaka oštrica reže strugotinu; $h_{m2}$ – srednja debljina strugotine gdje se uzastopne oštrice ne preklapaju i svaki drugi rezni brid reže strugotinu).

**Corresponding address:**

**ATIF HODŽIĆ**
University of Bihać, Faculty of Technical Engineering, dr Irfana Ljubijankića bb, 77000 Bihać, Bosnia and Herzegovina, E-mail: atif.hodzic@unbi.ba

Tuğba Yılmaz Aydın[1], Murat Aydın*[2]

# Non-Destructive Evaluation of Thermal Treatment Influence on Elastic Engineering Parameters of Poplar

# Ocjena utjecaja toplinske obrade na elastična svojstva drva topole nedestruktivnom metodom

**ORIGINAL SCIENTIFIC PAPER**
**Izvorni znanstveni rad**
Received – prispjelo: 23. 12. 2023.
Accepted – prihvaćeno: 2. 4. 2024.
UDK: 582.681.82; 674.04
https://doi.org/10.5552/drvind.2024.0180



**ABSTRACT** • *Twelve elastic constants (Young's modulus ($E_L$, $E_R$, and $E_T$), shear modulus ($G_{LR}$, $G_{LT}$, and $G_{RT}$) and Poisson's ratios ($v_{LR}$, $v_{LT}$, $v_{RT}$, $v_{TR}$, $v_{RL}$, and $v_{TL}$)) of Populus canadensis M. were determined by ultrasonic testing and evaluation, and the effect of thermal treatment on these constants was figured out. Samples were modified at 110, 160, and 210 °C for 3 and 6 h. The 2.25 MHz pressure and 1 MHz shear waves were propagated to calculate ultrasonic wave velocities, which were used to dynamically predict the constants. The control values for $E_L$, $E_R$, $E_T$, $G_{LR}$, $G_{LT}$, $G_{RT}$, $v_{LR}$, $v_{LT}$, $v_{RT}$, $v_{TR}$, $v_{RL}$, and $v_{TL}$ were 4361 MPa, 1438 MPa, 476 MPa, 771 MPa, 480 MPa, 107 MPa, 0.795, 0.296, 0.863, 0.335, 0.19, and 0.027, respectively. Yet, no data for full elastic constants were reported, and some remarkable differences were observed for moduli and Poisson ratios when compared to other poplar species. Elasticity and shear moduli reached their highest at 160 °C 3h and 110 °C 3h conditions, respectively. The common point of the treatment on moduli was that intense application caused the highest adverse effect, particularly for $E_T$ and $G_{RT}$. Contrary to moduli, apart from $v_{RT}$ and $v_{TR}$, the lowest values for Poisson's ratios were not obtained at the intense application. In general, none of the properties presented linear-like advancement or worsening by the increase in treatment conditions. Furthermore, not all the properties were significantly influenced by the treatment. Therefore, defining an optimum thermal treatment condition for improving the wood elastic constants is not easy when considering that the response to thermal treatment changes not only between the species but also within the species. Anyhow, preventing extended duration to elevated temperatures provides considerable advances.*

**KEYWORDS:** *poplar; thermal treatment; elastic constants; ultrasound; nondestructive test*

**SAŽETAK** • *Ultrazvučnim je ispitivanjem i ocjenjivanjem utvrđeno dvanaest konstanti elastičnosti: Youngov modul ($E_L$, $E_R$, i $E_T$), modul smicanja ($G_{LR}$, $G_{LT}$, i $G_{RT}$) i Poissonovi omjeri ($v_{LR}$, $v_{LT}$, $v_{RT}$, $v_{TR}$, $v_{RL}$ i $v_{TL}$) drva Populus canadensis M., a zatim je određen učinak toplinske obrade na te konstante. Uzorci su modificirani na 110, 160 i 210 °C tijekom tri i šest sati. Radi izračunavanja brzina ultrazvučnih valova koji su primijenjeni za dinamičko predviđanje konstanti, propagirani su tlačni valovi od 2,25 MHz i posmični valovi od 1 MHz. Kontrolne vrijednosti za $E_L$, $E_R$,*

* Corresponding author
[1] Author is researcher at Isparta University of Applied Sciences, Faculty of Forestry, Department of Forest Products Engineering, Isparta, Turkey. https://orcid.org/000-0002-3015-1868
[2] Isparta University of Applied Sciences, Keçiborlu Vocational School, Department of Machine, Isparta, Turkey. https://orcid.org/0000-0002-6792-9602

*$E_T$, $G_{LR}$, $G_{LT}$, $G_{RT}$, $v_{LR}$, $v_{LT}$, $v_{RT}$, $v_{TR}$, $v_{RL}$ i $v_{TL}$ bile su 4361 MPa, 1438 MPa, 476 MPa, 771 MPa, 480 MPa, 107 MPa, 0,795, 0,296, 0,863, 0,335, 0,19 i 0,027. Još nisu objavljeni potpuni podatci za elastične konstante, a uočene su i neke značajne razlike za module i Poissonove omjere u usporedbi s drvom drugih vrsta topole. Moduli elastičnosti i smicanja dosegnuli su najviše vrijednosti pri temperaturi modifikacije 160 °C u trajanju tri sata, odnosno pri 110 °C tijekom tri sata. Za sve je uzorke utvrđeno da intenzivna toplinska obrada ima najveći štetni učinak na module, posebice za $E_T$ i $G_{RT}$. Za razliku od modula, osim $v_{RT}$ i $v_{TR}$, najniže vrijednosti za Poissonove omjere nisu dobivene pri intenzivnoj toplinskoj obradi. Općenito, nijedno od svojstava nije pokazalo linearno povećanje ili smanjenje s pojačavanjem uvjeta toplinske obrade. Nadalje, toplinska obrada nije značajno utjecala na sva svojstva. Stoga definiranje optimalnih uvjeta toplinske obrade za poboljšanje elastičnih konstanti drva nije jednostavno ako se uzme u obzir da se reakcija na toplinsku obradu mijenja ne samo među različitim vrstama, već i unutar iste vrste drva. Zaključno se može reći da sprječavanje produljenog trajanja toplinske obrade pri povišenim temperaturama ima znatne prednosti.*

**KLJUČNE RIJEČI:** *drvo topole; toplinska obrada; elastične konstante; ultrazvuk; nedestruktivno ispitivanje*

## 1 INTRODUCTION
## 1. UVOD

External factor-related alterations should be known to ensure proper utilization of a biodegradable material (Kubovský *et al.,* 2020). Biomaterials such as wood do interact with environmental factors, which may cause significant changes in both physical and mechanical properties. As a result, due to the alterations that occurred in the structure, the life cycle of the material can be shortened. To prevent such adverse effects of environmental factors on the elements, lots of modification methods are in use. One of them is thermal treatment (TT), commonly used to advance some properties of wood. Shrinkage and swelling of the wood become stabilized by TT, and resistance to the degradation caused by biological attacks is increased. The fact remains that mechanical properties decrease, and so thermally treated wood is not suited for structural uses.

Studies generally reported the $E_L$ of *Populus deltoids* clones (Narasimhamurthy *et al.,* 2017), poplar (Aydın *et al.,* 2007), *Populus alba* and *Populus nigra* (Monteiro *et al.,* 2019), and *Populus euramericaha* cv. I-69/58 (Guo *et al.,* 2011). The effect of TT on $E_L$ of *Populus usbekistanica* was investigated by Sözbir *et al.* (2019). Orhan and Bal (2021) figured out the impact of TT on the mechanical features of *Populus subsps*. The influence of TT on the physical properties (Bytner *et al.,* 2022; Meija *et al.,* 2020; Taraborelli *et al.,* 2022; Villasante *et al.,* 2021, Yao *et al.,* 2023), modulus of elasticity (MOE) or modulus of rupture (MOR) (Bak and Nemeth, 2012; Bytner *et al.,* 2022; Goli *et al.,* 2015; Sözbir *et al.,* 2019; Todaro *et al.,* 2021), and tensile strength (Meija *et al.,* 2020) for solid wood obtained from different poplar species was evaluated. However, neither the twelve elastic constants nor the influence of TT on them were figured out for the *Populus x canadensis*. Advanced tool and method requirements are some of the obstacles that steer the researchers' focus on strength evaluation rather than orthotropic elastic behavior investigation. However, this study aimed to determine full elastic engineering parameters as a function of TT.

## 2 MATERIALS AND METHODS
## 2. MATERIJALI I METODE

Poplar (*Populus x canadensis* Moench.) was used in this study. Logs were obtained from the Atabey District of Isparta City of Türkiye and then sawn. Timbers were air dried and then defect-free samples were prepared. Thermal treatment was done using FN 500 (Nüve Co., Ankara, Türkiye) laboratory type oven operating in ambient air. Before separately placing each sample group, the oven was heated to experimental temperature levels (110, 160, and 210 °C) and samples were treated for exactly 3 and 6 h. Considering the oven drying temperature (103±2) °C, 110 °C was defined as the starting point of the treatment with 50 °C increments, which were within the range of the reported treatment temperatures. The temperature of approximately 220 °C is required for 2-4 h for a successful treatment, and the duration of heating up and cooling down changes according to wood dimension (Rapp and Sailer, 2001). Not only heating up but also cooling regimes cause additional treatment of wood particularly at high temperatures (Johansson, 2008). Furthermore, cooling down from higher temperatures extends this additional treatment. To evaluate the effects of exact exposure duration on elastic constants, pre-heating and equipment assisted cooling with remoistening was not performed as in industrial practice. Heat transfer and equilibration following the treatment took place in ambient air. The control samples were unmodified. Particularly for the samples treated at intense configurations, surfaces were controlled against the defects such as cracks, etc., and defected samples were not tested. Furthermore, samples presented with abnormal velocities were neglected due to assumption of inner faults.


**Figure 1** Samples and color changes regarding thermal treatment
**Slika 1.** Uzorci i promjene boje nakon toplinske obrade

**Table 1** Equations for determining matrix elements (Gonçalves *et al.,* 2014; Ozyhar *et al.,* 2013)
**Tablica 1.** Jednadžbe za određivanje elemenata matrice (Gonçalves *et al*., 2014.; Ozyhar *et al*., 2013.)

| **Propagation – Polarization** *Propagacija – polarizacija* | **Type of wave** *Vrsta vala* | | **Equation for diagonal and off-diagonal terms** *Jednadžba za dijagonalne i nedijagonalne članove* |
|---|---|---|---|
| Axis (L, R, and T) | $V_{LL}$ | Longitudinal *uzdužni* | $C_{11} = C_{LL} = \rho V_{LL}^2$ |
| | $V_{RR}$ | | $C_{22} = C_{RR} = \rho V_{RR}^2$ |
| | $V_{TT}$ | | $C_{33} = C_{TT} = \rho V_{TT}^2$ |
| | $V_{TR/RT}$ | Shear (Transverse) *posmični (poprečni)* | $C_{44} = C_{RT} = (\rho V_{RT}^2 + \rho V_{TR}^2)/2$ |
| | $V_{LT/TL}$ | | $C_{55} = C_{LT} = (\rho V_{LT}^2 + \rho V_{TL}^2)/2$ |
| | $V_{LR/RL}$ | | $C_{66} = C_{RL} = (\rho V_{RL}^2 + \rho V_{LR}^2)/2$ |
| Off-axis (RT45°) | $V_{RT/RT}$ | Quasi-shear (Transverse) *kvaziposmični (poprečni)* | $(C_{23} + C_{44}) n_2 n_3 = \pm\sqrt{[(C_{22} n_2^2 + C_{44} n_3^2 - \rho V_\infty^2)(C_{44} n_2^2 + C_{33} n_3^2 - \rho V_\infty^2)]}$ |
| Off-axis (LT45°) | $V_{LT/LT}$ | | $(C_{13} + C_{55}) n_1 n_3 = \pm\sqrt{[(C_{11} n_1^2 + C_{55} n_3^2 - \rho V_\infty^2)(C_{55} n_1^2 + C_{33} n_3^2 - \rho V_\infty^2)]}$ |
| Off-axis (LR45°) | $V_{LR/LR}$ | | $(C_{12} + C_{66}) n_1 n_2 = \pm\sqrt{[(C_{11} n_1^2 + C_{66} n_2^2 - \rho V_\infty^2)(C_{66} n_1^2 + C_{22} n_2^2 - \rho V_\infty^2)]}$ |

Where $\rho$ (kg/m) is density, $V_{lI}$ is longitudinal UWV (m/s), $V_{lJ}$ or $V_{Jl}$ is transverse UWV (m/s), and $V\alpha$ is quasi-transverse UWV (m/s) (Vázquez *et al.,* 2015), $n_1 = \cos\alpha$; $n_2 = \sin\alpha$, and $n_3 = 0$ for $C_{23}$, $n_1 = \cos\alpha$; $n_3 = \sin\alpha$, and $n_2 = 0$ for $C_{13}$, and $n^2 = \cos\alpha$; $n_3 = \sin\alpha$, and $n_1 = 0$ for $C_{12}$ (Gonçalves *et al.,* 2014).

Following the TT and cooling down, 20 mm × 20 mm × 20mm (through L, R, and T directions, and LR45°, LT45°, and RT45° off-axis planes) samples (Figure 1) were conditioned at 20±1°C and 65 % relative humidity using a laboratory-type chamber (Memmert Gmbh+Co. KG, Schwabach, Germany). To avoid the influence of ambient air, samples were stored in a desiccator for density determination and ultrasonic measurements. The density of the samples was determined according to TS ISO 13061-2 (2021) standard.

The ultrasonic wave velocity (UWV), required for elastic constant prediction, were calculated by ob-

tained wave propagation times in µs. Two different wave types, longitudinal or pressure (2.25 MHz) and transverse or shear (1MHz), were propagated through the essential directions (L, R, and T) and planes (LR, LT, and RT, and 45° off-axis-planes), respectively. The EPOCH 650 (Olympus NDT, USA) ultrasonic flaw detector, contact type piezoelectric transducers (Panametrics A133S-RM and V153-RM for pressure and shear waves, respectively), and ultrasonic couplants were used for propagation. For longitudinal waves, only propagation directions (L, R, and T) were used without polarization. However, for transverse waves, polarization with the propagation directions was used, which provided transmission through LR, LT, RT, RL, TL, and TR planes including 45° off-axis. The calculated UWVs were used to determine the stiffness matrix [*C*] (Eq. 1) elements using the equations presented in Table 1. Then compliance matrix [*S*] (Eq. 2) was calculated by inversing [*C*].

$$[C] = \begin{bmatrix} C_{11} & C_{12} & C_{13} & 0 & 0 & 0 \\ C_{21} & C_{22} & C_{23} & 0 & 0 & 0 \\ C_{31} & C_{32} & C_{33} & 0 & 0 & 0 \\ 0 & 0 & 0 & C_{44} & 0 & 0 \\ 0 & 0 & 0 & 0 & C_{55} & 0 \\ 0 & 0 & 0 & 0 & 0 & C_{66} \end{bmatrix} \quad (1)$$

Where $C_{ii}$ are the diagonal and $C_{ij}$ and $C_{ji}$ are the off-diagonal terms.

$$[S] = \begin{bmatrix} \frac{1}{E_L} & -\frac{\upsilon_{21}}{E_R} & -\frac{\upsilon_{31}}{E_T} & 0 & 0 & 0 \\ -\frac{\upsilon_{12}}{E_L} & \frac{1}{E_R} & -\frac{\upsilon_{32}}{E_T} & 0 & 0 & 0 \\ -\frac{\upsilon_{13}}{E_L} & -\frac{\upsilon_{23}}{E_R} & \frac{1}{E_T} & 0 & 0 & 0 \\ 0 & 0 & 0 & \frac{1}{G_{RT}} & 0 & 0 \\ 0 & 0 & 0 & 0 & \frac{1}{G_{LT}} & 0 \\ 0 & 0 & 0 & 0 & 0 & \frac{1}{G_{LR}} \end{bmatrix} \quad (2)$$

Where $E$ is Young's modulus, $G$ is the shear modulus, and $\boldsymbol{\upsilon}$ is Poisson's ratio.

## 3 RESULTS AND DISCUSSION
## 3. REZULTATI I RASPRAVA

The averages for the density are given in Table 2. Reported values for unmodified *Populus x canadensis* solid wood are 334-374 kg/m³ (Casado *et al.,* 2010), 395 kg/m³ (Papandrea *et al.,* 2022), 405.6 kg/m³ (Hodoušek *et al.,* 2016), 464 kg/m³ (Villasante *et al.,* 2021), and 372-468 kg/m³ (YingJie *et al.,* 2017), and averages of this study are comparable. As seen in the table, around 8.9 % decrease was observed for intensive treatment. Taraborelli *et al.* (2022) reported 2.5 % and 10 % decreases for *P.* × *canadensis* 'I-214' heat-treated at 160 °C for 3h and 200 °C for 45 min, respectively. However, in this study, a 0.7 % increase was observed for the same treatment level, while the adverse effect of intensive treatment is comparable. The means of the intensive treatment groups presented statistically significant differences from others.

The averages for the UWVs are presented in Table 3. No study reported all the UWVs required for full elastic characterization of *Populus x canadensis* solid wood. However, Aydın and Aydın (2023) noted 2, 4 and 6 annual rings related $V_{RR}$ (1607, 1782, and 1850 m/s), $V_{LR}$ (1463, 1494, and 1501 m/s), $V_{RL}$ (1491, 1567, and 1588 m/s), $V_{RT}$ (532, 536, and 565 m/s), and $V_{TR}$ (504, 512, and 522 m/s), respectively. The differences between the averages of the (Aydın and Aydın, 2023) and control values of this study are around 18 %, 1.1 %, -2.2 %, 3.5 %, and 9.2 %, respectively. Such diffractions are normal for wood material even for the same species. Zahedi *et al.* (2022) reported 3360 m/s ($V_{LL}$), 1850 m/s ($V_{RR}$), 1380 m/s ($V_{TT}$), 1370 m/s ($V_{LR}$), 1250 m/s ($V_{RL}$), 1140 m/s ($V_{LT}$), 1350 m/s ($V_{TL}$), 670 m/s ($V_{RT}$), 650 m/s ($V_{TR}$), 1510 m/s ($V_{LR\ 45°}$), 1210 m/s ($V_{LT\ 45°}$), and 740 m/s ($V_{RT\ 45°}$) for 390 kg/m³ *populus deltoides*. When compared, UWVs are generally comparable but Ettelaei *et al.* (2019) reported 5433-5887 m/s for $V_{LL}$ of *Populus Euroamericana* and around 35.2 % to 40.2 % diffractions between the lowest velocity and lower and upper bounds. Furthermore, 3877 to 4761 m/s $V_{LL}$ for the I-214 clone obtained by stress wave speed was reported (Casado *et al.,* 2010; Papandrea *et al.,* 2022). Contrary to (Ettelaei *et al.,* 2019), the lower bound (8.1 %) of stress wave velocity is comparable to this study.

In general, the UWVs oscillated instead of linearly increasing or decreasing with the treatment progress. The same fluctuations were reported for some UWVs of heat-treated Taurus cedar (Yılmaz Aydın, 2021), oak (Aydın, 2020; Yılmaz Aydın and Aydın, 2020), red pine (Aydın, 2022), and beech (Yılmaz Aydın and Aydın, 2018a). Furthermore, treatment levels caused different influences as seen in Table 3. Therefore, it is not possible to define a certain treatment level for optimum advancement through all the UWVs. However, except for quasi-shear wave velocities, the highest adverse effect was obviously observed for the prolonged duration at 210 °C. Furthermore, according to ANOVA results presented in Table 3, the influence of treatment is significant ($P$<0.05) for $V_{TT}$, $V_{LR}$, $V_{RL}$, $V_{LT}$, $V_{RT}$, and $V_{TR}$. Particularly the means of the intensively treated groups presented statistically significant diffractions.

The averages for moduli are presented in Table 4. Full elastic constants for unmodified *Populus x*

**Table 2** Statistics for density
**Tablica 2.** Statističke vrijednosti za gustoću

| Property | Groups | *N* | Mean, %** [CoV]*** | Std. Error | 95 % CI for mean (Bounds) | | Min. | Max. |
|---|---|---|---|---|---|---|---|---|
| | | | | | Lower | Upper | | |
| Density, kg/m³<br><br>s. (F 6.119, P 0.000) | Control | 10 | 339 a* [3,9] | 4.225 | 329.27 | 348.38 | 316 | 353 |
| | 110 °C 3 h | 10 | 346 a (2.3) [8,6] | 9.434 | 325.13 | 367.81 | 301 | 403 |
| | 110 °C 6 h | 10 | 335 a (-1.2) [3.2] | 3.387 | 327.24 | 342.56 | 321 | 351 |
| | 160 °C 3 h | 10 | 341 a (0.7) [4.6] | 5.001 | 329.88 | 352.50 | 324 | 375 |
| | 160 °C 6 h | 10 | 333 a (-1.7) [4.7] | 4.976 | 321.92 | 344.43 | 307 | 355 |
| | 210 °C 3 h | 10 | 310 b (-8.5) [5.4] | 5.248 | 298.14 | 321.89 | 288 | 330 |
| | 210 °C 6 h | 10 | 309 b (-8.9) [8.2] | 8.032 | 290.43 | 326.77 | 270 | 364 |

s – significant, *Duncan's homogeneity groups, ** % diffraction from the average of the control group, *** coefficient of variation
*s – značajan, *Duncanove grupe homogenosti, ** postotak difrakcije od prosječne vrijednosti kontrolne skupine, *** koeficijent varijacije*

**Table 3** Statistics for ultrasonic wave velocities
**Tablica 3.** Statističke vrijednosti za brzine ultrazvučnih valova

| Groups | Property | Mean, %** [CoV]*** | Property | Mean, % [CoV] | Property | Mean, % [CoV] |
|---|---|---|---|---|---|---|
| Control | $V_{LL}$, m/s n.s. (F 0.851, P 0.536) | 3585 a* [3.2] | $V_{RR}$, m/s n.s. (F 1.211, P 0.313) | 2060 a [3] | $V_{TT}$, m/s s. (F 5.945, P 0.000) | 1184 a [5.7] |
| 110 °C 3 h | | 3565 a (-0.6) [5.1] | | 2062 a (0.1) [9] | | 1182 a (-0.2) [4.1] |
| 110 °C 6 h | | 3564 a (-0.6) [3.0] | | 2110 a (2.4) [2.9] | | 1180 a (-0.4) [6.5] |
| 160 °C 3 h | | 3628 a (1.2) [3.3] | | 2103 a (2.1) [2.3] | | 1203 a (1.6) [7.4] |
| 160 °C 6 h | | 3632 a (1.3) [3.8] | | 2102 a (2.1) [2.7] | | 1191 a (0.6) [9.1] |
| 210 °C 3 h | | 3605 a (0.6) [3.4] | | 2059 a (0) [2.8] | | 1149 a (-3) [2.2] |
| 210 °C 6 h | | 3522 a (-1.8) [4.3] | | 2026 a (-1.6) [3.4] | | 1034 b (-12.6) [7.6] |
| Control | $V_{LR}$, m/s s. (F 2.428, P 0.036) | 1502 bc [2] | $V_{LT}$, m/s s. (F 4.636, P 0.001) | 1210 a [1.3] | $V_{RT}$, m/s s. (F 5.107, P 0.000) | 563 a [3.8] |
| 110 °C 3 h | | 1536 ab (2.3) [3.8] | | 1223 a (1.1) [1.8] | | 583 a (3.6) [6.9] |
| 110 °C 6 h | | 1554 a (3.5) [3.7] | | 1240 a (2.5) [2.7] | | 579 a (2.9) [4] |
| 160 °C 3 h | | 1531 abc (1.9) [3.9] | | 1234 a (2) [3] | | 585 a (3.9) [4.8] |
| 160 °C 6 h | | 1545 ab (2.8) [2.5] | | 1244 a (2.8) [2.5] | | 583 a (3.6) [4.7] |
| 210 °C 3 h | | 1524 abc (1.4) [3.3] | | 1221 a (0.9) [4.7] | | 561 a (-0.5) [5.7] |
| 210 °C 6 h | | 1485 c (-1.1) [2.8] | | 1174 b(-3) [2.8] | | 528 b (-6.2) [4.9] |
| Control | $V_{RL}$, m/s s. (F 2.969, P 0.013) | 1515 bc [1.5] | $V_{TL}$, m/s n.s. (F 1.600, P 0.162) | 1172 ab [3.1] | $V_{TR}$, m/s s. (F 2.749, P 0.019) | 560 a [5.3] |
| 110 °C 3 h | | 1530 abc (1) [4.6] | | 1197 ab (2.2) [5.5] | | 572 a (2.1) [8.8] |
| 110 °C 6 h | | 1555 ab (2.7) [2.6] | | 1188 ab (1.4) [3.9] | | 573 a (2.4) [7.9] |
| 160 °C 3 h | | 1545 ab (2) [3.3] | | 1191 ab (1.6) [6.1] | | 585 a (4.5) [5.8] |
| 160 °C 6 h | | 1562 a (3.1) [2.1] | | 1222 a (4.3) [4.7] | | 565 a (0.9) [7.9] |
| 210 °C 3 h | | 1555 ab (2.7) [2.5] | | 1164 b (-0.6) [3.4] | | 548 ab (-2.2) [9.2] |
| 210 °C 6 h | | 1496 c (-1.3) [3.1] | | 1157 b (-1.3) [5.2] | | 512 b (-8.6) [11.7] |
| Control | $V_{LR45°}$, m/s n.s. (F 1.986, P 0.081) | 1290 ab [5.3] | $V_{LT45°}$, m/s n.s. (F 1.760, P 0.122) | 1012 a [5.1] | $V_{RT45°}$, m/s n.s. (F 0.6989 P 0.659) | 639 a [5.9] |
| 110 °C 3 h | | 1245 ab (-3.5) [6.5] | | 1008 a (-0.4) [5.6] | | 633 a (-1) [4.0] |
| 110 °C 6 h | | 1232 b (-4.5) [5.9] | | 985 ab (-2.6) [5.1] | | 638 a (-0.2) [4.4] |
| 160 °C 3 h | | 1303 a (1.0) [1.4] | | 1006 a (-0.6) [3.2] | | 628 a (-1.8) [3.9] |
| 160 °C 6 h | | 1298 a (0.6) [5.1] | | 1006 a (-0.6) [4.1] | | 653 a (2.1) [5.9] |
| 210 °C 3 h | | 1286 ab (-0.4) [3.5] | | 1004 a (-0.8) [2.4] | | 645 a (0.9) [3.9] |
| 210 °C 6 h | | 1271 ab (-1.5) [4.1] | | 961 b (-5) [3.6] | | 633 a (-1) [6.3] |

n.s. – not significant, s – significant, *Duncan's homogeneity groups, ** % diffraction from the average of the control group, and *** coefficient of variation
*n.s. – nije značajno, s – značajno, *Duncanove grupe homogenosti, ** postotak difrakcije od prosječne vrijednosti kontrolne skupine, *** koeficijent varijacije*

*canadensis* solid wood are not available. However, Aydın and Aydın (2023) evaluated the influence of growth ring on $E_R$, $G_{LR}$, and $G_{RT}$ of *Populus x canadensis* (345-354 kg/m³ density) and reported 899-1211 MPa, 772-876 MPa, and 93-111 MPa, respectively. When compared, shear moduli are in harmony with the reported values. However, the control value for $E_R$ is around 18.8 % higher than the reported upper bound. Except for density, differences between the calculation methods of the studies may cause such diffractions as described in the materials and method headings. Due to a lack of full elastic properties for unmodified or thermally treated *Populus x canadensis* in the literature, results were compared to poplar subspecies. For exam-

**Table 4** Statistics for moduli
**Tablica 4.** Statističke vrijednosti za module

| Groups | Property | Mean, %** [CoV] *** | Property | Mean, %* [CoV] | Property | Mean, %* [CoV] |
|---|---|---|---|---|---|---|
| Control | $E_L$, MPa s. (F 3.258, P 0.007) | 4361 ab* [8.3] | $E_R$, MP Žs. (F 3.651, P 0.004) | 1438 ab [6.4] | $E_T$, MP s. (F 11.172, P 0.000) | 476 a [10.8] |
| 110 °C 3 h | | 4398 ab (0.9) [9.7] | | 1493 a (3.9) [21.6] | | 483 a (1.4) [7.5] |
| 110 °C 6 h | | 4256 ab (-2.4) [6.1] | | 1493 a (3.9) [8.4] | | 467 a (-1.8) [12.7] |
| 160 °C 3 h | | 4504 a (3.3) [10.2] | | 1508 a (4.9) [5.3] | | 495 a (4) [14] |
| 160 °C 6 h | | 4404 ab (1) [9.5] | | 1473 a (2.5) [7.2] | | 474 a (-0.4) [15.8] |
| 210 °C 3 h | | 4037 bc (-7.4) [9.9] | | 1313 bc (-8.6) [6.2] | | 409 b (-14) [6] |
| 210 °C 6 h | | 3841 c (-11.9) [13.3] | | 1270 c (-11.7) [12.1] | | 331 c (-30.4) [16] |
| Control | $G_{LR}$, MPa s. (F 6.176, P 0.000) | 771 ab [4.1] | $G_{LT}$, MP s. (F 11.946, P 0.000) | 480 a [3.6] | $G_{RT}$, MP s. (F 5.447, P 0.000) | 107 ab [10] |
| 110 °C 3 h | | 817 a (5.9) [13] | | 507 a (5.5) [8.4] | | 116 a (8.6) [18.2] |
| 110 °C 6 h | | 811 a (5.2) [8.4] | | 494 a (2.8) [5.9] | | 112 a (4.4) [13.5] |
| 160 °C 3 h | | 807 a (4.6) [5.4] | | 501 a (4.4) [5.8] | | 117 a (9.5) [11.9] |
| 160 °C 6 h | | 804 a (4.2) [4.7] | | 506 a (5.4) [5.1] | | 110 ab (2.9) [13.6] |
| 210 °C 3 h | | 734 ab (-4.8) [5.1] | | 441 b (-8.2) [7.3] | | 96 bc (-10.4) [17.1] |
| 210 °C 6 h | | 687 b (-11) [10.7] | | 419 b (-12.7) [9.5] | | 85 c (-21.1) [21.8] |

n.s. – not significant, s – significant, *Duncan's homogeneity groups, ** % diffraction from the average of the control group, and *** coefficient of variation
*n.s. – nije značajno, s – značajno, *Duncanove grupe homogenosti, ** postotak difrakcije od prosječne vrijednosti kontrolne skupine, *** koeficijent varijacije*

ple, Zahedi *et al.* (2022) determined $E_L$, $E_R$, $E_T$, $G_{LR}$, $G_{LT}$, and $G_{RT}$ of *Populus deltoides* by ultrasonic tests as follows: 4.52, 1.37, 0.74, 0.69, 0.62, and 0.17 GPa, respectively. When compared to the results of this study, differences between the moduli are -3.5 %, 5.0 %, -35.7 %, 11.7 %, -22.6 %, and -37.1 %, respectively. Considering the internal or external factors affecting wood properties, such differences are comparable.

The influence of treatment on both elasticity and shear moduli was significant ($P$<0.05). However, as can be seen in Table 4, a linear-like influence either positive or negative was not observed for moduli. Indeed, the fluctuation was the fact. As illustrated in Appendix 1, the treatment at 160 °C for 3 h provided the highest advancements in all elasticity modulus values. The positive impact of relatively low-level TT on $E_L$ of wood was reported by (Aydın, 2020; Güntekin *et al.,* 2017; Yılmaz Aydın, 2021; Yılmaz Aydın and Aydın, 2018a; Yılmaz Aydın and Aydın, 2020). The negative effect of TT even at a low-temperature level (110 °C) on some $E$ and $G$ of red pine was also reported (Aydın, 2022).

Considering the shear moduli, a common treatment condition for the highest advancement was not achieved because $G_{LR}$ and $G_{LT}$ reached their maximum value at 110 °C 3h, while $G_{RT}$ presented the highest values at 160 °C 3h treatment levels, contradicting the adverse effect of moderate treatment (Aydın, 2022).

Yue *et al.*, (2023) reported that modification at 160-170 °C caused insignificant discrepancies in the mechanical properties of Chinese poplar, while 180 °C and further levels caused differences. As seen in Table 4, elastic and shear moduli reached their highest values at different moderate temperature levels but the common point between them is that the intense treatment conditions caused the highest adverse effect. Therefore, extended exposure duration at high temperatures following 160 °C should be avoided so as not to weaken the moduli of wood.

The averages for Poisson ratios are presented in Table 5. In the literature, there is limited data for the Poisson ratio for poplar species. Furthermore, neither untreated nor heat-treated Poisson ratios of *Populus canadensis* were reported. The reported $\nu_{LR}$, $\nu_{LT}$, $\nu_{RT}$, $\nu_{TR}$, $\nu_{RL}$, and $\nu_{TL}$ ranges for hardwood species are 0.297-0.495, 0.374-0.651, 0.560-0.912, 0.213-0.496, 0.018-0.086, and 0.009-0.051, respectively (Kretschmann, 2010), and $\nu_{RL}$ and $\nu_{TL}$ are much smaller than other ratios. However, as can be seen in Table 5, this is only valid for $\nu_{TL}$. Furthermore, there are remarkable numerical differences between the reported LR and RL ratios and the results of this study. Moreover, Aydın (2022) reported -45 % to 109 % differences between the Poisson's ratios of heat-treated red pine. However, it should be taken into consideration that Poisson's ratios vary within and between species (Kretschmann, 2010) and there is no information about Poisson's ratio in the standards (Obara, 2018). Therefore, such numerically huge discrepancies in the literature are meaningful.

As for moduli, a stable behavior of ratios against the treatment progress was not observed as (Aydın, 2022) reported for red pine. Furthermore, among the properties, the highest adverse effect of the treatment was observed for ratios. In the literature, it was reported that Poisson's ratios are less sensitive (Yılmaz Aydın *et al.,* 2016) and insensitive (Luis Gómez-Royuela *et al.,* 2021) to TT. Furthermore, Al-musawi *et al*. (2023)

**Table 5** Statistics for Poisson's ratios
**Tablica 5.** Statističke vrijednosti za Poissonove omjere

| Groups | Property | Mean, %** [CoV]*** | Property | Mean, %* [CoV] | Property | Mean, %* [CoV] |
|---|---|---|---|---|---|---|
| Control | $\nu_{LR}$ n.s. (F 1.514, P 0.188) | 0.795 ab [13.7] | $\nu_{LT}$ n.s. (F 0.884, P 0.512) | 0.296 a [55.8] | $\nu_{RT}$ n.s. (F 1.451, P 0.210) | 0.863 ab [9.1] |
| 110 °C 3 h | | 0.864 a (8.7) [17.3] | | 0.347 a (17.2) [50.6] | | 0.845 ab (-2.1) [14.5] |
| 110 °C 6 h | | 0.843 ab (6.1) [14] | | 0.405 a (36.8) [68.8] | | 0.815 ab (-5.5) [13] |
| 160 °C 3 h | | 0.749 ab (-5.8) [17.2] | | 0.431 a (45.5) [57] | | 0.905 a (4.9) [8.3] |
| 160 °C 6 h | | 0.733 b (-7.8) [14.6] | | 0.499 a (68.6) [51] | | 0.821 ab (-4.8) [13.2] |
| 210 °C 3 h | | 0.818 ab (2.9) [14.7] | | 0.312 a (5.5) [65] | | 0.83 ab (-3.7) [10.8] |
| 210 °C 6 h | | 0.773 ab (-2.8) [16.8] | | 0.423 a (42.8) [78.9] | | 0.754 b (-12.6) [28.5] |
| Control | $\nu_{RL}$ n.s. (F 1.537, P 0.181) | 0.19 ab [21.6] | $\nu_{TL}$ n.s. (F 0.690, P 0.659) | 0.027 a [57.4] | $\nu_{TR}$ s. (F 3.625, P 0.004) | 0.335 a [13.2] |
| 110 °C 3 h | | 0.211 ab (11.2) [25.4] | | 0.034 a (24.7) [48.3] | | 0.338 a (1.1) [15.6] |
| 110 °C 6 h | | 0.225 a (18.5) [18.5] | | 0.042 a (54.2) [75.4] | | 0.310 a (-7.4) [20] |
| 160 °C 3 h | | 0.178 b (-6.7) [18.1] | | 0.038 a (40.8) [61.6] | | 0.337 a (0.7) [16.5] |
| 160 °C 6 h | | 0.192 ab (0.9) [24.4] | | 0.048 a (74.1) [55] | | 0.301 a (-10.2) [18.5] |
| 210 °C 3 h | | 0.202 ab (6.1) [17.6] | | 0.028 a (3.7) [65.1] | | 0.307 a (-8.4) [6.8] |
| 210 °C 6 h | | 0.214 ab (12.4) [17.5] | | 0.053 a (93.3) [148.7] | | 0.245 b (-26.7) [30.1] |

n.s. – not significant, s – significant, *Duncan's homogeneity groups, ** % diffraction from the average of the control group, and *** coefficient of variation
*n.s. – nije značajno, s – značajno, *Duncanove grupe homogenosti, ** postotak difrakcije od prosječne vrijednosti kontrolne skupine, *** koeficijent varijacije*

**Table 6** Linear regression $R^2$ values corresponding to Figure 1
**Tablica 6.** Vrijednosti $R^2$ linearne regresije koje odgovaraju uzorcima prikazanima na slici 1.

| | Density | $V_{LL}$ | $V_{RR}$ | $V_{TT}$ | $E_L$ | $E_R$ | $E_T$ | $G_{LR}$ | $G_{LT}$ | $G_{RT}$ | $V_{LR}$ | $V_{LT}$ | $V_{RT}$ | $V_{LR45}$ | $V_{LT45}$ | $V_{RT45}$ | $\nu_{RL}$ | $\nu_{TL}$ | $\nu_{LR}$ | $\nu_{TR}$ | $\nu_{LT}$ | $\nu_{RT}$ |
|---|---|---|---|---|---|---|---|---|---|---|---|---|---|---|---|---|---|---|---|---|---|---|
| **Density** | - | .010 | .079 | .011 | .498 | .593 | .224 | .575 | .477 | .626 | .002 | .004 | .332 | .001 | .017 | .002 | .019 | .058 | .041 | .028 | .074 | .045 |
| $V_{LL}$ | | - | .081 | .103 | .598 | .026 | .106 | .045 | .032 | .004 | .165 | .023 | .005 | .374 | .492 | .118 | .240 | .041 | .008 | .054 | .012 | .001 |
| $V_{RR}$ | | | - | .005 | .001 | .679 | .027 | .279 | .024 | .048 | .247 | .004 | .026 | .011 | .113 | .010 | .190 | .017 | .000 | .008 | .008 | .167 |
| $V_{TT}$ | | | | - | .085 | .010 | .849 | .059 | .205 | .054 | .079 | .269 | .088 | .018 | .295 | .004 | .280 | .001 | .028 | .616 | .007 | .134 |
| $E_L$ | | | | | - | .136 | .283 | .101 | .311 | .302 | .078 | .004 | .172 | .207 | .337 | .076 | .071 | .085 | .034 | .072 | .061 | .012 |
| $E_R$ | | | | | | - | .144 | .661 | .265 | .378 | .146 | .004 | .202 | .008 | .028 | .002 | .149 | .047 | .012 | .001 | .043 | .147 |
| $E_T$ | | | | | | | - | .251 | .445 | .251 | .066 | .192 | .223 | .019 | .281 | .001 | .182 | .009 | .008 | .556 | .000 | .149 |
| $G_{LR}$ | | | | | | | | - | .551 | .484 | .466 | .066 | .323 | .019 | .001 | .015 | .046 | .039 | .005 | .046 | .022 | .124 |
| $G_{LT}$ | | | | | | | | | - | .502 | .143 | .462 | .396 | .000 | .092 | .000 | .012 | .014 | .001 | .122 | .000 | .040 |
| $G_{RT}$ | | | | | | | | | | - | .036 | .029 | .902 | .001 | .026 | .000 | .001 | .049 | .024 | .079 | .041 | .076 |
| $V_{LR}$ | | | | | | | | | | | - | .229 | .059 | .047 | .026 | .061 | .025 | .004 | .010 | .028 | .003 | .108 |
| $V_{LT}$ | | | | | | | | | | | | - | .079 | .002 | .082 | .005 | .081 | .004 | .020 | .099 | .077 | .005 |
| $V_{RT}$ | | | | | | | | | | | | | - | .001 | .034 | .001 | .001 | .036 | .013 | .105 | .022 | .076 |
| $V_{LR45}$ | | | | | | | | | | | | | | - | .337 | .079 | .451 | .022 | .167 | .009 | .004 | .042 |
| $V_{LT45}$ | | | | | | | | | | | | | | | - | .091 | .280 | .103 | .023 | .335 | .147 | .009 |
| $V_{RT45}$ | | | | | | | | | | | | | | | | - | .008 | .091 | .011 | .214 | .010 | .506 |
| $\nu_{RL}$ | | | | | | | | | | | | | | | | | - | .017 | .338 | .244 | .082 | .074 |
| $\nu_{TL}$ | | | | | | | | | | | | | | | | | | - | .382 | .144 | .712 | .301 |
| $\nu_{LR}$ | | | | | | | | | | | | | | | | | | | - | .028 | .516 | .001 |
| $\nu_{TR}$ | | | | | | | | | | | | | | | | | | | | - | .097 | .426 |
| $\nu_{LT}$ | | | | | | | | | | | | | | | | | | | | | - | .098 |
| $\nu_{RT}$ | | | | | | | | | | | | | | | | | | | | | | - |

noted no obvious correlation between Poisson's ratios and intensity of the TT determined by ultrasonic tests. As can be seen in Table 5, except for $\nu_{TR}$, the influence of TT on Poisson's ratios is not significant ($P$<0.05). Contrary to moduli and except for $\nu_{RT}$ and $\nu_{TR}$, the lowest values were not observed at intensive treatment conditions. Furthermore, Yang *et al.* (2021) stated that Poisson's ratios of the bamboo slivers increased after the TT due to a decrease in the ductility in the loading direction and an increase in the transverse shrinkage. In this study, such an increase regarding the treatment was only observed for $\nu_{TL}$ but not linearly with the increase in treatment conditions. Moreover, $\nu_{TL}$ presented the highest value among the ratios at 210 °C applied for 6h. In the literature, small differences in the ratios between the unmodified and heat-treated samples were reported (Luis Gómez-Royuela *et al.,* 2021; Wetzig *et al.,* 2011). However, as seen in Table 5, the numerical differences between the control and modified means (-26.7 % to 93.3 %) are remarkably wide. Furthermore, variations in the ratios are high, particularly for $\nu_{LT}$ and $\nu_{TL}$ but this is not unusual as Luis Gómez-Royuela *et al.* (2021) state that it is a fact for wood material.

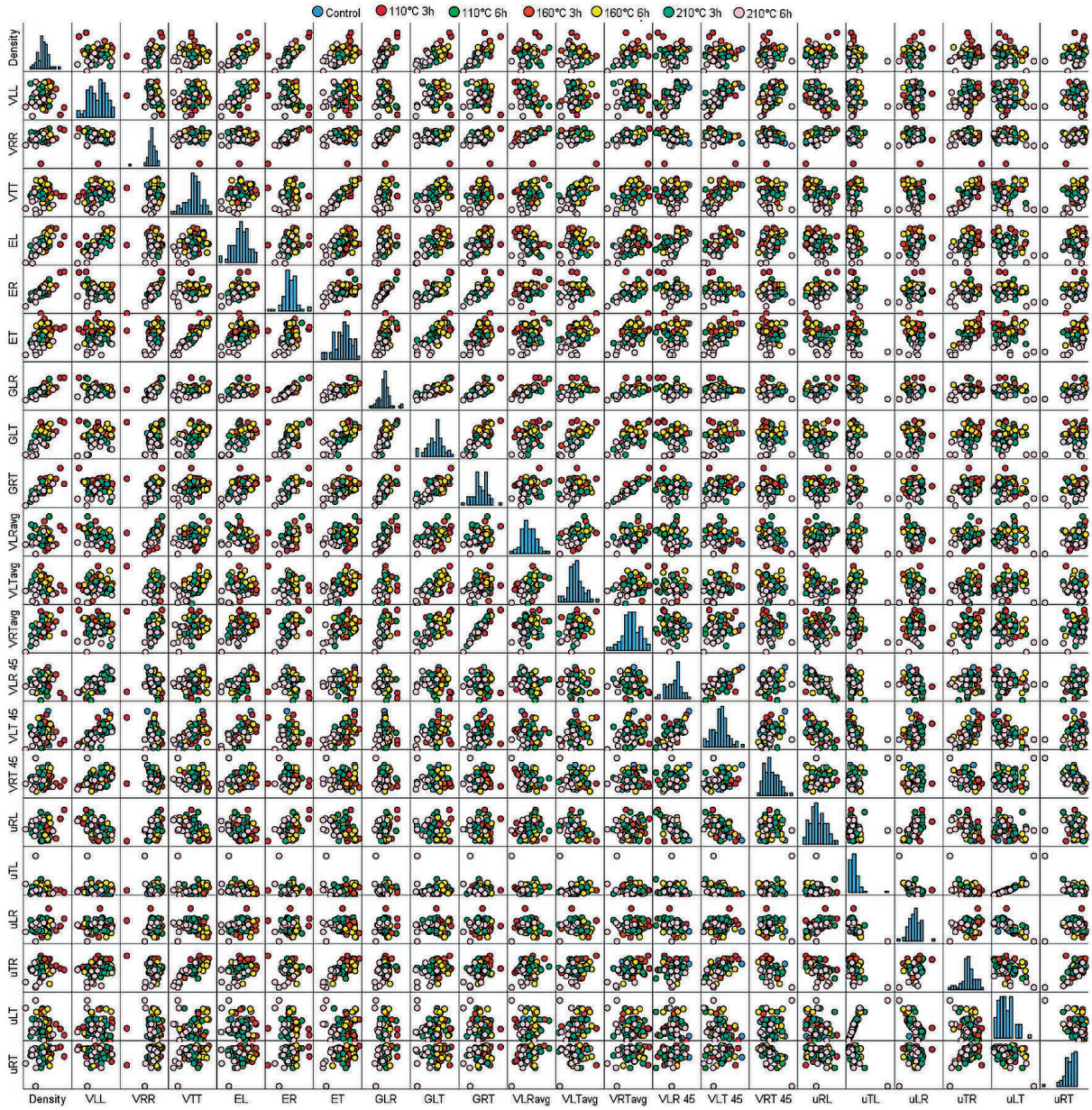


**Figure 2** Scatterplot matrix for all measured properties
**Slika 2.** Matrica dijagrama raspršenja za sva izmjerena svojstva

It is not evident from any of the above papers that Poisson's ratios and density or other elastic constants are highly correlated (Sliker and Yu, 1993). As can be seen in Table 6, $R^2$ values between the variables ranged from 0.001 ($V_{RR}$ *vs* $E_L$) to 0.849 ($V_{TT}$ *vs* $E_T$) for elasticity modulus, 0.004 ($V_{LL}$ *vs* $G_{RT}$) to 0.661 ($E_R$ *vs* $G_{LR}$) for shear modulus, 0.000 (νLR *vs* $V_{RR}$ and νLT *vs* $E_T$ or $G_{LT}$) to 0.712 (νLT *vs* νTL), and 0.001 ($V_{LL}$ *vs* density) to 0.593 (density *vs* $E_R$) for density. However, much higher $R^2$ values (0.64 to 0.91) for $V_{LL}$ *vs* density were reported (Yılmaz Aydın and Aydın, 2018b; Yılmaz Aydın and Aydın, 2018; Yılmaz Aydın and Aydın, 2018c). The scatterplot matrix illustrates the interaction between the variables with histograms in terms of treatment groups. Also, the interactions between the density vs UWVs and elastic constants are illustrated in Figures 2-4 by 3D scatters grouped by treatment conditions.

Changes in the structure of wood by TT are comprehensively reported in the literature and advertency is avoided so as not to fall into repetition. However, it should be kept in mind that one of the key points for the reduction in the mechanical properties is the degradation of hemicellulose (Yue *et al.,* 2023).

Apart from elastic constants, Kaymakçı and Bayram (2021) reported 7356 MPa (210 °C 4h) and 10231 MPa (untreated) *MOE* values for *Populus alba* L., and the decrease was linear instead of oscillating. Sözbir *et al.* (2019) heat-treated *Populus usbekistanica* and reported 5693 MPa *MOE* for untreated samples, while the *MOE* averages oscillated with the progress in TT

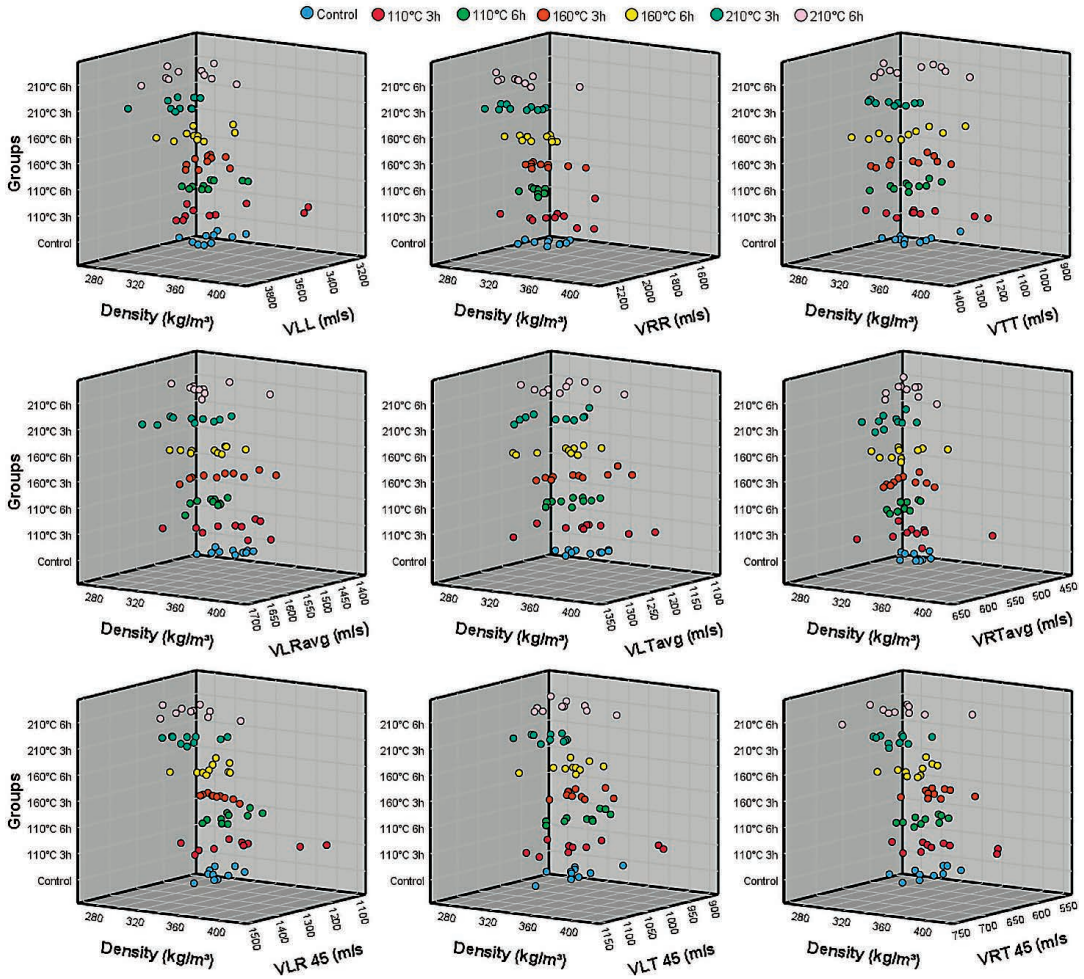


**Figure 3** Grouped 3D Scatters for velocities
**Slika 3.** Grupirana 3D raspršenja za brzine

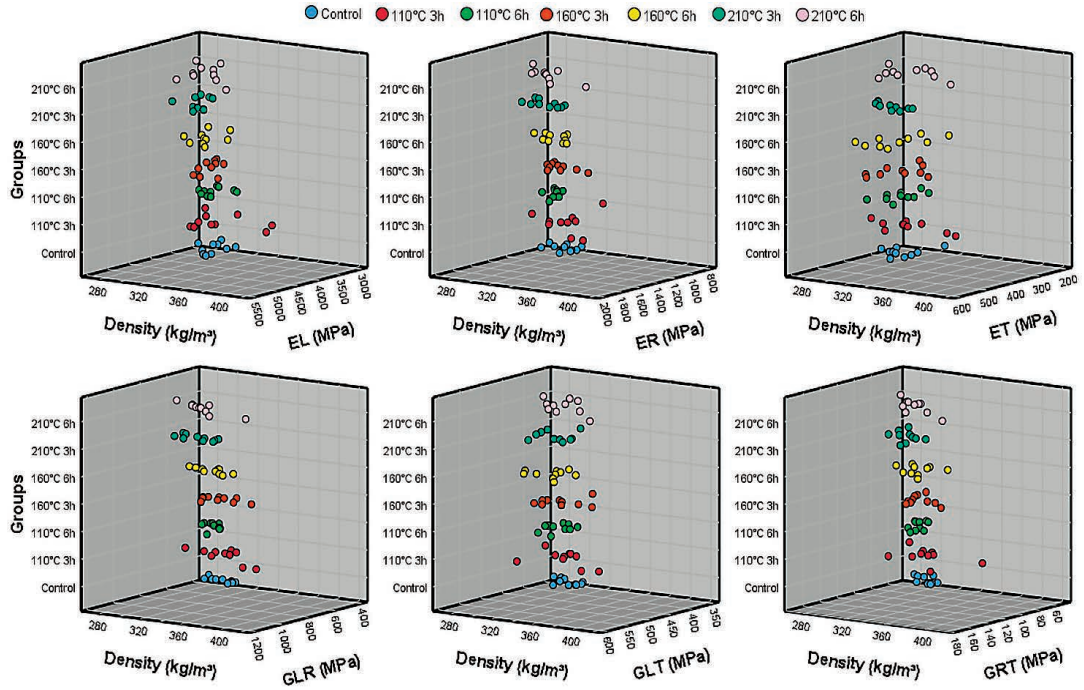


**Figure 4** Grouped 3D Scatters for moduli
**Slika 4.** Grupirana 3D raspršenja za module

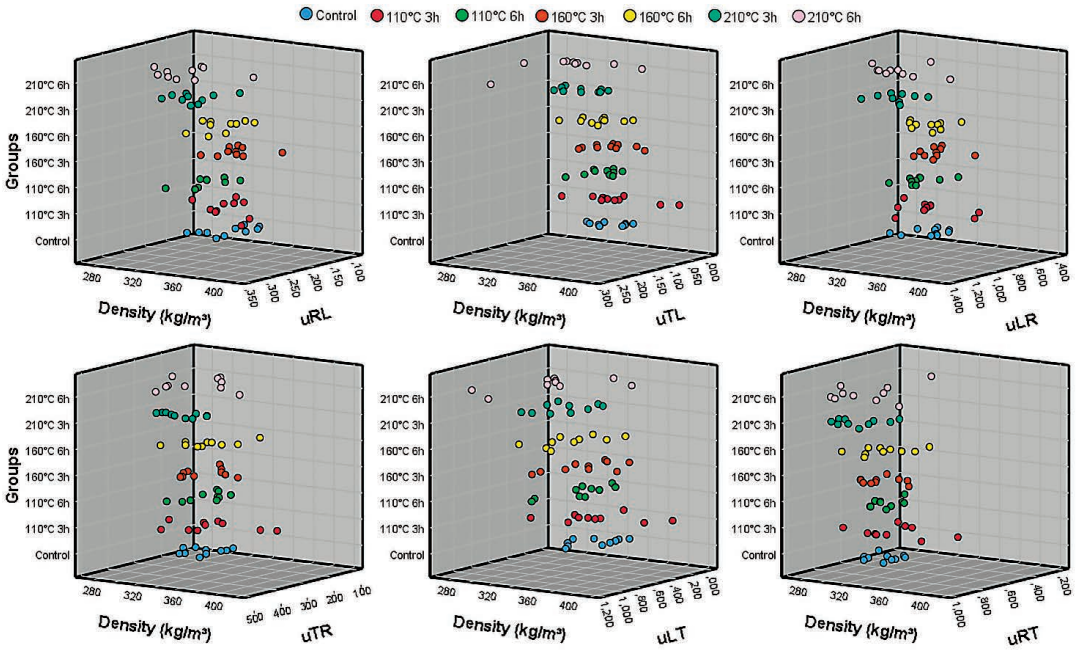


**Figure 5** Grouped 3D Scatters for Poisson's ratios
**Slika 5** Grupirana 3D raspršenja za Poissonove omjere

(120, 160, and 200 °C for 1 and 3h) and no statistically significant differences were found. For full elastic constants, fluctuation is the fact of this study. Therefore, the results of each study are generally unique or partially the same at moderate temperature levels but almost the same at intense conditions.

## 4 CONCLUSIONS
## 4. ZAKLJUČAK

Due to the polar orthotropic nature of wood, it is not an easy task to define factor-related properties, particularly for elastic properties through essential axes or planes. The reason is that not only specific tools are required but also a complex sample preparation due to anatomic complexity and inhomogeneous structure formation by the alignment of elements. Furthermore, samples used for the test are not similar even when prepared using the same laths.

Even though it was obvious that TT significantly affected the elastic characteristics of wood, a common expression of certain effects of TT on wood elastic constants should be avoided because the elastic engineering parameters were non-linearly and differently influenced by the treatment process. Moderate treatment conditions provided considerable advancements in the moduli of wood. However, intense treatment caused the highest decreases in moduli, while the same is not true for some Poisson's ratios. Common treatment conditions did not provide the highest improvements in all elastic constants. Therefore, prioritization should be taken into consideration for defining the application parameters.

## 5 REFERENCES
## 5. LITERATURA

1. Al-musawi, H.; Manni, E.; Stadlmann, A.; Ungerer, B.; Hassan Vand, M.; Lahayne, O.; Nobile, R.; Baumann, G.; Feist, F.; Müller, U., 2023: Characterisation of thermally treated beech and birch by means of quasi-static tests and ultrasonic waves. Scientific Reports, 13: 6348. https://doi.org/10.1038/s41598-023-33054-w
2. Aydin, T. Y., 2020: Ultrasonic evaluation of time and temperature-dependent orthotropic compression properties of oak wood. Journal of Materials Research and Technology, 9 (3): 6028-6036. https://doi.org/10.1016/j.jmrt.2020.04.006
3. Aydın, M.; Aydın, T. Y., 2023: Influence of growth ring number and width on elastic constants of poplar. BioResources, 18 (4): 8484-8502. https://doi.org/10.15376/biores.18.4.8484-8502
4. Aydın, S.; Yardımcı, M. Y.; Ramyar, K., 2007: Mechanical properties of four timber species commonly used in Turkey. Turkish Journal of Engineering and Environmental Sciences, 31 (1): 19-27.
5. Aydın, T. Y., 2022: Temperature influenced anisotropic elastic parameters of red pine. Russian Journal of Nondestructive Testing, 58: 548-562. https://doi.org/10.1134/S1061830922070099
6. Bak, M.; Nemeth, R., 2012: Modification of wood by oil heat treatment. In: Proceedings of the International Scientific Conference on Sustainable Development and Ecological Footprint. Sopron, Hungary.
7. Bytner, O.; Drożdżek, M.; Laskowska, A.; Zawadzki, J., 2022: Influence of thermal modification in nitrogen atmosphere on the selected mechanical properties of black poplar wood (*Populus nigra* L.). Materials, 15 (22): 7949. https://doi.org/10.3390/ma15227949
8. Casado, M.; Acuña, L.; Vecilla, D.; Relea, E.; Basterra, A.; Ramón, G.; López, G., 2010: The influence of size in predicting the elastic modulus of *Populus x euramericana* timber using vibration techniques. In: Proceedings of

the 1st International Conference on Structures and Architecture, ICSA 2010, Guimaraes, Portugal. https://doi.org/10.1201/b10428-282
9. Ettelaei, A.; Layeghi, M.; Zarea Hosseinabadi, H.; Ebrahimi, G., 2019: Prediction of modulus of elasticity of poplar wood using ultrasonic technique by applying empirical correction factors. Measurement, 135: 392-399. https://doi.org/10.1016/j.measurement.2018.11.076
10. Goli, G.; Cremonini, C.; Negro, F.; Zanuttini, R.; Fioravanti, M., 2015: Physical-mechanical properties and bonding quality of heat treated poplar (I-214 clone) and ceiba plywood. IForest, 8 (5): 687-692. https://doi.org/10.3832/ifor1276-007
11. Gonçalves, R.; Trinca, A. J.; Pellis, B. P., 2014: Elastic constants of wood determined by ultrasound using three geometries of specimens. Wood Science and Technology, 48: 269-287. https://doi.org/10.1007/s00226-013-0598-8
12. Güntekin, E.; Aydin, T. Y.; Üner, B., 2017: Physical, mechanical and bonding performance of Calabrian pine (*Pinus brutia* Ten.) as influenced by heat treatment. Drvna industrija, 68 (2): 99-108. https://doi.org/10.5552/drind.2017.1533
13. Guo, H.; Xu, C.; Lin, L.; Wang, Q.; Fu, F., 2011: The composite wood by poplar wood impregnated with $Na_2SiO_3$-polyacrylamide hybrid solution. Science and Engineering of Composite Materials, 18: 151-155. https://doi.org/10.1515/secm.2011.025
14. Hodoušek, M.; Dias, A. M. P. G.; Martins, C.; Marques, A.; Böhm, M., 2016: Comparison of non-destructive methods based on natural frequency for determining the modulus of elasticity of Cupressus lusitanica and *Populus x canadensis*. BioResources, 12 (1): 270-282. https://doi.org/10.15376/biores.12.1.270-282
15. Johansson, D., 2008: Heat Treatment of Solid Wood Effects on Absorption, Strength and Colour, PhD Thesis, Luleå University of Technology, Skellefteå, Sweden.
16. Kaymakci, A.; Bayram, B. Ç., 2021: Evaluation of heat treatment parameters' effect on some physical and mechanical properties of poplar wood with multi-criteria decision making techniques. BioResources, 16 (3): 4693-4703. https://doi.org/10.15376/biores.16.3.4693-4703
17. Kretschmann, D. E., 2010: Mechanical properties of wood. In: Wood Handbook-Wood as an Engineering Material, Ross, R. J. (ed.). Wisconsin, USDA Forest Product Laboratory, pp. 1-46. https://doi.org/10.1126/science.46.1195.516-a
18. Kubovský, I.; Kačíková, D.; Kačík, F., 2020: Structural changes of oak wood main components caused by thermal modification. Polymers (Basel), 12 (2): 1-12. https://doi.org/10.3390/polym12020485
19. Luis Gómez-Royuela, J.; Majano-Majano, A.; José Lara-Bocanegra, A.; Reynolds, T. P. S., 2021: Determination of the elastic constants of thermally modified beech by ultrasound and static tests coupled with 3D digital image correlation. Construction and Building Materials, 302. https://doi.org/10.1016/j.conbuildmat.2021.124270
20. Meija, A.; Irbe, I.; Morozovs, A.; Spulle, U., 2020: Properties of populus genus veneers thermally modified by two modification methods: Wood treatment technology and vacuumthermal treatment. Agronomy Research, 18 (3): 2138-2147. https://doi.org/10.15159/AR.20.184
21. Monteiro, S. R. S.; Martins, C. E. J.; Dias, A. M. P. G.; Cruz, H., 2019: Mechanical characterization of clear wood from Portuguese poplar. BioResources, 14 (4): 9677-9685. https://doi.org/10.15376/biores.14.4.9677-9685
22. Narasimhamurthy, U. V. K.; Kushwaha, P. K.; Mohanty, B. N., 2017: Study on anatomical and mechanical properties of plantation grown Melia dubia and *Populus deltoids* and its suitability for plywood manufacturing. International Journal of Engineering and Technical Research (IJETR), 7 (5): 211-214.
23. Obara, P., 2018: Verification of orthotropic model of wood. Archives of Civil Engineering, 64 (3): 31-44. https://doi.org/10.2478/ace-2018-0027
24. Orhan, H.; Bal, B. C., 2021: Effects of heat treatment in the presence of nitrogen gas on some mechanical properties of poplar wood. Turkish Journal of Forestry, 22 (2): 165-170. https://doi.org/10.18182/tjf.892685
25. Ozyhar, T.; Hering, S.; Sanabria, S. J.; Niemz, P., 2013: Determining moisture-dependent elastic characteristics of beech wood by means of ultrasonic waves. Wood Science and Technology, 47: 329-341. https://doi.org/10.1007/s00226-012-0499-2
26. Papandrea, S. F.; Cataldo, M. F.; Bernardi, B.; Zimbalatti, G.; Proto, A. R., 2022: The predictive accuracy of modulus of elasticity (MOE) in the wood of standing trees and logs. Forests, 13 (8): 1273. https://doi.org/10.3390/f13081273
27. Rapp, A. O.; Sailer, M., 2001: Oil-heat-treatment of wood – process and properties. Drvna industrija, 52 (2): 63-70.
28. Sliker, A.; Yu, Y.; 1993: Elastic constants for hardwoods measured from plate and tension tests. Wood and Fiber Science, 25 (1): 8-22.
29. Sözbir, G. D.; Bektaş, I.; Ak, A. K., 2019: Influence of combined heat treatment and densification on mechanical properties of poplar wood. Maderas: Ciencia y Tecnologia, 21 (4): 481-492. https://doi.org/10.4067/S0718-221X2019005000405
30. Taraborelli, C.; Monteoliva, S.; Keil, G.; Spavento, E., 2022: Effect of heat treatment on hardness, density and color of *Populus* × *canadensis* 'I-214' wood. Forest Systems, 31 (3): e023. https://doi.org/10.5424/fs/2022313-19558
31. Todaro, L.; Liuzzi, S.; Pantaleo, A.; Lo Giudice, V.; Moretti, N.; Stefanizzi, P., 2021: Thermo-modified native black poplar (*Populus nigra* L.) wood as an insulation material. IForest, 14 (3): 268-273. https://doi.org/10.3832/ifor3710-014
32. Vázquez, C.; Gonçalves, R.; Bertoldo, C.; Baño, V.; Vega, A.; Crespo, J.; Guaita, M., 2015: Determination of the mechanical properties of *Castanea sativa* Mill. using ultrasonic wave propagation and comparison with static compression and bending methods. Wood Science and Technology, 49: 607-622. https://doi.org/10.1007/s00226-015-0719-7
33. Villasante, A.; Vignote, S.; Fernandez-Serrano, A.; Laina, R., 2021: Simultaneous treatment with oil heat and densification on physical properties of *Populus* × *Canadensis* wood. Maderas. Ciencia y Tecnología, 24 (5): 1-12. https://doi.org/10.4067/S0718-221X2022000100405
34. Wetzig, M.; Heldstab, C.; Tauscher, T.; Niemz, P., 2011: Ermittlung ausgewählter mechanischer Kennwerte thermisch modifizierter Buche. Bauphysik, 33 (6): 366-373. https://doi.org/10.1002/bapi.201110794
35. Yang, T.-C.; Yang, Y.-H.; Yeh, C.-H., 2021: Thermal decomposition behavior of thin Makino bamboo (*Phyllostachys makinoi*) slivers under nitrogen atmosphere. Materials Today Communications, 26: 102054. https://doi.org/10.1016/j.mtcomm.2021.102054
36. Yao, T.; Zhu, Y.; Shu, Z.; Liu, S.; Hasanagić, R.; Leila, F.; Chu, D.; Li, Y., 2023: Thermal Modification Intensity of Heat-treated Poplar Wood, part 1. Drvna industrija, 74 (4): 447-457. https://doi.org/10.5552/drvind.2023.0125

37. Yılmaz Aydın, T., 2021: Evaluation of heating temperature and time on bending properties of Taurus cedar wood. Turkish Journal of Forestry, 22 (4): 432-438. https://doi.org/10.18182/tjf.1019032
38. Yılmaz Aydın, T.; Aydın, M., 2018: Prediction of bending properties of oriental beech wood exposed to temperature. In: Proceedings of the International Forest Products Congress. Trabzon, Türkiye.
39. Yılmaz Aydın, T.; Aydın, M., 2018a: Comparison of temperature dependent Young's modulus of oriental beech (*Fagus orientalis* L.) that determined by ultrasonic wave propagation and compression test. Turkish Journal of Forestry, 19 (2): 185-191. https://doi.org/10.18182/tjf.397907
40. Yılmaz Aydın, T.; Aydın, M., 2018b: Relationship between density or propagation length and ultrasonic wave velocity in cedar (*cedrus libani*) wood. In: Proceedings of the International Science and Technology Conference. Paris, France.
41. Yılmaz Aydın, T.; Aydın, M., 2018c: Relationship between density or propagation length and ultrasonic wave velocity in sessile oak (*Quercus petraea*) wood. In: Proceedings of the 4th International Conference on Advances in Mechanical Enginering. Yıldız Technical University, İstanbul, Türkiye.
42. Yılmaz Aydın, T.; Aydın, M., 2020: Influence of temperature and exposure duration on the bending properties of oak wood. Journal of Bartin Faculty of Forestry, 22 (3): 871-877. https://doi.org/10.24011/barofd.792268
43. Yılmaz Aydın, T.; Guntekin, E.; Aydın, M., 2016: Effects of heat treatment on some orthotropic mechanic properties of oak (*Quercus petraea*) wood. In: Proceedings of the 1st International Mediterranean Science and Engineering Congress. Adana, Türkiye.
44. Yingjie, Z.; Dejun, F.; Yanguang, D., 2017: Wood physical and mechanical properties of *Populus* × *canadensis* Moench and *Populus* × *euramericana* (Dode) Guinier cv. Gelrica. Agricultural Science and Technology, 18 (12): 2532-2535.
45. Yue, K.; Li, X.; Jiao, X.; Wu, P.; Song, X., 2023: Strength grading of Chinese poplar wood for structural use following thermal modification. Polymer Testing, 123: 108032. https://doi.org/10.1016/j.polymertesting.2023.108032
46. Zahedi, M.; Kazemi Najafi, S.; Füssl, J.; Elyasi, M., 2022: Determining elastic constants of poplar wood (*Populus deltoides*) by ultrasonic waves and its application in the finite element analysis. Wood Material Science and Engineering, 17 (6): 668-678. https://doi.org/10.1080/17480272.2021.1925962
47. TS ISO 13061-2, 2021: Physical and mechanical properties of wood, Test methods for small clear wood specimens. Part 2: Determination of density for physical and mechanical tests. Turkish Standards Institution, Ankara, Türkiye, 2021.

**Corresponding address:**

**MURAT AYDIN**
Isparta University of Applied Sciences, Keçiborlu Vocational School, Department of Machine, Keçiborlu, 32700, Isparta, TÜRKIYE, e-mail: murataydin@isparta.edu.tr

# APPENDIX
# DODATAK

## A.1 Tendency illustration regarding treatment conditions
## A.1. Prikaz trendova s obzirom na uvjete toplinske obrade


$G_{LR}$, MPa
850
800
750
700
650
$G_{LT}$, MPa
520
500
480
460
440
420
400
$G_{RT}$, MPa
120
110
100
90
80
$V_{LR\ 45°}$, m/s
1320
1300
1280
1260
1240
1220
$V_{LT\ 45°}$, m/s
1020
1010
1000
990
980
970
960
950
$V_{RT\ 45°}$, m/s
655
650
645
640
635
630
625
$\mu_{RL}$
0.230
0.210
0.190
0.170
0.150
$\mu_{TL}$
0.055
0.050
0.045
0.040
0.035
0.030
0.025
0.020
$\mu_{TR}$
0.360
0.340
0.320
0.300
0.280
0.260
0.240
0.220
$\mu_{LR}$
0.900
0.850
0.800
0.750
0.700
$\mu_{LT}$
0.550
0.500
0.450
0.400
0.350
0.300
0.250
$\mu_{RT}$
0.950
0.900
0.850
0.800
0.750
0.700
Control
110 °C 3h
110 °C 6h
160 °C 3h
160 °C 6h
210 °C 3h
210 °C 6h

Abdurrahman Karaman*[1], Hüseyin Yesil[2]

# Investigation of Some Physical and Mechanical Properties of Basalt Fiber-Reinforced Polymer (BFRP) Woven Fabrics and Plaster Mesh (PSM) Reinforced Glued Laminated Oak Lumber

# Istraživanje nekih fizičkih i mehaničkih svojstava lamelirane hrastove građe ojačane polimernim tkaninama s bazaltnim vlaknima (BFRP) i fasadnom mrežicom (PSM)

**ORIGINAL SCIENTIFIC PAPER**
**Izvorni znanstveni rad**
Received – prispjelo: 5. 12. 2023.
Accepted – prihvaćeno: 19. 3. 2024.
UDK: 630*83; 674,038,5
https://doi.org/10.5552/drvind.2024.0174



**ABSTRACT** • *In this study, some physical and mechanical properties of the basalt fiber-reinforced polymer (BFRP) woven fabrics (WF) and plaster mesh (PSM) reinforced glued laminated oak lumber were investigated. The BFRPWF and PSM were used in order to increase the mechanical properties of the laminated elements. One-component polyurethane glue (PUR) was used in the production of lumber. The BFRPWF and PSM were tested in three different locations using non-reinforced laminated oak lumber (LOL), reinforced laminated oak lumber with BFRPWF (LOL-BFRPWF), and reinforced laminated oak lumber with PSM (LOL-PSM). Tests were performed on the LOL, LOL-BFRPWF, and LOL-PSM to investigate their bending strength (MOR), air-dried density ($\delta_{12}$), and modulus of elasticity (MOE). The three-point MOR and MOE in bending tests were applied to the samples. The results showed that the highest value for MOR was found in the laminated wood samples (135.20 N/mm$^2$) that were prepared using the BFRPWF inter-layer. The lowest value of 112.82 N/mm$^2$ was found in the LOL samples. The highest value of modulus elasticity was found in the samples prepared with the BFRPWF inter-layer (16167 N/mm$^2$). The lowest value of 13786 N/mm$^2$ was found in the LOL samples. It was observed that the samples parallel to the glue line of the laminated material showed higher performance compared to those perpendicular to the glue line. The LOL-BFRPWF samples give better results than LOL-PSM and control samples. Accordingly, the LOL-BFRPWF and LOL-PSM samples have the potential to be used as viable options for both furniture and building materials.*

**KEYWORDS:** *bending strength; modulus of elasticity; plaster mesh; oak wood; polyurethane adhesive*

* Corresponding author
[1] Author is researcher at Usak University, Banaz Vocational School, Forestry Department, Usak, Turkey. https://orcid.org/0000-0002-5925-7519
[2] Author is researcher at Kutahya Dumlupınar University, Simav Vocational School, Interior Design Department, Kutahya, Turkey. https://orcid.org/0000-0003-2847-6492

**SAŽETAK** • *U radu su istražena neka fizička i mehanička svojstva lamelirane građe od hrastovine ojačane polimernim tkaninama s bazaltnim vlaknima (BFRPWF) i fasadnom mrežicom (PSM) kako bi se povećala mehanička svojstva lamelirane građe. U izradi lamelirane građe upotrijebljeno je jednokomponentno poliuretansko ljepilo (PUR). Tijekom ispitivanja određena je čvrstoća na savijanje (MOR), gustoća drva sušenog na zraku ($\delta_{12}$) i modul elastičnosti (MOE) neojačane lamelirane građe (LOL), lamelirane građe ojačane BFRPWF-om (LOL-BFRPWF) i lamelirane građe ojačane PSM-om (LOL-PSM). Za određivanje čvrstoće na savijanje i modula elastičnosti primijenjeno je savijanje u tri točke. Rezultati su pokazali da je čvrstoća na savijanje najveća na uzorcima lamelirane građe ojačane BFRPWF-om (135,20 N/mm$^2$), a najmanja na uzorcima bez ojačanja (112,82 N/mm$^2$). Najveća vrijednost modula elastičnosti izmjerena je na uzorcima ojačanim BFRPWF-om (16167 N/mm$^2$), a najmanja na uzorcima bez ojačanja (13786 N/mm$^2$). Uočeno je da su bolja svojstva uzoraka pri ispitivanju paralelno s lijepljenim spojem nego okomito na slijepljeni spoj. LOL-BFRPWF uzorci dali su bolje rezultate od uzoraka LOL-PSM i kontrolnih uzoraka. Prema dobivenim rezultatima, uzorci LOL-BFRPWF i LOL-PSM mogu poslužiti kao održive opcije u proizvodnji namještaja i proizvoda u graditeljstvu.*

**KLJUČNE RIJEČI:** *čvrstoća na savijanje; modul elastičnosti; fasadna mrežica; hrastovina; poliuretansko ljepilo*

## 1 INTRODUCTION
## 1. UVOD

The main goal in the development of laminated veneer lumber (LVL) is to enhance the dimensional stability of timber products, resulting in improved performance and reliability. In order to achieve the necessary strength levels, it is vital to ensure that the layer arrangement in the LVL is in accordance with the orientation of the timber fibers. An LVL product, characterized by veneers arranged perpendicularly, can be observed as a crossbanded material. Its elevated mechanical properties make it highly desirable for various structural applications (Rahayu *et al*., 2015). Typically, the production process of LVL involves the utilization of secondary-grade materials that exhibit characteristics such as the presence of numerous knots, lower density, and diminished mechanical properties. The composition of LVL can vary significantly as it can be manufactured using a wide range of wood species, including but not limited to Douglas fir, poplar, beech, spruce and others (Burdurlu *et al*., 2007).

To improve the physical and mechanical properties of LVL, FRP composites such as E-glass FRP (GFRP), carbon FRP (CFRP), and aramid FRP (AFRP) are commonly used as reinforcement materials (Johns and Lacroix, 2000; Lopez-Anido *et al*., 2003; Borri *et al*., 2005). While it is true that the manufacturing processes used for these fibers are known to be energy-intensive and come with high initial costs, the emergence of basalt FRP (BFRP), as a mineral-based natural FRP, has brought about notable changes.

BFRP, as supported by studies (Wang *et al*., 2014; Elgabbas *et al*., 2016; Fiore *et al*., 2015), offers the advantage of lower material costs and demonstrates a high level of ecological compatibility throughout its production. Furthermore, basalt fiber has beneficial properties (Patnaik *et al*., 2004) that, when combined with cost-effective production process (Wu *et al*., 2012; Sim *et al*., 2005), result in enhanced high temperature resistance (Sim *et al*., 2005), excellent freeze-thaw performance (Wu *et al*., 2010), and ease of manufacture (Sim *et al*., 2005). In addition, basalt fiber exhibits remarkable tensile properties, characterized by a high tensile strength ranging from 1.85 to 4.8 GPa (Zoghi, 2013).

Currently, there is growing interest in using BFRP as a type of FRP for reinforcing wood composites (Kufel and Kuciel, 2019; Kramár *et al*., 2020). As a newly introduced composite material, BFRP represents another technologically advanced fiber composite material, joining the ranks of carbon fibers (Subagia *et al*., 2014).

BFRP offers significant cost advantages over CFRP, with prices ranging from only one-eighth to one-sixth of CFRP (Wu, 2020). Additionally, BFRP exhibits superior mechanical properties, including higher elastic modulus and tensile strength, when compared to GFRP (Song *et al*., 2021).

Due to its lower density, with basalt weighing approximately one-third of the steel density (2.6 g/cm$^3$ compared to 7.68 g/cm$^3$), BFRP is considered a lighter and more robust construction material compared to steel. It is projected that the mechanical properties of BFRP as a construction material will exert an influence on its environmental performance (Garg and Shrivastava, 2019). The raw materials used in BFRP are characterized by their broad variety, while its production process adheres to environmentally friendly practices, and fulfills the requisites of green sustainable development (Gao *et al*., 2020).

Extensive study has been conducted on the use of BFRP in conjunction with LVL in various technological applications, including wood and LVL elements. These studies have demonstrated notable enhancements in mechanical properties when using different reinforcement configurations (Wang *et al*., 2019; Liu *et al*., 2020; Resvalvo *et al*., 2020; Wdowiak-Postulak and Swit, 2021; Cheng *et al*., 2022; Jian *et al*., 2022; Zhou *et al*., 2022; Núñez-Decap *et al*., 2023; Resvalvo *et al*., 2023).

The behavior of prismatic test specimens made from wild pinewood under compressive loads was examined by de la Rosa *et al*. (2021). The study focused on the effect of fabric confinement, with the use of three types of fabric: two BFRP fabrics with varying

grammages and CFRP. Lohmus *et al*. (2021) examined whether the tensile strength of basalt fiber-reinforced plywood can be affected by prestressing and temperature variations. Cheng *et al*. (2022) conducted a study to investigate a straightforward retrofitting technique that involved using small bamboo pieces and a BFRP wrap to enhance the structural strength of locally damaged laminated bamboo lumber (LBL) columns. Rescalvo *et al*. (2023) investigated the LVL mechanical behavior of poplar reinforced with BFRP subjected to shear and compressive stresses. Wdowiak-Postulak *et al*. (2023) conducted an analysis to assess the effectiveness of strengthening glued laminated timber beams through the use of pre-stressed BFRP.

Keskin (2004) investigated the bending properties of structural LVL made of Oak (*Quercus petrea* Lieble). The modulus of rupture, modulus of elasticity, and air-dry density of oak wood was measured to be 106 N/mm$^2$, 10742 N/mm$^2$, and 611 kg/m$^3$, respectively Keskin (2009) made an experiment to determine how timber species, loading direction and chemical impregnation affected the bending properties of LVL samples. The air-dry density for the chosen species was for beech (650 kg/m$^3$), oak (639 kg/m$^3$), Scotch pine (537 kg/m$^3$), spruce (403 kg/m$^3$) and Uludad fir (385 kg/m$^3$).

The literature review shows that there are not enough studies on some physical and mechanical properties of the BFRPWF and PSM reinforced glued laminated oak lumber. I believe that this study will contribute to the literature. The current study aimed to comparatively investigate some physical and mechanical properties of the control samples (LOL), the LOL-BFRPWF samples and LOL-PSM samples using polyurethane adhesive cured under room temperature.

## 2 MATERIALS AND METHODS
## 2. MATERIJALI I METODE

### 2.1 Materials
### 2.1. Materijali

For the study, the oak wood (*Quercus petrea* L.), widely used in the furniture sector, was chosen as the wood material. Its selection was conducted randomly from timber merchants located in Yenice-Karabuk, Turkey. As a test material, pieces of oak lumber (5 mm × 80 mm × 1000 mm) were used. It is a material whose full-dry density ($\delta_0$) is 650 kg/m$^3$, and $\delta_{12}$ is 690 kg/m$^3$. Also, the *MOE* is 12300 MPa, and the *MOR* is 105 MPa (Bozkurt and Erdin, 2000).

The BFRPWF for 200 gr/m$^2$ plain materials used in the study was obtained by Dost Chemical Industry Raw Material Industry and Trading Company (Turkey, Istanbul) (Figure 1a). It had the following values: density of 2.8 g/cm$^3$, thickness of 0.140 mm, modulus of elasticity of 89 GPa, tensile strength of 4.8 GPa, and elongation to fracture of 3.2 % (Fiore *et al*., 2011).

The plaster mesh (PSM) used had a weight of 160 g/m$^2$. It was alkali resistant and orange in color, with a 4 mm × 4 mm mesh pattern (Figure 1b).

The polyurethane adhesive (PUR) used in this the study was obtained by Apel Kimya Industrial Industry and Trade Company (Turkey, Istanbul) (Figure 1c). At a temperature of 20 °C, the density of the material is measured to be (1.11±0.02) g/cm$^3$, while at 25 °C, the viscosity is determined to be (14.000±3.000) mPas. When exposed to a temperature of (20 ±2) °C and a relative humidity of (65 ±3) %, the material undergoes hardening within 30 minutes.

### 2.2 Preparation of experimental samples
### 2.2. Priprema ispitnih uzoraka

Slats with dimensions of 5 mm thickness, 80 mm width, and 1000 mm length (T × W × L) were obtained from oak timber by a circular saw using the mowing technique. Once stacked, the slats were stored in a temperature-controlled room with a constant temperature of (20±2) °C and relative humidity of (65±5) %. The slats remained in the specified environment until they attained a moisture content of 12 %. The test samples were prepared in accordance with the guidelines outlined in the TS 5497 EN 408 (2006) standard. The PUR was used in the preparation of the samples.

As shown in Figure 2, reinforced laminated elements were produced by placing the BFRPWF or PSM

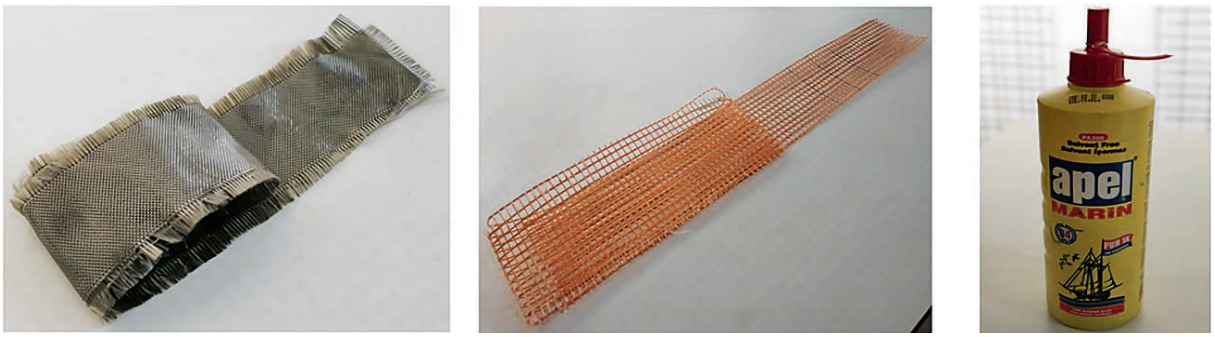


(a) (b) (c)

**Figure 1** Materials used in experiments: (a) BFRPWF, (b) PSM, (c) PUR adhesive
**Slika 1.** Materijali uključeni u istraživanju: (a) BFRPWF, (b) PSM, (c) PUR ljepilo

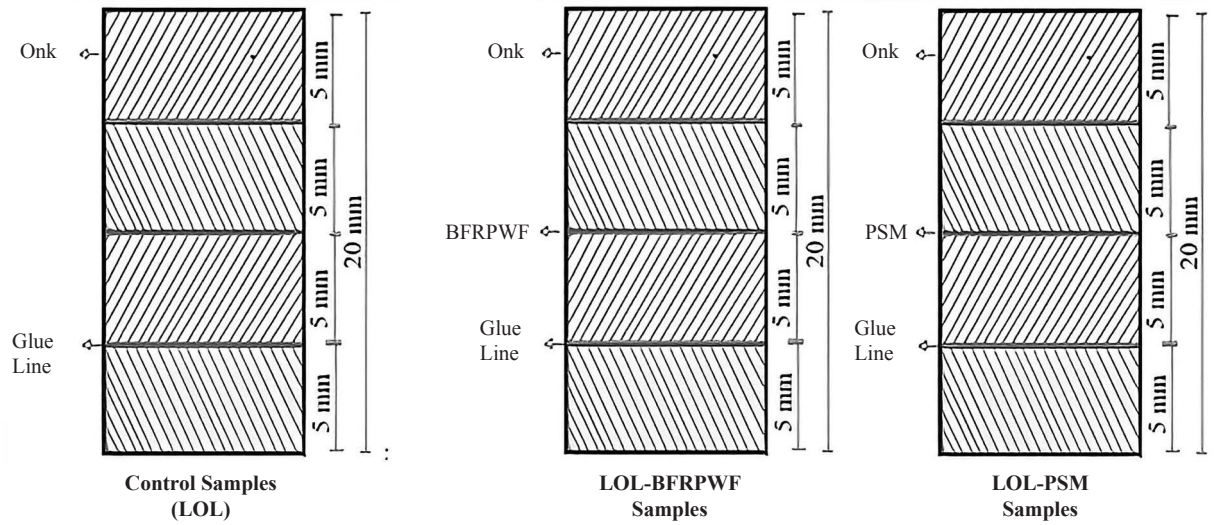


**Figure 2** All experimental samples
**Slika 2.** Svi ispitni uzorci


**Figure 3** Pressing of test samples
**Slika 3.** Prešanje ispitnih uzoraka

between each layer with the aim of inreasing the resistance. For interlayer samples, 3 layers of reinforced materials were used for intermediate support between solid layers. Approximately 200 g/m$^2$ of adhesive was used for the surface. The samples, which consisted of four layers, were placed into a hydraulic press (Hydraulic Veneer SSP-80; ASMETAL Wood Working Machinery Industry Inc., Ikitelli, Istanbul, Turkey) at room temperature. The press exerted a pressure of approximately 1.5 N/mm$^2$ on the samples for 3 hours. As a result, the desired laminated veneer lumbers were produced by cold pressure at (20 ±2) °C and (65±5) % relative humidity. Consequently, one wood species (oak), one adhesive type (PUR), two fiber reinforced polymers (BFRPWF, PSM, and control), two load types (perpendicular to the glue line and parallel to the glue line), and 10 samples of each material (1 × 1 × 3 × 2 × 10 = 60) were the variables, and the air-dry density tests were made for a total of 20 variables. A total of 80 specimens were prepared in this research. Prior to testing, all samples were conditioned in a humidity chamber controlled at (20±2) °C and (65±5) % relative humidity (RH) for two weeks. The pressing of test samples is shown in Figure 3.

## 2.3 Method of testing
## 2.3. Metode ispitivanja

The air-dry density was measured in accordance with the guidelines outlined in TS 2474 (1976). Test samples were prepared with dimensions of 20 mm × 20 mm × 30 mm for the purpose of determining the density. The samples were subjected to conditioning in an environment with a relative humidity of (65±5) % and a temperature of (20±2) °C. Conditioning was continued until the samples reached an equilibrium moisture content of 12 %. Subsequently, the samples were weighed using a digital precision scale, and their dimensions were determined using a digital precision compass. Next, the equations provided were used to compute the density values of the samples after air drying:

$$\delta_{12} = \frac{M_{12}}{\vartheta_{12}} \quad (1)$$

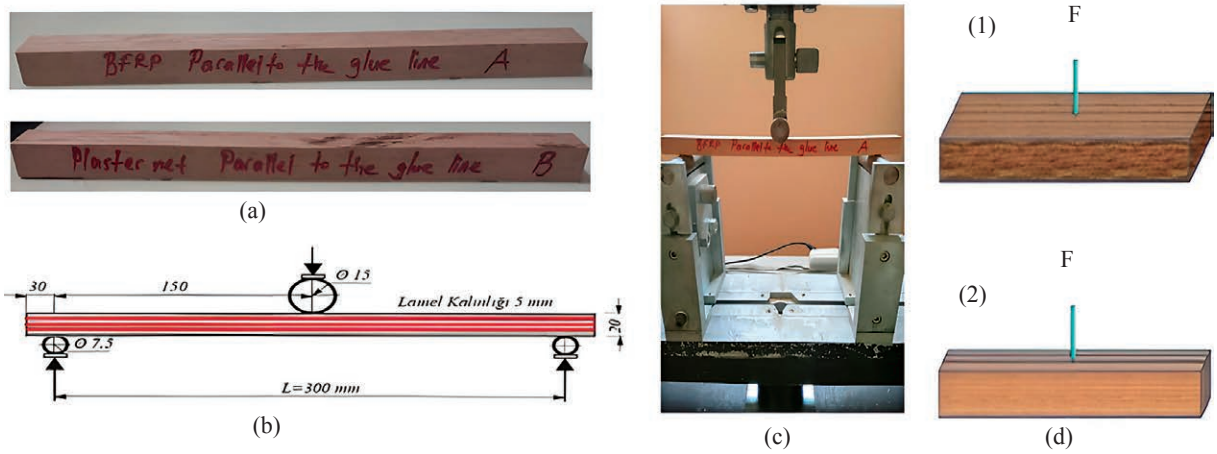


**Figure 4** Three-point bending test set-up for laminated samples: (a) vertical crosssection, (b) static system (in mm), (c) testing, (d) loading directions of test specimen according to glue lines: (1) perpendicular, (2) parallel
**Slika 4.** Postavljanje ispitivanja na savijanje u tri točke za lamelirane uzorke: (a) vertikalni presjek, (b) statički sustav (mm), (c) ispitivanje, (d) smjerovi opterećenja ispitnog uzorka u odnosu prema lijepljenom spoju: (1) okomito, (2) paralelno

Where, $\delta_{12}$ is the sample density (g/cm$^3$), $M_{12}$ is the weight, and $\vartheta_{12}$ is the volume (cm$^3$).

### 2.3.1 Bending strength and elasticity modulus
### 2.3.1. Čvrstoća na savijanje i modul elastičnosti

In accordance with the TS EN 326 (1999) standard, the test samples were prepared to facilitate the measurement of *MOR* and *MOE*. The *MOR* experiments were carried out in accordance with the guidelines outlined in the TS 2474 (1976) standard, while the modulus of elasticity tests adhered to the TS 2478 (1976) standard. Each test sample was prepared with dimensions of 20 mm × 20 mm × 360 mm, and two samples were used for each test. Three-point bending test method was carried out (Figure 4c). The bending tests were performed on an electromechanical universal testing machine (UTM) with a capacity of 10 kN. When performing the *MOR* tests, the force was applied to the edge wise position of the test sample in a direction parallel to the glue line and a direction perpendicular to glu line. The test speed was set at 5 mm/min, and the span between the supports was 300 mm. The preload amount was 10 N, and the test ended at 70 % of the maximum force. The *MOR* and *MOE* have been determined using the following equations:

$$MOR = \frac{3 \cdot F_{max} \cdot L}{2 \cdot b \cdot h^2} \quad (2)$$

In the given context, the variables are defined as follows: *MOR* (N/mm$^2$), $F_{max}$ represents the maximum load applied during testing, measured in N. *L* denotes the distance between the two supports, measured in mm, *b* represents the width of the test sample, also measured in mm. Lastly, *h* is the thickness of the test sample, measured in mm.

$$MOE = \frac{L_1^3 \cdot \Delta F}{4 \cdot b \cdot h^3 \cdot \Delta f} \quad (3)$$

In the given context, the variables are defined as follows:
*MOE* is the modulus of elasticity (N/mm$^2$), $\Delta F$ represents the load increment, measured in N, *L* denotes the distance between the two supports, measured in mm, $\Delta f$ represents the deflection increment, *b* is the width of the test sample, measured in mm, lastly, *h* is the thickness of the test sample, also measured in mm.

### 2.3 Data analyses
### 2.3. Analiza podataka

The statistical analysis of the experimental data involved calculating the arithmetic mean and standard deviation. Multiple analysis of variance (ANOVA) was used to assess the impact of various factors on the values obtained for all sample groups. Duncan's test was used to determine the significance level of the interaction between the factors, with a significance level set at 5 % ($p < 0{,}05$). This allowed to determine the degree of significance if the mutual strength of the factors exhibited a significant effect.

## 3 RESULTS AND DISCUSSION
## 3. REZULTATI I RASPRAVA

Table 1 presents a summary of the test results for some physical and mechanical properties of the samples. Descriptive statistics, including the maximum, minimum, mean, and standard deviation, were used to summarize the data. These statistical values provide an overview of the observed variability and central tendencies concerning the tested properties of the samples.

ANOVA analysis was performed to compare LOL, BFRPWF-LOL and LOL-PSM (Table 2). According to the analysis, the $\delta_{12}$, *MOR* perpendicular to the glue line ($\perp$*MOR*), *MOR* parallel to the glue line (// *MOR*), *MOE* perpendicular to the glue line ($\perp$*MOE*),

and *MOE* parallel to the glue line (//*MOE*) were statistically significant at the level of 0.05.

In cases where the observed differences between groups were deemed statistically significant, the Duncan's test was used to determine the specific differences between means. This analysis was conducted at a predetermined significance level of α=0.05. The results of the Duncan's test, indicating the significant differences between means, can be seen in Table 3.

This table shows that some physical and mechanical properties of LOL samples showed the lowest values, and some physical and mechanical properties of LOL-BFRPWF the highest. Some physical and mechanical properties of LOL-BFRPWF samples were

**Table 1** Descriptive statistical values of some physical and mechanical properties
**Tablica 1.** Deskriptivne statističke vrijednosti nekih fizičkih i mehaničkih svojstava lameliranih uzoraka

| Process | Values | $\delta_{12}$, kg/m$^3$ | ⊥ *MOR*, N/mm$^2$ | // *MOR*, N/mm$^2$ | ⊥ *MOE*, N/mm$^2$ | // *MOE*, N/mm$^2$ |
|---|---|---|---|---|---|---|
| LOL (Control) | *X* | 714 | 108.55 | 112.82 | 12501 | 13786 |
| | *SD* | 21.18 | 1.93 | 3.82 | 72.3 | 353 |
| | *COV* (%) | 0.45 | 3.71 | 14.61 | 5230 | 124558 |
| | *Min* | 680 | 106.15 | 108.00 | 12386 | 13076 |
| | *Max* | 753 | 112.65 | 122.30 | 12650 | 14199 |
| | *N* | 10 | 10 | 10 | 10 | 10 |
| PSM-LOL | *X* | 738 | 119.74 | 127.71 | 13558 | 15727 |
| | *SD* | 11.26 | 4.29 | 3.01 | 286 | 528 |
| | *COV* (%) | 0.13 | 18.40 | 9.07 | 81681 | 278257 |
| | *Min* | 718 | 110.05 | 122.55 | 13005 | 14719 |
| | *Max* | 755 | 125.29 | 132.30 | 14030 | 16612 |
| | *N* | 10 | 10 | 10 | 10 | 10 |
| LOL-BFRP-WF | *X* | 788 | 125.57 | 135.20 | 14526 | 16167 |
| | *SD* | 22.58 | 3.97 | 4.35 | 498 | 727 |
| | *COV* (%) | 0.51 | 15.73 | 18.95 | 248282 | 528799 |
| | *Min* | 758 | 120.71 | 129.65 | 13748 | 15245 |
| | *Max* | 831 | 132.73 | 141.65 | 15204 | 17394 |
| | *N* | 10 | 10 | 10 | 10 | 10 |

*X* – Mean values, *SD* – Standart deviation, *COV* (%) – Coefficient of variation, *N* – Number of samples, LOL – Non-reinforced laminated oak lumber (Control), PSM-LOL – Laminated oak lumber with reinforced PSM, LOL-BFRPWF – Laminated oak lumber with reinforced BFRPWF, ⊥ – perpendicular to glue line, // – paralell to glue line.
*X – srednje vrijednosti, SD – standardna devijacija, COV (%) – koeficijent varijacije, N – broj uzoraka, LOL – neojačani lamelirani uzorci od hrastovine (kontrolni uzorak), PSM-LOL – lamelirani uzorci od hrastovine ojačani PSM-om, LOL-BFRPWF – lamelirani uzorci od hrastovine ojačani BFRPWF-om, ⊥ – okomito na lijepljeni spoj, // – paralelno s lijepljenim spojem*

**Table 2** Result of ANOVA
**Tablica 2.** ANOVA rezultati

| | | | | | | |
|---|---|---|---|---|---|---|
| $\delta_{12}$, kg/m$^3$ | **Source** | ***SO*** | ***DF*** | ***MS*** | ***F* Value** | **Sig.** |
| | Between Groups | 0.03205 | 2 | 0.016027 | 44.29 | 0.000 |
| | Within Groups | 0.01086 | 30 | 0.000362 | | |
| | Total | 0.04291 | 32 | | | |
| ⊥*MOR*, N/mm$^2$ | **Source** | ***SO*** | ***DF*** | ***MS*** | ***F* Value** | **Sig.** |
| | Between Groups | 2452.2 | 2 | 1226.09 | 42.25 | 0.000 |
| | Within Groups | 870.7 | 30 | 29.02 | | |
| | Total | 2125.2 | 32 | | | |
| //*MOR*, N/mm$^2$ | **Source** | ***SO*** | ***DF*** | ***MS*** | ***F* Value** | **Sig.** |
| | Between Groups | 2750.7 | 2 | 1378.87 | 97.05 | 0.000 |
| | Within Groups | 426.20 | 30 | 14.21 | | |
| | Total | 3184.00 | 32 | | | |
| ⊥*MOE*, N/mm$^2$ | **Source** | ***SO*** | ***DF*** | ***MS*** | ***F* Value** | **Sig.** |
| | Between Groups | 22549729 | 2 | 11274865 | 100.91 | 0.000 |
| | Within Groups | 3351935 | 30 | 111731 | | |
| | Total | 25901664 | 32 | | | |
| //*MOE*, N/mm$^2$ | **Source** | ***SO*** | ***DF*** | ***MS*** | ***F* Value** | **Sig.** |
| | Between Groups | 59505749 | 2 | 29752874 | 115.14 | 0.000 |
| | Within Groups | 7752263 | 30 | 111731 | | |
| | Total | 67258012 | 32 | | | |

**Table 3** Result of Duncan's Test
**Tablica 3.** Rezultati Duncanova testa

| **Technological properties** *Tehnološka svojstva* | **Process** / *Proces* | | | | | |
|---|---|---|---|---|---|---|
| | **LOL** | | **PSM-LOL** | | **LOL-BFRPWF** | |
| | *X* | *HG* | *X* | *HG* | *X* | *HG* |
| $\delta_{12}$, g/cm$^3$ | 0.714 | C | 0.738 | B | 0.788 | A |
| ⊥ *MOR*, N/mm$^2$ | 108.55 | C | 119.74 | B | 125.57 | A |
| // *MOR*, N/mm$^2$ | 112.82 | C | 127.71 | B | 135.20 | A |
| ⊥ *MOE*, N/mm$^2$ | 12501 | C | 13558 | B | 14526 | A |
| // *MOE*, N/mm$^2$ | 13786 | C | 15727 | B | 16167 | A |

LOL – Non-reinforced laminated oak lumber, PSM-LOL – Laminated oak lumber with reinforced PSM, LOL-BFRPWF – Laminated oak lumber with reinforced BFRPWF , ⊥ – perpendicular to glue line, // – paralell to glue line.
*LOL – neojačani lamelirani uzorci od hrastovine (kontrolni uzorak), PSM-LOL – lamelirani uzorci od hrastovine ojačani PSM-om, LOL-BFRPWF – lamelirani uzorci od hrastovine ojačani BFRPWF-om, ⊥ – okomito na lijepljeni spoj, // – paralelno s lijepljenim spojem*

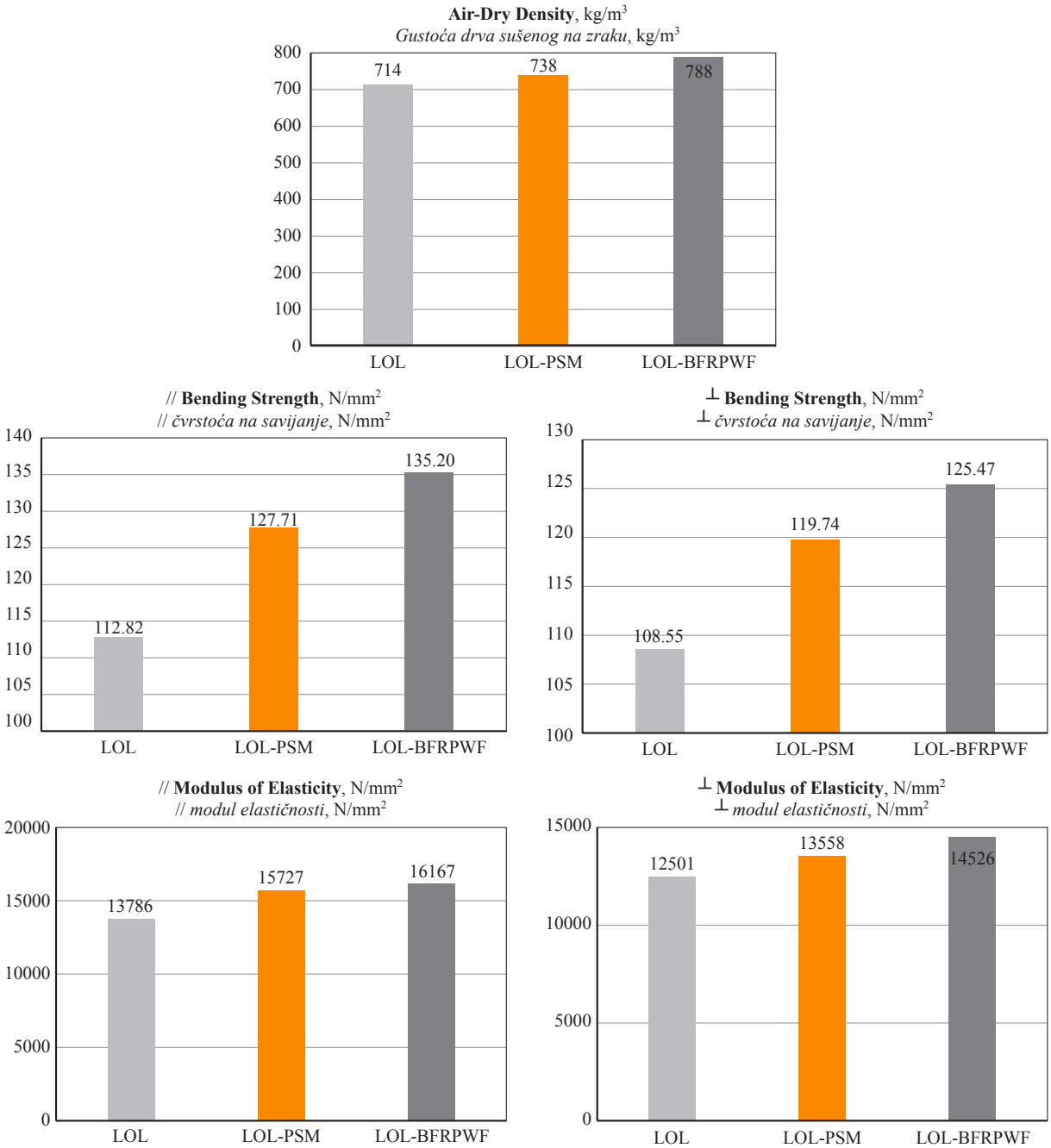


**Figure 5** Descriptive statistical values for various physical and mechanical properties such as δ12, // MOR, ⊥MOR, // MOE, and ⊥MOE of laminated oak lumber samples
**Slika 5.** Deskriptivne statističke vrijednosti za neka fizička i mehanička svojstva kao što su δ12, // MOR, ⊥MOR, // MOE i ⊥MOE uzoraka lamelirane hrastove građe

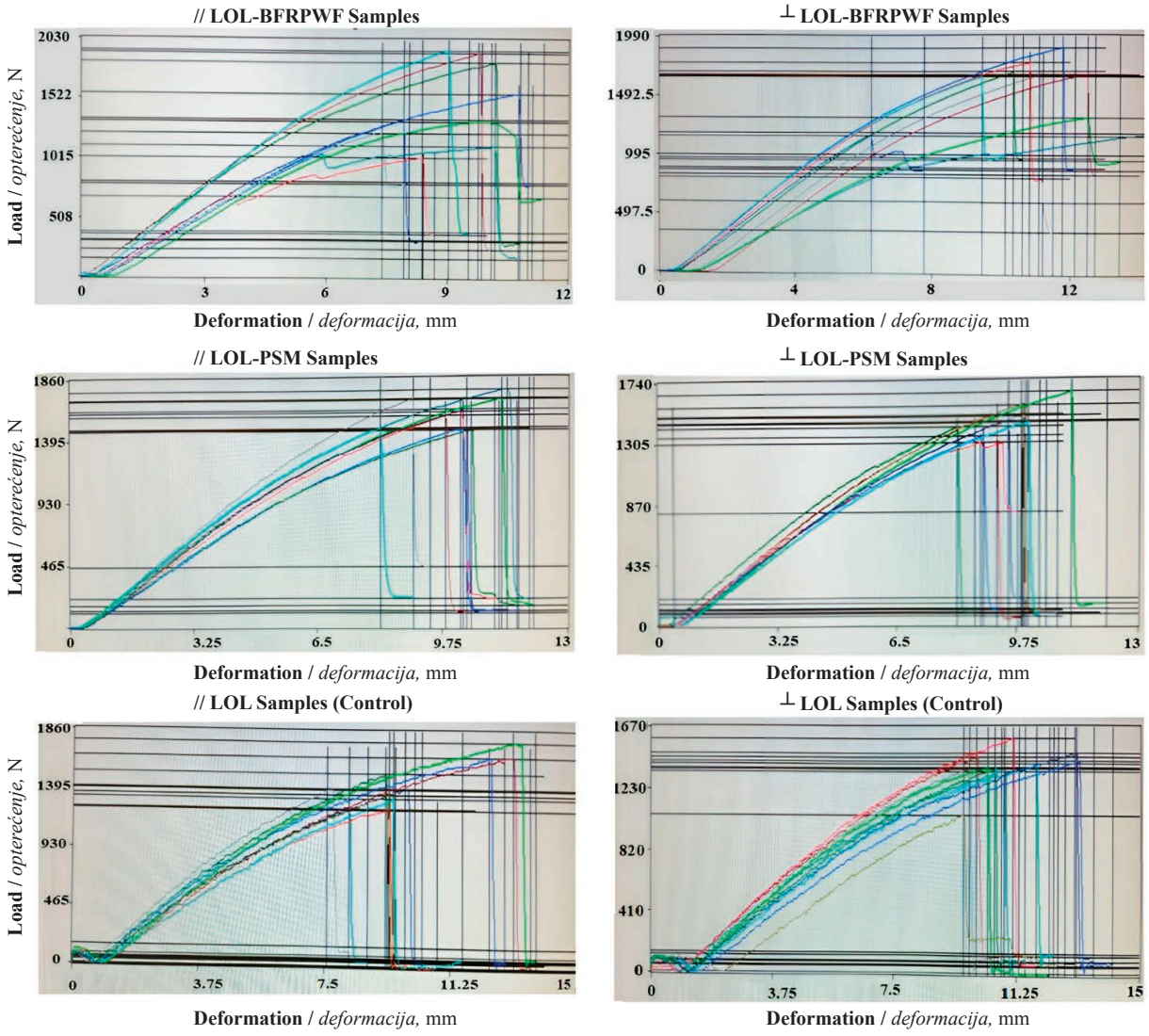


**Figure 6** Load – deformation graphs based on bending strength test results
**Slika 6.** Grafovi *opterećenje – deformacija* na temelju rezultata ispitivanja čvrstoće na savijanje

determined: $\delta_{12}$ 788 kg/m$^3$, //*MOR* 142.20 N/mm$^2$, ⊥*MOR* 129.66 N/mm$^2$, ⊥ *MOE* 17349 N/mm$^2$, //*MOE* 14526 N/mm$^2$, 90.44 N/mm$^2$. Thorough analysis of the results showed that the LOL-BFRPWF panels exhibited the most favorable properties. However, it is worth noting that the LOL samples demonstrated the lowest value among all the samples tested. Some physical and mechanical properties of the LOL-BFRPWF samples were higher than those of LOL samples, namely δ12 10.36 %, ⊥*MOR* 15.68 %, //*MOR* 19.83 %, ⊥ *MOE* 16.20 %, //*MOE* 17.27 %.

Similarly, some physical and mechanical properties of the LOL-PSM samples were higher than those of the LOL samples ($\delta_{12}$ 3.36 %, ⊥ *MOR* 10.31 %, // *MOR* 13.19 %, ⊥ *MOE* 8.45 %, //*MOE* 14.08 %). Based on the results, it can be concluded that laminated wood materials had higher values (LOL-PSM 14.08 %, LOL-BFRPWF 20.00 %) than the LOL samples that represented their species.

Borri *et al.* (2013) investigated some mechanical properties of low quality wooden beams reinforced with BFRP and flax. They reported that the bending strength of two-layer FFRP and BFRP reinforced low-quality wood beams increased by 38.6 % and 65.8 %, respectively, with the maximum mid-span deflection of 58.2 % and 40.2 %, respectively. Uzel *et al*. (2018) investigated flexural behavior of wooden beams reinforced with different bonding surface materials. The use of retrofitting nets resulted in 34 % increases in terms of load bearing capacity of test specimens.

The values of bending properties of BFRP-glulam beam samples, determined in edgewise samples of this investigation, were also higher than those of unreinforced samples, (Wdowiak-Postulak, 2021). Jinghui Wang and Wang (2020) conducted an investigation on applying BFRP fiber cloth at intervals as a means of reinforcing square long wooden columns. In comparison to the unreinforced wooden columns, the ultimate bearing capacity of the wooden columns with external

BFRP reinforcement exhibited an increase of 8.75 % and 30 %, respectively.

The $\delta_{12}$ increase varied between 3.36 % and 10.36 % in the LOL-PSM (738 kg/m$^3$) and LOL-BFRPWF (788 kg/m$^3$) samples, respectively. The increase of $\perp$*MOR* varied between 10.30 % and 15.68 % in the LOL-PSM (119.74 N/mm$^2$) and LOL-BFRPWF (125.57 N/mm$^2$) samples, respectively. The increase of // *MOR* varied between 13.19 % and 19.83 % in the LOL-PSM (127.71 N/mm$^2$) and LOL-BFRPWF (135.20 N/mm$^2$) samples, respectively. The increase of $\perp$*MOE* varied between 8.45 % and 16.20 % in the LOL-PSM (13558 N/mm$^2$) and LOL-BFRPWF (14526 N/mm$^2$) samples, respectively. The increase of // *MOE* varied between 14.08 % and 17.27 % in the LOL-PSM (15727 N/mm$^2$) and LOL-BFRPWF (16167 N/mm$^2$) samples, respectively (Figure 5).

In the bending strength test, after the maximum load (Fmax) of the test specimen against the applied force was reached, the end of the test varied with the toughness of the test specimen. The load–deformation graphs obtained during the bending strength tests are shown in Figure 6. With some wood materials, after reaching the maximum load, the test sample suddenly breaks, and the test is then completed. Such materials are referred to as brittle materials. With some materials, after reaching the maximum load, the test sample is broken slowly or gradually, before the test is completed.

## 4 CONCLUSIONS
## 4. ZAKLJUČAK

Some physical and mechanical properties of the LOL, LOL-BFRPWF and LOL-PSM samples prepared using PUR adhesive were investigated in this study.

Some physical and mechanical properties of LOL samples were determined: $\delta_{12}$ 714 kg/m$^3$, $\perp$*MOR* 108.55 N/mm$^2$, //*MOR* 127.71 N/mm$^2$, $\perp$*MOE* 12501 N/mm$^2$, // *MOE* 13786 N/mm$^2$, 71.72 N/mm$^2$. The values for LOL-PSM samples were as follows: $\delta_{12}$ 714 kg/m$^3$, $\perp$*MOR* 119.74 N/mm$^2$, //*MOR* 112.82 N/mm$^2$, $\perp$*MOE* 13558 N/mm$^2$, // *MOE* 5727 N/mm$^2$, 80, 90 N/mm$^2$. The values for LOL-BFRPWF samples were as follows: $\delta_{12}$ 788 kg/m$^3$, $\perp$*MOR* 125.57 N/mm$^2$, //*MOR* 135.20 N/mm$^2$, $\perp$*MOE* 14526 N/mm$^2$, // *MOE* 16167 N/mm$^2$.

According to the overall results, the LOL-BFRPWF samples demonstrated the best properties among all the tested samples. It should also be emphasized that the LOL samples exhibited the lowest values among all the samples.

Based on the empirical findings regarding the technical characteristics of BFRPWF and PSM as support materials, the strength of the laminated wood material was observed to be enhanced. Given the substantial enhancements in the resistance properties of the intermediate filling material used in laminated wood, it is advisable to prioritize high-strength properties in furniture and construction materials.

## 5 REFERENCES
## 5. LITERATURA


1. Borri, A.; Corradi, M.; Grazini, A., 2005: Method for flexural reinforcement of old wood beams with CFRP materials. Composites Part B. Engineering, 36: 143-153. https://doi.org/10.1016/j.compositesb.2004.04.013
2. Borri, A.; Corradi, M.; Speranzini, E., 2013: Reinforcement of wood with natural fibers. Composites Part B. Engineering, 53: 1-8. https://doi.org/10.1016/j.compositesb.2013.04.039
3. Bozkurt, A. Y.; Erdin, N., 2000: Wood Anatomy. Istanbul University publication number: 4263, Faculty of forestry publication number: 466, Istanbul, Turkey.
4. Burdurlu, E.; Kilic, M.; Ilce, A. C.; Uzunkavak, O., 2007: The effects of ply organization and loading direction on bending strength and modulus of elasticity in laminated veneer lumber (LVL) obtained from beech (*Fagus orientalis* L.) and lombardy poplar (*Populus nigra* L.). Construction and Building Materials, 21 (8): 1720-1725. https://doi.org/10.1016/j.conbuildmat.2005.05.002
5. Cheng, G.; Li, H.; Li, H.; Ashraf, M., 2022: Compression resistance of short LBL columns with local damage after retrofitting using basalt fiber reinforced polymer. Journal of Building Engineering, 48: 103941. https://doi.org/10.1016/j.jobe.2021.103941
6. de la Rosa, P.; González, M. D. L. N.; Prieto, M. I.; Gómez, E., 2021: Compressive behavior of pieces of wood reinforced with fabrics composed of carbon fiber and basalt fiber. Applied Sciences, 11 (6): 2460. https://doi.org/10.3390/app11062460
7. Elgabbas, F.; Vincent, P.; Ahmed, E. A.; Benmokrane, B., 2016: Experimental testing of basalt-fiber-reinforced polymer bars in concrete beams. Composites Part B. Engineering, 91: 205-218. https://doi.org/10.1016/j.compositesb.2016.01.045
8. Fiore, V.; Di Bella, G.; Valenza, A., 2011: Glass-basalt/epoxy hybrid composites for marine applications. Materials & Design, 32 (4): 2091-2099. https://doi.org/10.1016/j.matdes.2010.11.043
9. Fiore, V.; Scalici, T.; Di Bella, G.; Valenza, A., 2015: A review on basalt fibre and its composites. Composites Part B. Engineering, 74: 74-94. https://doi.org/10.1016/j.compositesb.2014.12.034
10. Gao, Y.; Zhou, Y.; Zhou, J.; Kong, X.; Zhang, B.; Liu, S., 2020: Blast responses of one-way sea-sand seawater concrete slabs reinforced with BFRP bars. Construction and Building Materials, 232: 117254. https://doi.org/10.1016/j.conbuildmat.2019.117254
11. Garg, N.; Shrivastava, S., 2019: Environmental and economic comparison of FRP reinforcements and steel reinforcements in concrete beams based on design strength parameter. In: Proceedings of the UKIERI Concrete Congress. Jalandhar, India.
12. Gao, P.; Huang, J. T.; Zhou, A.; Zhu, D.Y.; Wei, S.; Li, T.; Dai, D. J., 2019: Experimental research on axial compression of high-strength concrete column strengthened with BFRP and CFRP. Industrial Construction, 49: 139-144 + 160. https://doi.org/10.13204/j.gyjz201909024

13. Jian, B.; Li, H.; Zhou, K.; Ashraf, M.; Xiong, Z.; Zheng, X., 2022: Mechanical evaluation on BFRP laminated bamboo lumber columns under eccentric compression. Advances in Structural Engineering, 26 (5): 809-823. https://doi.org/10.1177/13694332221138312
14. Johns, K. C.; Lacroix, S., 2000: Composite reinforcement of timber in bending. Canadian Journal of Civil Engineering, 27: 899-906.
15. Kramár, S.; Trcala, M.; Chitbanyong, K.; Král, P.; Puangsin, B., 2020: Basalt-fiber-reinforced polyvinyl acetate resin: a coating for ductile plywood samples. Materials, 13 (1): 49. https://doi.org/10.3390/ma13010049
16. Keskin, H., 2004: Technological properties of laminated wood materials made up with the combination of oak (*Quercus petraea* Liebl.) wood and Scots pine (*Pinus sylvestris* Lipsky) wood and possibilities of using them. Gazi University Journal of Science, 17 (4): 121-131.
17. Keskin, H., 2009: Impact of impregnation chemical on the bending strength of solid and laminated wood materials. Materials & Design, 30 (3): 796-803. https://doi.org/10.1016/j.matdes.2008.05.043
18. Kufel, A.; Kuciel, S., 2019: Basalt/wood hybrid composites based on polypropylene: morphology, processing properties, and mechanical and thermal expansion performance. Materials, 12: 2557. https://doi.org/10.3390/ma12162557
19. Liu, Q.; Ma, S.; Han, X., 2020: Study on the flexural behavior of poplar beams externally strengthened by BFRP strips. Journal of Wood Science, 66: 1-13. https://doi.org/10.1186/s10086-020-01887-y
20. Lohmus, R.; Kallakas, H.; Tuhkanen, E.; Gulik, V.; Kiisk, M.; Saal, K.; Kalamees, T., 2021: The effect of prestressing and temperature on tensile strength of basalt fiber-reinforced plywood. Materials, 14 (16): 4701. https://doi.org/10.3390/ma14164701
21. Lopez-Anido, R.; Michael, A. P.; Sandford, T. C., 2003: Experimental characterization of FRP composite-wood pile structural response by bending tests. Marine Structures, 16: 257-274. https://doi.org/10.1016/S0951-8339(03)00021-2
22. Núñez-Decap, M.; Sandoval-Valderrama, B.; Opazo-Carlsson, C.; Moya-Rojas, B.; Vidal-Vega, M.; Opazo-Vega, A., 2023: Use of carbon and basalt fibers with adhesives to ımprove physical and mechanical properties of laminated veneer lumber. Applied Sciences, 13 (18): 10032. https://doi.org/10.3390/app12105114
23. Patnaik, A.; Puli, R.; Mylavarapu, R., 2004: Basalt FRP. A new FRP material for infrastructure market. In: Proceedings of the 4th International Conference Advanced Composite Materials in Bridges and Structures. ACMBS-IV, Montreal, Canada.
24. Rahayu, I.; Denaud, L.; Marchal, R.; Darmawan, W., 2015: Ten new poplar cultivars provide laminated veneer lumber for structural application. Annals of Forest Science, 72: 705-715. https://doi.org/10.1007/s13595-014-0422-0
25. Rescalvo, F. J.; Duriot, R.; Pot, G.; Gallego, A.; Denaud, L., 2020: Enhancement of bending properties of douglas-fir and poplar laminate veneer lumber (LVL) beams with carbon and basalt fibers reinforcement. Construction and Building Materials, 263: 120185. https://doi.org/10.1016/j.conbuildmat.2020.120185
26. Rescalvo, F. J.: Duriot, R.: Pot, G.; Gallego, A.; 2023: Mechanical behaviour of poplar laminated veneer lumber with fiber reinforced polymer under shear and compression stresses. Wood Material Science & Engineering, 18 (3): 893-901. https://doi.org/10.1080/17480272.2022.2086819
27. Sim, J.; Park, C.; Moon, D., 2005: Characteristics of basalt fiber as a strengthening material for concrete structures. Composites Part B. Engineering, 36 (6-7): 504-512. https://doi.org/10.1016/j.compositesb.2005.02.002
28. Song, J.; Gao, W. Y.; Ouyang, L. J.; Zeng, J. J.; Yang, J.; Liu, W. D., 2021: Compressive behavior of heat-damaged square concrete prisms confined with basalt fiber-reinforced polymer jackets. Engineering Structures, 242: 112504. https://doi.org/10.1016/j.engstruct.2021.112504
29. Subagia, I. A.; Kim, Y.; Tijing, L. D.; Kim, C. S.; Shon, H. K., 2014: Effect of stacking sequence on the flexural properties of hybrid composites reinforced with carbon and basalt fibers. Composites Part B. Engineering, 58: 251-258. https://doi.org/10.1016/j.compositesb.2013.10.027
30. Uzel, M.; Togay, A.; Anil, O.; Sogutlu, C., 2018: Experimental investigation of flexural behavior of glulam beams reinforced with different bonding surface materials. Construction and Building Materials, 158: 149-163. https://doi.org/10.1016/j.conbuildmat.2017.10.033
31. Wang, X.; Shi, J.; Liu, J.; Yang, L.; Wu, Z., 2014: Creep behavior of basalt fiber reinforced polymer tendons for prestressing application. Materials & Design, 59: 558-564. https://doi.org/10.1016/j.matdes.2014.03.009
32. Wang, B.; Bachtiar, E. V.; Yan, L.; Kasal, B.; Fiore, V., 2019: Flax, basalt, E-Glass FRP and their hybrid FRP strengthened wood beams: An experimental study. Polymers, 11 (8): 1255. https://doi.org/10.3390/polym11081255
33. Wang, J. H.; Wang, G. B.; 2020: Experimental research on the mechanical properties Xinjiang long rectangular-section popular column strengthened by basalt fiber alternately under axial compression. Industrial Construction, 50: 44-48.
34. Wdowiak-Postulak, A.; Swit, G., 2021: Behavior of glulam beams strengthened in bending with BFRP fabrics. Civil and Environmental Engineering Reports, 31 (2): 1-14 https://doi.org/10. 10.2478/ceer-2021-0016
35. Wdowiak-Postulak, A.; Bahleda, F.; Prokop, J., 2023: An experimental and numerical analysis of glued laminated beams strengthened by pre-stressed basalt fibre-reinforced polymer bars. Materials, 16 (7): 2776. https://doi.org/10.3390/ma16072776
36. Wu, G.; Gu, D. S.; Jiang, J. B.; Wu, Z. H.; Hu, X. Q., 2007: Comparative study on seismic performance of circular concrete columns strengthened with BFRP and CFRP composites. Industrial Construction, 37 (6): 19-23.
37. Wu, Z.; Wang, X.; Iwashita, K.; Sasaki, T.; Hamaguchi, Y., 2010: Tensile fatigue behaviour of FRP and hybrid FRP sheets. Composites Part B. Engineering, 41 (5): 396-402. https://doi.org/10.1016/j.compositesb.2010.02.001
38. Wu, Z.; Wang, X.; Wu, G., 2012: Advancement of structural safety and sustainability with basalt fiber reinforced polymers. In: Proceedings of the 6th International Conference on FRP Composites in Civil Engineering. CICE, Roma, Italy.
39. Wu, X., 2020: Research progress on application of basalt fiber in civil engineering. Bulletin of the Chinese Ceramic Society, 39 (4): 1043-1049.
40. Zhou, W.; Li, H.; Mohrmann, S.; Li, H.; Xiong, Z.; Lorenzo, R., 2022: Evaluation on the axial compression mechanical properties of short BFRP laminated bamboo lumber columns. Journal of Building Engineering, 5: 104483. https://doi.org/10.1016/j.jobe.2022.104483
41. Zoghi, M., 2013: The International Handbook of FRP Composites in Civil Engineering; CRC Press: Florida, FL, USA.

42. ***TS 5497 EN 408, 2006: Timber Structures – Structural and Glued Laminated Timber – Determination of Some Physical and Mechanical Properties. TSE, Ankara, Institute of Turkish Standards, Ankara, Turkey, 2006.
43. ***TS 2472, 1976: Wood – Determination of Density for Physical and Mechanical Tests. Institute of Turkish Standards, Ankara, Turkey, 1976.
44. ***TS 2474, 1976: Wood – Determination of Ultimate Strength in Static Bending. Institute of Turkish Standards, Ankara, Turkey, 1976.
45. ***TS EN 326-1, 1999: Wood – Based Samples – Sampling, Cutting and Inspection. Part 1: Sampling Test Pieces and Expression of Test Results. Institute of Turkish Standards, Ankara, Turkey, 1999.
46. ***TS 2478, 1976: Wood – Determination of Modulus of Elasticity in Static Bending. Institute of Turkish Standards, Ankara, Turkey, 1978.

**Corresponding address:**

**ABDURRAHMAN KARAMAN**
Usak University, Banaz Vocational School, Forestry Department, Usak, TURKEY,
e-mail: abdurrahman.karaman@usak.edu.tr

Bachir Bouhamida[1], Abderrazek Merzoug[1,2], Zouaoui Sereir[1], Ali Kilic[2], Zeki Candan*[3,4]

# Chemical, Thermal, and Morphological Properties of Sustainable Lignocellulosic Biomaterial

# Kemijska, toplinska i morfološka svojstva održivoga lignoceluloznog biomaterijala

**ORIGINAL SCIENTIFIC PAPER**
**Izvorni znanstveni rad**
Received – prispjelo: 8. 12. 2023.
Accepted – prihvaćeno: 29. 4. 2024.
UDK: 630*86; 674.8
https://doi.org/10.5552/drvind.2024.0176



**ABSTRACT** • *By the present paper, an experimental investigation was proposed to compare the morphological, chemical and mechanical properties of the Petiole Date Palm Wood (PDPW) collected from north and south of Algeria. Both regions have very distinctive climatic conditions – wet conditions in the north (near the Mediterranean Sea) and semi-arid conditions in the south Biskra. To achieve this aim, large quantities of waste from PDPW were collected, cleaned, and cut according to the normalization specific to each type of test. After that, scanning electron micrographs, infrared spectroscopy, dynamic mechanical thermal analysis (DMTA) and thermogravimetric analysis were made, and moisture content (MC) and water absorption (WA) were determined, to compare the effect of the different environmental conditions. From the results obtained, petiole date palm wood typical for the southern region had a high fiber content, attributed to its low porosity and excellent mechanical properties, which resulted in low water absorption. In contrast, the northern petiole wood reveals a higher glass transition temperature ($T_g$) and significant damping coefficient. At comparable relative density values, the specific properties were found to be comparable to those of balsa, foams and metallic honeycombs.*

**KEYWORDS:** *petiole date palm wood; mechanical properties; glass transition; porosity; damping*

**SAŽETAK** • *U radu je predstavljeno eksperimentalno istraživanje morfoloških, kemijskih i mehaničkih svojstava drva peteljki palme datulje (PDPW) prikupljenih na sjeveru i jugu Alžira. Te dvije regije imaju vrlo različite klimatske uvjete: na sjeveru su vlažni uvjeti (u blizini Sredozemnog mora), a na jugu Biskre klima je polusušna. Kako bi se postigao cilj istraživanja, skupljene su velike količine otpada PDPW-a, koje su očišćene i izrezane prema normi za svaku vrstu ispitivanja. Na pripremljenim uzorcima napravljena je pretražna elektronska mikrografija, infracrvena spektroskopija, dinamička mehanička toplinska analiza i termogravimetrijska analiza te je određen sadržaj vode (MC) i upijanje vode (WA) kako bi se odredio učinak različitih okolišnih uvjeta na svojstva PDPW-a. Rezultati istraživanja pokazali su da drvo peteljki palme datulje iz južne regije ima visok sadržaj vlakana, što se pripisuje njegovoj niskoj poroznosti i izvrsnim mehaničkim svojstvima, a rezultiralo je slabim upijanjem vode.*

* Corresponding author
[1] Authors are researchers at University of Science and Technology of Oran, Faculty of Mechanical Engineering, Laboratory of Composite Structures and Innovative Materials, Oran, Algeria.
[2] Authors are researchers at Istanbul Technical University, Faculty of Textile Technologies and Design, TEMAG Labs, Istanbul, Türkiye.
[3] Author is researcher at Department of Forest Industrial Engineering, Istanbul University-Cerrahpasa, İstanbul, Türkiye. https://orcid.org/0000-0002-4937-7904
[4] Author is researcher at Biomaterials and Nanotechnology Research Group & BioNanoTeam, İstanbul, Türkiye. https://orcid.org/0000-0002-4937-7904

*Nasuprot tome, drvo peteljke palme datulje iz sjeverne regije ima veću temperaturu staklišta ($T_g$) i koeficijent prigušenja. U usporedbi s materijalima podjednake relativne gustoće, utvrđeno je da su specifična svojstva PDPW-a usporediva s onima balze, pjene i metalnog saća.*

**KLJUČNE RIJEČI:** *drvo peteljke palme datulje; mehanička svojstva; staklište; poroznost; prigušenje*

## 1 INTRODUCTION
## 1. UVOD

Wood, a material composed of cellulose, hemicelluloses, lignin, and other components, exhibits viscoelastic properties. Its use in structural applications dates back to ancient times (Dave *et al*., 2018). Due to its renewability, affordability, specific strength, and ability to be tailored for various mechanical needs, wood is a promising ecological substitute for synthetic materials like carbon, glass fiber, and foams. These synthetic materials are commonly used in the construction of bridges, furniture, acoustic panels, and the interior structures of vehicles and aircraft. Consequently, researchers have increasingly focused on exploring wood, either independently or as an additive, in recent years (Candan *et al*., 2016). Atas *et al*. (2010) have used the balsa wood as a core of sandwich panels, demonstrating superior impact resistance compared to those using polyvinyl chloride (PVC) foam. Sofia *et al*. (2007) conducted a characterization study on cork oak wood, suggesting its potential application in solid wood structures due to its satisfactory physical properties. Hassanin *et al*. (2016) produced particleboards based on pine wood particles and polyester resins and observed significant increases of 19 % and 311.3 % in flexural strength and internal bending strength, respectively, compared to commercial wood particleboards.

Climate and environmental factors strongly influence the properties of biomass due to its hygroscopic nature (Makarona *et al*., 2017). Parameters such as density, wood species, temperature, water absorption (*WA*), and moisture content (*MC*) significantly impact wood performance (Hamdan *et al*., 2000). Hence, it is crucial to ascertain these factors to ensure the reliability of wood applications. Several studies have explored the relationship between moisture content and mechanical properties of wood. Oloyede *et al*. (2000) observed that drying wood in an oven at 50 °C increases tensile strength, while using a microwave at maximum power decreases tensile properties. However, the moisture content and damping properties of specimens were proportional during dynamic loading conditions. Benzidane *et al*. (2018) conducted experimental analyses on date palm wood under quasi-static and cyclic loading (fatigue), revealing that cutting wood in different directions significantly affects mechanical stiffness and dissipative energy. Srivaro *et al*. (2015) investigated the mechanical properties of oil palm wood in sandwich structures and observed that the longitudinal fiber direction exhibits greater rigidity compared to the perpendicular direction.

When using wood materials for industrial structures or as reinforcement for polymers, thermal stability becomes a crucial parameter to consider. Thermogravimetric analysis (TGA) stands out as the most employed technique for assessing the thermal decomposition of polymeric materials. Typically, the degradation of wood under the influence of temperature involves four main reactions: evaporation of water content, decomposition of hemicelluloses followed by cellulose, and ultimately, a gradual decomposition of lignin over a broader temperature range (Merzoug *et al*., 2020; Maache *et al*., 2017; Kamperidou, 2021).

The cross-linking of lignin and the orientation of wood grain significantly influence the viscoelastic properties of wood materials (Olsson *et al*., 1992; Placet *et al*., 2007). The harmonic test, dynamic thermal mechanical analysis (DMTA), is one of the high precision techniques to evaluate the viscoelastic properties and the glass transition of materials. Recently, there has been a growing interest among researchers in measuring the viscoelastic properties of wood materials along their longitudinal direction using DMTA (Backman *et al*., 2001; Li *et al.,* 2021; Li *et al.,* 2023). However, there remains a limited amount of research concerning the dynamic mechanical behavior of wood along different grain directions.

The date palm tree (*Phoenix dactylifera*), belonging to the palm tree family, is primarily grown for human consumption. These trees are widespread across the Middle East and Northern Africa, with significant potential. Globally, there are over 100 million date palm trees (Abdal-hay *et al*., 2012), and each harvest season results in approximately 2 million tons of date palm wood waste. Despite its lightweight nature (with an average density of 210 kg/m³), from an economic and environmental perspective, the utilization of date palm wood waste is a promising project. There appears to be a lack of investigation into the use of petiole date palm wood as a core for sandwich composites (Benzidane *et al*., 2022). However, no reference is found in the literature regarding the thermophysical, chemical, and dynamic mechanical properties of the petiole date palm wood. Knowledge of these properties enables the development of more effective industrial processes and mate-

rials. Thus, this research aims to assess the physical, thermal, and dynamic mechanical properties of petiole date palm wood coming from two distinct environmental regions. The results found suggest that the PDPW is suitable as a core for sandwich composite panels.

## 2 MATERIALS AND METHODS
## 2. MATERIJALI I METODE

### 2.1 Materials
### 2.1. Materijali

Around 18 million date palm trees planted in Algeria cover an area of 164 695 hectares. The petiole wood part is considered a natural unidirectional (UD)-composite structure. It has an Eiffel's tower feet shape, with a symmetry plane (Benzidane *et al*., 2018). PDPW used in this study was harvested in two different environmental growing regions: the first region was the oasis area in the south of Algeria (Biskra), where the climate is hot and dry. The second region is a humid region close to the Mediterranean (Sidi- bel abbes). The average age of PDP wood samples ranged from 70 to 80 years.

### 2.2 Methods
### 2.2. Metode

#### 2.2.1 Morphological analysis
#### 2.2.1. Morfološka analiza

Microscopic examinations of the PDPW specimens and their interfacial (fiber/matrix) characteristics were conducted using a Tescan Vega3 scanning electron microscope (SEM) at 10 kV and 15 kV. The specimens were coated with gold and mounted on aluminum holders using double-sided electrically conducting carbon adhesive tabs before analysis (Horiyama *et al*., 2023).

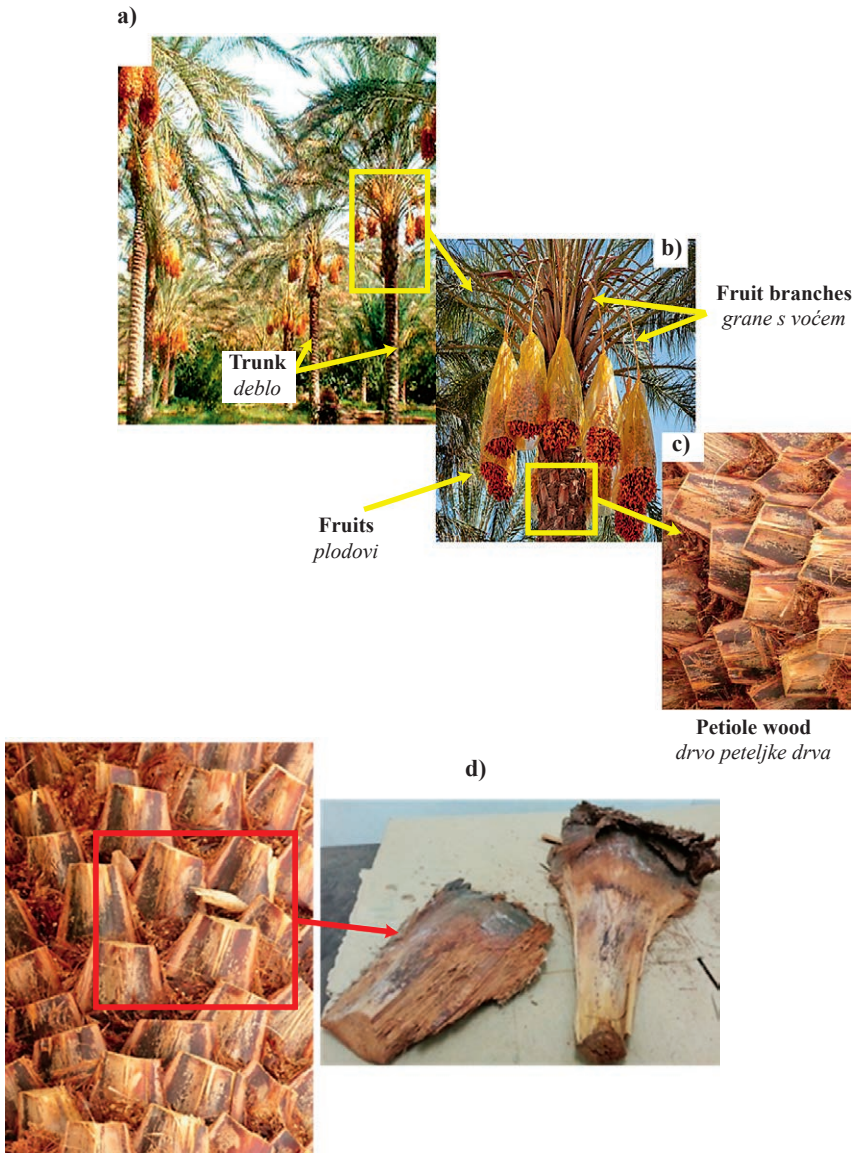


**Figure 1** Date palm tree morphology: a) Date palm trees, b) Zoom on top parts, c) Petiole wood, d) Petiole wood collected
**Slika 1.** Morfologija stabla palme datulje: a) stablo palme datulje, b) povećani gornji dijelovi, c) drvo peteljke, d) skupljeno drvo peteljke

a) b) c)

**Figure 2** Measurement steps of *MC*: a) Normalized specimens, b) Balance, c) Oven drying at 103 °C
**Slika 2.** Koraci pri mjerenju sadržaja vode: a) pripremljeni uzorci, b) vaganje, c) sušenje u sušioniku na 103 °C

### 2.2.2 Fourier transfer infrared spectroscopy (ATR-FTIR)
### 2.2.2. Infracrvena spektroskopija s Fourierovom transformacijom (ATR-FTIR)

The ATR-FTIR spectra of the PDPW (Northern / Southern) were carried out using a Thermo Scientific Nicolet iS10 type device with its own quantitative analysis software. The spectrum was obtained with a scanning speed of 32 acquisitions between 500 and 4000 $cm^{-1}$ with a resolution of 2 $cm^{-1}$.

### 2.2.3 Physical characterization
### 2.2.3. Određivanje fizičkih svojstava

*Moisture content*

The European standard (EN 322) was followed. The volume ($V$) was assessed through the water displacement method and the weights were measured both in wet and dry conditions (dried at 103 ± 2 °C). PDPW specimens were created with dimension 20 mm × 20 mm × 20 mm. The moisture content of both PDPW regions (Northern/ Southern) was evaluated using the following formula.

$$MC = \frac{M_h - M_o}{M_h} \cdot 100 \quad (1)$$

Where, $M_h$ (g) and $M_o$ (g) represent the wet and dry masses, respectively.

*Water absorption*

The water uptake was carried out for PDPW specimens for both regions based on ASTM D1037-99 Standard. First, the wood was dried in oven at (103±2) °C until the weight was constant. Next, the weight was measured, and it was considered as the initial weight when using a numerical balance. Then, the specimens were immersed in distilled water (20 °C) and weighed at a specific time (24, 48 and 72h). The gain weight difference was used for the estimation of water uptake of the specimens. The formula below represents the water uptake equation used.

$$WA = \frac{W_t - W_i}{W_t} \cdot 100 \quad (2)$$

Where, $W_t$ (g) represents the wet weight specimen and $W_i$ (g) represents the oven-dried specimen at $t=0$ time interval.

### 2.2.4 Thermogravimetric analysis (TGA/DTA)
### 2.2.4. Termogravimetrijska analiza (TGA/DTA)

Thermogravimetric analysis was conducted using a Mettler Toledo TGA/DSC 3+ star system (located at the University 8 Mai 1954, Guelma Algeria) under a dynamic nitrogen atmosphere heating at room temperature from (20 °C) to 600 °C at a heating rate of 10 °C/min. Specimens weighing approximately 6 mg were used, and their weight changes were measured throughout the process (Ma *et al.*, 2018).

### 2.2.5 Dynamic Mechanical Thermal Analysis (DMTA)
### 2.2.5. Dinamička mehanička toplinska analiza (DMTA)

Dynamic Mechanical Thermal Analyzer (Hitachi, Japan) located in the "Thermal Analysis Laboratory" and "Nanotechnology Laboratory" at Istanbul University-Cerrahpasa was used to evaluate viscoelas-

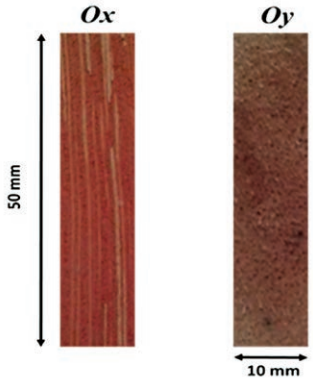


**Figure 3** DMTA specimens
**Slika 3.** Uzorci za DMTA analizu

tic performance properties of PDPW (North/South) specimens. Dimensions of the samples were 50 mm by 10 mm by 2 mm in both fiber directions (Figure 3). All analyses were conducted in dual cantilever mode (3-point bending) at a frequency of 1 Hz, with temperatures ranging from 30 °C to 150 °C and an increased heating rate of 5 °C/min. Three runs were performed for each group (Toubia *et al*., 2019).

## 3 RESULTS AND DISCUSSION
## 3. REZULTATI I RASPRAVA

### 3.1 Morphological analysis
### 3.1. Morfološka analiza

Scanning electron micrographs of petiole date palm wood (north and south) are shown in Figure 4. The transversal surface images of PDPW (northern/southern) showed quasi-unidirectional natural composite materials: technical and bundle fibers reinforced tissue parenchyma matrices. The surface of PDPW from the northern region exhibits a higher presence of holes compared to that from the southern region. However, the amount of fibers in PDPW from the southern region is notably higher than that in PDPW from the northern region, which significantly affects physical properties, especially density. Figure 4 (c and d) depicts the longitudinal surface of PDP woods, clearly showing the direction of fibers and their interface with the matrix. It is evident that PDPWs exhibits better adhesion between its components compared to PDPWn from the northern region. Micro-cracks are observed in the inflated parenchyma matrix of PDPW from the northern region due to environmental factors, a phenomenon also reported by Benzidane *et al*. (2018).

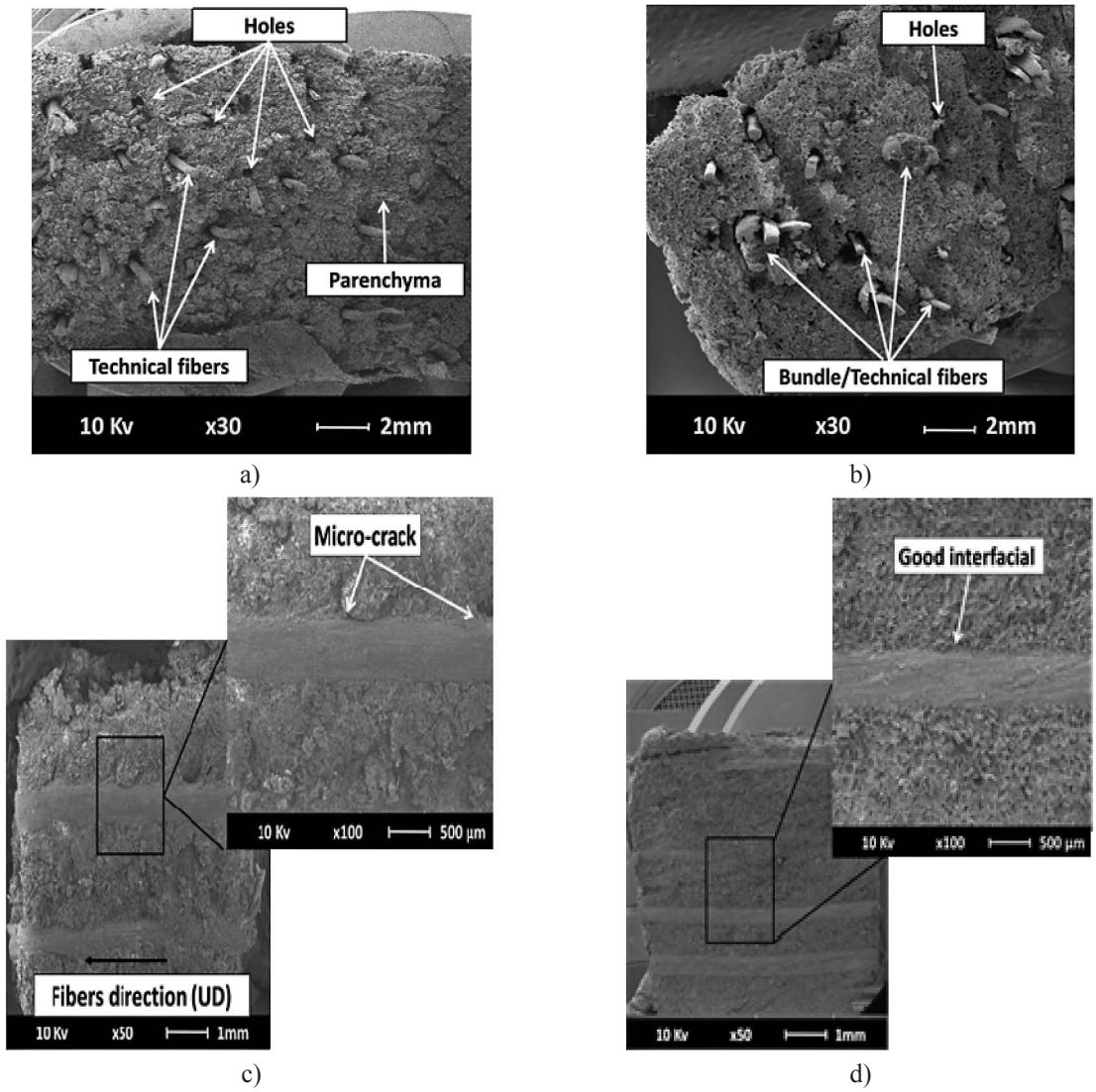


**Figure 4** SEM images of PDPW from north and south in both grain directions: a) *Ox* direction PDPW North, b) *Ox* direction PDPW South, c) *Oy* direction PDPW North, d) *Oy* direction PDPW South
**Slika 4.** SEM fotografije PDPW-a iz sjeverne i južne regije u oba smjera vlakanaca: a) *Ox* smjer PDPW-a iz sjeverne regije, b) *Ox* smjer PDPW-a iz južne regije, c) *Oy* smjer PDPW-a iz sjeverne regije, d) *Oy* smjer PDPW-a iz južne regije

### 3.2 Chemical analysis (FTIR)
### 3.2. Kemijska analiza (FTIR)

The infrared spectroscopy was used to define the chemical composition of PDPW of north and south regions as shown in Figure5. Similar peaks of both spectra correspond to northern and southern PDPW without deviation (1034, 1240, 1595, 2848, 2925 and 3351), but with different intensities. The band groups presented on the spectra are associated with hemicelluloses, α-cellulose and lignin. For instance, the strong peak at 1034 $cm^{-1}$ is associated with the O-H and C-O stretching mode of polysaccharides in cellulose groups (Romanzini *et al*., 2012). The band at 1240 $cm^{-1}$ is related to C-O ether, phenol and ester vibration groups, this being attributed to the presence of waxes, lignin and xylan units in the wood surface (Esteves *et al*., 2013). Further, both peaks 2925 and 2848 $cm^{-1}$ "C-$H_2$ and C-H bands" defined the acetyl group from hemicelluloses and cellulose components. A broad and intense peak was observed at 3351 $cm^{-1}$ associated with hydroxyl groups O-H present in the cellulose, water, and lignin structure (Gonultas *et al*., 2018). The transmittance intensity of the southern PDPW is the lowest observed, which means a lower amount of hydroxyl groups and lignin in this wood region compared to the north region.

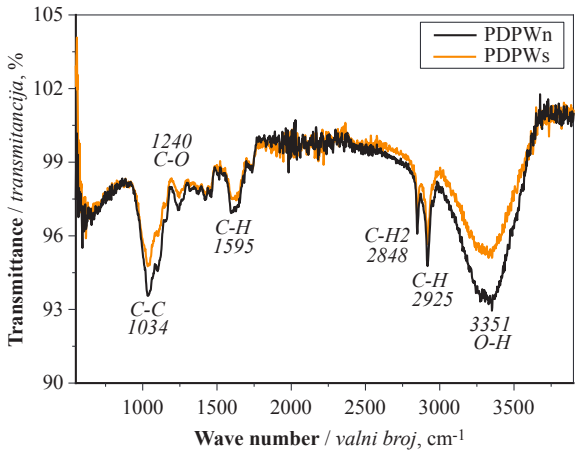


**Figure 5** Fourier transform infrared spectroscopy (FTIR) spectrogram of PDPW (North/South)
**Slika 5.** Spektar PDPW-a (sjever/jug) dobiven infracrvenom spektroskopijom s Fourierovom transformacijom (FTIR)

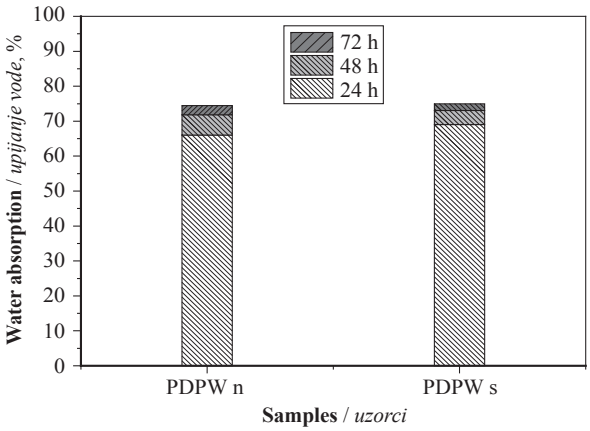


**Figure 6** Water absorption evaluation of PDPW specimens
**Slika 6.** Rezultati upijanja vode PDPW uzoraka

### 3.3 Physical analysis
### 3.3. Analiza fizičkih svojstava

#### 3.3.1 Water absorption
#### 3.3.1. Upijanje vode

Figure 6 presents the water absorption patterns for 24, 48, and 72 hours of PDPWn and PDPWs. The PDPWs shows a maximum water absorption rate of 74 %, which is 3 % higher than that of PDPWn. It could be explained by the filling up of capillaries, diffusion phenomena, and the cellular wall of wood. The high-water absorption phase was observed after 24h. The PDPWs absorbed 69.02 % of water, which was higher by 13 % than PDPWn due to the high fiber ratio and the presence of fewer holes. The free movement of water due to large holes and porosities in PDPWn resulted in a slow water uptake. Next, the immersion times of 48 hours and 72 hours showed a small amount of water absorption, where the PDPWs saw a slight increase of 5 % and 2 %, respectively, while PDPWn increased by 16 % and 4 %. The process of saturation occurs at a slow pace until the wood grain is completely saturated, including its fibers.

#### 3.3.2 Moisture content
#### 3.3.2. Sadržaj vode

Moisture content plays a crucial role in the thermal and mechanical properties of polymeric materials, especially biomass. Figure 7 presents the evaluation of PDPW moisture content of both regions Northern and Southern dried at 102 °C for 24 h. Similar curves are shown with different values. After one hour of drying, a high quantity of water was evaporated from both PDPW. In particular, the PDPWn (lost around 12 % of its initial weight) due the concentration of water in this wood region and the easier movement of water in large

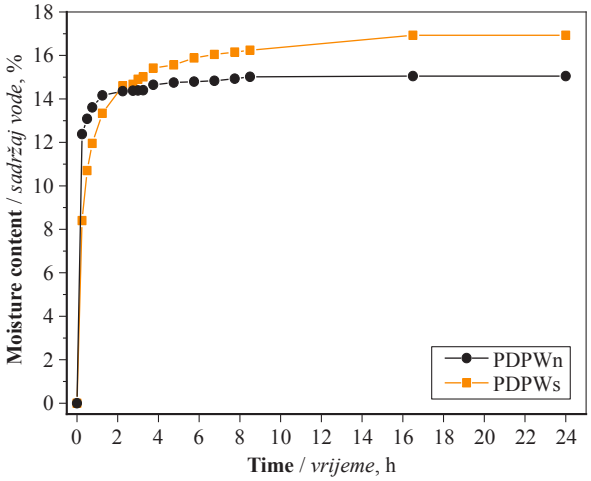


**Figure 7** Moisture content evaluation of PDPWood specimens
**Slika 7.** Evaluacija sadržaja vode PDPW uzoraka

holes of PDPWn. In comparison to PDPWs, the smaller hole dimensions, good adhesion between fibers and matrix, and higher fiber ratio result in less water evaporation. Subsequently, the moisture content gradually stabilizes for PDPW of both regions. The moisture content of PDPWs was around 17 %, which is 3 % higher than that of PDPWn. The morphologies and environmental factors of PDPW significantly influence its moisture content properties.

### 3.4 TGA/DTG
### 3.4. TGA/DTG

In order to study the thermal stability behavior of PDPW (Northern/ Southern), all specimens were subjected to heating in the Mettler Toledo TGA/DSC 3+ device. Figure 8 (a, b) displays the TGA curve and its DTG derivative obtained for the PDPW. Despite showing a similar trend, there were variations in weight loss percentages, with PDPWn and PDPWs losing 89.97 % and 92.43 % of their initial weight, respectively. During the initial heating of specimens, the water evaporation started at around 40 °C and was completed at roughly 128 °C. The same was observed in the case of balsa and oak wood (Tranvan *et al*., 2017; Ceylan *et al*., 2014). The first decomposition stage was attributed to water evaporation, accounting for 12.78 % and 11 % of weight loss for PDPW from the Northern and Southern regions, respectively. Subsequently, an active decomposition stage was evident, comprising three domains (Figure 8): 1) hemicellulose decomposition, 2) cellulose decomposition, and 3) lignin decomposition occurring between 405 and 500 °C (Todaro *et al.,* 2017). The decompositions of hemicelluloses and cellulose presented the major weight loss that occurred in the temperature range of 175-405 °C, where PDPWn gradually lost 54.87 % of its weight. Regarding the PDPWs, a dramatic weight loss of 61.57 % was noted. Ceylan *et al*. (2014) explained that decomposition in the temperature range of 180-350 °C is attributed to the depolymerization of hemicelluloses and the random cleavage of glycosidic linkages of cellulose. In addition, passive decomposition stages displayed quasi-constant values associated with lignin residues or char, accounting for 32.35 % PDPWn and 27.43 % of PDPWs. The products of cellulose degradation contain non-degraded fillers and carbon residues (Maache *et al*., 2017). The petiole date palm wood exhibited a similar thermal stability compared to that of balsa wood (Hellmeister *et al*., 2021; Marwanto *et al*., 2021).

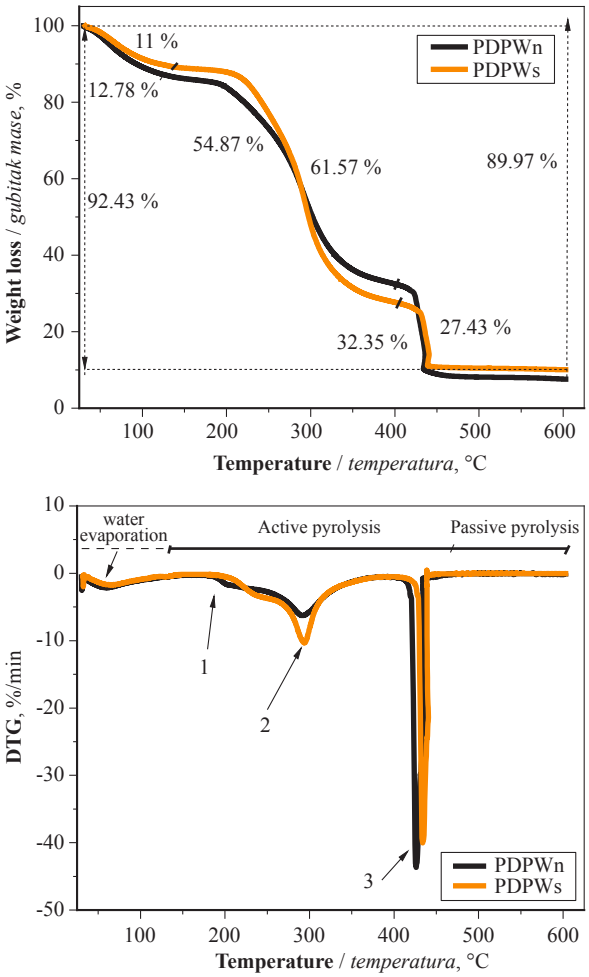


**Figure 8** Thermogravimetric analysis test results of PDPW (north/ south)
**Slika 8.** Rezultati termogravimetrijske analize PDPW-a (sjever/jug)

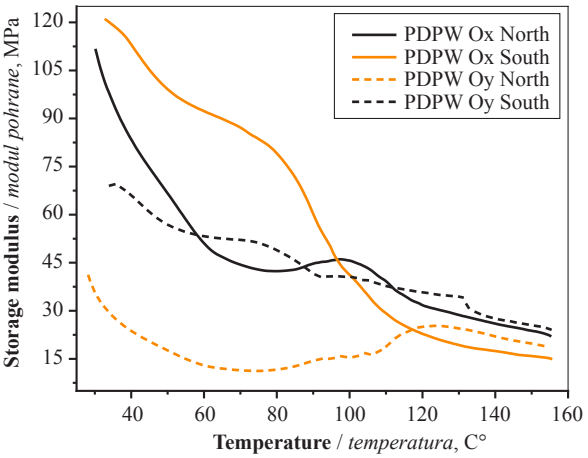


**Figure 9** Storage modulus of PDPW (north/south) for both directions (*Ox* and *Oy*)
**Slika 9.** Modul pohrane PDPW-a (sjever/jug) za oba smjera (*Ox* i *Oy*)

### 3.5 Dynamic Mechanical Thermal Analysis
### 3.5. Dinamička mehanička toplinska analiza

Stiffness, damping and glass transition of PDP Wood specimens were studied using dynamic mechanical thermal analysis (DMTA). The grain direction and environment region of specimens were considered as relevant parameters for the investigation. The results are plotted as storage modulus (*E*'), loss modulus (*E*") and loss factor (tan δ).

### 3.5.1 Storage modulus (E')
### 3.5.1. Modul pohrane (*E*')

The variation of storage modulus as the function of temperature for PDP wood specimens at the frequency of 1 Hz is given in Figure 9. The results have shown similar curves with different values for the same groups (regions). Values of the specimens of perpendicular fiber direction (*Ox*) were significantly higher than those of the corresponding parallel specimens, where the higher value of 120 MPa was noted for southern wood. Fiber rate, fiber performance and its length played a significant role for this property. In the case of perpendicular fiber direction (*Oy*), *E*' of PDPWs was considerably more important than that of PDPWn (higher by 40 %). This could be due to holes effect, poor interfacial adhesion (fiber/ matrix) and stat of parenchyma. The storage modulus of all specimens was unproportioned to the temperature, especially PDPWn wood (both directions), where its *E*' decreased dramatically until 70 °C. This diminution is due to the micro-Brownian movement of polymer chains as the polymer approaches the glass transition (Ornaghi *et al*., 2011). Plus, due to the augmentation of fully separated fibers, fibers are not susceptible to bonding again. It is known that PDPWs undergo a gradual diminution of E' before glass transition due to less holes, high fiber rate and strong interfacial adhesion (Sreekala *et al*., 2005). Below $T_g$, northern wood *E*' was increased slightly due to the final evaporation of water from fibers. However, the southern wood continued to diminish *E*' because the evaporation of water was the same for both fiber and parenchyma matrix.

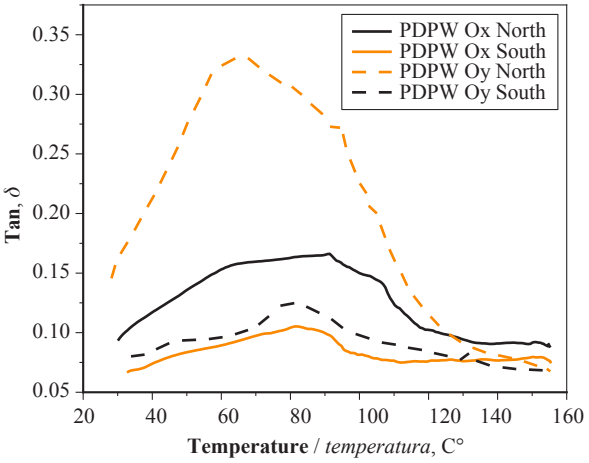


**Figure 10** Loss factor vs temperature of PDPW (north/south) for both directions (*Ox* and *Oy*)
**Slika 10.** Faktor gubitka s obzirom na temperaturu PDPW-a (sjever/jug) za oba smjera (*Ox* i *Oy*)

**Table 1** Glass transition temperature values at 1 Hz and damping of PDPW
**Tablica 1.** Vrijednosti temperature stakliša PDPW-a pri 1 Hz i prigušenje PDPW-a

| PDPW | Fiber direction *Smjer vlakana* | tan δ | Temperature, °C *Temperatura, °C* |
|---|---|---|---|
| **Northern** *sjeverna regija* | *Ox* | 0.15 | 67.7 |
| | *Oy* | 0.33 | 65.43 |
| **Southern** *južna regija* | *Ox* | 0.10 | 81.44 |
| | *Oy* | 0.12 | 79.55 |

### 3.5.2 Loss factor (tan δ)
### 3.5.2. Faktor gubitka (tan δ)

Loss factor variation of northern and southern PDPW for two different fiber directions as the function of temperature is shown in Figure 10. Tan δ is explained by the report of E"/E' and it can be called damping. It was very high in the parallel direction of PDPWn (0.33), due to the diminution of *E*' when the temperature increased. In addition, lower fiber rate and the presence of porosities led to free mobility of polymer molecules. Besides, it was observed that PDPWn in the perpendicular fibers was damper (higher by 20 %) than PDPWs in parallel direction even though its storage modulus was less than that of PDPWn (*Ox*). Furthermore, no considerable change between the fiber direction properties of southern PDPWood was observed. The glass transition of PDPW was similar in the case of the same regions (Table 1). In other words, the $T_g$ of PDPW was dependent on the environment more than on the fiber direction.

## 4 CONCLUSIONS
## 4. ZAKLJUČAK

Due to their lightweight nature and mechanical performance, foams, honeycomb structures, and balsa wood are widely used in mechanical technology as core materials for sandwich structures. However, their prices remain one of the major disadvantages. In this study, an experimental investigation on the physical, thermal and dissipative properties of new bio-mass potential, PDPW "Petiole Date Palm Wood", from two different Algerian regions was conducted. The Northern region (Sidi Bel Abbes), located near the Mediterranean Sea, is characterized by a humid and rainy climate, while the Southern region (Biskra) is a semi-arid area with hot and dry weather. The results of this study can be summarized as follows:

SEM images revealed that the morphology of PDPW resembles unidirectional composite materials. The wood from the southern region exhibited a higher fiber content (technical and bundle fibers) compared to that from the northern region. Additionally, the presence of voids was significant in the wood from the northern region.

The chemical composition of both PDPW was similar but with varying intensity.

There was a small difference (3 %) in moisture content between PDPW from both regions, despite the different climate conditions. The good interfacial adhesion and high fiber content of PDPW from the southern region led to gradual water evaporation compared to that from the northern region. For the latter, the presence of porosities facilitated easier water evaporation. Additionally, both PDPW types exhibited significant initial water absorption, especially in the case of PDPWs, due to their hydrophilic nature. Subsequently, fiber water absorption occurred.

The dissipative test was carried out on PDPW specimens for two different fiber directions (*Ox* and *Oy*) using DMTA. Due to the morphology of PDPWs (good interfacial adhesion, less voids and high fiber rate) and fiber properties, the storage modulus in perpendicular direction (*Ox*) was higher than in parallel (*Oy*) direction by 41 % for PDPWs and by 65 % for PDPWn. From a loss factor point of view, the fiber directions (perpendicular and parallel) were more affected by damping than by environmental regions.

The results of this study suggest that PDPW has the potential to be used as a sandwich core material in automotive, furniture, and boat interior structures.

**Acknowledgements** – Zahvala

The authors would like to thank Istanbul University-Cerrahpasa Research Fund for its financial support in this study (Project Nos. 4806, 19515, 31014, 43150, and 49525).

The authors would like to thank the Turkish Academy of Sciences (TÜBA) for its financial support throughout the study process. The authors would also like to thank the Biomaterials and Nanotechnology Research Group & BioNanoTeam for their valuable contributions during this work.

## 5 REFERENCES
## 5. LITERATURA

1. Dave, M. J.; Pandya, T. S.; Stoddard, D.; Street, J., 2018: Dynamic characterization of biocomposites under high strain rate compression loading with split Hopkinson pressure bar and digital image correlation technique. International Wood Products Journal, 9 (3): 115-121. https://doi.org/10.1080/20426445.2018.1482673
2. Candan, Z.; Gardner, D. J.; Shaler, S. M., 2016: Dynamic mechanical thermal analysis (DMTA) of cellulose nanofibril/nanoclay/pMDI nanocomposites. Composites Part B, 90: 126-132. https://doi.org/10.1016/j.compositesb.2015.12.016
3. Atas, C.; Sevim, C., 2010: On the impact response of sandwich composites with cores of balsa wood and PVC foam. Composite Structures, 93 (1): 40-48. https://doi.org/10.1016/j.compstruct.2010.06.018
4. Sofia, K.; José, L. L.; Sofia, L.; Helena, P., 2007: Original article Radial variation of wood density components and ring width in cork oak trees. Annals of Forest Science, 64: 211-218. https://doi.org/10.1051/forest:2006105
5. Hassanin, A. H.; Hamouda, T.; Candan, Z.; Kilic, A.; Akbulut, T., 2016: Developing high-performance hybrid green composites. Composites Part B. Engineering, 92: 384-394. https://doi.org/10.1016/j.compositesb.2016.02.051
6. Makarona, E.; Koutzagioti, C.; Salmas, C.; Ntalos, G.; Skoulikidou, M.-C.; Tsamis, C., 2017: Enhancing wood resistance to humidity with nanostructured ZnO coatings. Nano-Structures & Nano-Objects, 10: 57-68. https://doi.org/10.1016/j.nanoso.2017.03.003
7. Hamdan, B. S.; Dwianto, W.; Morooka, T.; Norimoto, M., 2000: Softening Characteristics of Wet Wood under Quasi Static Loading. Holzforschung, 54 (5): 557-560. https://doi.org/10.1515/HF.2000.094
8. Oloyede, A.; Groombridge, P., 2000: The influence of microwave heating on the mechanical properties of wood. Journal of Materials Processing Technology, 100 (1-3): 67-73. https://doi.org/10.1016/S0924-0136(99)00454-9
9. Benzidane, R.; Sereir, Z.; Bennegadi, M. L.; Doumalin, P.; Poilâne, C., 2018: Morphology, static and fatigue behavior of a natural UD composite: The date palm petiole 'wood'. Composite Structures, 203: 110-123. https://doi.org/10.1016/j.compstruct.2018.06.122
10. Srivaro, S.; Matan, N.; Lam, D. F., 2015: Stiffness and strength of oil palm wood core sandwich panel under center point bending. Materials & Design, 84: 154-162. https://doi.org/10.1016/j.matdes.2015.06.097
11. Merzoug, A.; Bouhamida, B.; Sereir, Z., 2020: Quasi-static and dynamic mechanical thermal performance of date palm/glass fiber hybrid composites. Journal of Industrial Textiles, 51 (5): 7599S-7621S. https://doi.org/10.1177/1528083720958036
12. Maache, M.; Bezazi, A.; Amroune, S.; Scarpa, F.; Dufresne, A., 2017: Characterization of a novel natural cellulosic fiber from Juncuseffusus L. Carbohydrate. Polymers, 171: 163-172. https://doi.org/10.1016/j.carbpol.2017.04.096
13. Kamperidou, V., 2021: Chemical and structural characterization of poplar and black pine wood exposed to short thermal modification. Drvna industrija, 72 (2): 155-167. https://doi.org/10.5552/drvind.2021.2026
14. Olsson, A. M.; Salmén, L., 1992: Viscoelasticity of in Situ Lignin as Affected by Structure. Viscoelasticity of Biomaterials. Chapter 9: 133-143. https://doi.org/10.1021/bk-1992-0489.ch009
15. Placet, V.; Passard, J.; Perré, P., 2007: Viscoelastic properties of green wood across the grain measured by harmonic tests in the range of 0-95 °C Hardwood vs. softwood and normal wood vs. reaction wood. Holzforschung, 61: 548-557. https://doi.org/10.1515/HF.2007.093
16. Backman, A. C.; Lindberg, K. H., 2001: Differences in wood material responses for radial and tangential direction as measured by dynamic mechanical thermal analysis. Journal of Materials Science, 36: 3777-3783. https://doi.org/10.1023/A:1017986119559
17. Li, Z.; Jiang, J. L.; Lyu, J. X.; Cao, J. Z., 2021: Orthotropic viscoelastic properties of chinese fir wood saturated with water in frozen and non-frozen states. Forest Products Journal, 71 (1): 77-83. https://doi.org/10.13073/FPJ-D-20-00069
18. Li, Z.; Jiang, J. L.; Lyu, J.; Cao, J. Z., 2023: Comparative investigation on the orthotropic viscoelastic properties of wood during cooling and heating variations. Wood Material Science & Engineering, 18 (1): 262-268. https://doi.org/10.1080/17480272.2021.2017478
19. Abdal-hay, A.; Ngakan Putu, G. S.; Jung, D. Y.; Kwang-Seog, C.; Jae Kyoo, L., 2012: Effect of diameters and alkali treatment on the tensile properties of date palm

fiber reinforced epoxy composites. International Journal of Precision Engineering and Manufacturing, 13: 1199-1206. https://doi.org/10.1007/s12541-012-0159-3
20. Benzidane, M. A.; Benzidane, R.; Hamamousse, K.; Adjal, Y.; Sereir, Z.; Poilâne, C., 2022: Valorization of date palm wastes as sandwich panels using short rachis fibers in skin and petiole 'wood' as core. Industrial Crops and Products, 177: 114436. https://doi.org/10.1016/j.indcrop.2021.114436
21. Horiyama, H.; Fujimoto, W.; Kojiro, K; Itoh, T.; Kajita, H.; Furuta, Y., 2023: Proposal for a new method for sustainable and advanced utilization of oil palm trunk waste. Bioresources and Bioprocessing, 10: 69. https://doi.org/10.1186/s40643-023-00688-7
22. Ma, Z.; Wang, J.; Yang, Y.; Zhang, Y.; Zhao, C.; Yu, Y.; Wang, S., 2018: Comparison of the thermal degradation behaviors and kinetics of palm oil waste under nitrogen and air atmosphere in tga-ftir with a complementary use of model-free and model fitting approaches. Journal of Analytical and Applied Pyrolysis, 13: 12-24. https://doi.org/10.1016/j.jaap.2018.04.002
23. Toubia, E. A.; Emami, S.; Klosterman, D., 2019: Degradation mechanisms of balsa wood and PVC foam sandwich core composites due to freeze/thaw exposure in saline solution. Journal of Sandwich Structures & Materials, 21 (3): 990-1008. https://doi.org/10.1177/1099636217706895
24. Gonultas, O.; Candan, Z., 2018: Chemical characterization and ftir spectroscopy of thermally compressed eucalyptus wood panels. Maderas. Ciencia y Tecnologia, 20 (3): 431-442.http://dx.doi.org/10.4067/S0718-221X2018005031301
25. Esteves, B.; Marques, A. V.; Pereira, H., 2013: Chemical changes of heat treated pine and eucalypt wood monitored by FTIR. Maderas. Ciencia y Tecnologia, 15 (2): 245-258. http://dx.doi.org/10.4067/S0718-221X2013005000020
26. Romanzini, D.; Júnior, H. L. O.; Amico, S. C.; Zattera, A. J., 2012: Preparation and characterization of ramie-glass fiber reinforced polymer matrix hybrid composites. Materials Research Ibero-American Journal of Materials, 15 (3): 415-420. https://doi.org/10.1590/S1516-14392012005000050
27. Tranvan, L.; Legrand, V.; Jacquemin, F., 2014: Thermal decomposition kinetics of balsa wood: Kinetics and degradation mechanisms comparison between dry and moisturized materials. Polymer Degradation and Stability, 110: 208-215. https://doi.org/10.1016/j.polymdegradstab.2014.09.004
28. Todaro, L.; Rita, A.; Pucciariello, R.; Mecca, M.; Hiziroglu, S., 2017: Influence of thermo-vacuum treatment on thermal degradation of various wood species. European Journal of Wood and Wood Products, 76: 541-547. https://doi.org/10.1007/s00107-017-1230-7
29. Ceylan, S.; Topçu, Y., 2014: Pyrolysis kinetics of hazelnut husk using thermogravimetric analysis. Bioresource Technology, 156: 182-188. https://doi.org/10.1016/j.biortech.2014.01.040
30. Hellmeister, V.; Barbirato, G.; Lopes Junior, W.; Santos, V.; Fiorelli, J., 2021: Evaluation of balsa wood (ochroma pyramidale) waste and osb panels with castor oil polyurethane resin. International Wood Products Journal, 12 (4): 267-276. https://doi.org/10.1080/20426445.2021.1977519
31. Marwanto, M.; Maulana, M. I.; Febrianto, F.; Wistara, N. J.; Nikmatin, S.; Masruchin, N.; Zaini, L. H.; Lee, S.-H.; Kim, N. H., 2021: Characteristics of nanocellulose crystals from balsa and kapok fibers at different ammonium persulfate concentrations. Wood Science and Technology, 55: 1319-1335. https://doi.org/10.1007/s00226-021-01319-0
32. Ornaghi Jr., H. L.; Pompeo da Silva, H. S.; Zattera, A. J.; Amico, S. C., 2011: Hybridization effect on the mechanical and dynamic mechanical properties of curaua composites. Materials Science and Engineering: A, 528 (24): 7285-7289. https://doi.org/10.1016/j.msea.2011.05.078
33. Sreekala, M. S.; Thomas, S.; Groeninckx, G., 2005: Dynamic mechanical properties of oil palm fiber/phenol formaldehyde and oil palm fiber/glass hybrid phenol formaldehyde composites. Polymer Composites, 26 (3): 388-400. https://doi.org/10.1002/pc.20095
34. *** EN 322, 1999: Wood based panels – Determination of moisture content. Institute of European Committee for Standardization, Brussels.
35. *** ASTM D1037, 1999: Standard test methods for evaluating properties of wood-base fiber and particle panel materials.

**Corresponding address:**

**ZEKI CANDAN**
Department of Forest Industrial Engineering, Istanbul University-Cerrahpasa, İstanbul, Türkiye; Biomaterials and Nanotechnology Research Group & BioNanoTeam, İstanbul, TÜRKIYE.
e-mail: zekic@istanbul.edu.tr
ORCID ID: Z. Candan https://orcid.org/0000-0002-4937-7904

Ayhan Gençer[1], Cengiz Keşmer*[2], Ayben Kılıç Pekgözlü[1], Mehmet Bebekli[3], Ahmet Can[1], Esra Ceylan[1]

# Using Dyestuff Obtained from Turkish Red Pine Bark Combined with Cationic Starch in Paper Dyeing

# Upotreba bojila dobivenog iz kore turskoga crvenog bora u kombinaciji s kationskim škrobom za bojenje papira

**ORIGINAL SCIENTIFIC PAPER**
**Izvorni znanstveni rad**
Received – prispjelo: 18. 1. 2024.
Accepted – prihvaćeno: 2. 4. 2024.
UDK: 630*84; 676.024.72
https://doi.org/10.5552/drvind.2024.0183



**ABSTRACT** • *This study will be important in reducing water pollution, especially by not using chemical agents in the dyeing process and using organic mordant in the paper dyeing process. The cationic starch (CS) is also used as a mordant. CS increases the dry strength properties of the paper as well as the dye adhesion, and it is important in terms of providing two functions to an additive at the same time. In this study, natural dyestuff was obtained from Turkish red pine (Pinus brutia Ten.) bark by boiling in water, and bleached eucalyptus pulp was dyed. CS, which can increase the paper dry strength, was used as a mordant in the dyeing process. CS was mixed with distilled water in a hot water bath at (95±2) ºC and gelled. Thanks to 1.5 % CS addition, the tensile index increased by 38 %. With the addition of dyestuff, the papers became red and yellow. Adding CS and increasing the amount of dyestuff darkened the tone of these colors. However, CS addition was more effective than increasing the amount of dyestuff. That is to say, increasing the amount of dye alone in CS-free papers was not as effective as in CS-added papers.*

**KEYWORDS:** *Turkish red pine bark; organic dyestuff; starch; mordant; UV-ΔL*

**SAŽETAK** • *Rezultati ove studije važni su za smanjenje onečišćenja vode, posebice zato što se u procesu bojenja papira ne rabe kemijska sredstva, kao i zato što se pritom kao organski fiksator upotrebljava kationski škrob (CS). On povećava svojstva čvrstoće suhog papira, kao i fiksiranje bojila, a važan je u smislu ostvarivanja dviju funkciju aditiva istodobno. U ovom je istraživanju prirodno bojilo dobiveno iz kore turskoga crvenog bora (Pinus brutia Ten.) kuhanjem u vodi, a njime je obojena izbijeljena pulpa eukaliptusa. Kationski škrob, koji može povećati čvrstoću suhog papira, poslužio je kao fiksator u procesu bojenja. Kationski je škrob pomiješan s destiliranom vodom u vrućoj vodenoj kupelji na (95 ± 2) ºC i želiran. Zahvaljujući dodatku 1,5 % kationskog škroba, vlačni indeks papira povećao se za 38 %. Nakon dodanog bojila papiri su postali crveni i žuti, a uz dodatak kationskog škroba i s povećanjem količine bojila ton boje postao je tamniji. Međutim, dodavanje kationskog škroba bilo je učinkovitije od povećanja količine bojila, tj. pokazalo se da povećanje količine bojila u papirima bez kationskog škroba nije dalo tako dobre rezultate kao u papirima s dodatkom kationskog škroba.*

**KLJUČNE RIJEČI:** *kora turskoga crvenog bora; organsko bojilo; škrob; fiksator; UV-ΔL*

* Corresponding author
[1] Authors are researchers at Bartin University, Faculty of Forestry, Department of Forest Industrial Engineering, Bartin, Türkiye.
[2] Author is researcher at Çukurova University, Aladağ Vocational High School Forestry Department, Adana, Türkiye.
[3] Author is researcher at Çukurova University, Faculty of Engineering, Department of Textile Engineering, Adana, Türkiye.

## 1 INTRODUCTION
## 1. UVOD

The substances found in nature are in different colors because their structures refract light at different angles. Many materials are used for recoloring for various reasons. The process of converting one color to another is done with dye or dyestuff. Dyestuffs are grouped into two main groups: natural and synthetic origin. Natural dyestuffs are obtained from plants, animals, and minerals. Natural dyestuffs obtained from plants and animals are renewable and therefore sustainable.

Dye is applied to a surface with a binder that can dry out, with brushes or spray guns. It can be removed from the applied surface by scraping. Dye is a colored substance that chemically bonds to the substrate to which it is applied (Devi, 2014). Dyestuff, on the other hand, is the substance used in the coloring of objects (fabric, fiber, etc.), and it cannot be removed by scraping (Önal, 2000).

Cellulose is known for its low affinity for anionic entities and therefore cannot form strong bonds with most natural dyes without mordant. The fact that the mordant used is cationic improves the aforementioned negative properties (Bechtold and Mussak, 2009).

The use of mordant in dyeing textile products with natural dyestuffs is common, with aluminum and iron salts, acids, and various minerals being preferred. By obtaining dyestuff from onion skin (*Allium cepa* L.) and using various metal salts as a mordant, high-fastness dyeing of hairy leather and cotton fabric has been carried out (Eser and Önal, 2010). Wool fabric was dyed with the dyestuff obtained from red pine bark. It has been stated that light, washing, and rubbing fastness are at the desired level and in usable condition (Akpınarlı and Yalçın, 2012). It has been emphasized that cotton fabrics are dyed in the presence of metal salts as a mordant with the dyestuff obtained by ethanol extraction from the pomegranate peel, and the colorfastness, washing fastness, and friction fastness of these fabrics are satisfactory. They also stated that this dyestuff can be used instead of banned arylamine dyes (Kulkarni *et al.,* 2011). Metal salts, aloe vera, and lemon juice were used as mordants in dyeing the cotton with dyestuff obtained from onion skin extract. It was stated that the best color yield was obtained with lemon juice mordant (Zubairu and Mshelia, 2015). Organic cotton fabrics were dyed with dyestuff from madder root, walnut shell, henna, horse chestnut, pomegranate peel, berberis vulgaris root, thyme, and sage tea. The color and fastness properties obtained from the dyed organic cotton fabrics were between good to excellent (Tutak and Korkmaz, 2012). In a study, the effect of different amounts of metals on the coloring scale of the pigments was investigated. For this purpose, the reaction of the dyestuffs present in buckthorn with aluminum(III), iron(II), and tin(II) was used to prepare natural pigments (Deveoglu *et al*., 2009). Natural yellow pigments from the hemp (*D. cannabina L.*) dye plant were prepared by using KAl $(SO_4)_2 \cdot 12H_2O$ (alum), $FeSO_4 \cdot 7H_2O$ and $SnCl_2 \cdot 2H_2O$ mordants (Deveoglu *et al.,* 2012). It has been reported that alum mordant is more suitable to accompany Turkish red pine bark extract in natural extract dyeing with one exception (flax); however, the use of oak ash natural mordant is beneficial when completely eco-friendly dyeing is desired (Avinc *et al.,* 2013). The enzymatic dyeing of Ferrulic Acid provides fabrics with multifunctional properties of antioxidant activity, UV protection, and deodorization (Sun *et al.,* 2015). A study used *Pistacia vera* hulls by-product extract as a dyestuff. Dyed samples exhibited good fastness to washing, rubbing, and light (Syrine *et al.,* 2020).

Onion peel, henna, pomegranate, pomegranate peel, and rose petals were extracted to produce natural dyestuffs. Alum was used as a mordant in dyeing the paper by dipping the paper into the dyestuff. Henna-dyed samples showed the highest color stability after aging in dyed papers, while pomegranate-dyed samples showed the least color stability (Çakar, 2012). A study extracted the dyestuff from eucalyptus bark with distilled water at different temperatures and stated that the dyestuff they obtained at the boiling temperature provided the best relative color strength in cotton dyeing (Ali *et al*., 2006).

In a study, dyestuff obtained from elderberry (*Sambucus nigra*) plants seeds used paper pulp dyeing by using alum as a mordant. It has been reported that dyestuff adhesion in papers obtained from pulps without mordant additions is weaker than in those with mordant additions (Gençer and Can, 2016). Wild cherry (*Cerasus avium* L.) tree bark extract is used as a dyestuff in paper production (Gençer *et al.,* 2019a). It has been stated that the UV resistance of the papers using alum as a mordant is high. The dyestuff obtained from the bark of wild cranberry (*Cornus australis* L.) was used to dye the pulp obtained from the mixture of waste papers of various origins. It has been reported that color homogeneity is achieved in the papers obtained from the mixture (Gençer *et al.,* 2019b). In a study to determine the dyestuffs used in manuscripts of the 15th century, non-destructive analyses were carried out with μXRF, Raman, and FTIR spectroscopy. Samples were taken from the fragments of these artifacts, and chromatographic analyses were performed. It was concluded that these papers were colored with Isgin (*Rheum ribes* L.) based on the compounds detected (Çakar, 2019).

Cellulose and hemicelluloses contain hydroxyl and carboxyl groups. They carry a negative charge due

to the carbonyl and carboxyl groups formed by the bleaching process (Eroğlu, 1989). Cationic groups in cationic starches have a positive charge effect on starch; showing interest in hydroxyl groups in cellulose, fiber-starch-fiber bonds are formed, and these bonds may be stronger than fiber-fiber bonds. In addition, very thin fibers remain on the paper surface like fluff due to the effect of static electricity charges, causing fluff. These papers run the risk of scattering the ink and losing dyeing homogeneity. Using starch, fine fibers are also drawn to the surface, making the paper surface smoother. Starch thermal properties and morphological structure vary according to the source from which it is obtained. It was stated that the granular structure of potato starch is larger than that of corn and cassava starch, and it is easier to gel with temperature (Abdullah *et al.,* 2018). In paper production, cooking gelatinization of starch is more effective, and it has been stated that potato starch is more effective than corn starch. Starch mixed in the Hollander tends to separate from the fibers with a mechanical effect. The starch is fixed to the paper by making a strong bond only after drying. This is because starch is not a wet-strength agent. In a study, 1.5 % CS obtained from potato was added to the pulp to produce paper from softwood. It was stated that there was a 64 % increase in the tensile index in the obtained CS-added papers compared to the control samples, and there was no significant difference when increasing the starch ratio (Gülsoy, 2014).

In a study regarding the morphologic properties of Eucalyptus pulp fibers, length (0.70–0.84 mm) and width (18.0–19.1 μm) were specified, and it was stated that papers with good mechanical properties could be obtained (Flávia Morais *et al.,* 2019). Unbleached pulps are difficult to dye because they contain lignin and other impurities. Because of these impurities and lignin, UV–Vis measurements of paper may include systematic errors (Małachowska *et al.,* 2020). On the other hand, bleached and high white pulps are easier to dye than other pulps. The bleached pulp was chosen to accurately determine the effect of dyestuff and mordant.

For a substance to be considered a dyestuff, it must be colored and tightly coupled to the fiber. Red pine bark contains Oligomeric Proantho Cyanidin (OPC). It has been reported that the ratio of OPC is high in the dyestuff that can be separated from the bark of red pine (Demir and Demir, 2012).

In Türkiye, 8,433,852 $m^3$ debarked Turkish red pine logs were produced in 2019 (OGM, 2020). The red pine bark remaining from this production is left to rot in the forests. Turkish red pine bark is burned after peeling to obtain energy. Although incineration is seen as a solution to energy production and removal of waste bark, emissions released into the atmosphere and some substances that pass into the ash can be problematic in terms of gas and solid waste disposal. For this reason, waste should be converted into useful products instead of incinerated. This will help reduce environmental pollution and positively affect the ecological balance.

Dyes are used traditionally or industrially to manufacture textiles, wood, and paper. In studies made from plant-derived dyestuffs, parts of plants containing chromophores such as bark, leaves, and flowers are used. Due to the low affinity of cellulose towards anionic substances, it must be cationic loaded in case of dyeing with natural dyestuffs. For this purpose, mordant is used. Most natural yellow colors are hydroxy and methoxy derivatives of flavones and isoflavones. Yellow dye mordants were noted to be tin, alum, and chrome (Vankar, 2000). Wastewater treatment from the metal mordants used is very costly. In addition, metal in products dyed for human use adversely affects human health. Instead of metal salts used as mordant in the literature, the dual advantage of using cationic starch, an organic substance, has been considered in this study. This paper aims to improve the paper dry strength properties, while increasing the dyestuff adhesion in the papers to be obtained in this way.

## 2 MATERIALS AND METHODS
## 2. MATERIJALI I METODE

### 2.1 Materials
### 2.1. Materijali

In this study, the pulp was dyed with natural dyestuff obtained from Turkish red pine (*Pinus brutia* Ten.) bark. In Turkey, the bark cut from coniferous trees is left in the forest after being debarked. For this reason, in our study, no trees were cut for bark production, and the waste bark remaining from log production was used. The Turkish red pine bark was taken from Türkiye's 35.33 longitude and 36.97 latitude region right after the tree was cut. The bark was ground and dried at room temperature, sieved, and the remaining part of the 60 mesh sieve was used. The high lignin concentration in the paper can even suppress some degradation pathways In unbleached pulps, the color of the pulp turns brown depending on the lignin ratio. Therefore, bleached Kraft pulp (21°SR) obtained from eucalyptus (*Eucalyptus grandis*) wood was used.

### 2.2 Methods
### 2.2. Metode

In our study, the 25 g bark sample was mixed with 500 ml of distilled water in a 1000 ml beaker and heated in a thermostated hot water bath with a sensitivity of ±2 ºC for 4 hours at 82 ºC and mixed with a glass baguette every 15 minutes. At the end of the process, the mixture was cooled at room temperature, filtered, and

made ready for use as dyestuff. The adhesive properties of CS adequately modified are better than those of natural starch. Modifying starch with different methods can even help adapt it, by considering its properties, for applications in areas such as food and papermaking. (Bismark *et al.,* 2018). Potato was the source of CS used as a mordant in the study. However, writing and printing processes have low ink and chemical costs (Hassaan and Nemr, 2017). The starch ratio was taken as 1.5 % by weight of the oven dry pulp. To prepare the starch solution, 500 ml of distilled water was poured into a 1-liter beaker, 3.6 g of CS was added and mixed in a hot water bath at (95±2) ºC and gelled. To obtain ten handsheets, 50 ml of gelled starch suspension was added and mixed in the mixer. In this case, 0.036 g of completely dry starch is added to 2.4 g of paper. Then, using a laboratory-type Rapid Köthen paper machine, paper groups with (75±2) g/m$^2$ were obtained according to ISO 5269-2 standard (ISO 5269-2, 2013).

The papers obtained were conditioned according to TAPPI T 402 sp-03 (2003) standard. The tensile properties of the paper are measured according to the TAPPI T 494 om-01 (2001) standard.

The morphological features of the papers and how the starch forms a bridge between the fibers were visualized in SEM. By measuring the ΔL, Δa, Δb, and, ΔE values of the obtained paper groups after UV, the dyestuff ratio and the effect of cationic starch were determined. Test sample color measurements before and after accelerated aging were made with Konica Minolta CD-600 colorimeter in accordance with ISO 7724 standard (ISO 7724-1, 2, 3, 1984). Accelerated weathering (50 ºC, 0.75 W/m$^2$) test was carried out on Q-Panel Lab Products instrument according to Eser and Önal, 2015. The dyed paper aging (UV) treatment was applied at four time intervals: 24, 48, 96, and 120 hours. The tests were carried out at 50 ºC while UV treatment was applied; no other conditioning process was applied.

## 3 RESULTS AND DISCUSSION
## 3. REZULTATI I RASPRAVA

### 3.1 Morphological analysis
### 3.1. Morfološka analiza

A low $L^*$ value means a high dye yield. Compared to the reference sample, a higher $L^*$ value indicates a brighter appearance and lighter color, while a lower $L^*$ value indicates a duller and darker color. Paper groups and their $L^*a^*b^*$ values are given in Table 2.

In the samples without starch and dyestuff, yellow was at low values, and red was not observed. The red color was also observed with the addition of dyestuff, and the red and yellow color tone became darker with the increase in the amount of dyestuff. These colors are even darker in the samples with the same amount of dyestuff with starch added. The low L value, proof of dye adhesion, showed a rapid decrease with adding 50 ml of dyestuff. The lower L value of the same amount of dyestuff-added papers with starch added is proof that starch increases dye adhesion. As the amount of dyestuff was increased by more than 50 ml, the decrease in L value was not much. Therefore, the optimum value of the amount of dyestuff can be accepted as 50 ml. This is also seen in the red color change. There is an increase in yellow-colored CS-added papers samples at high dyestuff usage. This is because starch increases adhesion. This is also confirmed by the fact that the yellow color of C2 is more dominant than the green. After the UV treatments, the color measurements of the dyed papers were made by spectroscopy. The results obtained from the color measurements are shown in Table 3.

Table 3 shows that the yellow color (+Δ$b^*$) turned into blue color (-Δ$b^*$) after 24 hours of UV application on papers dyed with mordant-free dyestuff. In papers using cationic starch, the color transformation occurred after 96 hours. This shows that starch is effective as a mordant and that its UV resistance is greater

**Table 1** Paper groups; suspension was mixed by mixer at low speed
**Tablica 1.** Skupine papira (suspenzija je malom brzinom izmiješana u mikseru)

| **Groups** / *Skupine* | **Abbreviation** *Kratica* | **Explanation** / *Objašnjenje* |
|---|---|---|
| Control 1 / *kontrolna skupina 1.* | C1 | Test papers were made without starch and dye<br>*ispitni papiri bez škroba i bojila* |
| Control 2 / k*ontrolna skupina 2.* | C2 | Starchy papers were obtained by adding only gelled CS<br>*papiri s dodatkom samo želiranoga kationskog škroba* |
| Only dyed papers<br>*samo obojeni papiri* | D50 | 50 ml of dyestuff was added<br>*s dodatkom 50 ml bojila* |
| | D100 | 100 ml of dyestuff was added<br>*s dodatkom 100 ml bojila* |
| Dyed CS-added papers<br>*obojeni papiri s dodatkom kationskog škroba* | D50+CS | 50 ml of dyestuff and 1.5 % of CS were added<br>*s dodatkom 50 ml bojila i 1,5 % kationskog škroba* |
| | D100+CS | 100 ml of dyestuff and 1.5 % of CS were added<br>*s dodatkom 100 ml bojila i 1,5 % kationskog škroba* |

**Table 2** Paper groups and their $L^*a^*b^*$ values
**Tablica 2.** Skupine papira i njihove $L^*a^*b^*$ vrijednosti

| **Paper groups** *Skupine papira* | **Dyestuff, ml** *Bojilo,* ml | **Cationic starch, %** *Kationski* ***škrob****,* % | $L^*$ | $a^*$ | $b^*$ |
|---|---|---|---|---|---|
| Control 1 (C1) *kontrolna skupina 1. (C1)* | 0.0 | 0.0 | 91.58 | -0.14 | 2.16 |
| Control 2 (C2) *kontrolna skupina 2. (C2)* | 0.0 | 1.5 | 89.31 | -0.38 | 3.34 |
| Only dyed papers (D50) *obojeni papiri (D50)* | 50 | 0.0 | 76.45 | 8.46 | 14.49 |
| Starchy dyed (D50+CS) *obojeni papiri uz dodatak škroba (D50+CS)* | 50 | 1.5 | 70.96 | 9.56 | 16.55 |
| Only dyed papers (D100) *obojeni papiri (D100)* | 100 | 0.0 | 75.73 | 9.00 | 15.50 |
| Starchy dyed (D100+CS) *obojeni papiri uz dodatak škroba (D100+CS)* | 100 | 1.5 | 70.20 | 9.77 | 20.18 |

**Table 3** $\Delta L^*\Delta a^*\Delta b^*$ values after UV treatment
**Tablica 3.** Vrijednosti $\Delta L^*\Delta a^*\Delta b^*$ nakon UV tretmana

| **Paper groups** *Skupine papira* | **UV, hours** *UV, sati* | **ΔI*** | **Δ*a**** | **Δ*b**** | **Δ*E**** |
|---|---|---|---|---|---|
| Control 1 (C1) *kontrolna skupina 1.* | 24 | -0.33 | -0.14 | 0.61 | 0.99 |
| | 48 | 0.38 | -0.18 | -0. 10 | 0.77 |
| | 96 | 0.90 | -0.17 | -0.23 | 0.87 |
| | 120 | 1.40 | -0.15 | -0.40 | 1.20 |
| Control 2 (C2) *kotrolna skupina 2. (C2)* | 24 | 0.98 | -0.75 | 1.51 | 0.90 |
| | 48 | 1.20 | -0.83 | 1.00 | 0.86 |
| | 96 | 2.34 | -0.88 | -1.60 | 1.34 |
| | 120 | 2.61 | -0.90 | -2.78 | 1.54 |
| Only dyed papers (D50) *obojeni papiri (D50)* | 24 | 2.69 | -2.44 | -0.11 | 1.24 |
| | 48 | 5.29 | -3.73 | -1.62 | 2.21 |
| | 96 | 8.49 | -5.46 | -3.15 | 4.02 |
| | 120 | 9.45 | -5.60 | -3.87 | 4.74 |
| Starchy dyed (D50+CS) *obojeni papiri uz dodatak škroba (D50+CS)* | 24 | 3.00 | -2.70 | 2.04 | 4.17 |
| | 48 | 5.53 | -3.10 | 0.30 | 6.48 |
| | 96 | 8.60 | -5.27 | -3.16 | 10.58 |
| | 120 | 9.55 | -5.63 | -3.89 | 11.50 |
| Only dyed papers (D100) *obojeni papiri (D100)* | 24 | 4.24 | -3.18 | -1.02 | 2.55 |
| | 48 | 5.63 | -3.43 | -1.51 | 3.10 |
| | 96 | 7.68 | -5.50 | -2.33 | 9.25 |
| | 120 | 9.61 | -6.10 | -3.00 | 11.40 |
| Starchy dyed (D100+CS) *obojeni papiri uz dodatak škroba (D100+CS)* | 24 | 4.24 | -3.25 | 2.51 | 4.66 |
| | 48 | 5.63 | -3.43 | 1.02 | 5.85 |
| | 96 | 7.68 | -5.50 | -2.33 | 10.42 |
| | 120 | 9.61 | -6.10 | -3.00 | 11.61 |

for 72 hours. When $\Delta a$ values were examined, it was observed that the results were negative (-). It has been determined that the values of paper groups using starch are higher, especially when adding the same amount of dyestuff. The increase in $\Delta a$ values to minus (-) indicates that the colors of post-UV dyed papers move towards darker shades of green. In a study conducted on onion skin dyestuff, after 12 days of aging, the $a^*$ value increased and shifted from green to red (Akyol and Çakar Sevim, 2023).

A decrease in the $\Delta E$ value means that the compared colors are getting closer, and an increase in its value means that the colors are moving away from each other. It was determined that the lowest/highest $\Delta E^*$ values of 50 ml dyed and starch-free papers were 1.24/4.74, respectively. It was observed that $\Delta E$ values increased as UV duration increased. Therefore, as the aging time increased, the colors diverged from each other. It was determined that D50+CS paper groups had a score of 4.17, and D100+CS had a score of 4.66.

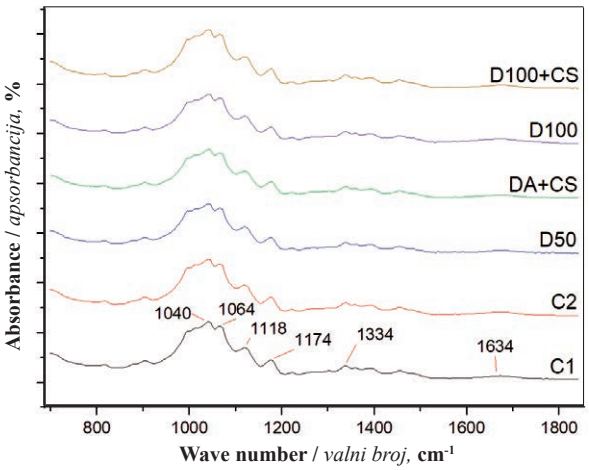


**Figure 1** FTIR results of samples
**Slika 1.** Rezultati FTIR-a

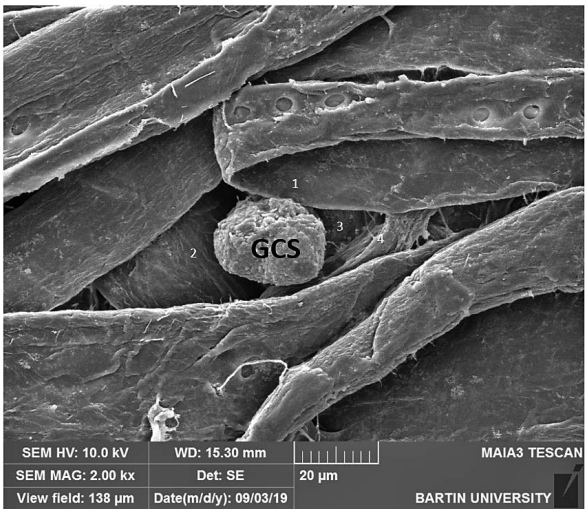


**Figure 2** SEM images of samples (GCS – Gelled cationic starch, 1, 2, 3, 4 – Gelled cationic starch bridges with fibers)
**Slika 2.** SEM slike uzoraka (GCS – želirani kationski škrob, 1, 2, 3, 4 – želirani kationski škrobni mostovi s vlaknima)

Figure 1 shows the FTIR results of the obtained papers.

Figure 1 shows that there is no difference between the papers along the *x*-axis. It can be seen that there are differences in the y-axis due to the difference in color tones. In the figure, the formation of a higher peak in the same wavelength range as the amount of dyestuff increases is due to intensity. This is because there are darker shades of the same color.

It is seen that the addition of dyestuff does not affect the tensile effect of the paper. The reason for this can be explained by the fact that dyestuffs do not have a positive effect because they are not dry-strength substances, they are not the size of a filler, and they do not harm the connection between fibers.

Figure 2 shows the surface SEM image of the gelled cationic starch (GCN) added paper obtained at 27 ºSR from bleached pulp obtained from eucalyptus wood by the Kraft method.

The polar hydroxyl groups present in starch increase the strength of the paper by forming 'fiber-starch-fiber' bonds with the hydroxyl groups in cellulose fibers (Casey, 1960). Figure 2 shows that starch settles in the space of the paper and forms an interfiber bridge there. In our study, there was a 38 % increase in tensile index with the addition of 1.5 % cationic starch, thanks to the bonds made by cationic starch in contact with at least four (1-2-3-4) fibers at the same time on the visible surface. Additionally, it is noteworthy that it fills the space between fibers. This will also have a positive effect on increasing surface smoothness. In addition, the roughness of the starch surface due to gelation increases the contact area. In the literature, it is stated that the average tensile index of papers produced at 27 $^0$SR from bleached eucalyptus pulp without a dry strength agent is 41.3 Nm/g (Gonzàlez *et al.,* 2012). This study determined the tensile index as 44 (N·m/g) in starchless paper groups at 21 $^0$SR. The difference occurs with the increase in the amount of beating.

## 4 CONCLUSIONS
## 4. ZAKLJUČAK

When starting this study, the aim was to provide an alternative dyeing to synthetic dyes and inorganic mordants in paper dyeing. For this purpose, Turkish red pine bark extract was chosen as the natural dyestuff in paper dyeing. Cationic starch was used as a mordant. It aimed to increase the dry strength properties of the paper with the same mordant while increasing the dye adhesion by taking advantage of its adhesive properties.

The degree of paint adhesion is the $\Delta L^*$ value. The fact that this value is higher than the control samples means that adhesion increases. $\Delta L^*$ values in paper groups obtained using Turkish red pine bark extract and cationic starch together are significantly higher than in paper groups without cationic starch. This is because starch works well as an organic mordant. There was no significant increase in $\Delta L^*$ values by increasing the amount of dyestuff from 50 ml to 100ml in mordant samples. Therefore, the optimum amount of dyestuff can be considered to be 50 ml. When $\Delta b$ values are examined, it has been observed that it gives different results than $\Delta a^*$ values. At $\Delta E^*$ values, it was determined that the average of starch paper groups was 248.70 % higher than the average of non-starch paper groups. It has been observed that cationic starch, together with the natural dyestuff of Turkish red pine bark, adheres well to the paper pulp. The use of cationic starch has made a significant difference in the adhesion of the natural dyestuff of Turkish red pine bark to papers produced from wood pulp before UV and after UV and in increasing the durability of the paper. These findings will contribute to the literature and be useful to future studies.

In this study, it was seen that natural wastes such as Turkish red pine bark can be converted into benefits and, if used, become an important biomass. We believe that Turkish red pine bark can be used in the board industry or agricultural applications since it does not lose significant mass after obtaining natural dyestuff.

**Acknowledgements** – Zahvala

Ahmet CAN and Esra CEYLAN were not involved in the project named BAP:2018-FEN-A-002 but contributed to FTIR experiments.

## 5 REFERENCES
## 5. LITERATURA

1. Abdullah, A. H. D.; Chalimah, S.; Primadona I.; Hanantyo, M. H. G., 2018: Physical and chemical properties of corn, cassava and potato starches. IOP Conference Series: Earth and Environmental Science 160: 012003. https://doi:10.1088/1755-1315/160/1/012003
2. Akpınarlı, H. F.; Yalçın, M., 2012: Obtaining Red Pine Pigment and Its Usage Properties in Wool Yarn Dyeing. Arış Dergisi, 7: 10-17 (in Turkish).
3. Akyol, E.; Çakar Sevim, P., 2023: Dyes used for Colouring manuscripts and their effect on cellulose degradation. Restaurator, International Journal for the Preservation of Library and Archival Material, 44 (4): 345-360. https://doi.org/10.1515/res-2023-0014
4. Ali, S.; Nisar, N.; Hussain, T., 2006: Dyeing properties of natural dyes extracted from eucalyptus. Taylor&Francis.
5. Avinc, O.; Celik, A.; Gedik, G.; Yavas, A., 2013: Natural dye extraction from waste barks of Turkish red pine (*Pinus brutia* Ten.) timber and eco-friendly natural dyeing of various textile fibers. Fibers and Polymers, 14: 866-873. https://doi.org/10.1007/s12221-013-0866-0
6. Bechtold, T.; Mussak, R., 2009: Handbook of Natural Colorants. John Wiley & Sons, Ltd., Chichester, UK.
7. Bismark, S.; Zhifeng, Z.; Benjamin, T., 2018: Effects of differential degree of chemical modification on the properties of modified starches: Sizing. The Journal of Adhesion, 94 (2): 97-123. https://doi.org/10.1080/00218464.2016.1250629
8. Casey, J. P., 1960: Pulp and Paper Chemistry and Chemical Technology, Vol. II, 2nd ed. Wiley Interscience Publisher Inc., New York, pp. 770-771.
9. Çakar, P., 2012: Investigation of the Effect of Copper-Based Pigments and Dyestuffs on Manuscripts. MSc Thesis, Republic of Turkey, Ministry of Culture and Tourism, Süleymaniye Manuscript Library Directorate, İstanbul, p. 128 (in Turkish).
10. Çakar, P., 2019: Determination of Dyes Used in Manuscripts and Investigation of Their Effects on the Ageing Kinetics of Paper. PhD Thesis, Yıldız Technical University, Institute of Science, Department of Chemical Engineering, Department of Chemical Engineering, p. 219 (in Turkish).
11. Demir, N.; Demir, Y., 2012: Obtainment and Industrial Use of OPC (Oligomeric Proanthocyanidin, Antioxidant), Dyestuff, Resin and Other Active Substances from Red Pine Bark (*Pinus brutia*). In: Proceedings of XXVI National Chemistry Congress, pp. 94-95.
12. Deveoglu, O.; Karadağ, R.; Yurdun, T., 2009: Preparation and HPLC analysis of the natural pigments obtained from buckthorn (*Rhamnus petiolaris* Boiss) dye plants. Jordan Journal of Chemistry, 4 (4): 377-385.
13. Deveoglu, O.; Çakmakcı, E.; Taşköprü, T.; Torgan, E.; Karadağ, R., 2012: Identification by RP-HPLC-DAD, FTIR, TGA and FESEM-EDAX of natural pigments prepared from *Datisca cannabina* L. Dyes an Pigments, 94 (3): 437-442. https: doi.org//10.1016/j.dyepig.2012.02.002
14. Devi, A. A., 2014: Extraction of natural dyes from fungus – an alternate for textile dyeing. Journal of Natural Sciences Research, 4 (7): 1-7.
15. Eroğlu, H., 1989: Kağıt ve Karton Üretim Teknolojisi. Karadeniz Teknik Üniversitesi Basımevi, Trabzon, 623 s.
16. Eser, F.; Seyfikli, D.; Önal, A., 2010: Usage of Willow Extract as Mordant Agent and Dyeing of Wooden and Fiber Samples with Onion Allium Cepa Shell. Rasayan Journal of Chemistry, 3(1), 1-8. No: 2012131.
17. Eser, F.; Önal, A., 2015: Dyeing of Wool and Cotton with Extract of the Nettle (*Urtica dioica* L.) Leaves. Journal of Natural Fibers, 12(3): 222-231.
18. Flávia Morais, P.; Raquel Bértolo, A. C.; Joana Curto, M. R.; Maria, E. C. C.; Amaral Ana Carta, M. M. S.; Dmitry, V., 2019: Comparative Characterization of eucalyptus fibers and softwood fibers for tissue papers application. Materials Letters: X, 4: 100028. https://doi.org/10.1016/j.mlblux.2019.100028
19. Gençer, A.; Can, A., 2016: Investigation of dyestuff obtained from Elderberry (*Sambucus Nigra* L.) seeds in the coloring process of paper. In: Proceedings of International Forestry Symposium (IFS 2016), 07-10, Kastamonu, Turkey.
20. Gençer, A.; Can, A.; Mustak, A.; Gitti, Ü. B., 2019a: The effect of using alum mordant in wild cherry bark dyestuff for the production of UV resistant colored paper. Drvna industrıja, 70 (4) 383-390. https://doi.org/10.5552/drvind.2019.1854
21. Gençer, A.; Can, A.; Gitti, Ü. B.; Mustak, A., 2019b: Determination of the effect on the color homogeneity of the use of natural dye stuff in paper obtained from recycled paper by accelerated weathering. Sigma Journal of Engineering and Natural Sciences, 10 (1): 69-80.
22. Gonzàlez, I. T.; Boufi, S.; Pélac, M. A.; Alcàla, M.; Vilaseca, F.; Mutjé, P., 2012: Nanofibrillated cellulose as paper additive in eucalyptus pulp. BioResource, 7 (4): 5167-5180.
23. Gülsoy, S. K., 2014: Effects of cationic starch addition and pulp beating on strength properties of softwood kraft pulp. Starch, 66 (7-8): 655-659. https://doi.org/10.1002/star.201300247
24. Hassaan, A. A.; El Nemr, M., 2017: Health and environmental impacts of dyes: mini-review. American Journal of Environmental Science and Engineering, 1 (3): 64-67.
25. Kulkarni, S. S.; Gokhale, A. V.; Bodake, U. M.; Pathade, G. R., 2011: Cotton dyeing with natural dye extracted from pomegranate (*Punica granatum*) peel. Universal Journal of Environmental Research & Technology, 1 (2): 135-139.
26. Małachowska, E.; Dubowik, M.; Boruszewski, P.; Łojewska, J.; Przybysz, P., 2020: Influence of lignin content in cellulose pulp on paper durability. Scientific Reports, 10 (1): 19998. https://doi.org/10.1038/s41598-020-77101-2
27. Onal, A., 2000: Natural dyestuffs (Extraction-Dyeing), Gaziosmanpaşa University Faculty of Science and Letters Publications, No. 7. Tokat (in Turkey).
28. Sun, S. S.; Xing, T.; Tang, R. C., 2015: Enzymatic dyeing and functional finishing of textile fibres with ferulic acid.

Indian Journal of Fibre & Textile Research (IJFTR), 40 (1): 62-69.
29. Syrine, L.; Jabli, M.; Abdessalem, S. B.; Almalki, S. G., 2020: FT-IR spectroscopy and morphological study of functionalized cellulosic fibers: Evaluation of their dyeing properties using biological Pistacia vera hulls by-product extract. International Journal of Biological Macromolecules, 145: 1106-1114. https://doi.org/10.1016/j.ijbiomac.2019.09.204
30. Tutak, M.; Korkmaz, N. E., 2012: Environmentally friendly natural dyeing of organic cotton. Journal of Natural Fibers, 9: 51-59. https://doi.org/10.1080/15440478.2011.651830
31. Vankar, P. S., 2000: Natural Dyes for Textiles, Elsevier, ISBN:978-08-101884-2.
32. Zubairu, A.; Mshelia, Y. M., 2015: Effects of selected mordants on the application of natural dye from onion skin (*Allium cepa*). Science and Technology, 5 (2): 26-32. https://doi.org/10.5923/j.scit.20150502.02
33. ***ISO 7724-1, 2, 3, 1984: Paints and varnishes – Colorimetry.
34. ***ISO 5269-2, 2013: Pulps preparation of laboratory sheets for physical testing. Part 2: Rapid-Köthenmethod.
35. ***OGM, 2020: Ormancılık İstatistikleri 2019. T. C. Tarım ve Orman Bakanlığı, Orman Genel Müdürlüğü, 36 s.
36. ***TAPPI T 494 om-01, 2001: Tensile properties of paper and paperboard.
37. ***TAPPI T 402 sp-03, 2003: Standard conditioning and testing atmospheres for paper, board, pulp hand sheets and related products.

**Corresponding address:**

**CENGIZ KEŞMER**
Çukurova University, Aladağ Vocational High School Forestry Department, Adana, TURKEY, e-mail:

Kennedy Kinikanwo Aleru*[1], Nwiisuator David-Sarogoro[1], Burabarı Jephter[2]

# Evaluation of Some Mechanical Properties of *Cola pachycarpa* (K. Schum.) Wood in the Tropical Rainforest Ecosystem of Rivers State, Nigeria

# Procjena nekih mehaničkih svojstava drva *Cola pachycarpa* K. Schum. iz ekosustava tropske prašume u saveznoj državi Rivers, Nigerija

**ORIGINAL SCIENTIFIC PAPER**
**Izvorni znanstveni rad**
Received – prispjelo: 26. 1. 2024.
Accepted – prihvaćeno: 24. 6. 2024.
UDK: 630*81; 674.038.17
https://doi.org/10.5552/drvind.2024.0184



**ABSTRACT** • *The wood mechanical properties of Cola pachycarpa K Schum. were investigated within one of the tropical rainforest ecosystems of Rivers State. Three mature wood stands of Cola pachycarpa were harvested and used for the study. Samples of wood were collected from each of the different sections of the tree: the base (10 % height), middle (50 % height), and top (90 % height) along the axial plane. These samples were then divided into innerwood, corewood, and outerwood based on their radial position. Afterwards, the samples underwent oven drying until they reached a moisture content (MC) level of 12 %. The study was conducted using a 3 × 3 nested design in a completely randomized design (CRD). In cases where there were significant differences, the Duncan multiple range test (DMRT) was employed to separate the means. The results revealed that the MOR mean value was 5.89 N/mm² with an increase from top to base along the axial plane and with an increase from outer to inner wood across the bole of the tree radially. The MOE mean value was 810.87 N/mm² and it showed an increase from the base to the top axially, with an increase from the outer to inner wood radially. The mean value of CS//G recorded 34.62 N/mm². It showed that there was an increase from base to top across the grain radially, and an increase from outer to inner wood. The findings of this study offer quantitative data on the potential use of Cola pachycarpa wood, which could be competitive with other well-known wood species and serve as a good replacement for commercially overexploited wood species.*

**KEYWORDS:** *Cola pachycarpa; mechanical properties; axial plane; radial plane*

**SAŽETAK** • *U radu su istražena mehanička svojstva drva Cola pachycarpa K Schum., uzetoga iz jednog od ekosustava tropske prašume u saveznoj državi Rivers. Tri zrela stabla drva Cola pachycarpa posječena su i iskorištena za istraživanje. Uzorci drva pripremljeni su iz različitih dijelova stabla: iz baze (na 10 % visine), sa sredine (na 50 % visine) i s vrha (na 90 % visine) duž aksijalne osi. Ti su uzorci na temelju njihova radijalnog*

* Corresponding author
[1] Authors are researchers at Rivers State University, Faculty of Agriculture, Department of Forestry and Environment, Port Harcourt, Rivers State, Nigeria. https://orcid.org/0009-0002-2570-5106
[2] Author is researcher at Rivers State University, Faculty of Engineering, Department of Civil Engineering, Port Harcourt, Rivers State, Nigeria.

*položaja zatim podijeljeni na uzorke iz unutarnje, srednje i vanjske zone. Uzorci su sušeni u sušioniku do sadržaja vode (MC) od 12 %.*
*Istraživanje je provedeno uz pomoć 3 × 3 potpuno randomiziranog dizajna (CRD) studije. Ako su postojale znatnije razlike, za razdvajanje srednjih vrijednosti primjenjivan je Duncanov test višestrukih raspona (DMRT). Rezultati su pokazali da je srednja vrijednost MOR-a iznosila 5,89 N/mm², s porastom od vrha prema dnu debla u uzdužnom smjeru i s porastom od vanjske prema unutarnjoj zoni u radijalnom smjeru debla. Srednja vrijednost MOE-a bila je 810,87 N/mm² i povećavala se od dna prema vrhu u uzdužnom smjeru te od vanjske prema unutarnjoj zoni u radijalnom smjeru debla. Srednja vrijednost CS//G iznosila je 34,62 N/mm², s porastom od dna prema vrhu u uzdužnom smjeru i od vanjske prema unutarnjoj zoni u radijalnom smjeru debla. Rezultati ove studije nude kvantitativne podatke o potencijalnoj uporabi drva Cola pachycarpa, koje bi moglo konkurirati drugim poznatim vrstama drva i poslužiti kao dobra zamjena za komercijalno prekomjerno iskorištavane vrste drva.*

**KLJUČNE RIJEČI:** Cola pachycarpa*; mehanička svojstva; aksijalna ravnina; radijalna ravnina*

## 1 INTRODUCTION
## 1. UVOD

Wood is a biological structure whose complexity is based on several cell kinds and chemistries working together to meet the demands of living plants (Wiedenhoeft, 2010). Wood has been used for centuries and decades for so many things ranging from furniture, structural, construction, acoustics, biofuel, etc. It is an indispensable material for people, and as such it is used for many utility and industrial purposes. Wood has a variety of qualities/properties originating from different wood species and within the same wood species due to varying factors and/or characteristics of wood. This is why wood species are classified based on their mechanical/strength properties thus providing timely information to science, wood-based industries, etc. Kretschmann (2010) opined that due to the dissimilarity of structural traits in wood, it helps to ascertain the mechanical attributes which in turn affect its potential for use. The modulus of rupture (*MOR*), which is also known and called the flexural strength of wood, is the load-carrying capacity (LCC) of a member. It measures the wood ability to resist deformation under bending. This property is essential in determining the structural integrity and suitability of wood for various applications. In contrast, the modulus of elasticity (*MOE*) quantifies the stiffness and stress-resiliency of wood. This property is crucial for figuring out how wood behaves under load, and whether it is appropriate for a given structural application. The resistance of wood to deformation when force is applied along the direction of the wood fibres is known as wood compressive strength parallel to the grain.

The African tropical sub-regions are home to many important edible tree species that have vast utilitarian potential and are rarely tapped. *Cola pachycarpa* happens to be one of them. *Cola pachycarpa* belongs to the Cola genus in the Malvaceae family and is a lesser-known plant species. In Nigeria, its fruits are recognized as edible, although it should be noted that the seeds within the fruit are not suitable for consumption like the commonly known "Kolanut" from the Cola genus (Jonny and Bassey, 2020). It is a forest tree which is over 30 feet high, little-branched with pale red flowers and white within. It is also, known as and commonly called Monkey or Bush Kola. Ogbu and Umeokechukwu (2014) asserted that Monkey Kola, also known as *Cola pachycarpa, Cola lepidota*, and *Cola lateritia*, are native tree species in the tropics originating from West Africa.

Despite their abundance, these edible wild relatives are underutilized. This underutilized indigenous tropical edible tree species is commonly consumed and relished by Nigerians and the Cameroons. It was reported by Anya (1982) that the south-eastern part of Nigeria has a wide array and diversity of *Cola pachycarpa* and other Cola spps. They are regarded as one of the epicentres for the early domestication of these forest tree species.

The aim of this work is to fill the knowledge gap regarding the mechanical properties of wood in most fruit tree species, with a focus on *Cola pachycarpa.* The goal is to better understand this fruit and food tree characteristics, as well as the possibilities of its utilization in construction works and plantation establishment.

## 2 MATERIALS AND METHODS
## 2. MATERIJALI I METODE

### 2.1 Study area
### 2.1. Područje istraživanja

The research was carried out in Rivers State, located in the South-South region of Nigeria (Figure 1). The state is primarily focused on agricultural activities and has a land area of approximately 11,077 km² (4,277 sq mi), which places it as the 26th largest state in Nigeria. It is situated along the coastal plain of the eastern Niger Delta, extending towards the ocean from the Benue Trough. Rivers State is primarily known for the many rivers that run through it, such as the Bonny River. It lies between 4°45′N 6°50′E North of the Equator.

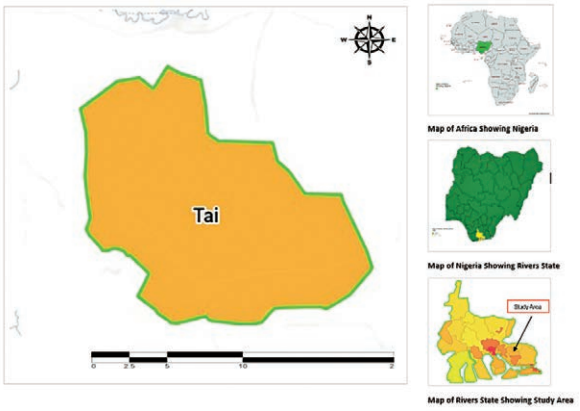


**Figure 1** Map showing study area
**Slika 1.** Karta koja prikazuje područje istraživanja

Its surface geology consists of predominantly fluvial sediments. Rivers State experiences heavy, erratic, and seasonal rainfall. The average yearly temperature in the State stands at 26 °C.The hottest period is from February to May. For the majority of the year, relative humidity ranges from 90 % to 100 %, seldom falling below 60 % (Niger Delta Budget Monitoring Group, 2022). Specifically, wood species samples of Bush Kola (*Cola pachycarpa*) were obtained from Kpite, Bunu Tai in Tai LGA in Rivers State, Nigeria bordering between latitude: 4° 42' 59.99"N, longitude: 7° 17' 60.00" E.

## 2.2 Sample preparation
## 2.2. Priprema uzoraka

Three trees of *Cola pachycarpa* were selected due to their good quality. Measurements were taken for both the length and diameter of the chosen trees. Three samples of bolts (logs) were taken from the base (10 % height), middle (50 % height), and top (90 % height) of the trees along the axial plane or merchantable height (Figure 2). Bolts were taken to the sawmill workshop for conversion and divided into six equal zones: labelled 1 to 6 from bark to bark. Sections 1 and 6 formed the outerwood portion, section 2 and 5 formed the corewood, and 3 and 4 formed the innerwood portion in-line with the recommendations of Aguda *et al.*, (2020). The sawn wood samples were further cut and trimmed to the specified dimensions of 20 mm × 20 mm × 60 mm and 20 mm × 20 mm × 300 mm for testing the mechanical properties. The blocks were prepared for testing by undergoing a process of drying and sterilization in an oven until reaching a constant weight at (103±2) °C for a duration of 24 hours. The weight of each wood sample was first measured, both when wet and dry in an oven, before being placed in a sealed nylon bag to avoid moisture absorption. 45 test samples were taken from each tree, with dimensions of 20 mm × 20 mm × 60 mm, totalling 135 samples. An additional 45 test samples were collected with dimensions of 20 mm × 20 mm × 300 mm, also totalling 135 samples, resulting in a grand total of 270 test samples (ASTM, 2014 and BS, 2012).

## 2.3 Determination of some mechanical test properties
## 2.3. Određivanje nekih mehaničkih svojstava

### 2.3.1 Modulus of rupture (*MOR*)
### 2.3.1. Modul loma (*MOR*)

The static bending tests were conducted using British standard BS: EN 408 (2012) and ASTM (2014) standard for small clear specimens of wood. The experiment was carried out at the Structural Unit of the Civil Engineering Laboratory, Rivers State University, Port Harcourt, using an improvised wood bending strength frame with a digital dial gauge (Improvised Universal Testing Machine) as shown in Figure 3. The dimensions of the test specimens are shown in Figure 4. The test specimens were loaded on a radial face, and the force applied to the sample at the point of failure was noted. The load carrying capacity (LCC) or bending strength was determined. This is typically expressed as the MOR, which is equivalent to the fibre stress in extreme fibres of the specimen at the point of failure.

$$MOR = \frac{3 \cdot P \cdot L}{2 \cdot b \cdot d^2} \, (\mathrm{N/mm^2}) \qquad (1)$$

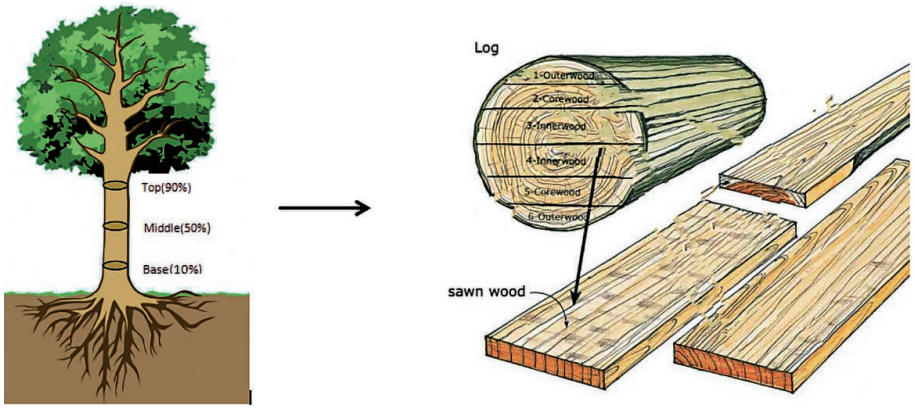


**Figure 2** Selected parts of tree samples
**Slika 2.** Odabrani dijelovi uzoraka stabala

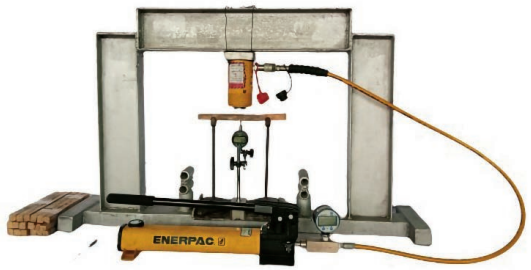


**Figure 3** *MOR* test sample setup
**Slika 3.** Oprema i postavljanje uzorka pri ispitivanju modula loma

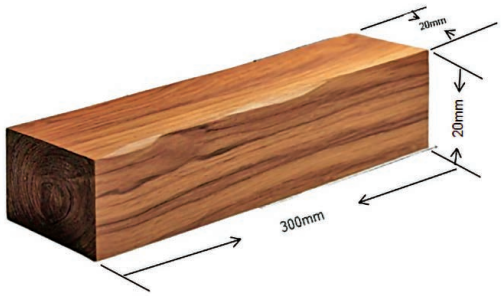


**Figure 4** Wood sample geometry for *MOR* and *MOE* test
**Slika 4.** Geometrija uzorka drva za ispitivanje *MOR-a* i *MOE-a*

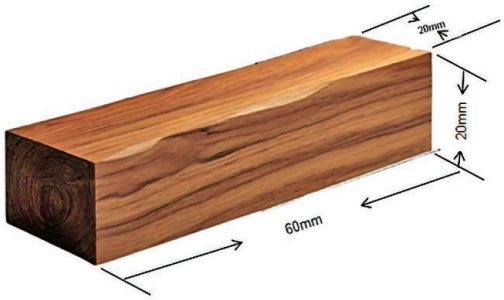


**Figure 5** Wood sample geometry for compressive strength test
**Slika 5.** Geometrija uzorka drva za ispitivanje čvrstoće na tlak

Where:

*MOR* – Modulus of Rupture
*P* – load (N)
*L* – length of the sample (mm)
*b* – width of the sample (mm)
*d* – thickness of the sample (mm)

### 2.3.2 Modulus of elasticity (*MOE*)
### 2.3.2. Modul elastičnosti (*MOE*)

The values obtained at the point of failure and recorded during the *MOR* test were used to calculate the *MOE*. This made it possible to compute the deflection, which was then used to estimate the *MOE* by the following formula:

$$MOE = \frac{P \cdot L^3}{4 \cdot \Delta b \cdot d^3} (\mathrm{N/mm^2}) \qquad (2)$$

Where:

*P* – load (N)
*L* – span (mm)
*b* – width (mm)


**Figure 6** Compression stress parallel to grain test setup
**Slika 6.** Oprema za ispitivanje čvrstoće na tlak paralelno s vlakancima

*d* – depth (mm)
Δ – deflection at the beam centre at a proportional limit (mm)

### 2.3.3 Compressive strength parallel to grain (*CS//G*)
### 2.3.3. Čvrstoća na tlak paralelno s vlakancima (*CS//G*)

The maximum compressive strength parallel to the grain was ascertained in line with the guidelines of BS: EN 408 (2012) method of testing small clear specimens of timber with test samples measuring 20 mm × 20 mm × 60 mm (Figure 5). At a rate of 0.01 mm/sec, wood samples were loaded, and the corresponding force was measured directly at the point of failure. The maximum compressive strength parallel to the grain was calculated by dividing this by the test specimen cross-sectional area. The CRB machine was used for this task (Figure 6).

(3)

Where:

*CS//G* – compressive strength parallel to grain
*F* – force at failure (N)
*L* – length of specimen (mm)
*b* – width in (mm)
**Note:** $L \cdot b$ – Cross-sectional area of specimen ($mm^2$)

## 2.4 Experimental design and data analysis
## 2.4. Dizajn eksperimenta i analiza podataka

The experiment was laid out in a Completely Randomized Design (CRD), and the samples were replicated three (3) times and data was analyzed using Minitab

statistical software version 16. One-way analysis of variance (ANOVA) was carried out to determine the level of significance among the various treatment means at a 0.05 % probability level. Duncan Multiple Range Test (DMRT) was used to separate the means.

## 3 RESULTS AND DISCUSSION
## 3. REZULTATI I RASPRAVA

### 3.1 Modulus of rupture (*MOR*)
### 3.1. Modul loma (*MOR*)

*MOR* is the load-carrying capacity (LCC) of a member. As shown in Table 1, the *MOR* mean values range from 5.81 N/mm$^2$ to 6.03 N/mm$^2$ with an increase from top to base along the axial length and with an increase from outer to inner wood across the bole of the tree radially with mean values ranging from 5.43 N/mm$^2$ to 6.64 N/mm$^2$, respectively. The findings align with the studies conducted by Aleru and David-Sarogoro (2016) on *Mangifera indica*, Izekor (2010) on *Tectona grandis*, Aguda *et al*. (2014) on *Funtumia elastica*, Oriowo *et al*. (2015) on *Terminalia superba,* Kiaei and Farsi (2016) on *Albizia julibrissin* (Persian silk wood), and Ojo (2016) on *Borassus aethiopum*, as well as the recent research by Aguda *et al*. (2020) on *Ficus vallis-choudae* wood. However, the mean values are far less than those of the above authors but agree with the mean *MOR* range values (1.6067±0.62 to 5.5133±2.33 N/mm$^2$) of the work conducted by David-Sarogoro, and Emerhi (2021) on *Ficus exasperata*. The addition of more mature wood, an increase in annual growth rings, and the ageing of the cambium as the tree grows in girth could all be contributing factors to the axial increase of *MOR* from top to base (Izekor and Fuwape, 2010). The radial increase from the outerwood to the innerwood of the tree bole could be a result of the formation of annual growth rings, wherein the innerwood seems older than the core and outerwood. Accumulation of wood extractives at the heartwood area tends to boost the wood weight-bearing ability, and this may also have contributed to the increase from the outerwood to the innerwood (Aguda *et al.*, 2020). In accordance with BS 5268-2 (2002) wood strength grading as reported in the BVRIO Guide by Blackham *et al.* (2020), the mean *MOR* (5.89 N/mm$^2$) falls under the deciduous class (D40), making it a very weak wood in terms of bending. This is also corroborated according to MS 544 Part 2 (2001), which falls under the strength group (SG-7).

### 3.2 Modulus of elasticity (*MOE*)
### 3.2. Modul elastičnosti (*MOE*)

*MOE* is the ability of a material, in this case wood, to exhibit its level of retention to its original size and shape before deformation. As such, the evaluation of the wood elastic modulus has great significance in determining its suitability for specific end uses. The mean data of the *MOE* is presented in Table 2. The mean values range from 756.72 N/mm$^2$ to 878.41 N/mm$^2$ with an increase from base to top (axially). Radially, there was an increase from outer to inner wood with mean values ranging from 761.96 N/mm$^2$ to 869.32 N/mm$^2$, respectively. The results at the axial position agree with the results of Fasiku and Ogunsanwo (2020) in the work carried out on *Anogeissus leiocarpus* (DC.) Guill & Perr and with the work of Aguda. *et al*. (2020.) on *Ficus vallis-choudaea* wood in their radial position. The increase in MOE at the top of the tree could be attributed to the dynamic nature of the tree canopy area. Wood from the canopy zone is often prone to wood defects because the area is gnarled (i.e., filled with knots). This zone is where photosynthetic activity is predominantly carried out and it is impacted more when compared to the base region of the wood. This report corresponds with the work carried out by Sanwo (1983) in the study of the plantation-grown *Tectona grandis* and Aguma, and by Ogunsanwo (2019) on *Khaya grandifoliola.* Given that age in the cambium and the accumulation of extractives in the heartwood when compared to the outerwood are major determinants of wood mechanical properties, the increase in MOE from the outer to the innerwood may have resulted from the annual formation of growth rings. This report contradicts the study(ies) on *Tectona grandis* by Izekor (2010) and Aguda *et al.* (2020), Ojo (2016) on *Borassus aethiopum* and (2012, 2014, and 2015) on *Staudtia stipitata, Funtumia elastica, and Chrysophyllum albidum.* Consequently, a combination of juvenile wood properties, growth stresses, nutrient distribution, cell structure variation, environmental influences and

**Table 1** Mean *MOR* (N/mm$^2$) values of Cola (*Cola pachycarpa*)
**Tablica 1.** Srednje vrijednosti modula loma (N/mm$^2$) drva *Cola pachycarpa*

| **Axial position** / *Pozicija u uzdužnom smjeru* | | | | | |
|---|---|---|---|---|---|
| **Radial position** *Pozicija u radijalnom smjeru* | **Top (90 %)** | **Middle (50 %)** | **Base (10 %)** | **Mean** | **COV, %** |
| Inner / *unutarnja zona* | 6.19a±0.97 | 7.16a±0.60 | 6.56a±1.36 | 6.64±0.99 | 14.91 |
| Core / *srednja zona* | 5.44b±0.65 | 5.49b±0.97 | 5.91b±0.74 | 5.61±0.99 | 17.64 |
| Outer / *vanjska zona* | 5.81ab±1.29 | 4.86b±0.14 | 5.61b±0.73 | 5.43±0.55 | 10.13 |
| Mean | 5.81±0.86 | 5.84±0.19 | 6.03±0.85 | 5.89±0.12 | 2.04 |

The means in the same column that have the same superscript are not statistically significant ($p < 0.05$).
*Srednje vrijednosti u istom stupcu koje imaju jednak indeks nisu statistički značajne ($p < 0,05$).*

**Table 2** Mean *MOE* (N/mm²) values of Cola (*Cola pachycarpa*)
**Tablica 2.** Srednje vrijednosti modula elastičnosti (N/mm²) drva *Cola pachycarpa*

| **Axial position** / *Pozicija u uzdužnom smjeru* | | | | | |
|---|---|---|---|---|---|
| **Radial position** *Pozicija u radijalnom smjeru* | **Top (90 %)** | **Middle (50 %)** | **Base (10 %)** | **Mean** | **COV, %** |
| Inner / *unutarnja zona* | 977.16[a]±168.17 | 871.12[a] ±185.72 | 759.68[a]±97.70 | 869.32 ±164.17 | 18.88 |
| Core / *srednja zona* | 880.55[b]±91.06 | 766.54[b]±127.65 | 754.80[c]±38.89 | 801.34±99.64 | 12.43 |
| Outer / *vanjska zona* | 777.52[c]±10.04 | 754.80[c]±38.89 | 753.55[a]±310.50 | 761.96 ±157.03 | 20.61 |
| Mean | 878.41±61.32 | 797.49 ±65.04 | 756.72±117.21 | 810.87±61.94 | 7.64 |

The means in the same column that have the same superscript are not statistically significant ($p < 0.05$).
*Srednje vrijednosti u istom stupcu koje imaju jednak indeks nisu statistički značajne ($p < 0,05$).*

**Table 3** Mean *CS//G* (N/mm²) values of Cola (*Cola pachycarpa*)
**Tablica 3.** Srednje vrijednosti *CS//G*-a (N/mm²) drva *Cola pachycarpa*

| **Axial position** / *Pozicija u uzdužnom smjeru* | | | | | |
|---|---|---|---|---|---|
| **Radial position** *Pozicija u radijalnom smjeru* | **Top (90 %)** | **Middle (50 %)** | **Base (10 %)** | **Mean** | **COV, %** |
| Inner / *unutarnja zona* | 38.98[a]±3.60 | 33.37[a]±3.54 | 35.26[a]±4.23 | 35.87±2.86 | 7.97 |
| Core / *srednja zona* | 38.30[a]±6.10 | 33.18[a]±0.95 | 33.32[a]±3.08 | 34.93±2.92 | 8.36 |
| Outer / *vanjska zona* | 35.02[b]±6.81 | 33.11[a]±7.67 | 31.02[b]±2.11 | 33.05±2.00 | 6.05 |
| Mean | 37.43±4.55 | 33.22±2.33 | 33.20±0.77 | 34.62±2.44 | 7.04 |

The means in the same column that have the same superscript are not statistically significant ($p < 0.05$).
*Srednje vrijednosti u istom stupcu koje imaju jednak indeks nisu statistički značajne ($p < 0,05$).*

genetic factors can cause the wood at the top of the tree to grow harder and exhibit a higher MOE compared to the wood in the middle and base of the tree. In the same vein, the mean *MOE* (10.87 N/mm²) also falls under the D30 and SG-7 category, making it a very weak wood in elasticity in line with BS 5268-2(2002) and MS 544 Part 2 (2001), respectively.

### 3.3 Compressive strength parallel to grain (*CS//G*)
### 3.3. Čvrstoća na tlak paralelno s vlakancima (*CS//G*)

The mean compressive strength parallel to the grain of wood species is presented in Table 3. The values at their axial length range from 33.20 N/mm² to 37.43 N/mm² with an increase from base to top across the grain radially, and from 33.05 N/mm² to 35.87 N/mm² with an increase from outer to inner wood. The result agrees with the works carried out by Aguda *et al.* (2020) on *Ficus vallis-choudae* (Delile) wood and Fasiku and Ogunsanwo (2020) on *Anogeissus leiocarpus* (DC.) Guill & Perr wood. Conversely, the orientation trend goes contrary to the works of Izekor and Fuwape (2010) on *Tectona grandis* and Aguma and Ogunsanwo (2019) in both their axial and radial plan. This variation could also be a result of the top tree being close to photosynthetic activities as against the base of the tree, as seen in the *MOE* of the tree. Since age is one of the factors that determine wood strength properties, the radial variation that is highest in the innerwood may be the result of the annual growth ring formation, as the growth ring of the innerwood is older than that of the core and outerwood. Furthermore, these variations could be attributed to the fact that juvenile wood has a high density at the top due to rapid growth and high lignin content, which contributes to increased compressive strength (Larson *et al.*, 2001). The genetic composition and/or hormonal factors of the tree could also have resulted in this variation. Some tree species adapt to environmental conditions that favour stronger wood formation at the top for enhanced stability and resistance to mechanical forces (Wimmer and Downes,2003). The hormonal regulation of growth, particularly the influence of auxins produced at the apical meristem (top of the tree), can also cause this variation. These hormones can regulate cell division and differentiation, potentially leading to variations in wood strength along the tree height (Hoad *et al.*, 1981). Conversely, the wood in *CS//G* (34.62 N/mm²) falls under SG-1 and D70 in line with MS 544 Part 2 (2001) and BS 5268 – 2 (2002) grading standards, respectively. This shows that the wood is stronger in *CS//G* and very weak in *MOR* and *MOE*.

## 4 CONCLUSIONS
## 4. ZAKLJUČAK

In conclusion, the research has provided baseline data on the suitability of *Cola pachycarpa* K Schum and its utilization potentials. Through meticulous analysis, the investigation results indicate that the *MOR* and *MOE* are low in line with the British and Malaysian Standard while *CS//G* wood is comparatively high. As such, having a relatively high compressive strength parallel to the grain, the wood will be suitable for applications where wood will be subjected to axial loads, such as columns, post, beams and joists (where the load is applied parallel to the grain), rafters and trusses and it could be competitive with other well-

known wood species and be used as a good replacement for commercially overexploited wood species. Moving forward, further research is recommended to explore additional properties and applications of *Cola pachycarpa*, ensuring the conservation and responsible utilization of this valuable resource in the context of the rich biodiversity of the tropical rainforests of Rivers State, Nigeria.

## 5 REFERENCES
## 5. LITERATURA


1. Aguda, L. O.; Adejoba, O. R.; Areghan, S. E.; Ogunleye, M. B.; Aba, O. D., 2014: Mechanical properties of *Funtumia elastica* wood. In: Proceedings of 4th Biennial National Conference of the Forests and Forest Products Society, Abeokuta, Nigeria, pp. 351-356.
2. Aguda, L.; Ajayi, B.; Areghan, S.; Olayiwola, Y.; Kehinde, A.; Idowu, A.; Aguda, Y., 2020: Mechanical properties of *Ficus vallis-choudae* (Delile), a lesser utilized species in Nigeria. BioResources, 15 (3): 6550-6560. https://doi.org/10.15376/biores.15.3.6550-6560
3. Aguma, Q.; Ogunsanwo, O. Y., 2019: Variations pattern in selected mechanical properties ofstem and branch woods of *Khaya grandifoliola* (Welw.). C. DC. Journal of Research in Forestry, Wildlife & Environment, 11 (1): March, 2019.
4. Aleru, K. K.; David-Sarogoro, N., 2016: Mechanical strength properties of *Mangifera indica* in axial direction at different moisture regimes. International Journal of Advanced Research, 4 (11): 1520-1526. https://doi.org/10.21474/ijar01/2242
5. Anya, A. O., 1982: The Ecology and Sociology of Igbo Cultural and Development.1982 Ahiaojku Lecture Series. Owerri, Nigeria. Government Press.
6. Blackham, G.; Núñez del Prado, I.; Parker, J.; Tavares de Bastos, C., 2020: Lesser-known & lesser-used timber species utilizing ghana's sustainable timber resources. BVRio Responsible Timber Exchange.
7. David-Sarogoro, N.; Emerhi, E. A., 2021: Correlation between density and other mechanical wood properties of *Ficus exasperata* (Vahl) along axial plane. African Journal of Wood Science and Forestry, 9 (6): 001-007.
8. Fasiku, O. O; Ogunsanwo, O. Y., 2020: Selected physico-mechanical properties of wood of *Anogeissus leiocarpus* (DC.) Guill & Perr. International Journal of Research Studies in Science, Engineering and Technology, 7 (1): 9-17.
9. Hoad, G. V.; Lenton, J. R.; Jackson, M. B.; Atkin, R. K., 1981. Hormone Action in Plant Development – A Critical Appraisal. Butterworth-Heinemann Ltd.
10. Izekor, D. N.; Fuwape, J. A., 2010: Variations in mechanical properties among trees of the same and different age classes of teak (*Tectona grandis* L.F) wood. Journal of Applied Sciences Research, 6 (4): 562-567.
11. Izekor, D. N., 2010: Physico-mechanical characteristics and anatomy of teak (Tectona grandis L. F.) wood grown in Edo State, Nigeria. PhD Thesis, Federal University of Technology, Akure, Nigeria.
12. Jonny, I. I.; Bassey, M. E., 2020: Pharmacognostic and taxonomic studies of cola *Cola pachycarpa* K. Schum. (Malvaceae). Asian Plant Research Journal, 6 (3): 33-45. https:doi.org/10.9734/aaaaprj/2020/v6i330132
13. Kiaei, M.; Fars, M., 2016: Vertical variation of density, flexural strength and stiffness of Persian silk wood. Madera y Bosques, 22 (1): 169-175. https:doi.org/10.21829/myb.2016.221484
14. Kretschmann, D. E., 2010: Mechanical properties of wood. In: Wood handbook – Wood as an engineering material. Chapter 4: General Technical Report FPL-GTR-190. Department of Agriculture, Forest Service, Forest Products Laboratory, Madison, WI. p. 508.
15. Larson, P. R.; Kretschmann, D. E.; Clark, A.; Isebrands, J. G., 2001: Formation and Properties of Juvenile Wood in Southern Pines. Forest Product Society.
16. Ogbu, J. U.; Umeokechukwu, C. E., 2014: Aspects of fruit biology of three wild edible monkey kola species fruits (*Cola* spp. Malvaceae). Annual Research and Review in Biology, 4 (12): 2007-2014. https:doi.org/10.9734/ARRB/2014/8066
17. Ojo, A. R., 2016: Intra-tree variation in physico-mechanical properties and natural durability of *Borassus aethiopum* Mart. Woods in Savanna Zones of Nigeria. PhD Thesis, University of Ibadan, Ibadan, Nigeria.
18. Oriowo, B. F.; Amusa, N. A; Aina, K. S., 2015: Evaluation of Mechanical Properties of the *Terminalia Catappa* Trees and Stems from South Western Nigeria. International Journal of Novel Research in Electrical and Mechanical Engineering, 2 (3): 132-138.
19. Sanwo, S. K., 1983: Variations in the wood characteristics of plantation grown teak *Tectona grandis* in Nigeria. PhD Thesis, University of Wales, Cardiff.
20. Wiedenhoeft, A., 2010: Structure and function of wood. Wood handbook: wood as an engineering material. In: Wood handbook – Wood as an engineering material. Chapter 3: General Technical Report FPL-GTR-190. Department of Agriculture, Forest Service, Forest Products Laboratory, Madison, WI, p. 3.1-3.18.
21. Wimmer, R.; Downes, G. M., 2003. Temporal and Spatial Variation of Climate-related Tree ring Growth. Springer Series in Wood Science.
22. ***ASTM D143-14, 2014: Standard Test Methods for Small, Clear Specimens of Timber, West Conshohocken, PA.
23. ***BS EN 408, 2012: Timber Structures – Structural Timber and Glued Laminated Timber-Determination of Some Physical and Mechanical Properties. British Standard Institute, London.
24. ***BS 5268-2, 2002: Structural use of Timber. Part 2: Code of Practice for Permissible Stress Design, Materials and Workmanship. British Standard Institute, London.
25. ***MS 544, 2001: Code of Practice for Structural Use of Timber. Part 2: Permissible Stress Design of Solid Timber (First Revision). Department of Standards Malaysia, Shah Alam.
26. ***Niger Delta Budget Monitoring Group. 2022: Overview of Rivers State.


**Corresponding address:**

**KENNEDY KINIKANWO ALERU**
Rivers State University, Faculty of Agriculture, Department of Forestry and Environment, Port Harcourt, Rivers State, NIGERIA, e-mail: alerukennedy@gmail.com

Viljem Vek*, Ida Poljanšek, Urša Osolnik, Primož Oven[1]

# Analysis of Extractives in Liquid and Headspace Samples of Silver Fir Using Gas Chromatography Coupled with a Mass Selective Detector

# Analiza tekuće i parne faze ekstraktivnih tvari jelovine primjenom plinske kromatografije sa spektrometrom masa

**ORIGINAL SCIENTIFIC PAPER**
**Izvorni znanstveni rad**
Received – prispjelo: 15. 2. 2024.
Accepted – prihvaćeno: 7. 10. 2024.
UDK: 630*81; 674.032.475.2
https://doi.org/10.5552/drvind.2024.0193



**ABSTRACT** • *The main objective of the study is to present a chromatographic method that allows rapid and accurate quality control of extractives in liquid and headspace samples of wood and bark of European silver fir (Abies alba Mill.). The chemical identity of silver fir extractives in liquid and headspace samples was investigated. Mature silver firs were harvested and samples of sapwood, heartwood, knotwood and bark were prepared. Liquid samples were obtained by solvent extraction at higher temperature and pressure, while the volatile extractives of silver fir tissues were collected by headspace sampling. The extractives in the liquid silver fir samples were silylated prior to chromatographic analysis. The samples were then measured using gas chromatography (GC) coupled with a mass selective detector (MSD). The samples were introduced into the GC-MSD system using the Automatic Liquid Sampler (ALS) and the Headspace Sampler (HS). A total of 55 compounds were detected in the silver fir wood and bark samples. The liquid samples consisted of a variety of carboxylic/dicarboxylic acids, sugars with sugar alcohols (inositols) and sugar acids, with citric acid, quininic acid and sucrose being the most frequently represented. The liquid bark samples contained mainly sugar-like compounds, while the knotwood extracts contained large amounts of phenolic compounds and lignans. D-pitinol was confirmed as the most characteristic GC-MSD peak of the silver fir extracts. Analysis of the headspace of silver fir revealed α-pinene, camphene, D-limonene, β-myrcene, ocimene, 2-bornanone or D-camphor and α-terpineol as the characteristic monoterpenes. It was shown that the presented GC-MSD method is a suitable analytical tool for the chemical screening of low molecular weight compounds in both liquid and headspace samples of wood and bark. However, the analysis of higher molecular weight extractives requires a different analytical approach supported by other analytical methods such as LC/MS.*

**KEYWORDS:** *Abies alba Mill.; wood; bark; extractives; headspace; polyphenols; gas chromatography-mass selective detection (GC-MSD)*

* Corresponding author
[1] Authors are researchers at University of Ljubljana, Biotechnical Faculty, Department of Wood Science and Technology, Ljubljana, Slovenia. https://orcid.org/0000-0002-5091-0091

**SAŽETAK** • *Glavni cilj rada jest predstavljanje kromatografske metode koja omogućuje brzu i preciznu kontrolu kvalitete tekuće i parne faze ekstraktivnih tvari drva i kore jelovine (Abies alba Mill.). Ispitivan je kemijski sastav tekuće i parne faze ekstraktivnih tvari jelovine. Posječena su stabla zrele jele i pripremljeni su uzorci bjeljike, srži, kvrge i kore. Tekući uzorci ekstraktivnih tvari dobiveni su ekstrakcijom otapalom pri povišenoj temperaturi i tlaku, dok su hlapljive ekstraktivne tvari tkiva jelovine prikupljene injektiranjem parne faze. Ekstraktivne su tvari u tekućim uzorcima jelovine sililirane prije kromatografske analize. Uzorci su zatim izmjereni primjenom plinske kromatografije sa spektrometrom masa (GC-MSD) te su uneseni u GC-MSD sustav uz pomoć automatskog uzorkivača tekućina (ALS) i uzorkivača za hlapljive spojeve (HS). U uzorcima drva i kore jelovine detektirano je ukupno 55 spojeva. Tekući uzorci sastojali su se od različitih karboksilnih/dikarboksilnih kiselina, šećera sa šećernim alkoholima (inozitolima) i šećernih kiselina, a najčešće su bile zastupljene limunska kiselina, kininska kiselina i saharoza. Tekući uzorci kore sadržavali su uglavnom spojeve slične šećeru, dok su ekstrakti kvrga sadržavali velike količine fenolnih spojeva i lignana. D-pitinol je potvrđen kao najkarakterističniji GC-MSD vrh ekstrakata jelovine. Analiza parne faze ekstraktivnih tvari jelovine otkrila je α-pinen, kamfen, D-limonen, β-mircen, ocimen, 2-bornanon ili D-kamfor i α-terpineol kao karakteristične monoterpene. Pokazalo se da je predstavljena GC-MSD metoda prikladan analitički alat za kemijski pregled spojeva male molekularne mase u tekućoj i parnoj fazi ekstraktivnih tvari u uzorcima drva i kore. Međutim, analiza ekstraktivnih tvari veće molekularne težine zahtijeva drukčiji analitički pristup podržan drugim analitičkim metodama kao što je LC/MS.*

**KLJUČNE RIJEČI:** *Abies alba Mill.; drvo; kora; ekstraktivne tvari; parna faza; fenoli; plinska kromatografija sa spektrometrom masa (GC-MSD)*

## 1 INTRODUCTION
## 1. UVOD

Silver fir (*Abies alba* Mill.) is a tree species that plays an important role in the main processing streams of the timber industry in Europe. In addition, silver fir could even gain industrial importance with regard to the model prediction of future wood stock in European forests as a result of climate change (Dyderski *et al.*, 2018). The side streams of forestry and wood processing industry hold great underutilized potential (Verkasalo *et al.*, 2019). The idea of biorefining biomass products from wood industry side streams has been around for some time, and there are already value chains involving the extraction of valuable phytochemicals from low-value biomass of trees, such as knotwood or bark (Holmbom, 2011; Domazet *et al.*, 2023). The bioactive extractives are usually obtained from wood and bark tissues using various extraction methods and different more or less polar organic solvents (Holmbom, 1999). The choice of extraction method and analytical instruments depends on the objectives of the investigation and the type of extracts to be analyzed.

The literature review shows different analytical approaches for the analysis of extractives in the tissues of silver fir. The silver fir bark was extracted in different studies using various solvents and different extraction methods. These methods are based on the use of cold and/or hot water (Tavčar Benković *et al.*, 2014; Bianchi *et al.*, 2015), mixtures of water and ethanol (50:50, v/v) (Brennan *et al.*, 2020) or water and methanol (65:35, v/v) (Hamad *et al.*, 2019). The bark was also extracted sequentially, e.g. with hexane, then with acetone and finally with a mixture of toluene and ethanol (50:50, v/v), as shown by Brennan *et al.* (2020). Silver fir barks were extracted conventionally (Soxhlet, maceration, shaker) and with more advanced techniques such as sonication and accelerated solvent extraction (ASE). The bark extracts are analyzed with gas (GC-MS) and liquid chromatography (UPLC-PDA, HPLC-MS), with mass spectrometry (MALDI-TOF MS) and with NMR ($^{13}$C) spectroscopy (Bianchi *et al.*, 2015; Hamad *et al.*, 2019; Brennan *et al.*, 2020; Schoss *et al.*, 2022).

The silver fir wood, especially the knotwood, was most frequently extracted sequentially with less polar solvents, followed by extraction with polar solvents. This approach allows efficient removal of both lipophilic and hydrophilic extractives from silver fir wood and knots. For the extraction of knotwood, hexane and mixtures of water and acetone were used in the Soxhlet apparatus (Kebbi-Benkeder *et al.*, 2017) or in the ASE system (Willför *et al.*, 2004). Stemwood with sapwood and heartwood of silver fir was effectively extracted with a mixture of toluene and ethanol (2:1, v/v) and ethanol as reported by Hamada *et al.* (2018). An example of using only hot water as a solvent was shown by Schoss *et al.* (2022), who extracted sawdust consisting of both bark and wood tissue from branches using ultrasound. Silver fir branchwood samples were also extracted with aqueous methanol under reflux or/and successively with hexane and methanol under sonication as suggested by Patyra *et al.* (2022). It can be summarized from the literature that GC-MS and LC-MS are frequently used methods for the chemical screening of extractives in silver fir wood and bark. Thus, GC-MSD is a well-known analytical tool for the identification of low molecular weight compounds in wood samples.

In addition to the lipophilic and hydrophilic extractives of the liquid samples, the volatile terpenes of silver fir were analyzed both in the liquid and volatile

emission samples. As suggested by Salem *et al.* (2015), silver fir terpenes can be obtained by extracting wood and bark by soaking the ground samples in hexane for 14 days. Terpenes can also be extracted from wood by shaking the ground samples in hexane, as presented by Kačík *et al.* (2012). The volatile terpenes of silver fir are then separated and analyzed using various GC methods. An interesting sampling technique was demonstrated by Moukhtar *et al.* (2006), who measured volatile organic compound (VOC) emissions from silver fir branches using a large cuvette in which a selected branch was enclosed. The captured monoterpenes were then thermodesorbed and analyzed by GC-FID analysis (Moukhtar *et al.*, 2006).

However, due to the recent policy of the EU Commission Green Deal with green transition strategies, more attention is being paid to the use of so-called greener solvents with less hazardous effects on the environment and human health. Ethanol or water are suggested as such (Tekin *et al.*, 2018; Brennan *et al.*, 2021). However, extraction with such polar solvents usually results in complex extracts consisting of a variety of different compounds, e.g. from simple acids to sugar-like compounds to low and high molecular weight polyphenols. In this context, the choice of a suitable analytical approach for rapid and accurate chemical screening of the compounds in the wood and bark extracts is a difficult decision. The aim of the present study was to improve to some extent our published data on silver fir extractives by analyzing the wood and bark samples with GC-MSD for characteristic extractives that may have been overlooked or not detected in our previous TLC and HPLC analyses. The extractives in the liquid sample, i.e. the extracts of silver fir wood and bark, and the presence of volatile extractives in the headspace over the solid silver fir samples were analyzed by a gas chromatograph (GC) with a mass selective detector (MSD). Our aim is also to present a method for the chemical screening of extractives in liquid and headspace samples of wood and bark using a GC-MSD instrument in combination with simple and fast sample preparation.

## 2 MATERIALS AND METHODS
## 2. MATERIJALI I METODE

### 2.1 Chemicals
### 2.1. Kemikalije

The chemicals used for the silylation of silver fir extracts, i.e. pyridine, chlorotrimethylsilane (TMCS), N,O-bis(trimethylsilyl)trifluoroacetamide (BSTFA), heneicosanoic acid (C21:0) and betulinol, were purchased from Merck (Sigma-Aldrich Chemie, Taufkirchen, Germany). Water, methanol and absolute ethanol were purchased from J.T. Baker (Phillipsburg, NJ, USA). All chemicals used are commercially available, all were of pure/analytical grade and used without further purification.

### 2.2 Material
### 2.2. Materijal

The material for this analysis was taken from mature silver firs (*Abies alba* Mill.) with a height of 30 to 35 meters and an age of up to 189 years. The silver firs were felled in the forests of Kočevska Reka, Slovenia (45°34'31.5" N, 14°46'27.8" E) (45°34'31.5" N, 14°46'27.8" E) (Vek *et al.* 2021, 2023). Silver fir wood and bark were randomly sampled from the 15 cm thick stem discs and homogenized into sapwood (SW), heartwood (HW), knotwood (KW) and bark (B) (Figure 1). Sapwood and heartwood on the stem discs were differentiated using an iodine-starch test by applying iodine solution to the surface of the discs with a brush. In the case of knotwood, only a dark-colored middle section was sampled, leaving out the adjacent light-colored tissue of knots. The bark samples were prepared as a mixture of inner (living) tissues, including phloem and periderm, and dead/outer bark with all tissues outside the youngest/deepest phellogen (rhytidome) (Figure 1). The samples were then dried overnight in an oven at 50 °C and ground using a Retsch SM 2000 cutting mill. For the GC-MSD analysis, the four samples were prepared by mixing the mass aliquots of each sample for the analysis of wood and bark tissue. The material for headspace analysis was taken directly from the stem discs using a drill, and the fresh samples were then stored in airtight vials until the start of chromatographic analysis. The samples of sapwood, heartwood, sapwood and bark prepared for solvent extraction were stored in PP bottles and kept in a cool and dark place until extraction. PP bottles were used for storage and to facilitate handling of the material prior to solvent extraction, and only glassware was used for later processing of the extracts.

### 2.3 Extraction
### 2.3. Ekstrakcija

The method for extracting wood and bark samples was similar to that already described (Vek *et al.* 2021, 2023). Prior to extraction, all wood and bark ground samples were freeze-dried overnight in a Telstar LyoQuest CC1930 lyophilizator at 0.045 mbar and - 85 °C. The silver fir samples were extracted in an automated extraction system at a temperature above the boiling point of the solvent and at higher pressure. The obtained extracts were filtered and the sample to solvent ratio of the final extracts was 1:100 (w/v). After extraction, all extracts were filtered into dark (amber) 20 mL bottles, which were hermetically sealed with screw caps with silicone/PTFE septum. Prior to the


**Figure 1** A scheme of analysis: Trees of silver fir (*Abies alba* Mill.) were felled in the forests of Kočevska Reka, Ravne district. Sapwood (SW), heartwood (HW), knotwood (KW) and bark (B) of silver fir were prepared for extraction, the extracts were analyzed with a GC-MSD system equipped with automatic samplers for liquid samples and headspace samples.
**Slika 1.** Shema analize: stabla jelovine (*Abies alba* Mill.) posječena su u šumama Kočevske Reke, kotar Ravne. Bjelika (SW), srž (HW), kvrga (KW) i kora (B) jelovine pripremljeni su za ekstrakciju, a ekstrakti su analizirani sustavom GC-MSD opremljenim automatskim uzorkivačima za tekuću i hlapljivu fazu ekstraktivnih tvari.

analysis, all bottles containing the extracts were stored in a refrigerator at 4 °C.

### 2.4 Chromatographic analysis of silver fir wood and bark extractives
### 2.4. Kromatografska analiza ekstraktivnih tvari drva i kore jelovine

#### 2.4.1 Preparation of silver fir samples for GC-MSD analysis
#### 2.4.1. Priprema uzoraka jelovine za GC-MSD analizu

Prior to analysis by gas chromatography coupled with mass selective detector (GC-MSD), liquid samples of silver fir wood and bark were chemically modified by silylation as described by Willför *et al.* (2004). The extracts of SH, HW, KW and B were pipetted into a boro- glass tube. Heneicosanoic acid (C21) and betulinol were used as internal standards (ISTD). The extracts were dried to constant weight in a vacuum chamber at 0.050 bar and RT. The silver fir extracts were then silylated by adding 20 µL pyridine, 20 µL TMCS and 80 µL BSTFA. The reaction mixture was kept at 75 °C for 45 minutes. Silylation was used to chemically modify the extractives of the liquid silver fir samples into silyl derivatives, making the modified compounds more volatile and thermally stable and thus easier to analyze qualitatively and quantitatively (Sigma-Al-

drich©, 1997). The silylated samples were then transferred to 1.5 mL glass vials with 100 µL inserts using glass Pasteur pipettes.

For headspace analysis with GC-MSD, 1 gram of ground fresh sample was placed in a 20 mL glass vial, which was sealed airtight with an aluminum cap and a 20 mm PTFE/silicone septum. Headspace is the gas space in a valet above the fresh sample. Headspace analysis is therefore the analysis of the components present in this gas (Anthias Consulting, 2018).

#### 2.4.2 Gas chromatography of headspace and liquid samples of silver fir
#### 2.4.2. Plinska kromatografija parne i tekuće faze ekstraktivnih tvari jelovine

Injection of 1 µL of derivatized silver fir extracts containing internal standards (ISTD, C21:0 and betulinol) was performed in a split mode of 1:20. The sample was introduced into the column via an ultra-inert inlet liner for split injection with glass wool measuring 4 mm (ID) × 78.5 mm (length) and a volume of 870 µL. The inlet heater temperature was set to 250 °C.

The headspace of 1.00 g of a silver fir sample in 20 mL vials was sampled using the Agilent 7697A Headspace Sampler (HS). The HS oven temperature was set to 80 °C, the HS loop temperature to 90 °C, and the HS transfer line temperature to 100 °C. The samples were extracted from the vials for 1.00 minute. The headspace extractives were then transferred to the GC system at a temperature of 115 °C. Due to this increase in temperature from the HS oven to the transfer line unwanted condensation was avoided. The silver fir headspace samples were introduced into the column through an ultra-inert inlet liner for splitless injection without glass wool; this splitless liner had the same dimensions as the split liner mentioned above. The inlet temperature was 250 °C.

The silver fir extractives of the liquid and headspace samples were analyzed with an Agilent 8890 gas chromatograph (GC) coupled with an Agilent 5997B mass selective detector (MSD). The GC-MSD system is supported by the 7693A Automatic Liquid Sampler (ALS), which is a 16-vial injector tower complemented by the Agilent 7693A Autosampler with a 150-vial tray, and the Agilent 7697A Headspace Sampler with a 12-vial tray. The chromatography of the silver fir extractives, both the derivatized extractives and the headspace extractives, was carried out on an Agilent 19091S-433 Ultra Inert (5 % phenyl)-Methylpolysiloxane Fused Silica Capillary Column (HP-5ms) with a film thickness of 0.25 µm, an inner diameter (ID) of 0.25 mm and a length of 30 m. Helium was used as carrier gas at flow of 1.2 mL/min. The separation of the extractives from the liquid samples was achieved by the following temperature program: 100 °C (1 min)→ 4 °C $min^{-1}$ to 220 °C →20 °C $min^{-1}$ to 320 °C (8 min). The headspace samples of silver fir were separated in a similar temperature range as mentioned above using the temperature program: 40 °C (2 min) → 15 °C $min^{-1}$ to 200 °C →10 °C $min^{-1}$ to 280 °C (5 min) →10 °C $min^{-1}$ to 300 °C (5 min). The separated extractives were detected with the following MSD parameters: MS source and transfer line temperatures were 230 and 250 °C, respectively, MS quadrupole temperature was 150 °C, ionization was performed in electron impact (EI) mode at an ionization energy of 70 eV, and the scan time segments were set for the mass range of 20 m/z to 800 m/z. The solvent delay was set to 3 min. GC/MS chromatograms were analyzed using Agilent MassHunter Workstation 10.0 software, and peak assignment and peak identification were performed by comparison with spectra from the NIST 2017 Mass Spectral Library. The results of the qualitative analysis of the extractives present in the liquid and headspace samples of silver fir were confirmed with a high probability value (Prob. %). The chromatograms obtained were also compared with the GC/MS analysis data for silver fir samples from the literature.

## 3 RESULTS AND DISCUSSION
## 3. REZULTATI I RASPRAVA

### 3.1 Chemical identities of extractives in liquid silver fir samples
### 3.1. Kemijski sastav ekstraktivnih tvari u tekućim uzorcima jelovine

GC-MSD analysis revealed the presence of 33 compounds (excluding the two ISTDs) in the liquid samples. The extractives identified in the liquid silver fir samples are listed in Table 1. GC-MSD of the silylated compounds revealed the presence of various simple and carboxylic acids, monosaccharides, disaccharides and polyphenols, including simple phenols, flavonoids and lignans (Table 1). Figure 2 and Figure 3 show clear differences in the GC-MSD chromatograms of stemwood, knotwood and bark extracts of silver fir. With GC-MSD, significantly more compounds were separated and detected from the samples of silver fir KW and B (Figure 2), whereby the chromatograms of KW and B were richer than those of SW and HW (Figure 3). The extended peaks 26 and 35 with retention times of 18.480 minutes and 26.240 minutes are assigned to the internal standards (ISTD), i.e. heneicosanoic acid (linear/unbranched C21:0 fatty acid) and betulin or betilinol (triterpene/sterol) (Figure 2 and Figure 3). The ISTDs are used to quantitatively evaluate the separated compounds of the chemically analyzed samples, but quantitative analysis was not the aim of the present preliminary investigation. Detailed information on the amounts of the identified compounds in the silver fir wood and bark extracts will be

presented in our future reports. In the present study, the characteristic and abundant peaks of ISTD are mostly used for easier orientation and reading of the chromatograms. As can be seen from Figure 2, the obvious difference between the extracts of KW (DK in the upper chromatogram) and B is in the MSD responses for the extractives/peaks eluted before the retention time of 18.480 minutes, i.e. before the ISTD C21:0 fatty acid, and the detector responses for the extractives/peaks eluted between two ISTDs (C21:0 and betulinol), between 18.480 and 26.240 minutes (Figure 2).

The B extracts of silver fir were found to be characterized by a large number of carboxylic/dicarboxylic acids, sugar acids, sugar alcohols and monosaccharides, with inositols/sugar alcohols (peaks #20 and #23), citric acid (peak #19), quininic acid (peak #21) and sucrose (peak #17) being among the most abundant peaks (Figure 2) (Table 1). The GC-MSD analysis also showed the presence of flavonoids (peak #29 and #31) and lignans (peak #33), which were found in rather low amounts (Figure 2) (Table 1). However, it has already been proven that silver fir bark contains polyphenols with a simple chemical structure, such as gallic acid, homovanillic acid, protocatechuic acid, vanillic acid, ferulic acid, p-coumaric acid, catechin, epicatechin, taxifolin, isorhamnetin (or 3-methylquercetin), gallocatechin, epigallocatechin, taxiresinol, lariciresinol, secolariciresinol, but also more complex

**Table 1** Chemical composition of hydrophilic extractives of silver fir (*Abies alba* Mill.)
**Tablica 1.** Kemijski sastav hidrofilnih ekstrakata jelovine (*Abies alba* Mill.)

| **Peak** *Vrh #* | **Retention time, min** *Retencijsko vrijeme,* min | **Group of extractives** *Skupine ekstraktivnih tvari* | **Identified compound** *Identificirani spoj* |
|---|---|---|---|
| **1** | 3.190 | Polysiloxane | Tetrasiloxane |
| **2** | 3.381 | Carboxylic acid | Lactic Acid |
| **3** | 3.505 | Carboxylic acid | Glycolic acid |
| **4** | 4.055 | Dicarboxylic acid | Oxalic acid |
| **5** | 4.570 | Polysiloxane | Pentasiloxane |
| **6** | 5.762 | Sugar alcohol | Glycerol |
| **7** | 6.193 | Carboxylic acid | Butanedioic acid |
| **8** | 6.474 | Dicarboxylic acid | Glyceric acid |
| **9** | 8.415 | Dicarboxylic acid | Malic acid |
| **10** | 8.713 | Carboxylic acid | 2,3,4-Trihydroxybutyric acid |
| **11** | 8.795 | Monosaccharide | Ribofuranose-type 1 |
| **12** | 9.346 | Carboxylic acid | 2,3,4-Trihydroxybutyric acid |
| **13** | 9.441 | Monosaccharide | 3-O-Methyl-β-D-Glucopyranose |
| **14** | 10.013 | Monosaccharide | Ribofuranose-type 2 |
| **15** | 10.765 | Monosaccharide | Xylose |
| **16** | 11.496 | Dihydroxybenzoic acid | Vanillic Acid |
| **17** | 11.894 | Sugar acid | Ribonic acid |
| **18** | 12.066 | Cyclohexanecarboxylic acid | Shikimic acid |
| **19** | 12.227 | Carboxylic acid | Citric acid |
| **20** | 12.456 | Sugar alcohol | D-Pinitol |
| **21** | 12.733 | Cyclohexanecarboxylic acid | Quininic acid |
| **22** | 13.317 | Sugar alcohol | Acrylic acid |
| **23** | 13.780 | Sugar alcohol | Inositol 1 |
| **24** | 14.185 | Sugar acid | D-Gluconic acid |
| **25** | 14.988 | Sugar alcohol | Inositol 2 |
| **26** | 18.480 | Internal standard ISTD | C21:0 Heneicosanoic acid |
| **27** | 19.670 | Disaccharide | Sucrose |
| **28** | 19.916 | Fatty acid | Tricosanoic acid |
| **29** | 21.184 | Flavonoid | Catechin |
| **30** | 21.263 | Disaccharide | Melibiose |
| **31** | 21.476 | Flavonoid | Gallocatechin-type 1 |
| **32** | 21.588 | Flavonoid | Gallocatechin-type 2 |
| **33** | 21.748 | Lignan | Isolariciresinol |
| **34** | 25.193 | Disaccharide | Disaccharide-type |
| **35** | 26.240 | Internal standard ISTD | Betulinol |

ISTD, internal standard. The identified compounds with their peaks are shown in the GC-MSD chromatograms at Figure 2 and Figure 3, with the peak numbers given in the table.
*ISTD – interni standard. Identificirani spojevi sa svojim vrhovima prikazani su u GC-MSD kromatogramima na slici 2. i 3., s brojevima vrhova navedenima u tablici.*

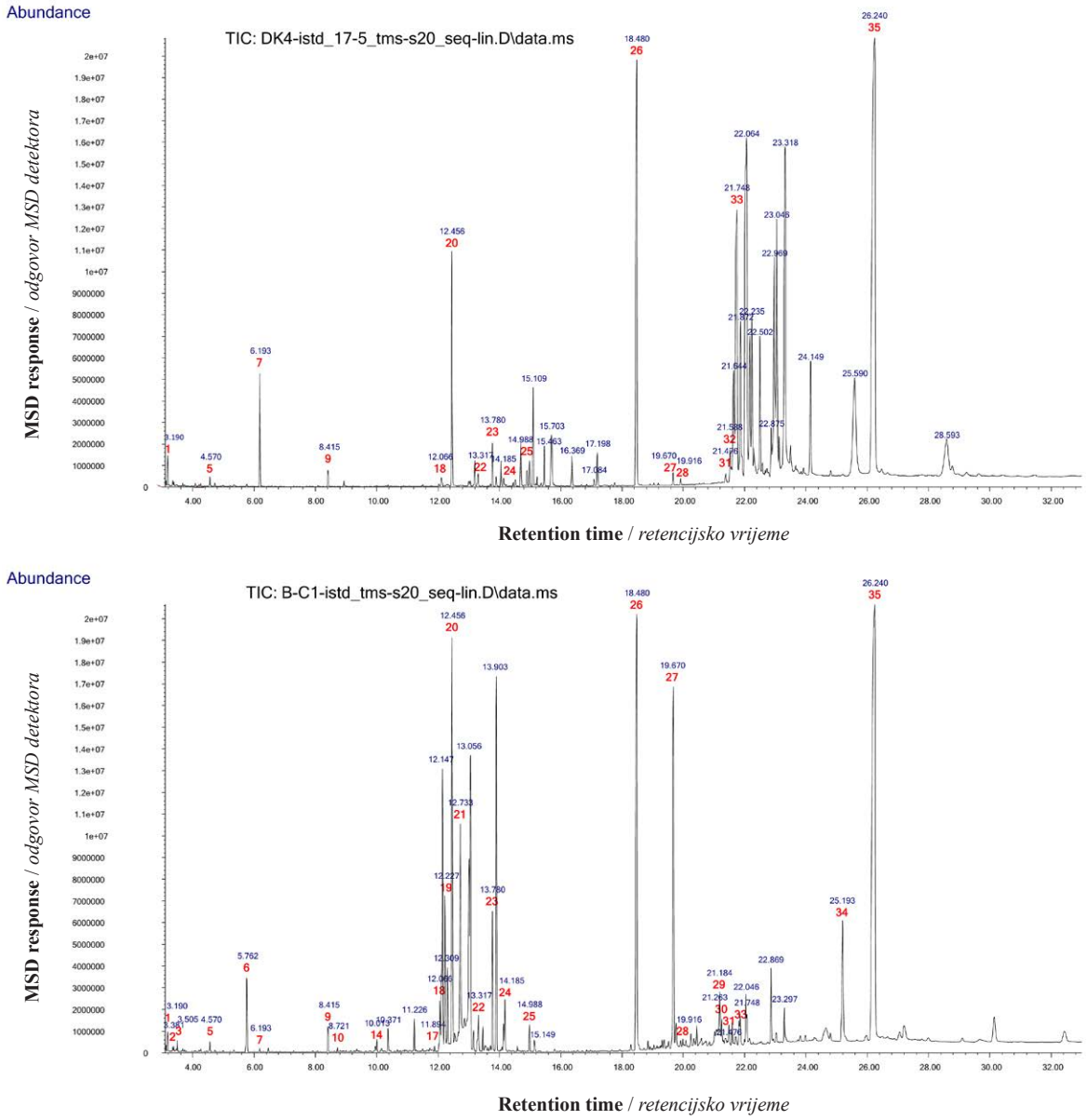


**Figure 2** GC-MSD chromatograms (TIC) of silylated extracts of silver fir (*Abies alba* Mill.) (DK – knotwood, B – bark, TIC – total ion chromatogram, #1 – #35, for peak assignment see Table 1)
**Slika 2.** GC-MSD kromatogrami (TIC) siliranih ekstraktivnih tvari jelovine (*Abies alba* Mill.) (DK – kvrga, B – kora, TIC – ukupni ionski kromatogram za pikove #1 – #35 prikazane u tablici 1.)

compounds such as gallocatechin gallate, various flavonoid glycosides (e.g. quercetin glycoside, isorhamnetin glucoside, astringin), gallocatechin dimers and various prodelphinidins. It has also been confirmed that dimeric and trimeric procyanidins are part of the hydrophilic extractable fraction of silver fir samples (Patyra *et al.*, 2022). The compounds mentioned are characterized by a higher molecular mass, therefore LC-MS methods are the usual choice of analytical approach for the analysis of polyphenols from silver fir bark (Tavčar Benković *et al.*, 2014; Bianchi *et al.*, 2015; Brennan *et al.*, 2020; Patyra *et al.*, 2022; Vek *et al.*, 2023).

On the other hand, the KW extracts were richer in phenolic compounds that eluted at retention times intermediate to those of the two ISTDs (Figure 2). Of the compounds that eluted at retention times between 18.80 and 26.40 minutes (Figure 2), the presence of gallocatechins and isolariciresinol could be confirmed using the NIST spectral database. Silver fir knots have previously been described as a rich source of lignans, of which secoisolariciresinol, lariciresinol, nortrachelogenin, liovil, hydroxymatairesinol, matairesinol, cyclolariciresinol, and pinoresinol were qualitatively assessed by GC-MS analysis (Willför *et al.*, 2004). Analysis on a short GC column also revealed the presence of sesquilignans, dilignans and higher oligolignans in silver fir knotwood (Willför *et al.*, 2004). Similar results were reported by Brennan *et al.* (2021), who used GC-MS analysis and their spectral database to

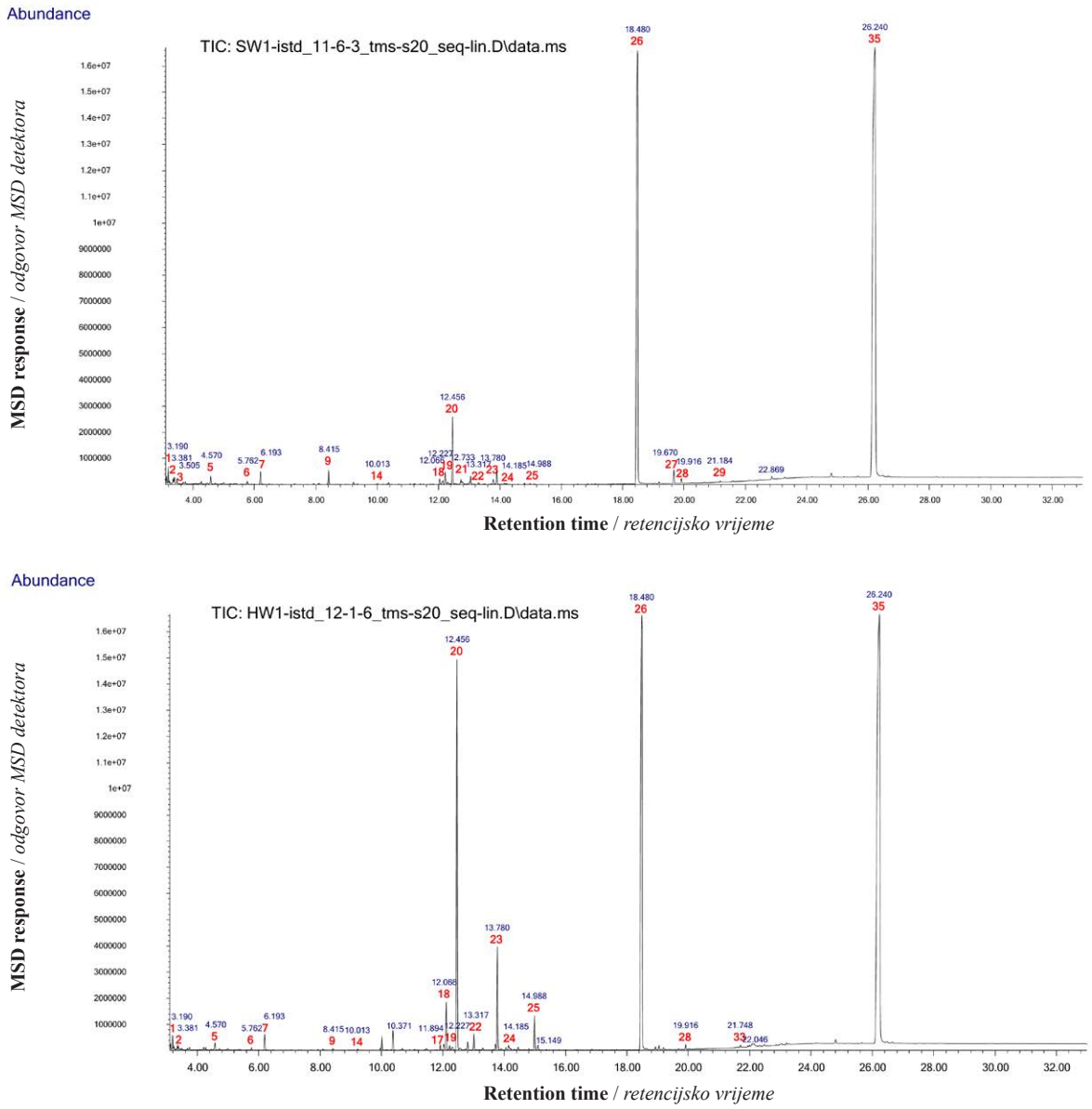


**Figure 3** GC-MSD chromatograms (TIC) of silylated extracts of silver fir (*Abies alba* Mill.) (SW – sapwood, HW – heartwood, TIC – total ion chromatogram, #1 – #35, for peak assignment see Table 1)
**Slika 3.** GC-MSD kromatogrami (TIC) siliranih ekstraktivnih tvari jelovine (*Abies alba* Mill.) (SW – bjeljika, HW – srž, TIC – ukupni ionski kromatogram za pikove #1 – #35 prikazane u tablici 1.)

detect silylated secoisolariciresinol, lariciresinol, hydroxymatairesinol and isolariciresinol in silver fir knotwood extracts. In addition, the extraction of silver fir KW also produces sugars with mono- and disaccharides as well as sugar alcohols (Table 1, Figure 2). D-pitinol (peak #20) was confirmed as a characteristic GC-MSD peak for both the KW and B samples, which agrees well with the literature data (Brennan *et al.*, 2021) (Figure 2).

Our recent investigations using other chromatographic methods (TLC, HPLC) on the silver fir samples from Kočevska also showed the presence of simple phenolic acids (homovanillic acid, coumaric acid, ferulic acid), flavonoids (epicatechin, taxifolin, quercetin) and, of course, lignans, as already mentioned in the literature review. With regard to the GC-MSD results (Table 1, Figure 2), our HPLC-PDA analysis of lignans in KW proved to be a convenient and rapid method for the separation and detection of not only isolariciresinol, but also lariciresinol, secoisolariciresinol, pinoresinol and matairesinol, with secoisolariciresinol being confirmed as the most abundant (Vek *et al.*, 2021). Therefore, the peaks between the retention times of 21.00 and 23.00 minutes could represent the presence of these lignans, with secoisolariciresinol being the predominant peak of the KW extracts presumably at 22,064 minutes (Figure 2) (Willför *et al.*, 2004).

Furthermore, our results confirmed that the extraction of silver fir stemwood samples, i.e. SW and HW samples, yielded a significantly lower amount of

extractives than the extracts from B and KW (Figure 2), as shown by the low detector responses for the separate extractives of SW and HW extracts (Figure 3). Similar results have been reported by other research groups (Willför *et al.*, 2004; Ul'yanovskii *et al.*, 2022). The hydrophilic extracts of silver fir SW and HW consisted mainly of various carboxylic acids (lactic acid #2, glycolic acid #3, butanedioic acid #7, malic acid #9, shikimic acid #18, citric acid #19, quininic acid #21), various sugar compounds (sugar alcohols, sugar acids, monosaccharides and disaccharides), of which D-pinitol was the most abundant peak (Figure 3, Table 1). Phenolic compounds (#29 and #33) were only present in trace amounts in the liquid SW and HW samples (Figure 3). It is evident that the peaks for the internal standard (peak 26 and peak 35) were high compared to the peaks of the other compounds present in both the SW and HW extracts (Figure 3). However, due to the same preparation of the liquid samples for chromatographic analysis, the differences in the chemical composition and the amount of extractives between the SW, HW, KW and B samples are very clear (Figure 2 and Figure 3).

Finally, regarding our liquid silver fir samples, all hydrophilic extracts (SW, HE, KW and B) were also characterized by the presence of small amounts of tricosanoic acid (peak #28), a C23:0 fatty acid (Figure 2 and Figure 3). Other research groups have also reported the presence of compounds with lower polarity, i.e. epimanool, neoabietic acid and abietic acid, extracted from silver fir wood with more polar solvents such as ethanol or aqueous methanol (Brennan *et al.*, 2021; Patyra *et al.*, 2022).

### 3.1 Chemical identities of silver fir extractives in headspace samples
### 3.1. Kemijski sastav parne faze ekstraktivnih tvari uzoraka jelovine

The GC-MSD analysis of volatile extractives in silver fir samples confirmed the presence of 22 compounds. The extractives identified in the silver fir headspace (HS) samples are listed in Table 2. Compared to the analysis of the liquid silver fir sample (Figure 2 and Figure 3), the headspace analysis could be performed in a much shorter time – the chromatographic run took 12.5 minutes as can be seen in the figure. As mentioned above, the samples analyzed in this preliminary headspace analysis were selected for their good sensory properties and pleasant characteristic odor. The headspace GC-MSD analysis revealed the presence of volatile monoterpenes, sesquiterpenes as well as volatile esters of low molecular weight carboxylic acids (Table 2, Figure 4).

**Table 2** Chemical composition of volatile extractives in headspace samples of silver fir (*Abies alba* Mill.)
**Tablica 2.** Kemijski sastav parne faze ekstraktivnih tvari uzoraka jelovine (*Abies alba* Mill.)

| **Peak** *Vrh #* | **Retention time, min** *Retencijsko vrijeme,* min | **Group of extractives** *Skupine ekstraktivnih tvari* | **Identified compound** *Identificirani spoj* |
|---|---|---|---|
| 1 | 2.757 | Polysiloxane | Disiloxane, hexamethyl- |
| 2 | 4.671 | Monoterpene, bicyclic | α-Pinene |
| 3 | 4.806 | Monoterpene, bicyclic | α-Pinene |
| 4 | 4.881 | Monoterpene, bicyclic | Camphene |
| 5 | 4.901 | Monoterpene, bicyclic | Dehydrosabinene |
| 6 | 5.136 | Monoterpene, acyclic | β-Myrcene |
| 7 | 5.442 | Monoterpene, cyclic | D-Limonene |
| 8 | 5.479 | Monoterpene, cyclic | D-Limonene |
| 9 | 5.702 | Monoterpene, bicyclic | γ-Terpinene |
| 10 | 5.968 | Monoterpene, bicyclic | L-Fenchone |
| 11 | 6.163 | Monoterpene, bicyclic | Fenchol, exo- |
| 12 | 6.217 | Monoterpene | Ocimene |
| 13 | 6.249 | Monoterpene | α-Campholenal |
| 14 | 6.427 | Monoterpene | 2-Bornanone/D-Camphor |
| 15 | 6.578 | Monoterpene, bicyclic | endo-Borneol |
| 16 | 6.647 | Monoterpene | Terpinen-4-ol |
| 17 | 6.738 | Monoterpene | α-Terpineol |
| 18 | 6.790 | Monoterpene | Myrtenol |
| 19 | 8.070 | Sesquiterpene | Ylangene |
| 20 | 8.099 | Sesquiterpene | Copaene |
| 21 | 8.421 | Sesquiterpene | Caryophyllene |
| 22 | 9.421 | LMW carboxylic acid | Valeric acid, volatile esters |

LMW, low-molecular weight compound. The identified compounds with their peaks are shown in the GC-MSD chromatogram in Figure 4, with the peak numbers given in the table.
*LMW – spoj niske molekularne mase. Identificirani spojevi sa svojim vrhovima prikazani su u GC-MSD kromatogramu na slici 4., s brojevima vrhova navedenima u tablici.*

As shown in Figure 4, the characteristic volatile compounds of the silver fir headspace samples were monoterpenes, which eluted from the column between 4.20 and 7.00 minutes. The peaks in the GC-MSD chromatogram (Figure 4) were assigned to the monoterpenes α-pinene (peak #2 and #3), camphene (peak #4), D-limonene (#7 and #8), β-myrcene (#6), ocimene (#12), (+)-2-bornanone or D-(+)-camphor (#14), and α-terpineol (#17) (Table 2). It is obvious that the concentration of α-pinene and D-limonene in the extracted headspace sample was very high, so the interactions of the compounds with the stationary phase led to the formation of the split peaks, which means that the molecules of both α-pinene and D-limonene came out of the column and eluted at two retention times (Figure 4). Therefore, improving the existing headspace sampling method and determining the exact timing for sampling the headspace of wood and bark from the HS vials will be one of the important goals of our future research activities.

Monoterpenes from various tree tissues are extracted by simple steam distillation, supercritical $CO_2$ distillation, solid phase extraction (SPE), purge and trap (P&T), thermal desorption (TD) and solid phase microextraction (SPME) as well as by solvent extraction (Fengel and Wegener, 1989; Moukhtar *et al.*, 2006; Holmbom, 2011; Kačík *et al.*, 2012; Salem *et al.*, 2015; Turner, 2018). As described by Kačík *et al.* (2012) α-pinene, camphene, β-pinene, α-phellandrene, cymene, limonene, fenchol, borneol, thymol, myrtenal and verbenone are extracted from silver fir wood using hexane as a solvent. Using the present GC-MSD method, we were also able to detect sesquiterpene structures, i.e. terpenes consisting of three isoprene units, in the silver fir headspace samples; these volatile extractives were eluted after 8 minutes, as shown in Figure 4. Ylangene (peak #19), copaene (#20) and caryophyllene (#21) were described as sesquiterpenes with the spectral database used (Table 2). Brennan *et al.* (2021) report the detection of juvabiones, i.e. dehydrojuvabione and juvabione, among the eluted sesquiterpenes in the liquid sample of silylated KW silver fir extracts by GC-MSD analysis. However, the first detailed report on the presence of juvabiones (4'-dehydrojuvabione, todomatuic acid and 4'-dehydrotodomatuic acid) in extracts from silver fir stemwood and knotwood was presented two decades ago (Willför *et al.*, 2004). Interestingly, dehydrojuvabione was also detected in methanolic extracts of silver fir wood using the LC-DAD-ESI-MS/MS method, demonstrating that liquid chromatography/mass spectrometry is also an effective analytical approach for the analysis of terpenes in liquid samples (Patyra *et al.*, 2022).

However, the collection of volatile extractives from wood and bark using the headspace sampling method described is a rapid and accurate technique that requires no additional pretreatment of the sample prior to analysis. When taking headspace samples, it is important that the sample is fresh and has not been subjected to any thermal treatment that could negatively influence the results of the subsequent chromatographic analysis. Our results are in good agreement with existing literature data, and small differences in the composition of the volatile extracts of silver fir samples

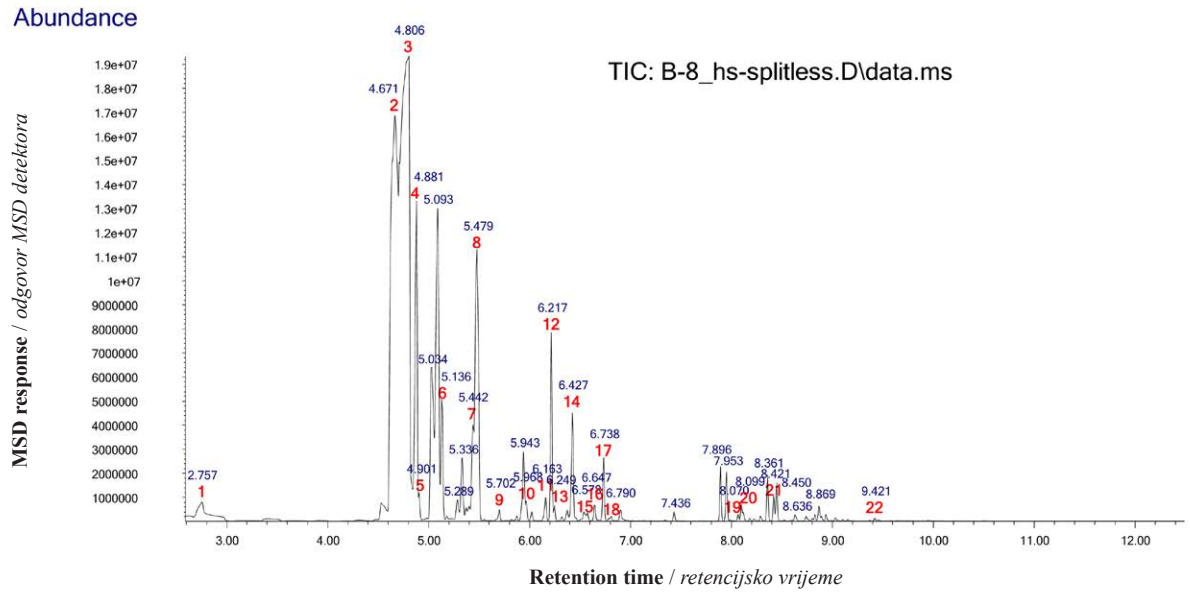


**Figure 4** GC-MSD chromatograms (TIC) of headspace extractives of silver fir (*Abies alba* Mill.) (B – bark, TIC – total ion chromatogram, #1 – #22, for peak assignment see Table 2)
**Slika 4.** GC-MSD kromatogrami (TIC) parne faze ekstraktivnih tvari jelovine (*Abies alba* Mill.) (B – kora, TIC – ukupni ionski kromatogram za pikove #1 – #22 prikazane u tablici 2.)

could be due to the fact that the terpenoid profiles of conifers are geographically, taxa, genotype, temperature and light dependent (Manninen *et al.*, 2002; Moukhtar *et al.*, 2006; Kačík *et al.*, 2012).

## 4 CONCLUSIONS
## 4. ZAKLJUČAK

This research report presents a rapid and accurate method for analyzing the solvent-soluble and volatile extractives of silver fir tissues. The demonstrated gas chromatograph-mass selective detector (GC-MSD) method allows both the analysis of liquid wood and bark samples, where the extracts have been previously silylated, and the analysis of the headspace (HS) of freshly prepared silver samples. A total of 55 extractives in silver fir wood and bark samples were qualitatively evaluated using the HS-GC-MSD method. Gas chromatography of silylated compounds confirmed that silver fir bark extracts are characterized by a large number of carboxylic/dicarboxylic acids, sugar acids, sugar alcohols and monosaccharides, with inositols/sugar alcohols, citric acid, quininic acid and sucrose reaching the most abundant peaks. Larger amounts of phenolic extractives in the bark were not found, which does not mean that the bark does not contain phenolic extractives, but that the GC results should also be supported by other analytical methods. The liquid samples of knotwood extracts were rich in phenolic compounds and lignans. These compounds include gallocatechins and isolariciresinol. D-pitinol was confirmed as the most characteristic chromatographic peak in the GC traces of both the silver fir wood and bark samples. On the other hand, headspace analysis revealed the monoterpenes α-pinene, camphene, D-limonene, β-myrcene, ocimene, 2-bornanone or D-camphor and α-terpineol as the characteristic volatile extractives of silver fir. Headspace sampling has proven to be a fast and convenient method for analyzing volatile extractives, but still needs some fine-tuning. Finally, gas chromatography in combination with a mass selective detector and automatic samplers for liquid and headspace samples is an excellent analytical tool for the chemical screening of low molecular weight compounds in wood and tree bark. However, the analysis of higher molecular weight extractives requires a different analytical approach.

**Acknowledgements** – Zahvala

The authors would like to thank the Slovenian Research and Innovation Agency (ARIS) for supporting the project L4-2623 (ArsAlbi), the project V4-2017 and the programme group P4-0015. Special thanks go to Ars Pharmae d.o.o. for supporting the research activities and co-financing the HS-GC-MSD system. Many thanks also to the company Kočevski les d.o.o. for providing the silver fir material and to Samo Grbec, Anže Lopatič and Peter Hrovatič for their help and support in the field and in the laboratory.

## 5 REFERENCES
## 5. LITERATURA

1. Bianchi, S.; Kroslakova, I.; Janzon, R.; Mayer, I.; Saake, B.; Pichelin, F., 2015: Characterization of condensed tannins and carbohydrates in hot water bark extracts of European softwood species. Phytochemistry, 120: 53-61. https://doi.org/10.1016/j.phytochem.2015.10.006
2. Brennan, M.; Fritsch, C.; Cosgun, S.; Dumarcay, S.; Colin, F.; Gerardin, P., 2020: Quantitative and qualitative composition of bark polyphenols changes longitudinally with bark maturity in *Abies alba* Mill. Annals of Forest Science, 77 (1): 14. https://doi.org/10.1007/s13595-019-0916-x
3. Brennan, M.; Hentges, D.; Cosgun, S.; Dumarcay, S.; Colin, F.; Gérardin, C.; Gérardin, P., 2021: Intraspecific variability of quantity and chemical composition of ethanolic knotwood extracts along the stems of three industrially important softwood species: *Abies alba*, *Picea abies* and *Pseudotsuga menziesii*. Holzforschung, 75 (2): 168-179. https://doi.org/10.1515/hf-2020-0108
4. Domazet, M.; Zaloker, U.; Vek, V., 2023: Ars Pharmae®: Innovative natural approach to prevent and reduce diseases of modern times; food supplements from wood extractives. BioRural Knowledge-exchange Workshops (online), 2023.
5. Dyderski, M. K.; Paź, S.; Frelich, L. E.; Jagodziński, A. M., 2018: How much does climate change threaten European forest tree species distributions? Global Change Biology, 24 (3): 1150-1163. https://doi.org/10.1111/gcb.13925
6. Fengel, D.; Wegener, G., 1989: Wood: chemistry, ultrastructure, reactions. Berlin – New York, Walter de Gruyter. https://doi.org/10.1515/9783110839654
7. Hamad, A. M. A.; Ates, S.; Olgun, C.; Gur, M., 2019: Chemical Composition and Antioxidant Properties of Some Industrial Tree Bark Extracts. BioResources, 14 (3): 5657-5671. https://doi.org/10.15376/biores.14.3.5657-5671
8. Hamada, J.; Petrissans, A.; Ruelle, J.; Mothe, F.; Colin, F.; Petrissans, M.; Gerardin, P., 2018: Thermal stability of *Abies alba* wood according to its radial position and forest management. European Journal of Wood and Wood Products, 76 (6): 1669-1676. https://doi.org/10.1007/s00107-018-1353-5
9. Holmbom, B., 1999: Extractives. In: Sjöström, E.; Alén, R. (eds.): Analytical methods in wood chemistry, pulping and papermaking. Berlin, Springer-Verlang, pp. 316. https://doi.org/10.1007/978-3-662-03898-7_5
10. Holmbom, B., 2011: Extraction and utilisation of non-structural wood and bark components. In: Alén, R. (ed.): Biorefining of forest resources. Helsinki, Paper Engineers' Association/Paperi ja Puu Oy, pp. 178-224.
11. Kačík, F.; Veľková, V.; Šmíra, P.; Nasswettrová, A.; Kačíková, D.; Reinprecht, L., 2012: Release of Terpenes from Fir Wood during Its Long-Term Use and in Thermal Treatment. Molecules, 17 (8): 9990-9999. https://doi.org/10.3390/molecules17089990
12. Kebbi-Benkeder, Z.; Manso, R.; Gérardin, P.; Dumarçay, S.; Chopard, B.; Colin, F., 2017: Knot extractives: a model for analysing the eco-physiological factors that control the within and between-tree variability. Trees, 31 (5): 1619-1633. https://doi.org/10.1007/s00468-017-1573-z

13. Manninen, A. M.; Tarhanen, S.; Vuorinen, M.; Kainulainen, P., 2002: Comparing the Variation of Needle and Wood Terpenoids in Scots Pine Provenances. Journal of Chemical Ecology, 28 (1): 211-228. https://doi.org/10.1023/A:1013579222600
14. Moukhtar, S.; Couret, C.; Rouil, L.; Simon, V., 2006: Biogenic Volatile Organic Compounds (BVOCs) emissions from *Abies alba* in a French forest. Science of The Total Environment, 354 (2): 232-245. https://doi.org/10.1016/j.scitotenv.2005.01.044
15. Patyra, A.; Dudek, M. K.; Kiss, A. K., 2022: LC-DAD – ESI-MS/MS and NMR Analysis of ConiferWood Specialized Metabolites. Cells, 11 (20): 3332. https://doi.org/10.3390/cells11203332
16. Salem, M.; Zeidler, A.; Böhm, M.; Mohamed, M.; Ali, H., 2015: GC/MS Analysis of Oil Extractives from Wood and Bark of *Pinus sylvestris*, *Abies alba*, *Picea abies* and *Larix decidua*. BioResources, 10: 7725-7737. https://doi.org/10.15376/biores.14.3.5657-5671
17. Schoss, K.; Benedetič, R.; Kreft, S., 2022: The Phenolic Content, Antioxidative Properties and Extractable Substances in Silver Fir (*Abies alba* Mill.) Branches Decrease with Distance from the Trunk. Plants, 11 (3): 333. https://doi.org/10.3390/plants11030333
18. Tavčar Benković, E.; Grohar, T.; Žigon, D.; Švajger, U.; Janeš, D.; Kreft, S.; Štrukelj, B., 2014: Chemical composition of the silver fir (*Abies alba*) bark extract Abigenol® and its antioxidant activity. Industrial Crops and Products, 52: 23-28. https://doi.org/10.1016/j.indcrop.2013.10.005
19. Tekin, K.; Hao, N.; Karagoz, S.; Ragauskas, A. J., 2018: Ethanol: A Promising Green Solvent for the Deconstruction of Lignocellulose. ChemSusChem, 11 (20): 3559-3575. https://doi.org/10.1002/cssc.201801291
20. Turner, D., 2018: Hands-on Sample Preparation. Headspace, Solid-Phase Micro-Extraction (SPME), Thermal Desorption (TD), Purge and Trap (P&T). Hands-on Sample Preparation Training Course, Ljubljana, 2018.
21. Ul'yanovskii, N. V.; Onuchina, A. A.; Faleva, A. V.; Gorbova, N. S.; Kosyakov, D. S., 2022: Comprehensive characterization of chemical composition and antioxidant activity of lignan-rich coniferous knotwood extractives. Antioxidants, 11 (12): 2338. https://doi.org/10.3390/antiox11122338
22. Vek, V.; Keržič, E.; Poljanšek, I.; Eklund, P.; Humar, M.; Oven, P., 2021: Wood Extractives of Silver Fir and Their Antioxidant and Antifungal Properties. Molecules, 26 (21): 6412. https://doi.org/10.3390/molecules26216412
23. Vek, V.; Šmidovnik, T.; Humar, M.; Poljanšek, I.; Oven, P., 2023: Comparison of the content of extractives in the bark of the trunk and the bark of the branches of silver fir (*Abies alba* Mill.). Molecules, 28 (1): 225. https://doi.org/10.3390/molecules28010225
24. Verkasalo, E.; Leppälä, J.; Muhonen, T.; Korpinen, R.; Möttönen, V.; Kurppa, S., 2019: Novel industrial ecosystems and value chains to utilize side-streams of wood products industries – Finnish approach. Pro Ligno Journal, 15 (4): 157-165.
25. Willför, S.; Nisula, L.; Hemming, J.; Reunanen, M.; Holmbom, B., 2004: Bioactive phenolic substances in industrially important tree species. Part 2: Knots and stemwood of fir species. Holzforschung, 58 (6): 650-659. https://doi.org/10.1515/HF.2004.119

**Corresponding address:**

**VILJEM VEK**
University of Ljubljana, Biotechnical Faculty, Department of Wood Science and Technology, Jamnikarjeva ulica 101, Ljubljana, SLOVENIA, e-mail: viljem.vek@bf.uni-lj.si

Çağlar Altay*[1], Davut Çiftçi[2], Hilmi Toker[2], Ergün Baysal[2]

# Physical, Mechanical and Weathering Characteristics of Oriental beech Heat Treated with Waste Engine Oil

# Fizička i mehanička svojstva te otpornost na vremenske utjecaje drva kavkaske bukve toplinski tretirane otpadnim motornim uljem

**ORIGINAL SCIENTIFIC PAPER**
**Izvorni znanstveni rad**
Received – prispjelo: 21. 3. 2024.
Accepted – prihvaćeno: 29. 8. 2024.
UDK: 630*84; 674.04
https://doi.org/10.5552/drvind.2024.0203



**ABSTRACT** • *In general, vegetable oils are chosen for oil heat treatment. Oil heat treatment with waste engine oil, which is quite limited in the literature, was used in this study. After the wood material was subjected to oil heat treatment with waste motor oil, several physical parameters such as oven-dry and air-dry density, water absorption (WA) levels, and mechanical properties such as compression strength parallel to the grain (CSPG) were examined. The color changes of waste engine oil heat treated (WEOHT) specimens were examined after three months of weathering.*

*The results showed that when oven-dry and air-dry density of WEOHT specimens increased, WA levels decreased. The WEOHT specimens had greater CSPG values than the control group. WEOHT specimens and control group revealed negative ΔL*, Δa*, and Δb* values following weathering. The WEOHT specimens had smaller total color changes (ΔE*) than the control group after weathering. Our results showed that higher temperature and durations resulted in lower WA, and higher air-dry density and total color changes of WEOHT specimens.*

**KEYWORDS:** *oil heat treatment; oriental beech; physical properties; mechanical properties; color; waste engine oil; weathering*

**SAŽETAK** • *Za toplinski tretman drva uljem najčešće se biraju biljna ulja. U ovom je radu za toplinski tretman drva upotrijebljeno otpadno motorno ulje, o čemu postoji malo podataka u literaturi. Nakon što je drvo toplinski tretirano otpadnim motornim uljem, ispitano je nekoliko njegovih fizičkih svojstava kao što su gustoća apsolutno suhog drva i drva sušenog na zraku, upijanje vode (WA) te mehanička svojstva poput čvrstoće na tlak paralelno s vlakancima (CSPG). Osim toga, promatrana je promjena boje uzoraka toplinski tretiranih otpadnim motornim uljem (WEOHT) nakon tri mjeseca izlaganja vremenskim utjecajima. Rezultati su pokazali da se pri povećanju gustoće toplinski tretiranih uzoraka apsolutno suhog drva i drva sušenog na zraku smanjilo upijanje vode. Toplinski tretirani uzorci imali su veće vrijednosti čvrstoće na tlak paralelno s vlakancima nego kontrolni. Nakon*

* Corresponding author
[1] Author is researcher at Aydın Adnan Menderes University, Vocational School of Aydın, Aydın, Turkey. https://orcid.org/0000-0003-1286-8600
[2] Authors are researchers at Muğla Sıtkı Koçman University, Technology Faculty, Muğla, Turkey. https://orcid.org/0009-0000-3756-8079, https://orcid.org/0000-0002-4109-458X, https://orcid.org/0000-0002-6299-2725

*izlaganja vremenskim utjecajima toplinski tretirani i kontrolni uzorci pokazali su negativne vrijednosti ΔL*, Δa* i Δb*. Nakon izlaganja vremenskim utjecajima toplinski tretirani uzorci imali su manje promjene boje (ΔE*) od kontrolnih uzoraka. Rezultati istraživanja pokazali su da su viša temperatura i dulje trajanje toplinskog tretmana rezultirali nižim upijanjem vode, većom gustoćom uzoraka drva sušenog na zraku i ukupnim promjenama boje toplinski tretiranih uzoraka.*

**KLJUČNE RIJEČI:** *toplinski tretman uljem; drvo kavkaske bukve; fizička svojstva; mehanička svojstva; boja; otpadno motorno ulje; izlaganje vremenskim utjecajima*

## 1 INTRODUCTION
## 1. UVOD

Compared to other materials, wood has a number of advantages, such as a high strength-to-weight ratio, high impact resistance, the ability to be used in a variety of technical processes, etc (Popescu and Popescu, 2013). Wood chemical structure contains a lot of hydroxyl groups, which makes it vulnerable to atmospheric influences. These influences can cause wood to change in size and perform differently, as well as significantly shorten product service lives and cause biological decomposition (Korkut and Hızıroğlu, 2014; Okon *et al.,* 2017; Li *et al.,* 2015; Kasemsiri *et al.,* 2012). Enhancing these characteristics makes thermally treated wood suitable for outdoor use (Németh *et al.,* 2016). One of the best methods for reducing the hygroscopicity of wood is thermal treatment in an inert atmosphere, which involves treating the wood at temperatures between 160 °C and 260 °C (Esteves and Pereira, 2008; Candelier *et al.,* 2016). Making long-lasting wood products without the use of biocides is crucial (La Mantia and Morreale, 2011). Oil heat treatment (OHT), which uses oil as the heating medium, is thought to be a slightly different approach to wood modification and a more cost-effective, sustainable, and ecologically friendly way to treat wood. OHT, which combines heat treatment and oil impregnation, has proven to be the most effective method for enhancing wood qualities (Sailer *et al.,* 2000). Linseed, rapeseed, palm, soy, and coconut oils are among the industrial vegetable oils that are used for thermal treatments. (Welzbacher and Rapp, 2005; Wang and Cooper, 2005). OHT is commonly conducted at temperatures ranging from 180 to 260 °C using rapeseed, linseed, or sunflower oil as the heat transfer medium. These oils have exceptional heat transmission properties and effectively exclude oxygen from the wood during treatment (Militz, 2002). Typically, OHT process is conducted in a closed vessel with hot oil circulating around the wood. According to recent studies, heating wood with oil is a perfect substitute for it. Because of their non-toxicity and environmentally benign composition, plant oils have long been used to preserve wood against fungal and mold deterioration as well as to minimize the accessibility of moisture to the wood (Yingprasert *et al.,* 2015). According to Tomak *et al.* (2011), oil absorption during treatment produces a protective layer on the wood surface that improves the treated wood dimensional stability. According to Tang *et al.* (2019), tung oil improved the structural stability and hydrophobicity of bamboo after oil heat treatment by being evenly distributed across the cell walls and lumens. Wood can also be improved for outdoor use and have its surface uniformly colored with oil heat treatment (Sailer *et al.,* 2000). Bak and Németh (2012) heated sunflower, rapeseed, and linseed oils to 160 °C and 200 °C for two hours, four hours, and six hours, respectively, to cure Poplar (*Populus* × *euramericana* Pannónia) and Robinia (*Robinia pseudoacacia* L.) woods. It is noteworthy to observe that poplar wood treated with oil heat treatment has a 15 % – 25 % improvement in compression strength. Additionally, black locust wood compression strength rose by 5 % to 15 % at 160 °C; however, it began to decrease by 5 % to 10 % at 200 °C. Mastouri *et al.* (2021) investigated the water absorption rates of eastern cotton (*Populus deltoides*) wood for four hours at 190 °C using silicone and rapeseed oil. The results show that heat treatment using silicon has a higher potential to improve the water-related qualities of wood than heat treatment using rapeseed oil. Özkan (2013) heated Turkish fir (*Abies nordmanniana* subsp. *bornmulleriana* Mattf.) wood to 150 °C, 180 °C, and 200 °C for two, four, and six hours, allowing the wood to naturally weather. Consequently, it was shown that an oil heat treatment given for two hours at 150 °C increased water absorption by 76 % and weathering color stability by 35 %. While coal oils and creosote are classified as highly hazardous materials, waste engine oil is classified as a moderately hazardous waste under the Russian Federation current criteria (Belchinskaya *et al.,* 2021). Research on the application of waste engine oil as preservative, anticorrosive and stabilizing agents to produce the hydrophobizing composition required for impregnation of railway sleepers is limited (Belchinskaya *et al.,* 2020).

Waste engine oil may pose some problems if it leaches. The Regulation on the Control of Waste Oils intends to record waste engine oils that are hazardous to the environment and human health, collect them under proper conditions, and dispose of them in accordance with European Union standards. If waste oils are

not handled properly, they can damage the environment, injure living animals, and cause harm when tossed into soil or water. Furthermore, heavy metal and chlorine compounds in waste oils are discharged into the atmosphere, contaminating the air and endangering human health (CSB, 2024).

This study used waste engine oil, which is not often used in the literature instead of vegetable oils, for oil heat treatment of Oriental beech wood. The main aim of this study is to examine certain physical and mechanical properties of Oriental beech wood, thermally modified with waste engine oil, and color changes of this material after weathering.

## 2 MATERIALS AND METHODS
## 2. MATERIJALI I METODE

### 2.1 Materials
### 2.1. Materijali

Wood specimens were prepared from Oriental beech (*Fagus orientalis* L.) wood. The oven-dry and air-dry density of Oriental beech wood is 0.645 g/cm$^3$ and 0.669 g/cm$^3$, respectively. In this study, waste engine oil was used for the oil heat treatment. Engine oils that have exceeded their useful life and can no longer be reused are called waste engine oil. Waste engine oil was supplied from the oils drained after the engine maintenance of the vehicles of different auto mechanics in the auto industry site in Muğla city of Turkey.

Compared to unused oils, waste engine oils can become contaminated by mixing with dirt, metal friction, water or chemicals during use. Furthermore, the 20W-50 engine oil used in the study is in viscosity class and is a high-performance engine oil that provides proven protection for diesel engines operating in harsh road and off-road applications (Mobil, 2024). The density of the original engine oil (20W/50) is 0.87 g/cm$^3$ at 15 degrees, its viscosity is 91.0 at 40 degrees (Vural, 2020). In our study, the viscosity of waste engine oil at 15 degrees was found to be 108.24 and its density was 0.9387 g/cm$^3$ at 40 degrees

### 2.2 Methods
### 2.2. Metode

#### 2.2.1 Preparation of wood specimens
#### 2.2.1. Priprema uzoraka drva

Oriental beech (*Fagus orientalis* L.) was cut to the measurements found in the tests and subjected to oven-dry density, air-dry density, *WA*, *CSPG*, and color tests.

#### 2.2.2 Treatment process
#### 2.2.2. Postupak modifikacije

To be prepared for waste engine oil heat treatment (WEOHT), specimens were dried in an oven at (103±2) °C until they reached a constant weight. Before the oil heat treatment, the test specimens were immersed in an oil bath and weighted to keep them from floating in the oil. The specimens were then poured with waste engine oil at room temperature and heated for 3 and 6 hours at 160 and 220 °C, respectively. Following their removal from the oil bath, the specimens were wrapped in aluminum foil and left to cool. Following the therapy, weight percent gain (WPG) of specimens was determined using Equation 1:

$$WPG\,(\%) = \frac{m_2 - m_1}{m_1} \cdot 100 \qquad (1)$$

Weights before and after oil heat treatment by $m_1$ and $m_2$, respectively.

Then, wood specimens were conditioned at 20 °C and 65 % relative humidity for two weeks before physical, mechanical and weathering tests.

#### 2.2.3 Oven-dry density test
#### 2.2.3. Ispitivanje gustoće uzoraka drva u apsolutno suhom stanju

The TS ISO 13061-2 2472 (TS ISO, 2021) standard was used to ascertain the oven-dry density of the specimens. In this test, specimen were prepared with the dimensions of 20 mm × 20 mm × 20 mm. A total of 50 specimens were prepared, 10 from each specimen group. The test specimens needed to be dried at (103±2) °C in order to reach a consistent weight. The specimens were allowed to cool before measuring their diameters with a 0.01 mm fine calliper, estimating their volumes with the stereo metric method, and recording their weights with an analytical balance to the accuracy of 0.01 g.

The oven-dry density ($\delta_0$), oven-dry weight ($M_0$), and oven-dry volume ($V_0$) were then determined using Formula 2:

$$\delta_0 = \frac{M_0}{V_0}\left(\mathrm{g/cm^3}\right) \qquad (2)$$

#### 2.2.4 Air-dry density test
#### 2.2.4. Ispitivanje gustoće uzoraka drva sušenih na zraku

The air-dry density values of specimens were computed using TS ISO 13061-2 (2021). In this test, specimens were prepared in dimensions of 20 mm × 20 mm × 20 mm. A total of 50 specimens were prepared, 10 from each specimen group. Until they reached a constant weight, specimens were maintained in the cabinet at 20 °C and 65 % relative humidity. Following that, an analytical balance with a sensitivity of 0.01 g was used to weigh the air-dry density, which was then determined using the stereometric method and the dimensions measured with a calliper with a sensitivity of 0.01 mm. Next, using the air-dry weight ($M_{12}$) and volume ($V_{12}$) data, the air-dry density ($\delta_{12}$) was calculated from Equation 3.

$$\delta_{12} = \frac{M_{12}}{V_{12}}\left(\mathrm{g/cm^3}\right) \qquad (3)$$

### 2.2.5 Water absorption test
### 2.2.5. Ispitivanje upijanja vode

In this test, specimen were prepared in dimensions of 20 mm × 20 mm × 20 mm. A total of 50 specimens were prepared, 10 from each specimen group. Specimens were stored in distilled water for 5, 10, 20, 40, 60, 80, 100, and 120 hours in a room setting. Specimens were taken out of the water, wiped dry with paper, and weighed following each soaking time. The *WA* of each specimen was therefore determined using Formula 4.

$$WA = \frac{M_f - M_{oi}}{M_{oi}} \cdot 100 \quad (4)$$

In this section;

$WA$ – water absorption (%),

$M_f$ – specimen's weight following absorption of water (g),

$M_{oi}$ – the specimen's oven-dry weight following impregnation (g).

### 2.2.6 Compression strength parallel to the grain (CSPG)
### 2.2.6. Čvrstoća na tlak paralelno s vlakancima (*CSPG*)

A universal test machine with a 4000 N capacity and a 6-mm/min loading period was used to execute the *CSPG* test in compliance with TS 2595 (TS, 1977) standard. All specimens were conditioned at 20 °C and 65 % relative humidity for 2 weeks before *CSPG* test. In this test, specimens dimensions were prepared as 20 mm × 20 mm × 30 mm. A total of 50 specimens were prepared, 10 from each specimen group. *CSPG* was calculated using Formula 5.

$$\sigma_B = \frac{P}{a \cdot b} \quad (5)$$

In this section:

$\sigma_B$ – *CSPG* (N/mm$^2$),

$P$ – load at break (N),

$a$, $b$ – specimen cross-section dimensions (mm)

### 2.2.7 Color test
### 2.2.7. Ispitivanje boje

In this test, specimen were prepared in dimensions of 10 mm × 100 mm × 150 mm. A total of 50 specimens were prepared, 10 from each specimen group. The $L^*$, $a^*$, and $b^*$ color characteristics of the specimens were ascertained for the color test using the CIEL*a*b* method. The $a^*$ and $b^*$ axes in this diagram stand for the chromaticity coordinates, and the $L^*$ axis for darkness (black-white axis). In addition, the hues red and green are represented by the symbols $+a^*$ and $-a^*$, respectively. Furthermore, the variables $+b^*$ and $-b^*$ stand in for yellow and blue, respectively. Zhang (2003) states that the $L^*$ value ranges from 0 (black) to 100 (white). The overall color difference ($\Delta E^*$) was determined using equations 6 through 9 in accordance with ASTM D1536-58T (ASTM 1964) standards. Color analysis was performed in the radial direction of wood.

$$\Delta a^* = a_{final}{}^* - a_{initial}{}^* \quad (6)$$

$$\Delta b^* = b_{final}{}^* - b_{initial}{}^* \quad (7)$$

$$\Delta L^* = L_{final}{}^* - L_{initial}{}^* \quad (8)$$

$$(\Delta E^*) = \left[ (\Delta a^*)^2 + (\Delta b^*)^2 + (\Delta L^*)^2 \right]^{1/2} \quad (9)$$

Where:

The discrepancies between the values of the first and last intervals are represented by the symbols $\Delta a^*$, $\Delta b^*$, and $\Delta L^*$, respectively.

### 2.2.8 Weathering test
### 2.2.8. Izlaganje vremenskim utjecajima

The ASTM D 358-55 (ASTM, 1970) standard states that wood panels should expose specimens to weathering. The specimens were then weathered for three months (10 November 2023–10 February 2024) in panels located in the province of Muğla in the South Aegean Region of Turkey (Table 1). The specimens

**Table 1** Meteorological data of Muğla
**Tablica 1.** Meteorološki podatci za Muğlu

| **Muğla** | **10 November-10 December 2023** *10. studenog-10. prosinca 2023.* | **11 December-10 January 2024** *11. prosinca-10. siječnja 2023.* | **11 January-10 February 2024** *11. siječnja-10. veljače 2023.* |
|---|---|---|---|
| Average temperature per month, °C *prosječna mjesečna temperatura,* °C | 10.51 | 8.61 | 6.21 |
| Average humidity per month, % *prosječna mjesečna vlažnost zraka,* % | 90.00 | 92.00 | 78.00 |
| Average wind speed per month, m/s *prosječna mjesečna brzina vjetra*, m/s | 1.00 | 1.20 | 0.97 |
| Average sun exposure time per month, hours *prosječno mjesečno vrijeme izloženosti suncu,* h | 0.42 | 0.15 | 0.87 |
| Total rainfall per month, mm = kg/m$^{-2}$ *ukupna mjesečna količina padalina,* mm = kg/m$^{-2}$ | 10.46 | 4.88 | 7.19 |

faced south at a 45° angle and were set up on panels about 50 cm above the ground.

### 2.2.9 Statistical evaluation
### 2.2.9. Statistička obrada rezultata

The Duncan test, at a 95 % confidence level, and variance analysis were evaluated by the SPSS computer once the test results were obtained. Statistical studies were performed on homogeneity groups (HG), with various letters indicating statistical significance.

## 3 RESULTS AND DISCUSSION
## 3. REZULTATI I RASPRAVA

### 3.1 Weight percent gain of treated oriental beech wood
### 3.1. Postotno povećanje mase toplinski modificiranog drva kavkaske bukve

Weight percent gain (*WPG*) values of WEOHT specimens are given in Table 2. *WPG* values of WEOHT specimens were ranged from 23 % to 44 %. Higher duration and temperatures resulted in higher *WPG* of WEOHT specimens.

**Table 2** *WPG* of WEOHT specimens
**Tablica 2.** *WPG* za WEOHT uzorke

| Treatment type *Vrsta tretmana* | Temperature, °C *Temperatura,* °C | Duration, h *Trajanje,* h | *WPG*, % | Std. dev. |
|---|---|---|---|---|
| Control | - | - | - | - |
| WEOHT | 160 | 3 | 23 | 5.1 |
| WEOHT | 160 | 6 | 26 | 4.2 |
| WEOHT | 220 | 3 | 37 | 4.8 |
| WEOHT | 220 | 6 | 44 | 6.3 |

WEOHT – Waste engine oil heat treatment; *WPG* – Weight percent gain; Std. dev. – Standard deviations
*WEOHT – toplinski tretman otpadnim motornim uljem; WPG – postotno povećanje mase; Std. dev. – standardna devijacija*

### 3.2 Oven-dry density
### 3.2. Gustoća apsolutno suhog drva

The oven-dry density and and air-dry density values of the WEOHT specimens are given in Table 3.

Compared to the control group, the oven-dry density values of the WEOHT specimens are higher. While the volume of wood either stays the same or only slightly changes, the density may rise as a result of the WEOHT specimens increased mass and oil filling in the wood cells (Azis *et al.,* 2020). A longer heating period will result in a greater amount of oil filling the wood cells, raising the wood density (Daud and Coto, 2009). In contrast to the control group, which had the lowest oven-dry density, the specimens heat treated at 220 °C for six hours had the highest oven-dry density, according to the study. The specimens heat treated at 160 °C and 220 °C for 6 hours showed statistically significant differences in oven dry density values when compared to the control group.

The WEOHT specimens had a higher air-dry density than the control group. The study discovered that specimens heated for six hours at 220 °C had the highest air-dry density, whereas the control group had the lowest. The air dry density values of the specimens that were heat treated at 220 °C for 3 and 6 hours differed statistically significantly from the control group. Azis *et al.,* (2020) investigated the density variations of bulk oil-heated candlenut wood (*Aleurites moluccanus* (L.) Willd.). The average density of the control group was 0.38 g/cm³. The density of the oil-heated wood increased dramatically from 18.85 % to 25.13 % when compared to the control. Bayraktar and Pelit (2022) investigated the air dry density values of European beech and Scots pine linseed oil heated to three different temperatures (170 °C, 190 °C, and 210 °C). They discovered that European beech and Scots pine specimens heat-treated with linseed oil increased their air dry density values by 29 % and 31 %, respectively.

During our examination, the oven dry and air dry density values of WEOHT Oriental beech increased by 16.66 % to 39.39 % and 22.05 % to 44.11 %, respectively. Overall, our findings are consistent with past research.

### 3.3 Water absorption
### 3.3. Upijanje vode

The water absorption (*WA*) values of WEOHT specimens and decreases of *WA* values of WEOHT specimens compared to the control group (%) are given in Table 4 and Table 5, respectively.

The results confirmed previous finding (Yalınkılıç *et al.,* 1995) and demonstrated that throughout the early stages of *WA*, particularly within 5, 10 and 20 hours, *WA* levels of the control group were significantly higher. This may be a result of water being absorbed by wood during the initial soaking period and gradually decreasing wood gaps (Richardson, 1987). The *WA* levels of the control group were higher during the first and subsequent *WA* periods when compared to WEOHT specimens. The application of waste engine oil provides a thickening and water-repellent quality that greatly lowers *WA*. The results of the *WA* test indicate that as the temperature and length of the oil heat treatment increase, the *WA* of all wood decreases. This is consistent with the claim made in (Hidayat *et al.,* 2015; Jamsa and Viitaniemi, 2001) that wood loses water absorption as treatment duration and temperature increase because the cell walls become more hydrophobic due to a decrease in hydroxyl groups as a result of chemical reactions during heat treatment. Wood dimensional stability will rise as a result of its decreased capacity to absorb water (Ma'ruf *et al.,* 2021). The wood external and partially inner surfaces retain waste engine oil, which fills the cell lumen and increases the surface hydrophobicity. Water enters wood pores

**Table 3** Oven- and air-dry density values of WEOHT specimens
**Tablica 3.** Vrijednosti gustoće WEOHT uzoraka u apsolutno suhom stanju i sušenih na zraku

| **Treatment type** *Vrsta tretmana* | **Temperature, °C** *Temperatura, °C* | **Duration, h** *Trajanje, h* | **Oven-dry density, g/cm³** *Gustoća apsolutno suhog drva, g/cm³* | **Increase compared to control, %** *Povećanje u odnosu prema kontrolnim uzorcima, %* | **Std. dev.** | **H.G.** | **Air-dry density, g/cm³** *Gustoća drva sušenog na zraku, g/cm³* | **Std. dev.** | **H.G.** | **Increase compared to control, %** *Povećanje u odnosu prema kontrolnim uzorcima, %* |
|---|---|---|---|---|---|---|---|---|---|---|
| Control | - | - | 0.66 | - | 0.05 | A | 0.68 | 0.05 | A | - |
| WEOHT | 160 | 3 | 0.77 | 16.66 | 0.06 | AB | 0.83 | 0.05 | AB | 22.05 |
| WEOHT | 160 | 6 | 0.87 | 31.81 | 0.08 | B | 0.84 | 0.08 | AB | 23.52 |
| WEOHT | 220 | 3 | 0.78 | 18.18 | 0.02 | AB | 0.92 | 0.07 | B | 35.29 |
| WEOHT | 220 | 6 | 0.92 | 39.39 | 0.10 | B | 0.98 | 0.09 | B | 44.11 |

WEOHT – Waste engine oil heat treatment; Std. dev. – Standard deviation; H.G. – Homogeneity group
*WEOHT – toplinski tretman otpadnim motornim ulje; Std. dev. – standardna devijacija; H.G. – grupe homogenosti*

**Table 4** Water absorption values of WEOHT specimens
**Tablica 4.** Vrijednosti upijanja vode WEOHT uzoraka

| **Treatment type** *Vrsta tretmana* | **Temperature, °C** *Temperatura, °C* | **Duration, h** *Trajanje, h* | **Water absorption** / *Upijanje vode, %* | | | | | | | | | | | | | | | |
|---|---|---|---|---|---|---|---|---|---|---|---|---|---|---|---|---|---|---|
| | | | 5 h | H.G | 10 h | H.G | 20 h | H.G | 40 h | H.G | 60 h | H.G | 80 h | H.G | 100 h | H.G | 120 h | H.G |
| Control | - | - | 32.41 | A | 37.59 | A | 47.35 | D | 57.26 | C | 59.80 | C | 63.14 | C | 63.31 | C | 64.33 | C |
| WEOHT | 160 | 3 | 9.60 | B | 11.89 | B | 17.97 | C | 27.24 | B | 31.72 | B | 33.12 | B | 34.55 | B | 36.06 | B |
| WEOHT | 160 | 6 | 7.46 | B | 9.91 | B | 16.46 | BC | 24.85 | B | 29.80 | B | 31.31 | B | 32.87 | B | 34.68 | B |
| WEOHT | 220 | 3 | 7.34 | B | 9.27 | B | 14.61 | AB | 21.28 | A | 26.60 | A | 28.83 | AB | 30.64 | AB | 31.87 | AB |
| WEOHT | 220 | 6 | 6.46 | B | 8.86 | B | 12.83 | A | 19.45 | A | 24.07 | A | 26.43 | A | 28.27 | A | 29.83 | A |

WEOHT – Waste engine oil heat treatment H.G – Homogeneity group / *WEOHT – toplinski tretman otpadnim motornim uljem; H.G. – grupe homogenosti*

**Table 5** Decreases of water absorption values of WEOHT specimens compared to control group
**Tablica 5.** Smanjenje vrijednosti upijanja vode WEOHT uzoraka u usporedbi s kontrolnim uzorcima

| **Treatment type** *Vrsta tretmana* | **Temperature, °C** *Temperatura, °C* | **Duration, h** *Trajanje, h* | **Decrease in water absorption values compared to the control, %** *Smanjenje vrijednosti upijanja vode u odnosu prema kontrolnim uzorcima, %* | | | | | | | |
|---|---|---|---|---|---|---|---|---|---|---|
| | | | 5 h | 10 h | 20 h | 40 h | 60 h | 80 h | 100 h | 120 h |
| Control | - | - | - | - | - | - | - | - | - | - |
| WEOHT | 160 | 3 | 70.4 | 68.4 | 62.0 | 52.4 | 47.0 | 47.5 | 45.4 | 43.9 |
| WEOHT | 160 | 6 | 77.0 | 73.6 | 65.2 | 56.6 | 50.2 | 50.4 | 48.1 | 46.1 |
| WEOHT | 220 | 3 | 77.3 | 75.3 | 69.1 | 62.8 | 55.5 | 54.3 | 51.6 | 50.5 |
| WEOHT | 220 | 6 | 80.1 | 76.4 | 72.9 | 66.0 | 59.7 | 58.1 | 55.3 | 53.6 |

WEOHT – Waste engine oil heat treatment / *toplinski tretman otpadnim motornim uljem*

through capillary action, which lowers the amount of water absorption (Koski, 2008). Our results proved that *WA* of control group maintained a stronger trend than WEOHT specimens for total durations ranging from 5 hours to 120 hours. Every phase showed a statistically significant difference between the WEOHT specimens and the control group. Dubey *et al.* (2012) stated that higher temperatures led to various chemical alterations that affected dimensional stability, and hydrophobic oils in the lumens stopped water from penetrating the walls. According to studies conducted in Hyvonen *et al.* (2005) and Hofland and Tjeerdsma (2005), heating wood with tall oil or rapeseed oil, respectively, reduced the water absorption properties of wood. Our findings and those of the previously cited researcher are fairly consistent. According to our research, after 120 hours of *WA*, the *WA* levels of the control group increased to 64.33 %, while WEOHT specimens showed a shift from 29.83 to 36.06 %. Therefore, after 120 hours *WA* period, WEOHT specimens took up 43.9 to 53.6 % less water than the control group (Table 5)

### 3.4 Compression strength parallel to grain (*CSPG*)
### 3.4. Čvrstoća na tlak paralelno s vlakancima (*CSPG*)

The *CSPG* values of WEOHT specimens are given in Table 6.

The highest *CSPG* values in our study were 46.04 N/mm$^2$ for WEOHT specimens at 220 °C for three hours, compared to 39.57 N/mm$^2$ for the control group; the values for WEOHT specimens were changed from 43.56 to 46.04 N/mm$^2$. After oil heat treatment, the wood strength properties are impacted because heat causes the chemical structure of the wood cell wall components to change. The strength quality of wood is influenced by the contributions of hemicellulose, cellulose, and lignin, the three primary components of the cell wall, in distinct ways (Lee *et al.,* 2018). Our results proved that WEOHT specimens had higher *CSPG* values than the control group, ranging from 10.08 % to 16.35 %. However, there were no statistically significant differences between the WEOHT specimens and the control group at the 95 % confidence level. Cheng *et al.* (2014) found that following oil heat treatment, poplar wood *CSPG* rose. The high oil uptake thickened the fibers and increased their longitudinal strength, which was primarily responsible for this. The results were ascribed by Windeisen *et al.* (2009) to the rise in lignin condensation caused by heat treatment. The increase in compression strength may be explained by a number of factors, including reduced bound water content in heat-treated wood, an increase in crystalline cellulose, and restricted movement perpendicular to the grain as a result of increased lignin polymer network cross-linking (Boonstra *et al.,* 2007). Our findings are consistent with the previously cited research. However, it has been reported in the literature that the compression strength decreases in oil heat treated wood, especially at temperatures of 200 °C (Bak and Németh 2012). In our study, *CSPG* values were higher in a 3 h heat time at 160 °C compared to a 6 h heat time; For 220 °C, 6 h of heat time gave lower CSPG values than 3 hours of heat time.

### 3.5 Color changes
### 3.5. Promjene boje

The color and total color change values of the WEOHT specimens are shown in Table 7 both before and after weathering. The specimens' total color change values upon weathering are also shown in Figure 1.

Consideration should be given to the hardwood color in addition to its durability, as it plays a significant role in defining both its aesthetic appeal and market value (Baar and Gryc, 2012). The chemical components of wood material, such as extractives, interact with light to determine its hue. The surface color of the wood material varies depending on the abundance, scarcity, or modification of the extractives effects (Hon and Minemura, 2001). The $L^*$ value for the control group was found to be 65.85 before weathering. The $L^*$ values of the WEOHT specimens' ranged from 28.14 to 32.24. Because of this, WEOHT specimens' $L^*$ values were lower than those of the control group. Furthermore, WEOHT specimens $L^*$ values declined with increasing duration. As a result of the oil heat treatment process, the Oriental beech specimens darkened. It is more likely that the darkening effect in the oxygen-excluded treatment medium, such as oil, is

**Table 6** *CSPG* values of WEOHT specimens
**Tablica 6.** *CSPG* vrijednosti WEOHT uzoraka

| **Treatment type** *Vrsta tretmana* | **Temperature, °C** *Temperatura,* °C | **Duration, h** *Trajanje,* h | ***CSPG*, N/mm$^2$** | **Standard deviation** *Standardna devijacija* | **Homogeneity group** *Grupe homogenosti* | **Increase compared to control, %** *Povećanje u odnosu prema kontrolnim uzorcima, %* |
|---|---|---|---|---|---|---|
| Control | - | - | 39.57 | 6.81 | A | - |
| WEOHT | 160 | 3 | 45.67 | 7.31 | A | 15.41 |
| WEOHT | 160 | 6 | 44.20 | 5.44 | A | 11.70 |
| WEOHT | 220 | 3 | 46.04 | 5.79 | A | 16.35 |
| WEOHT | 220 | 6 | 43.56 | 6.92 | A | 10.08 |

WEOHT – Waste engine oil heat treatment / *toplinski tretman otpadnim motornim uljem*

**Table 7** Color and total color differences of WEOHT specimens as a result of weathering
**Tablica 7.** Boja i ukupne promjene boje WEOHT uzoraka kao posljedica izlaganja vremenskim utjecajima

| **Treatment type** *Vrsta tretmana* | Temperature, °C *Temperatura, °C* | Duration, h *Trajanje,* h | **Color differences before weathering** *Vrijednosti boje prije izlaganja vremenskim utjecajima* | | | **Color differences after weathering** *Vrijednosti boje nakon izlaganja vremenskim utjecajima* | | | **Total color differences** *Ukupne promjene boje* | |
|---|---|---|---|---|---|---|---|---|---|---|
| | | | *L** | *a** | *b** | Δ*L** | Δ*a** | Δ*b** | Δ*E** | *H.G* |
| Control | - | - | 65.85 | 11.69 | 22.07 | -16.82 | -9.67 | -12.59 | 23.12 | B |
| WEOHT | 160 | 3 | 30.28 | 3.66 | 6.74 | -2.31 | -1.62 | -0.04 | 2.82 | A |
| WEOHT | 160 | 6 | 29.95 | 4.12 | 7.30 | -1.98 | -2.08 | -0.82 | 2.98 | A |
| WEOHT | 220 | 3 | 32.24 | 4.35 | 8.83 | -1.96 | -2.67 | -1.31 | 3.56 | A |
| WEOHT | 220 | 6 | 28.14 | 3.77 | 7.35 | -3.29 | -2.22 | -1.09 | 4.11 | A |

WEOHT – Waste engine oil heat treatment; Std. dev. – Standard deviation / *WEOHT – toplinski tretman otpadnim motornim uljem; Std. dev. – standardna devijacija*

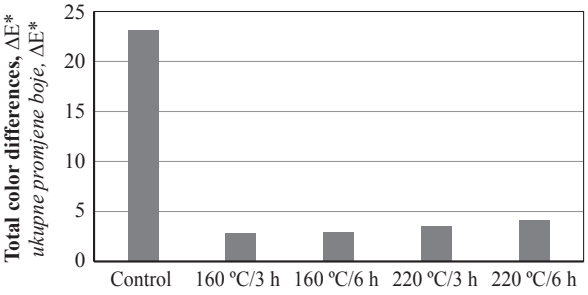


**Figure 1** Total color differences of WEOHT specimens
**Slika 1.** Ukupne promjene boje WEOHT uzoraka

caused by the caramelization of soluble sugars and heat treatment, which forms an oil coating on the wood surface (Lee *et al.,* 2018). According to Németh *et al.* (2016), the level of darkening is strongly influenced by the extractive content of wood. The effect of further darkening generated by the oxidation process is more noticeable in wood with a higher extractive content. According to our research, WEOHT specimens had lower *a** and *b** values than the control group before weathering. The WEOHT and control groups experienced negative Δ*L** values due to weathering. The best parameter to describe the color evolution of a wood surface is Δ*L**. Consequently, the wood surface became rougher and darker with age. In Oriental beech, photodegradation and leaching of lignin and other non-cellulosic polysaccharides result in weathering-related darkening (Sönmez *et al.*, 2011; Petric *et al.*, 2004; Hon and Chang, 1985). Both the WEOHT and control groups saw negative Δ*a** and Δ*b** values due to weathering. The surfaces of oriental beech have negative values for Δ*a** and Δ*b**, corresponding to greenish and blueish tones. Our study found that WEOHT specimens thermally treated at 160 °C for 3 hours had the lowest total color change value (2.82), while the control group had the highest total color change value (Δ*E**). Our findings indicated that there were substantial differences in overall color changes between WEOHT specimens and the control group. Németh *et al.,* (2016) studied the photostability of sunflower oil heat-treated locust and poplar wood when subjected to short-term UV radiation. They discovered that oil heat treated wood specimens had better photostability than the control group. Our findings are consistent with data from Németh *et al.* (2016). Given that a low total color change value is sought, WEOHT specimens heated at 160 °C for 3 hours demonstrated the best color stability.

In our investigation, the control group had the highest total color change value (Δ*E**) while the WEOHT specimens, which were thermally treated for three hours at 160 °C, had the lowest (1.82). Based on our research, the control group and WEOHT specimens had significantly different overall color alterations. Short-term UV radiation treatment of locust and poplar wood treated with sunflower oil was investigated by Németh *et al.* (2016) for photostability. Compared to the control group, the wood specimens that had undergone oil heat treatment demonstrated superior photostability. The data from Németh *et al.* (2016) agrees with our conclusions. The maximum color stability was achieved by WEOHT specimens heat treated at 160 °C for three hours; this is because a low total color change value is required.WEOHT specimens higher color stability could be explained by the increased lignin stability caused by oil heat treatment (Ayadi *et al.,* 2003; Deka *et al.,* 2008). In our study, the total color changes of WEOHT specimens increased as the temperatures and durations increased.

## 4 CONCLUSIONS
## 4. ZAKLJUČAK

This study was designed to recycle engine oils, which are widely used in the automotive industry, and use them in the wood preservation industry. In the study, some physical, mechanical and color changes of Oriental beech wood specimens heat treated with waste engine oils were evaluated.

According to the results obtained, oven-dry and air-dry density values of WEOHT specimens increased compared to the control group. After all *WA* periods, all WEOHT specimens absorbed less water than the control group. Additionally, a statistically significant dif-

ference was found in *WA* levels between WEOHT specimens and the control group. Higher duration and temperature values resulted in lower *WA* levels of WEOHT specimens. Although the *CSPG* values of WEOHT specimens were increased compared to the control group, no statistically significant difference was found between all specimens. Our results showed that weathering caused darkening and reduced $a^*$ and $b^*$ values in WEOHT specimens and the control group. Additionally, the total color change of WEOHT specimens was lower than that of the control group.

In summary, the physical and mechanical properties of WEOHT specimens improved. Color stability of WEOHT specimens were higher than those of the control group after weathering. While there were statistically significant differences in oven-dry density, air-dry density, and *WA* levels between WEOHT specimens and the control group, there was no statistical difference in *CSPG* values between WEOHT specimens and the control group. Increased air-dry densities as well as total color changes, were seen in WEOHT specimens with decreased *WA* at higher temperatures and durations. As a result, WEOHT specimens are an alternate structural material that can be used outside when especially physical properties and color stability are needed.

**Acknowledgements** – Zahvala

The data used in this study came from Davut Çiftçi's Engineering Project course at Technology Faculty of Muğla Sıtkı Koçman University, specifically from an undergraduate student at the Department of Woodworking and Industrial Engineering.

## 5 REFERENCES
## 5. LITERATURA

1. Ayadi, N.; Lejeune, F.; Charrier, F.; Charrier, B.; Merlin, A., 2003: Color stability of heat-treated wood during artificial weathering. Holz als Roh- und Werkstoff, 61: 221-226. https://doi.org/10.1007/s00107-003-0389-2
2. Azis, A.; Yunianti, A. D.; Agussalim, A., 2020: Changes in the density, specific gravity and dimensional stability of candlenut wood (*Aleurites moluccanus* (L.) Willd.) from several variation temperatures with oil-heat treatment. In: IOP Conference Series: Materials Science and Engineering, Volume 935, International Conference on Forest Products (ICFP) 2020: 12th International Symposium of IWORS, 1 September 2020, Bogor, Indonesia.
3. Baar, J.; Gryc, V., 2012: The analysis of tropical wood discoloration caused by simulated sunlight. European Journal of Wood and Wood Products, 70 (1-3): 263-269. https://doi.org/10.1007/s00107-011-0551-1
4. Bayraktar, S.; Pelit, H., 2022: Determination of density and bending strength of heat-treated wood materials with different methods. Ormancılık Araştırma Dergisi, 9: 355-362 (in Turkish). https://doi.org/10.17568/ogmoad.1090574
5. Bak, M.; Németh, R., 2012: Modification of wood by oil heat treatment. In: Proceedings of the International Scientific Conference on Sustainable Development & Ecological Footprint. March 26-27, Sopron, Hungary.
6. Belchinskaya, L.; Zhuzhukin, K.; Dmitrenkov, A.; Roessner, F., 2020: Studying and Imparting Moisture Absorption Qualities of the New Wood Based Bio-Composite Material. In: IOP Conference Series: Earth and Environmental Science, Volume 595, International Forestry Forum "Forest ecosystems as global resource of the biosphere: calls, threats, solutions", 23 October 2020, Voronezh, Russian Federation.
7. Belchinskaya, L.; Zhuzhukin, K. V.; Ishchenko, T.; Platonov, A., 2021: Impregnation of wood with waste engine oil to increase water-and bio-resistance. Forests, 12 (12): 1-14. https://doi.org/10.3390/f12121762
8. Boonstra, M. J.; Van Acker, J.; Tjeerdsma, B. F.; Kegel, E. V., 2007: Strength properties of thermally modified softwoods and its relation to polymeric structural wood constituents. Annals of Forest Science, 64: 679-690. https://doi.org/10.1051/forest:2007048
9. Candelier, K.; Thevenon, M. F.; Petrissans, A.; Dumarcay, S.; Gerardin, P.; Petrissans, M., 2016: Control of wood thermal treatment and its effects on decay resistance: a review. Annals of Forest Science, 73 (3): 571-583. https://doi.org/10.1007/s13595-016-0541-x
10. Cheng, D.; Chen, L.; Jiang, S.; Zhang, Q., 2014: Oil uptake percentage in oil-heat-treated wood, its determination by soxhlet extraction and its effects on wood compression strength parallel to the grain. BioResources, 9 (1): 120-131. https://doi.org/10.15376/biores.9.1.120-131
11. Deka, M.; Humar, M.; Rep, G.; Kričej, B.; Šentjurc, M.; Petrič, M., 2008: Effects of UV light irradiation on colour stability of thermally modified, copper ethanolamine treated and non-modified wood: EPR and DRIFT spectroscopic studies. Wood Science and Technology, 42: 5-20. https://doi.org/10.1007/s00226-007-0147-4
12. Daud, M.; Coto, Z., 2009: Peningkatan sifat fisis dan mekanis kayu durian (durio sp) dengan penggorengan. In: Simposium Forum Teknologi Hasil Hutan, October 2009.
13. Dubey, M. K.; Pang, S.; Walker, J., 2012: Oil uptake by wood during heat-treatment and post-treatment cooling and effects on wood dimensional stability. European Journal of Wood and Wood Products, 70: 183-190. https://doi.org/10.1007/s00107-011-0535-1
14. Esteves, B.; Pereira, H., 2008: Wood modification by heat treatment: A review. BioResources, 4 (1): 370-404.
15. Hon, D. N. S.; Minemura, N., 2001: Color and Discoloration. Wood and Cellulosic Chemistry. DNS, 525.
16. Hon, D. N. S.; Chang, S. T., 1985: Photoprotection of Wood Surfaces by Wood-ion Complexes. Wood Fiber and Science, 17: 92-100.
17. Hidayat, W.; Jang, J. H.; Park, S. H.; Qi, Y.; Febrianto, F.; Lee, S. H.; Kim, N. H., 2015: Effect of temperature and clamping during heat treatment on physical and mechanical properties of okan (*Cylicodiscusgabunensis* [Taub.] Harms) wood. BioResources, 10 (4): 6961-6974. https://doi.org/10.15376/biores.10.4.6961-6974
18. Hofland, A.; Tjeerdsma, B. F., 2005: Wood protection by chemical modification. ECOTAN 3rd Report, Part 3.
19. Hyvonen, A.; Piltonen, P.; Nelo, M.; Niinimaki, J., 2005: Wood protection of tomorrow – Potential of modified crude tall oil formulations in wood protection. In: Proceedings of the Seventh Finnish Conference of Environmental Sciences. Jyväskylä, Finland.
20. Jamsa, S.; Viitaniemi, P., 2001: Heat treatment of wood: Better durability without chemicals. In: Proceeding of special seminar held in Antibes, France.
21. Koski, A., 2008: Applicability of crude tall oil for wood protection. Acta Universitatis Ouluensis C Technica 293, Oulu.
22. Kasemsiri, P.; Hızıroğlu, S.; Rimdusit, S., 2012: Characterization of heat treated eastern redcedar (*Juniperus Virginiana* L.). Journal of Materials Processing Technology, 212 (6): 1324-1330. https://doi.org/10.1016/j.jmatprotec.2011.12.019

23. Korkut, D. S.; Hızıroğlu, S., 2014: Experimental test of heat treatment effect on physical properties of red oak (*Quercus Falcate* Michx.) and southern pine (*Pinus Taeda* L.). Materials, 7 (11): 7314-7323. https://doi.org/10.3390/ma7117314
24. Lee, S. H.; Ashaari, Z.; Lum, W. C.; Halip, J. A.; Ang, A. F.; Tan, L. P.; Chin, K. L.; Tahir, P. M., 2018: Thermal treatment of wood using vegetable oils: A review. Construction and Building Materials, 181: 408-419. https://doi.org/10.1016/j.conbuildmat.2018.06.058
25. La Mantia, F.; Morreale, M., 2011: Green composites: A brief review. Composites. Part A: Applied Science and Manufacturing, 42 (6): 579-588. https://10.1016/j.compositesa.2011.01.017
26. Li, W.; Wang, H.; Ren, D.; Yu, Y.; Yu, Y., 2015: Wood modification with furfuryl alcohol catalysed by a new composite acidic catalyst. Wood Science and Technology, 49: 845-856. https://doi.org/10.1007/s00226-015-0721-0
27. Mastouri, A.; Efhamisisi, D.; Shirmohammadli, Y.; Oladi, R., 2021: Physicochemical properties of thermally treated poplar wood in silicone and rapeseed oils: A comparative study. Journal of Building Engineering, 43: 102511. https://10.1016/j.jobe.2021.102511
28. Ma'ruf, S. D.; Bakri, S.; Febryano, I. G.; Setiawan, A., Haryanto, A., Suri, I. F.; Kim, N. H.; Hidayat, W., 2021: Effects of eco-frendly hot oil treatment on the wood properties of gmelina aborea and cocos nucifera. In: International Conference on Sustainable Biomass (ICSB 2019), 4 June 2021, Atlantis Press.
29. Militz, H., 2002: Heat treatment technologies in Europe: Scientific background and technological state-of-art. In: Proceedings of conference on "Enhancing the durability of lumber and engineered wood products", Kissimmee, Orlando. Forest Products Society, Madison, US.
30. Németh, R.; Tolvaj, L.; Bak, M.; Alpar, T., 2016: Colour stability of oil-heat treated black locust and poplar wood during short-term UV radiation. Journal of Photochemistry and Photobiology. A: Chemistry, 329: 287-292. https://doi.org/10.1016/j.jphotochem.2016.07.017
31. Okon, K. E.; Lin, F.; Chen, Y.; Huang, B., 2017: Effect of silicone oil heat treatment on the chemical composition, cellulose crystalline structure and contact angle of chinese parasol wood. Carbohydrate Polymers, 164: 179-185. https://doi.org/10.1016/j.carbpol.2017.01.076
32. Özkan, O. E., 2013: Biological, mechanical, physical and outdoor durability properties of heat treated fir wood. MSc Thesis, Kastamonu Üniversitesi Fen Bilimleri Enstitüsü, 95 s. Kastamonu (in Turkish).
33. Petric, M.; Kricej, B.; Humar, M.; Pavlic M.; Tomazic, M., 2004: Patination of cherry wood and spruce wood with ethanolamine and surface finishes. Surface Coatings International, Part B, 87: 195-201. https://doi.org/10.1007/BF02699635
34. Popescu, C. M.; Popescu, M. C., 2013: A near infrared spectroscopic study of the structural modifications of lime (*Tilia Cordata* Mill.) wood during hydro-thermal treatment. Spectrochimica Acta. Part A: Molecular and Biomolecular Spectroscopy, 115: 227-233. https://doi.org/10.1016/j.saa.2013.06.002
35. Richardson, B., 1987: Wood preservation. Lancester: The Construction Press Ltd.
36. Sailer, M.; Rapp, A. O.; Leithoff, H.; Peek, R. D., 2000: Upgrading of wood by application of an oil heat treatment. Holz als Roh- und Werkstoff, 58: 15-22. https://doi.org/10.1007/s001070050379 (in German).
37. Sönmez, A.; Budakcı, M.; Pelit, H., 2011: The effect of moisture content of the wood on layer performance of water-borne varnishes. BioResources, 6 3166-3177. https://doi.org/10.15376/biores.6.3.3166-3177
38. Tomak, E. D.; Hughes, M.; Yıldız, Ü. C.; Viitanen, H., 2011: The combined effects of boron and oil heat treatment on beech and Scots pine wood properties. Part 1: Boron leaching, thermogravimetric analysis and chemical composition. Journal of Materials Science 46: 598-607. https://doi.org/10.1007/s10853-010-4859-8
39. Tang, T.; Zhang, B.; Liu, X.; Wang, W.; Chen, X.; Fei, B., 2019: Synergistic effects of tung oil and heat treatment on physicochemical properties of bamboo materials. Scientific Reports, 9: 12824. https://doi.org/10.1038/s41598-019-49240-8.
40. Welzbacher, C.; Rapp, A., 2005: Durability of different heat treated materials from industrial processes in ground contact. International Research Group on Wood Protection, Document No IRG/WP, 05-40312.
41. Wang, J.; Cooper, P., 2005: Effect of oil type, temperature and time on moisture properties of hot oil-treated wood. Holz als Roh-und Werkstoff, 63 (6): 417-422. https://doi.org/10.1007/s00107-005-0033-4
42. Windeisen, E.; Bächle, H.; Zimmer, B.; Wegener, G., 2009: Relations between chemical changes and mechanical properties of thermally treated wood. Holzforschung, 63: 773-778. https://doi.org/10.1515/HF.2009.084
43. Vural, U., 2020: Waste mineral oils re-refining with physicochemical methods. Turkish Journal of Engineering, 4 (2): 62-69. https://doi.org/10.31127/tuje.616960
44. Yalınkılıç, M. K.; Baysal, E.; Demirci, Z., 1995: Leaching rates of boron from Douglas wood impregnated with boron compounds and prevention of leaching with various water repellents. Atatürk Üniversitesi, Çevre Sempozyumu Eylül, Erzurum, Türkiye (in Turkish).
45. Yingprasert, W.; Matan, N.; Chaowana, P., 2015: Fungal resistance and physico-mechanical properties of cinnamon oil and clove oil-treated rubberwood particleboards. Journal of Tropical Forest Science, 27 (1): 69-79. https://www.jstor.org/stable/43150976
46. Zhang, X., 2003: Photo-resistance of alkyl ammonium compound treated wood. MSc Thesis, University of British Colombia, Vancouver, Canada.
47. ***ASTM D358-55, 1970: Standard specification for wood to be used panels in weathering tests of paints and varnishes. West Conshohocken, PA, USA.
48. ***ASTM D1536-58, 1964: Tentative method of test color difference using the color master differential colorimeter. West Conshohocken, PA, USA.
49. ***CSB, 2024: Ministry of Environment, Urbanization and Climate Change of the Republic of Türkiye (in Turkish).
50. ***Mobil, 2024: https://www.mobiloil.com.tr/tr-tr/industrial-products/mobil-delvac-super-20w-50 (Accessed Jul. 22, 2024).
51. ***TS ISO 13061-2, 2021: Physical and mechanical properties of wood – Test methods for small clear wood specimens. Part 2: Determination of density for physical and mechanical tests.
52. ***TS 2595, 1977: Wood-determination of ultimate stress in compression parallel to grain. Turkish Standardization Institute.

**Corresponding address:**

**ÇAĞLAR ALTAY**
Aydın Adnan Menderes University, Vocational School of Aydın, Aydın, TURKEY, e-mail: caglar.altay@adu.edu.tr

Miglena Valyova*[1], Daniel Koynov[2]

# Bonding Strength of Beech Plywood Glued with Alcohol-Soluble Phenol-Formaldehyde Resin

# Čvrstoća lijepljenja bukove furnirske ploče fenol-formaldehidnom smolom topljivom u alkoholu

**ORIGINAL SCIENTIFIC PAPER**
**Izvorni znanstveni rad**
Received – prispjelo: 15. 4. 2024.
Accepted – prihvaćeno: 2. 10. 2024.
674.81; 691.116
https://doi.org/10.5552/drvind.2024.0208



**ABSTRACT** • *The present study examines the bonding strength of five-layer plywood made from beech wood (Fagus sylvatica L.). An alcohol-soluble phenol-formaldehyde (PF) resin as an adhesive between the veneer sheets was used. Various pressing factors, showing the effect of the varying ratio between them, were applied. The experimental samples both in a dry state and after immersion in boiling water for one hour were tested. The results clearly demonstrated that the bonding strength is very high when using the alcohol-soluble PF resin and meets the requirements of the standard BDS EN 314-2: 2002. The best bonding strength values were obtained at a press temperature of 145 °C, adhesive spread of 150 to 170 g/m², and initial adhesive temperature of 30-40 °C.*

**KEYWORDS:** *plywood; PF resin; bonding strength; Fagus sylvatica L.*

**SAŽETAK** • *U radu se ispituje čvrstoća lijepljenja peteroslojne furnirske ploče izrađene od bukovine (Fagus sylvatica L.). Za lijepljenje listova furnira upotrijebljena je fenol-formaldehidna (PF) smola topljiva u alkoholu. Proučavani su različiti parametri prešanja te njihovi međusobni odnosi. Ispitivani su suhi uzorci i uzorci nakon jednosatnog potapanja u kipućoj vodi. Rezultati su jasno pokazali da je čvrstoća lijepljenja furnirske ploče vrlo visoka kada se rabi PF smola topljiva u alkoholu te da zadovoljava zahtjeve standarda BDS EN 314-2: 2002. Najbolje vrijednosti čvrstoće lijepljenja dobivene su pri temperaturi prešanja od 145 °C, uz količinu nanosa ljepila 150 – 170 g/m² i uz početnu temperaturu ljepila 30 – 40 °C.*

**KLJUČNE RIJEČI:** *furnirska ploča, PF smola; čvrstoća lijepljenja; Fagus sylvatica L.*

* Corresponding author
[1] Author is researcher at University of Forestry, Faculty of Ecology and Landscape Architecture, Department of Plant Pathology and Chemistry, Sofia, Bulgaria. https://orcid.org/0000-0003-4072-2537
[2] Author is researcher at University of Forestry, Faculty of Forest Industry, Department of Mechanical Technology of Wood, Sofia, Bulgaria. https://orcid.org/0000-0001-5370-9468

## 1 INTRODUCTION
## 1. UVOD

Plywood is a composite material mainly applied in the furniture and construction industries. It consists of several thin layers of veneer tightly glued together with an odd number of layers with the grain direction of adjacent layers oriented perpendicular to one another.

Obtaining quality adhesive joints between veneer sheets in the production of laminated wood and more specifically plywood is directly dependent on the main process factors. These factors can be briefly considered as factors characterizing the veneer and plywood package; factors characterizing the properties and use of the adhesive; and factors characterizing the conditions of pressing (Hong and Park, 2017).

The type of wood used directly affects the performance indicators of the finished plywood. In Bulgaria, various types of wood for plywood production are applied, but the most commonly used are beech (*Fagus sylvatica* L.) and poplar (*Populus* sp.). The reason for this is that beech wood has very good physical and mechanical properties (Gryc *et al.*, 2008; Rais *et al.*, 2022). In addition, this wood species is present in relatively large quantities in our country (approximately 144 million $m^3$). The distribution of beech is approximately 20 % of the total stock of the country (Executive Forest Agency, 2020).

In the process of developing logs and obtaining veneer sheets, roughness has a significant impact on the bonding process (Dundar *et al.,* 2008; Bekhta *et al.,* 2009). Micro and macro irregularities on the veneer surface are formed. Studies show that the strength of the adhesive layer increases with increasing roughness of the veneer, but up to certain values, after which a significant decrease is observed (Aydin, 2004; Wang *et al.,* 2006). The moisture content of the veneer should be in the range of 6 to 12 % (Aydin *et al.*, 2006; Quiao, 2014), and when bonding with multi-component adhesives, it should not be higher than 7 %. The investigations regarding the moisture content of the veneer show that at very low values, the adhesive viscosity significantly increases because of intensive moisture absorption from the applied adhesive (Resnik and Šernek, 2000). The viscosity of the adhesive decreases in cases of very high moisture content of the veneer. Both cases are a prerequisite for creating internal stresses, leading to reduction in the quality of the bonding joints. The piezo-thermal treatment process creates conditions for an increased amount of steam-gas mixture at high moisture content in the veneer. This can contribute to thermal degradation of the resin (Resnik and Šernek, 2000; Bekhta *et al.,* 2012; Bekhta *et al.,* 2020).

The initial temperature of the wood also has an influence on the quality of adhesive bonds. The viscosity of the resin decreases at higher temperatures of the wood due to the increased thermal movement of molecules. This, in turn, is a prerequisite for better adhesive bonds and penetration of the adhesive into the veneer sheets during the pressing process of the plywood package (Frihart, 2012; Tran *et al.,* 2020). The initial temperature of the adhesive affects the improvement of the contact between the adhesive and the wood, thus creating conditions for speeding up the curing process (Demirkir *et al.,* 2017; Bliem *et al.,* 2019; Sutiawan *et al.,* 2022).

The adhesive consumption and its optimal thickness are essential both practically and technologically (Apsari and Tanaka, 2023). The curing time of the resin in the adhesive bond is crucial. Insufficient pressing time results in the defect of weak bonding. Excessive pressure and temperature can lead to the destruction of the already cured resin, resulting in poor adhesive bond, and hence a decrease in the quality of the finished plywood (Kurowska *et al.,* 2010; Li *et al.,* 2020; Wei *et al.,* 2021).

The condition of the adhesive is primarily determined by its concentration, viscosity, and temperature (Gomez-Bues and Haupt, 2010). Phenol formaldehyde (PF) resins are widely used in the manufacture of construction plywood and oriented strand board (OSB) for exterior applications. PF adhesives are characterized with excellent bonding strength, water resistance, bioresistance and weather durability (Gomez-Bueso and Haupt 2010; Karthäuser *et al.,* 2024). Depending on the conditions under which the reaction is carried out, two types of resins can be obtained, resole (thermosetting) and novolac (thermoplastic). Resole resins are obtained by condensing phenol with an excess of formaldehyde, in the presence of a basic catalyst. They have the ability to transform into an insoluble and unmeltable state upon heating, as they undergo three stages of structural change – resole, resitol, and resite (Figure 1).

The high content of polar groups (hydroxyl and methylol) provides excellent adhesion of resol resins to wood, as well as their solubility in alcohol, bases, and water. The chain molecules of resols consist of phenolic nuclei linked together by methylene groups or ether bonds. Novolac resins are obtained in excess of phenol in the presence of an acidic catalyst. Upon heating, these resins cannot be converted into an unmeltable and insoluble state as easily as resol resins. The rapid curing of novolac resins only occurs in the presence of special curing agents (Sarika *et al.,* 2020).

Alcohol-soluble PF resins are of interest, because the glued products are characterized by high strength and resistance to external influences (Lee *et al.,* 2014; Popovska *et al.,* 2014; Shishlov *et al.,* 2015; Chi and Trang, 2021). The literature data show that research in this area is scarce. Therefore, the aim of the present study was to examine the properties of this adhesive under different bonding technological factors, as well as its influence on the quality characteristics of ply-

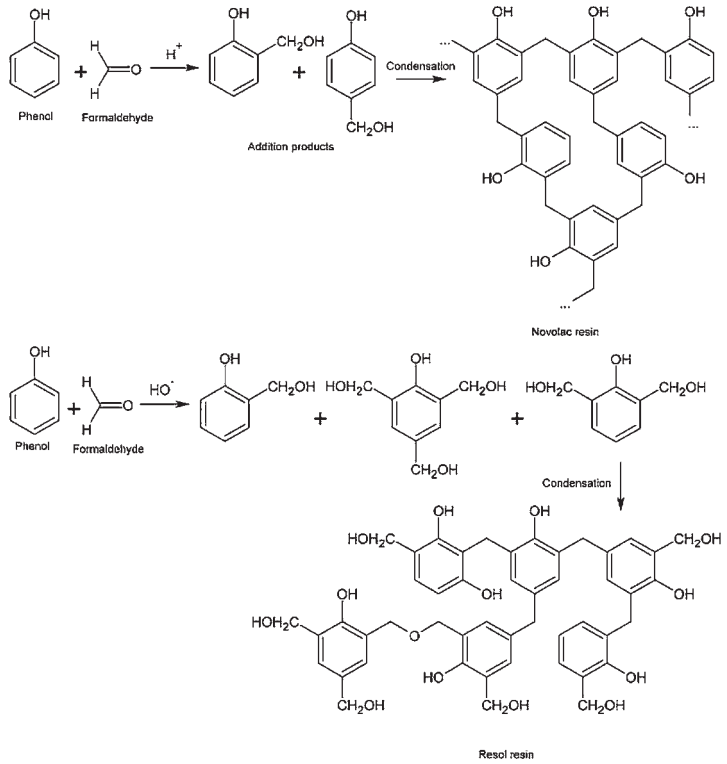


**Figure 1** Synthesis of novolac and resol resin
**Slika 1.** Sinteza novolaka i rezol smole

wood products (in dry condition and after immersion of the test specimens in boiling water for one hour).

## 2 MATERIALS AND METHODS
## 2. MATERIJALI I METODE

The experimental studies in the present work were performed using high-quality beech veneer (*Fagus sylvatica* L.) with a thickness of 1.5 mm, free from wood defects, with a smooth surface and without processing defects. The veneer was obtained and dried to a moisture content of 6-8 % under production conditions (Cooperation "Obnova", Cherni Osam village). A total of 12 pieces of laboratory-glued five-layer plywood were produced in order to establish the strength indicators of the adhesive joints between the veneer sheets. After piezo-thermal treatment, the panels were removed from the hot press and arranged in tight formations for 24 hours. Before testing the strength parameters of the adhesive joints, the plywood panels were conditioned for seven days at a temperature of 20 °C and an air humidity of 65 %.

Thirty specimens were cut from each plywood sheet, half of which were tested in a dry condition and the other half in boiling water for 1 hour. The alcohol-soluble PF resin Prefere 14J350 (Prefere Resins Austria GmbH) with a solids content of 46 %, viscosity- 372 MPas at 20 °C, and pH- 6-8, was used as an adhesive.

The research was conducted in the laboratory of wood-based panels at the University of Forestry, Sofia according to the standards BDS EN 314-1:2006 and BDS EN 314-2:2002. The five-layer plywood samples were made in a hydraulic press with dimensions of 600/600 mm. The adhesive was applied to the veneer sheets using a roller applicator. This study presents the influence of certain technological factors on the bonding strength. Test specimens for determining the bonding strength of plywood were prepared according to BDS EN 315:2002.

The bonding strength at the farthest adhesive joints from the face layers, namely the second and third adhesive joints, was established. The strength characteristics of the laboratory-produced veneer sheets of beech wood was determined according to Eq. 1.

$$f_v = \frac{F}{l_1 \cdot b_1} \quad (1)$$

Where: $f_v$ – bonding strength, N/mm$^2$;
$F$ – breaking force of test specimens, N;
$l_1$ – bonding area length, mm;
$b_1$ – bonding area width, mm.

The dimensions of the test specimens were determined as the arithmetic mean values of two measurements in the middle and their length. The experiments were performed on a universal testing machine with an accuracy of 0.1 N under the following conditions: in dry state at a moisture content of plywood not exceeding 8 %, and after immersion of the test specimens in boiling water for one hour. After testing the specimens, it was recorded whether the failure occurred at the ad-

hesive joint or not. This is an additional indicator for characterizing the quality of the adhesive bond.

The influence of bonding duration on the bonding strength of plywood was investigated at three different press temperatures (135 °C, 145 °C, and 155 °C), an adhesive spread of 130 g/m$^2$ and a pressure of 1.8 MPa. The effect of adhesive consumption on bonding strength was also established at the following parameters: pressing pressure of 1.8 MPa, pressing temperature of 145 °C, pressing time of 6.15 minutes, and different adhesive consumption ranging from 110 to 190 g/m$^2$ (Pipíška *et al.,* 2023).

Studies related to the effect of the adhesive initial temperature at the moment of its application on the bonding strength of plywood were performed. Under all the above conditions, a glue spread of 130 g/m$^2$ was applied.

The obtained values were processed by the method of variational statistics, and the values between two samples were processed using the T-test.

## 3 RESULTS AND DISCUSSION
## 3. REZULTATI I RASPRAVA

In order to establish the influence of the pressing time on the bonding strength of plywood, experiments with different pressing time and at different temperatures (135 °C, 145 °C and 155 °C) were conducted. A glue spread of 130 g/m$^2$ and a pressing pressure of 1.8 MPa were applied.

The relationship between the press temperature and the pressing time on the bonding strength in a dry state at 135 °C is graphically illustrated in Figure 2a.

The results obtained showed a significant increase in bonding strength of 27 % in the range of 4:30 – 5:30 min. At this temperature, the highest bonding strength was found at a pressing time of 8:30 min. Lowering the pressing time in all cases led to a decrease in bonding strength.

The results of the conducted T-test showed statistical significance when comparing bonding strength at different pressing times. In the first case, from 4:30 to 5:30 min., p-value = 0.00007; between 5:30 and 6:30 min, p-value = 0.00015. The results were not statistically significant in the range of 6:30 to 7:30 min (p-value = 0.41110). In the last mode range from 7:30 to 8:30 min, the results displayed statistical significance again (p-value = 0.00039).

The presented results indicate that the bonding strength significantly decreased after immersion of the test specimens in boiling water for 1 hour (Figure 2b).

The lowest values were found at press temperature of 135 °C and pressing time of 4:30 minutes (1.00 N/mm$^2$), and the highest values (1.58 N/mm$^2$) when the pressing time reached 8:30 minutes. In this case, as well as in the case of testing in a dry state, the same dependence was observed, namely that with an increase in the pressing time, the bonding strength also increased. The enhancement of the adhesive joint strength with increasing pressing time was in the range of 8 to 18 %.

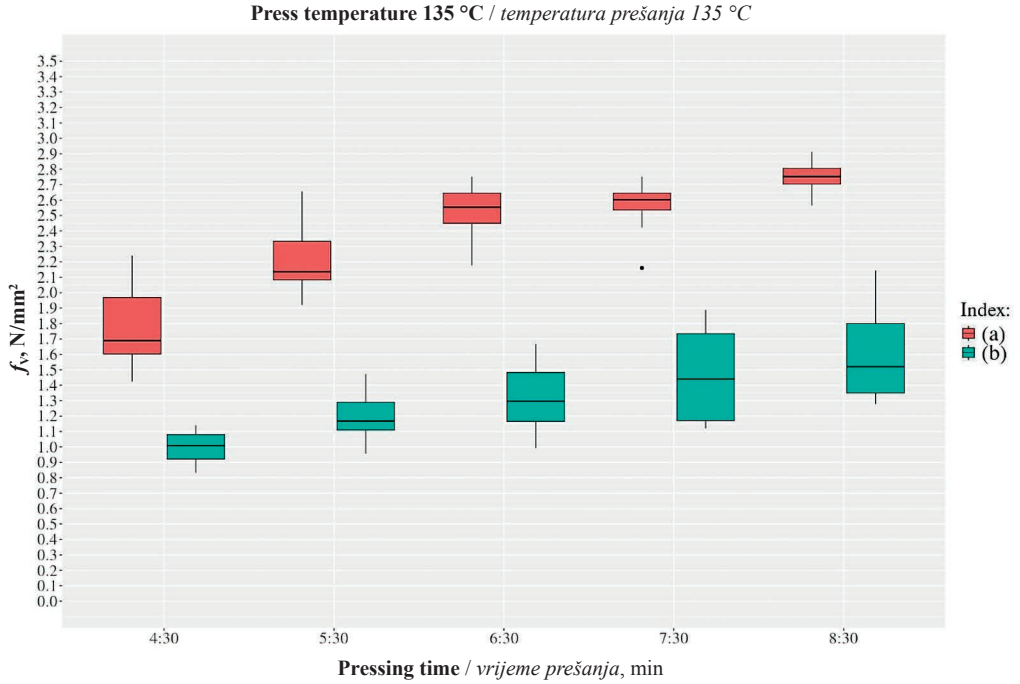


**Figure 2** Influence of pressing time on bonding strength in a dry state (a) and after immersion of test specimens in boiling water for 1 hour (b) at press temperature of 135 °C

**Slika 2.** Utjecaj vremena prešanja na čvrstoću lijepljenja furnirske ploče u suhom stanju (a) i nakon jednosatnog potapanja uzoraka u kipućoj vodi (b) pri temperaturi prešanja od 135 °C

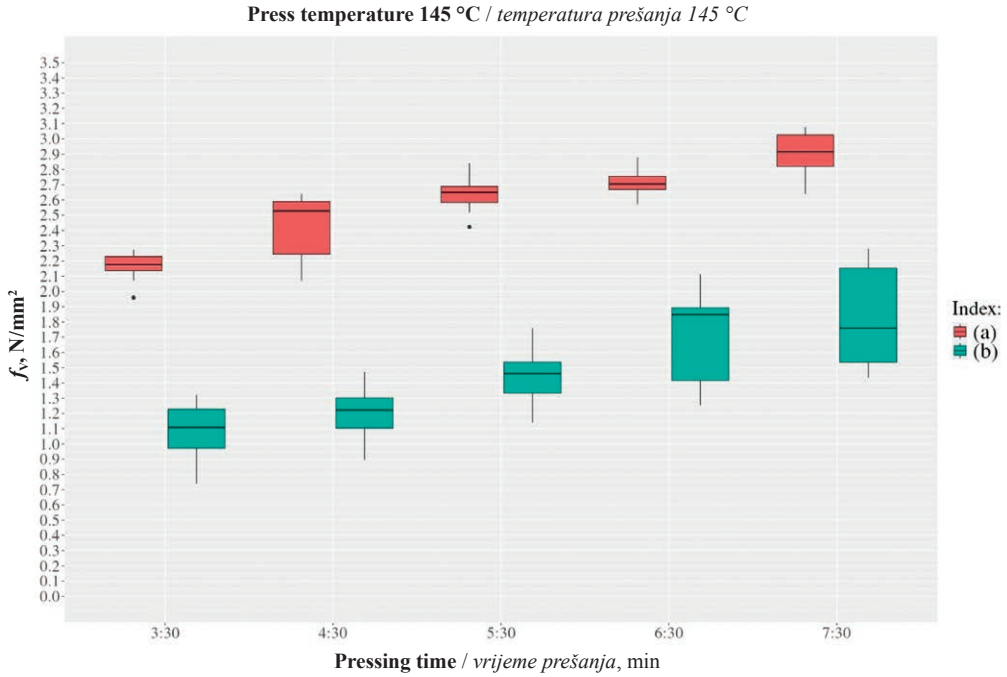


**Figure 3** Influence of pressing time on bonding strength in a dry state (a) and after immersion of test specimens in boiling water for 1 hour (b) at press temperature of 145 °C
**Slika 3.** Utjecaj vremena prešanja na čvrstoću lijepljenja furnirske ploče u suhom stanju (a) i nakon jednosatnog potapanja uzoraka u kipućoj vodi (b) pri temperaturi prešanja od 145 °C

Increasing the press temperature from 135 °C to 145 °C in a dry state led to rising of bonding strength from 5 to 24 % (Figure 3a).

In this case, with increasing pressing time, the bonding strength rises from 6 to 11 %. The lowest bonding strength was observed at 3:30 min. (2.17 N/mm$^2$), while the highest value was found at 7:30 min (2.91 N/mm$^2$).

The results of the T-test showed the same dependence. In the first case, from 3:30 to 4:30 min, the p-value was 0.00026 and between 4:30 and 5:30 min, the p-value was 0.00101. In the range of 5:30 to 6:30 min, the p-value was 0.04331. In the last regime mode from 6:30 to 7:30 min, the results of the T-test were very small, which again shows statistical significance.

The results found at press temperature of 145 °C and immersion of the test specimens in boiling water for one hour showed similar dependencies to the previous cases (Figure 3b).

The lowest value was obtained with the shortest pressing time of 3:30 min. (1.09 N/mm$^2$), while the highest value was achieved with a pressing time of 7:30 min. (1.82 N/mm$^2$). The results clearly indicate that with rising pressing time in the specified range, the strength properties of the adhesive joints after a 1-hour stay in boiling water increased by approximately 67 %.

Increasing the temperature to 155 °C in a dry state exhibited the same dependence as in the other two cases (Figure 4a).

The most significant increase in the bonding strength was observed in the range between 5:30 and 6:30 min (approximately 9 %).

The values obtained from the performed T-test showed the same trend as in the previous cases. In the range from 2:30 to 3:30 min, p-value = 0.00034 and between 3:30 and 4:30 min, p-value = 0.00018. The values were negligibly small (significantly ≤0.05) from 4:30 to 6:30 min, which again showed statistical significance.

The action of boiling water influenced a negative effect on the bonding strength at a temperature of 155 °C (Figure 4b).

It increased to the greatest extent in the interval of 4:30-5:30 min, and the highest value (3.25 N/mm$^2$) was found at a pressing time of 6:30 min. The results of testing the experimental specimens, both in a dry state and after immersion in boiling water for 1 hour, showed that with increasing the press temperature and the pressing time, the bonding strength significantly enhanced. Pressing at higher temperatures results in higher bonding strength. In addition, a shorter pressing time at higher temperatures was used.

The results clearly show that this does not have a negative impact on the bonding strength of plywood glued with alcohol-soluble PF resin. This in turn is a prerequisite for intensifying the bonding process, which is an opportunity to increase the economic effect.

When determining the bonding strength in a dry state, the failure of the adhesive joints was from 75 to 90 % in the wood zone, due to the significantly large adhesion bonds. Another part of the specimens failed 100 % in the wood zone (8:30 min in Figure 2 as well as 7:30 min in Figure 3 and 6:30 min in Figure 4). The failure of the adhesive joints in the bonding strength test after im-

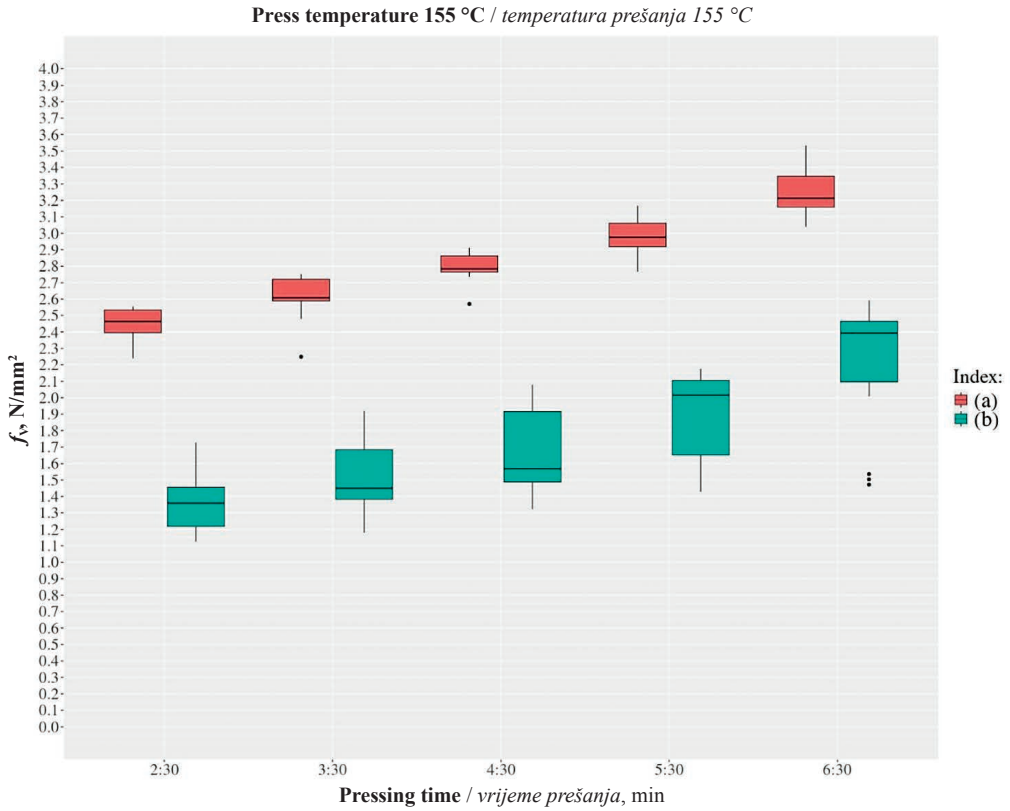


**Figure 4** Influence of pressing time on bonding strength in a dry state (a) and after immersion of test specimens in boiling water for 1 hour (b) at press temperature of 155 °C
**Slika 4.** Utjecaj vremena prešanja na čvrstoću lijepljenja furnirske ploče u suhom stanju (a) i nakon jednosatnog potapanja uzoraka u kipućoj vodi (b) pri temperaturi prešanja od 155 °C

mersion of the test specimens in boiling water for 1 hour occurred from 10 to 40 % in the wood zone.

The obtained results were compared with the research of some authors in studies conducted in a similar area. Pipiška *et al*. (2024) applied different regimes, examining three types of specimens obtained under the following conditions: after conditioning at a temperature of 20 °C and relative humidity of 65 %; at soaking in water at 20 °C for 24 h; at boiling in water for 6 h and cooling in water at 20 °C at least 1 h. The determined shear strength of the adhesive joint was in the range of 1.1 to 1.82 N/mm$^2$ and the wood failure was from 33 to 85 %.

Other authors, such as Kallakas *et al*. (2020) considered different combinations of hardwood species (gray alder, black alder and aspen), the aim being to replace birch veneer in plywood. A consumption of PF adhesive of 152 to 179 g/m$^2$ was applied. The highest bonding strength value obtained was 2.39 N/mm$^2$, and the failure in the wood zone ranged from 43.3 to 79.8 % depending on the different processing parameters and combinations of wood species.

Interesting dependencies were found by Bekhta *et al*. (2020), who conducted a study on the bonding of birch plywood with phenol-formaldehyde resin at different pressing parameters and binder content. The shear strength found, depending on the applied conditions and adhesive consumption, was in the range of 1.2 to 2.93 N/mm$^2$. Other authors optimized some of the pressing processes when gluing birch plywood with phenol-formaldehyde resin. They investigated bond strength after soaking the test specimens at 20 °C for a period of 24 hours, as well as after boiling them in water for 4 hours. The established bond strength, depending on the selected pressing parameter, was in the range from 1.1 to 2.5 N/mm$^2$ (Kawalerczyk *et al*., 2022).

The above cases clearly show that not only the main pressing parameters but also the amount and type of the binder have a significant influence on the bonding strength of plywood.

The choice of optimal adhesive consumption for bonding plywood is of great importance. The adhesive consumption affects the cost of the final product. The influence of adhesive consumption on the bonding strength of plywood was determined by the following technological factors: pressing temperature of 145 °C; pressing time of 5:30 min; pressing pressure of 1.8 MPa. Glue spreading of 110, 130, 150, 170, and 190 g/m$^2$ was selected.

The results demonstrated that with increasing consumption of phenol-formaldehyde resin, the bonding strength in dry condition also increased. This was valid, however, only in the range of 110-170 g/m$^2$ (Figure 5).

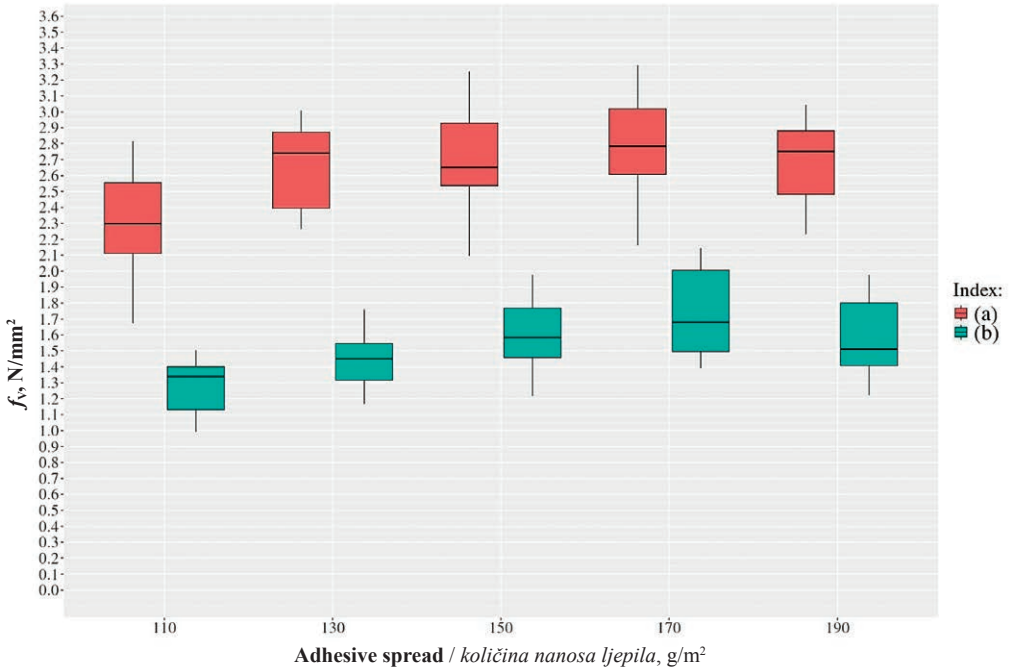


**Figure 5** Influence of adhesive spread on bonding strength of plywood in a dry state (a) and after immersion in boiling water for one hour (b)
**Slika 5.** Utjecaj količine nanosa ljepila na čvrstoću lijepljenja furnirske ploče u suhom stanju (a) i nakon jednosatnog potapanja u kipućoj vodi (b)

A significant rise in bonding strength of about 15 % was observed when the adhesive consumption was increased from 110 to 130 g/m$^2$.

The bonding strength enhanced by about 3 % from 130 to 150 g/m$^2$. This dependency was repeated in the range of 150 to 170 g/m$^2$. When the adhesive spread reached 190 g/m$^2$, a decrease in bonding strength of plywood was observed. This is due to the formation of a thick adhesive joint, leading to significant stress within it. These results indicated that excessive increase in adhesive consumption is not advisable.

The results of the conducted T-test showed that there is no statistically significant difference in bonding strength when comparing different adhesive amounts. In the range of 110 to 130 g/m$^2$, $p$-value = 0.00644; from 130 to 150 g/m$^2$, $p$-value = 0.53025. Similar values were found for adhesive spread between 150 and 170 g/m$^2$ ($p$-value = 0.46423) and between 170 and 190 g/m$^2$ ($p$-value = 0.23646).

Testing of the specimens after immersion in boiling water for one hour showed a similar dependence as in the dry state, with the difference that the values were lower (Figure 5b).

In this case, there was again a sharp increase of about 13 % in the bonding strength from 110 to 130 g/m$^2$.

From the above, it becomes clear that the optimal consumption of alcohol-soluble phenol-formaldehyde resin can be assumed to be in the range of 150-170 g/m$^2$.

The initial temperature of the adhesive also influenced the bonding strength. The same process factors were applied as in the study of the adhesive consumption. When testing the samples in a dry state, the lowest bonding strength was obtained at an adhesive temperature of 10 °C – 2.02 N/mm$^2$ (Figure 6a).

As the adhesive temperature rises, the bonding strength also increases. It changed insignificantly (about 7 %) in the range of 10 to 20 °C. Further increase in temperature leads to a considerable enhancement in bonding strength (about 19 %) in the range of 20 to 30 °C. The increase of 19 % was also observed from 30 to 40 °C. The graphical representation shows that as the temperature rises in the range of 20 to 40 °C, the bonding strength of plywood increases from 2.26 to 3.32 N/mm$^2$, or by approximately 42 %.

Figure 6b illustrates the results of testing the samples after immersion in boiling water for one hour. A similar dependence was found as in the dry state, with the most intensive increase in bonding strength in the range of 30-40 °C. However, in this case, the values were lower compared to those in the dry state. The best bonding strength was achieved at the highest temperature.

The results of the conducted T-test showed that when comparing the bonding strength at different temperatures of the adhesive, in most cases statistical significance was assessed. When increasing the temperature from 10 to 20 °C, the results were not statistically significant ($p$-value = 0.10001). In a temperature range from 20 to 30 °C, p-value = 0.00019. In the final variant of 30 to 40 °C, $p$-value = 0.00053. The performed studies demonstrate that the optimal temperature of

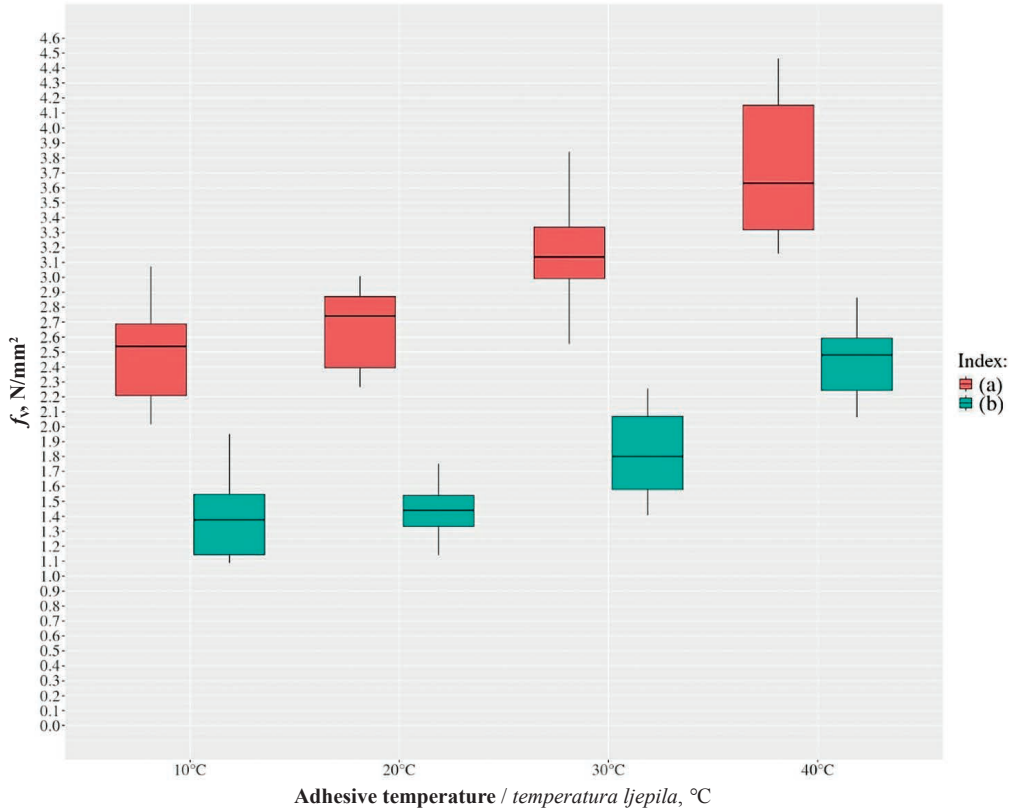


**Figure 6** Influence of adhesive temperature on bonding strength in a dry state (a) and after immersion in boiling water for one hour (b)
**Slika 6.** Utjecaj temperature ljepila na čvrstoću lijepljenja furnirske ploče u suhom stanju (a) i nakon jednosatnog potapanja u kipućoj vodi (b)

alcohol-soluble PF resin can be assumed to be in the range of 30-40 °C.

## 4 CONCLUSIONS
## 4. ZAKLJUČAK

The use of alcohol-soluble PF resin for the production of plywood showed very high strength characteristics of the adhesive joint. The established results strongly indicate that these properties apply both to the dry state and to treatment in boiling water. This is of considerable interest when plywood is subjected to adverse weather conditions.

The strength of the adhesive joints rised almost linearly with increasing pressing time and temperature from 135 to 155 °C.

The established optimal mode factors after the conducted research were: temperature of 145 °C, adhesive spread of 150 g/m² and initial temperature of the glue 30-40 °C.

## 5 REFERENCES
## 5. LITERATURA

1. Aydin, I., 2004: Activation of wood surfaces for glue bonds by mechanical pre-treatment and its effects on some properties of veneer surfaces and plywood panels. Applied Surface Science, 233 (1-4): 268-274. https://doi.org/10.1016/j.apsusc.2004.03.230
2. Aydin, I.; Colakoglu, G.; Çolak, Ş.; Demirkir, C., 2006: Effects of moisture content on formaldehyde emission and mechanical properties of plywood. Building and Environment, 41 (10): 1311-1316. https://doi.org/10.1016/j.buildenv.2005.05.011
3. Apsari, A. N.; Tanaka, T., 2023: Effects of glue spreading rate and veneer density on sugi (*Cryptomeria japonica*) plywood adhesive penetration. Maderas. Ciencia y Tecnología, 25 (8): 1-10. https://dx.doi.org/10.4067/s0718-221x2023000100408
4. Bekhta, P.; Hiziroglu, S.; Shepelyuk, O., 2009: Properties of plywood manufactured from compressed veneer as building material. Materials & Design, 30 (4): 947-953. https://doi.org/10.1016/j.matdes.2008.07.001
5. Bekhta, P.; Niemz, P.; Sedliacik, J., 2012: Effect of pre-pressing of veneer on the glueability and properties of veneer-based products. European Journal of Wood and Wood Products, 70: 99-106. https://doi.org/10.1007/s00107-010-0486-y
6. Bekhta, P.; Sedliačik, J.; Bekhta, N., 2020: Effects of selected parameters on the bonding quality and temperature evolution inside plywood during pressing. Polymers, 12 (5): 1035. https://doi.org/10.3390/polym12051035
7. Bliem, P.; Konnerth, J.; Frömel-Frybort, S.; Gartner, C.; Mauritz, R.; van Herwijnen, H. W. G., 2020: Influence of drying and curing parameters on phenol-formaldehyde impregnated wood veneers. The Journal of Adhesion, 96 (1-4): 253-271. https://doi.org/10.1080/00218464.2019.1657015
8. Chi, M. T. P.; Trang, N. H. P., 2021: Application of alcohol soluble phenol formaldehyde resin for manufacturing

cut-off wheel in Vietnam. International Journal of Latest Engineering Research and Applications, 6 (4): 76-83.
9. Demirkir, C.; Öztürk, H.; Çolakoğlu, G., 2017: Effects of press parameters on some technological properties of polystyrene composite plywood. Kastamonu University Journal of Forestry Faculty, 17 (3): 517-522. https://doi.org/10.17475/kastorman.285645
10. Dundar, T.; Akbulut, T.; Korkut, S., 2008: The effects of some manufacturing factors on surface roughness of sliced Makoré (*Tieghemella heckelii* Pierre Ex A. Chev.) and rotary-cut beech (*Fagus orientalis* L.) veneers. Building and Environment, 43 (4): 469-474. https://doi.org/10.1016/j.buildenv.2007.01.002
11. Frihart, Ch., 2012: Wood Adhesion and Adhesives. In: Handbook of Wood Chemistry and Wood Composites, Chapter 9. CRC Press Taylor & Francis Group, pp. 255-321. https://doi.org/10.1201/b12487-13
12. Gomez-Bueso, J.; Haupt, R., 2010: Wood Composite Adhesives. In Phenolic Resins: A Century of Progress, Chapter 8. Springer-Verlag: Berlin Heidelberg, p 545.
13. Gryc, V.; Vavrčík, H.; Gomola, Š., 2008: Selected properties of European beech (*Fagus sylvatica* L.). Journal of Forest Science, 54 (9): 418-425. https://doi.org/10.17221/59/2008-JFS
14. Hong, M.-K.; Park, B.-D., 2017: Effect of urea-formaldehyde resin adhesive viscosity on plywood adhesion. Journal of the Korean Wood Science and Technology, 45 (2): 223-231. https://doi.org/10.5658/WOOD.2017.45.2.223
15. Kallakas, H.; Rohumaa, A.; Vahermets, H.; Kers, J., 2020: Effect of different hardwood species and lay-up schemes on the mechanical properties of plywood. Forests, 11 (6): 649. https://doi.org/10.3390/f11060649
16. Karthäuser, J.; Raskop, S.; Slabohm, M.; Militz, H., 2024: Modification of plywood with phenol-formaldehyde resin: substitution of phenol by pyrolysis cleavage products of softwood kraft lignin. European Journal of Wood and Wood Products, 82: 309-319. https://doi.org/10.1007/s00107-023-02029-z
17. Kawalerczyk, J.; Dziurka, D.; Mirski, R., 2022: The effect of a phenol-formaldehyde adhesive reinforcement with nanocellulose on the pressing parameters of plywood. Wood Research, 67 (5): 796-808. https://doi.org/10.37763/wr.1336-4561/67.5.7968088
18. Kurowska, A.; Borysiuk, P.; Mamiński, M.; Zbieć, M., 2010: Veneer densification as a tool for shortening of plywood pressing time. Drvna industrija, 61 (3): 193-196.
19. Lee, W.; Tseng, I.; Kao, Y.; Lee, Y.; Hu, M., 2014: Synthesis of alcohol-soluble phenol-formaldehyde resins from pyrolysis oil of *Cunninghamia lanceolata* wood and properties of molding plates made of resin-impregnated materials. Holzforschung, 68 (2): 217-222. https://doi.org/10.1515/hf-2013-0068
20. Li, W.; Zhang, Z.; Zhou, G.; Leng, W.; Mei, C., 2020: Understanding the interaction between bonding strength and strain distribution of plywood. International Journal of Adhesion and Adhesives, 98: 102506. https://doi.org/10.1016/j.ijadhadh.2019.102506
21. Pipíška, T.; Bekhta, P.; Král, P.; Paschová, Z., 2024: Effects of different pressures and veneer moisture content in adjacent layers on properties of PUF bonded plywood. Journal of Adhesion Science and Technology, 38 (7): 1043-1052. https://doi.org/10.1080/01694243.2023.2248694
22. Popovska, V. J.; Iliev, B.; Mihaylova, J., 2014: Water resistance of plywood bonded with alcohol-soluble phenol-formaldehyde resin. Innovation in Woodworking Industry and Engineering Design, 5 (1): 127-136.
23. Qiao, J. Z., 2014: Bonding properties of poplar plywood with high moisture content veneer. Applied Mechanics and Materials, 618: 86-89. https://doi.org/10.4028/www.scientific.net/AMM.618.86
24. Rais, A.; Kovryga, A.; Pretzsch, H.; van de Kuilen, J. W. G., 2022: Timber tensile strength in mixed stands of European beech (*Fagus sylvatica* L.). Wood Science and Technology, 56 (4): 1239-1259. https://doi.org/10.1007/s00226-022-01398-7
25. Resnik, J.; Šernek, M., 2000: Influence of veneer moisture content on shear strength of plywood adhesive bond. Drvna industrija, 51 (1): 3-8.
26. Sarika, P. R.; Nancarrow, P.; Khansaheb, A.; Ibrahim, T., 2020: Bio-based alternatives to phenol and formaldehyde for the production of resins. Polymers, 12 (10): 2237. https://doi.org/10.3390/polym12102237
27. Shishlov, O. F.; Troshin, D. P.; Baulina, N. S.; Glukhikh, V. V.; Stoyanov, O. V., 2015: Synthesis and properties of glues for densified laminated wood based on alcohol-soluble phenol-cardanol-formaldehyde resolic resins. Polymer Science, Series D, 8: 37-41. https://doi.org/10.1134/S199542121501013X
28. Sutiawan, J.; Hermawan, D.; Massijaya, M. Y.; Kusumah, S. S.; Lubis, M. A. R.; Marlina, R.; Purnomo, D.; Sulastiningsih, I. M., 2022: Influence of different hot-pressing conditions on the performance of eco-friendly jabon plywood bonded with citric acid adhesive. Wood Material Science & Engineering, 17 (6): 400-409. https://doi.org/10.1080/17480272.2021.1884898
29. Tran, A.; Mayr, M.; Konnerth, J.; Gindl-Altmutter, W., 2020: Adhesive strength and micromechanics of wood bonded at low temperature. International Journal of Adhesion and Adhesives, 103: 102697. https://doi.org/10.1016/j.ijadhadh.2020.102697
30. Wang, B. J.; Dai, Ch.; Ellis, S., 2006: Veneer surface roughness and compressibility pertaining to plywood/LVL manufacturing. Part I: Experimentation and implication. Wood and Fiber Science, 38 (3): 535-545.
31. Wei, Q.; Wu, Z.; Wei, W.; Aladejana, J. T.; Yves, K. G.; Li, D.; Hou, X.; Wang, X.; Xie, Y., 2021: Optimization of hot-press parameters for plywood with environmental aluminophosphate adhesive. BioResources, 16 (1): 1702-1712. https://doi.org/10.15376/biores.16.1.1702.1712
32. ***BDS EN 314-1, 2006: Plywood – Bonding quality. Part 1: Test methods.
33. ***BDS EN 314-2, 2002: Plywood – Bonding quality. Part 2: Requirements.
34. ***BDS EN 315, 2002: Plywood – Tolerances for dimensions.
35. ***Executive Forest Agency, 2020: Annual report on the afforested area until December 31, 2020. Forest fund of Bulgaria: forms 2, 3 (in Bulgarian).

**Corresponding address:**

**MIGLENA VALYOVA**
University of Forestry, Faculty of Ecology and Landscape Architecture, Department of Plant Pathology and Chemistry, 10 Kliment Ohridsky Blvd., 1797 Sofia, BULGARIA, e-mail: mvalyova@abv.bg

# Drvo crnog oraha
## *Juglans nigra* L.

## MIKROSKOPSKA OBILJEŽJA

Drvo crnog oraha rastresito je porozno do poluprstenasto porozno. Traheje su brojne (6 – 14 na 1 mm$^2$ poprečnog presjeka), srednje veličine i promjera do 260 µm. Veličina im se postupno smanjuje od ranoga prema kasnom drvu. Raspoređene su pojedinačno, u skupinama i u kratkim radijalnim nizovima. Volumni udio traheja je oko 18 %. Uzdužni parenhim apotrahealno je difuzan, volumnog udjela oko 4 %. Staničje drvnih trakova je homogeno do jedva heterogeno. Drvni su traci široki 1 – 3 stanice, visoki do 25 stanica, gustoće od 8 do 13 na 1 mm tangentnog smjera. Volumni udio drvnih trakova iznosi oko 11 %. Drvna su vlakanca libriformska, a pojavljuju se i u obliku vlaknastih traheida duljine od 1,1 do 1,85 mm. Debljina staničnih stijenki kreće se od 3,0 do 9,0 µm, a promjer njihovih lumena od 7,0 do 23,0 µm. Volumni udio drvnih vlakanaca iznosi oko 67 %.

## RELEVANTNE SPOZNAJE O STRUKTURI I VARIJACIJAMA DRVA CRNOG ORAHA

Pregled ograničenog broja istraživanja strukture i varijacije svojstava drva crnog oraha donosi spoznaje: a) o drvu crnog oraha uzgojenom na otvorenome, koje je imalo veću gustoću od drva oraha uzgojenoga u šumi (Paul, 1943.); b) o mehaničkim i tehnološkim svojstvima drva crnog oraha koja su bila zadovoljavajuća bez obzira na anatomska obilježja (Schumann, 1973.); c) o plantažno uzgojenim stablima crnog oraha koja su imala šire godove, sa širom zonom kasnog drva, što rezultira smanjenjem površine pora i lošijom teksturom drva (Phelps i Workman, 1992.); d) o duljini vlakanaca na koju neznatno utječu postupci suzbijanje korova i obrada usjeva (Cutter i Garrett, 1993.).

## MICROSCOPIC CHARACTERISTICS

Black walnut wood is diffuse porous to semi-ring porous. Vessels are numerous (6 to 14 on 1 mm$^2$ cross section), medium in size and with diameter up to 260 µm. Their size gradually decreases from early to late wood. They are arranged individually, in pairs and in short radial rows. The volume fraction of vessels is around 18 %. Axial parenchyma is apotracheal diffuse, with volume fraction of around 4 %. Wood ray tissue is homogeneous to barely heterogenous. Wood rays are 1 to 3 cells in width, to 25 cells in height, with the density of 8 to 13 per tangential mm. The volume fraction of wood rays is around 11 %. Wood fibres are libriform, and also appear in the form of fibrous tracheids, with a length of 1.1 to 1.85 mm. The cell wall thickness ranges from 3.0 to 9.0 µm, and lumen diameter from 7.0 to 23.0 µm. The volume fraction of wood fibres is around 67 %.

## RELEVANT KNOWLEDGE ABOUT BLACK WALNUT WOOD STRUCTURE AND VARIATIONS

A review of the limited research on wood structure and properties variations provides the following information: (a) open-grown black walnut wood had higher density than did forest-grown walnut (Paul, 1943); (b) mechanical and machining properties of black walnut wood were satisfactory regardless of anatomical characteristics (Schumann, 1973); (c) black walnut plantation trees had wider growth rings with wider latewood zones, resulting in a reduction in vessel area and poorer wood texture (Phelps and Workman, 1992.); (d) fiber length was found to be weakly affected by weed control and cropping practices (Cutter and Garrett, 1993).

## REFERENCES


1. Cutter, B. E.; Garrett, H. E., 1993: Wood quality in alleycropped eastern black walnut. Agroforestry Systems, 22: 25-32.
2. Paul, B. H., 1943: Black walnut for gunstocks. Southern Lumberman, 166 (2089): 32-33.
3. Phelps, J. E.; Workman, C. E., 1992: Vessel area studies in black walnut (*Juglans nigra* L.). Wood Fiber Sci., 24 (1): 60-67.
4. Schumann, D. R., 1973: Mechanical, physical and machining properties of black walnut from Indiana and Missouri. Wood and Fiber Science, 5 (1): 14-20.
5. Wagenführ, R.; Scheiber, C., 2006: HOLZATLAS. VEB Fachbuchverlag, Leipzig, pp. 551-554.


*doc. dr. sc. Iva Ištok Pandur*

**SVEUČILIŠTE U ZAGREBU • FAKULTET ŠUMARSTVA I DRVNE TEHNOLOGIJE**
***UNIVERSITY OF ZAGREB • FACULTY OF FORESTRY AND WOOD TECHNOLOGY***
Svetošimunska 23, 10000 Zagreb, Hrvatska / *Croatia* IBAN: HR0923600001101340148
tel: 00385 1 2352 454 e-mail: dcvetan@sumfak.hr OIB / *VAT ID*: HR07699719217

# PRETPLATNI LIST / *SUBSCRIPTION SHEET*

Uskoro izlazi **volumen 76 (2025. godina)** časopisa Drvna industrija. Pozivamo Vas da obnovite svoju pretplatu ili se pretplatite na časopis, te na taj način pomognete njegovo izdavanje. Cijena sva četiri broja jednog godišta (volumena) je 55,00 EUR bez PDV-a. Ukoliko ste suglasni s uvjetima pretplate za jedno godište časopisa, molimo Vas da popunite obrazac za pretplatu i pošaljete ga na našu poštansku ili elektroničku adresu.

***Volume 76 (2025)*** *of the journal Drvna industrija will be published soon. We invite you to renew your subscription or subscribe to a journal to support it. The price of all four issues of one year (volume) is 55 EUR without VAT. If you agree to the subscription terms for one volume, please complete the subscription form and send it to our postal or e-mail address.*

Predsjednik Izdavačkog savjeta
časopisa Drvna industrija
*President of Publishing Council*

izv. prof. dr. sc. Vjekoslav Živković

Glavna i odgovorna urednica
časopisa Drvna industrija
*Editor-In-Chief*

prof. dr. sc. Ružica Beljo Lučić

or Copy/Scan

## PRETPLATA NA ČASOPIS
## *SUBSCRIPTION TO JOURNAL*

DRVNA INDUSTRIJA

Pretplaćujemo se na časopis *Drvna industrija* u količini od ___ godišnje pretplate (četiri broja).
Cijena jednog godišta (volumena) iznosi 55 EUR, bez PDV-a. Pretplata obuhvaća sve brojeve jednog godišta.
*We subscribe to the journal* Drvna industrija *in amount of ___ annual subscription(s) (four issues).*
*Price of one volume (year) is 55 EUR, without VAT. The subscription covers all issues of one volume.*

Hrvatska:
HR0923600001101340148
s naznakom "Za časopis Drvna industrija"
poziv na broj: 3-02-03

EU / World:
Bank: Zagrebačka banka
IBAN: HR0923600001101340148
Swift: ZABA HR 2X

Osoba / *Name*: _____ e-mail: _____

Tvrtka, ustanova / *Company, institution*: _____

OIB / *VAT ID*: _____ Telefon / *Phone*: _____

Adresa / *Address*: _____ Pošta. broj: _____
*(ulica / street)* *Postal code:*

Grad / *City*: _____ Regija / *Region*: _____

Država / *Country*: _____

HRVATSKA KOMORA
INŽENJERA ŠUMARSTVA
I DRVNE TEHNOLOGIJE

# HRVATSKA KOMORA INŽENJERA ŠUMARSTVA I DRVNE TEHNOLOGIJE

Osnovana je na temelju Zakona o Hrvatskoj komori inženjera šumarstva i drvne tehnologije.

Komora je samostalna i neovisna strukovna organizacija koja obavlja povjerene joj javne ovlasti, čuva ugled, čast i prava svojih članova, skrbi da ovlašteni inženjeri obavljaju svoje poslove savjesno i u skladu sa zakonom, promiče, zastupa i usklađuje njihove interese pred državnim i drugim tijelima u zemlji i inozemstvu.

## Članovi komore:

inženjeri šumarstva i drvne tehnologije koji obavljaju stručne poslove iz područja šumarstva, lovstva i drvne tehnologije.

## Stručni poslovi:

projektiranje, izrada, procjena, izvođenje i nadzor radova iz područja uzgajanja, uređivanja, iskorištavanja i otvaranja šuma, lovstva, zaštite šuma, hortikulture, rasadničarske proizvodnje, savjetovanja, ispitivanja kvalitete proizvoda, sudskoga vještačenja, izrade i revizije stručnih studija i planova, kontrola projekata i stručne dokumentacije, izgradnja uređaja, izbor opreme, objekata, procesa i sustava, stručno osposobljavanje i licenciranje radova u šumarstvu, lovstvu i preradi drva.

## Zadaci Komore:

- promicanje razvoja struke i skrb o stručnom usavršavanju članova,
- poticanje donošenja propisa kojima se utvrđuju javne ovlasti Komore,
- reagiranje struke na pripremu propisa iz područja šumarstva, lovstva i drvne tehnologije,
- suradnja s nadležnim institucijama i zastupanje struke u odnosu prema njima,
- organizacija stručnoga usavršavanja,
- zastupanje interesa svojih članova,
- izdavanje pečata i iskaznice ovlaštenim inženjerima,
- briga i nadzor poštivanja kodeksa strukovne etike,
- osiguravanje članova Komore za štetu koja bi mogla nastati investitorima i trećim osobama i sl.

Članovima Komore izdaje se rješenje, pečat i iskaznica ovlaštenoga inženjera.
Za uspješno obavljanje zadataka te za postizanje ciljeva ravnopravnoga i jednakovrijednoga zastupanja struka udruženih u Komoru, članovi Komore organizirani su u razrede:

- Razred inženjera šumarstva
- Razred inženjera drvne tehnologije

HRVATSKA KOMORA INŽENJERA ŠUMARSTVA I DRVNE TEHNOLOGIJE
Prilaz Gjure Deželića 63
10000 ZAGREB

telefon:
++ 385 1 376-5501
e-mail:
info@hkisdt.hr

www.hkisdt.hr


**Drvodjelac d.o.o.**
**Petra Preradovića 14, Ivanec, Hrvatska**
**+385 (0)42 781 922 | www.drvodjelac.hr**